



<https://theses.gla.ac.uk/>

Theses Digitisation:

<https://www.gla.ac.uk/myglasgow/research/enlighten/theses/digitisation/>

This is a digitised version of the original print thesis.

Copyright and moral rights for this work are retained by the author

A copy can be downloaded for personal non-commercial research or study,
without prior permission or charge

This work cannot be reproduced or quoted extensively from without first
obtaining permission in writing from the author

The content must not be changed in any way or sold commercially in any
format or medium without the formal permission of the author

When referring to this work, full bibliographic details including the author,
title, awarding institution and date of the thesis must be given

Enlighten: Theses

<https://theses.gla.ac.uk/>
research-enlighten@glasgow.ac.uk

M A T H E M A T I C A L M O D E L S

O F

L U N G F U N C T I O N

A thesis submitted for the degree of

Doctor of Philosophy

by

ALLAN IAN PACK

Centre for Respiratory Investigation
Glasgow Royal Infirmary.

August 1976.

ProQuest Number: 10662668

All rights reserved

INFORMATION TO ALL USERS

The quality of this reproduction is dependent upon the quality of the copy submitted.

In the unlikely event that the author did not send a complete manuscript and there are missing pages, these will be noted. Also, if material had to be removed, a note will indicate the deletion.



ProQuest 10662668

Published by ProQuest LLC (2017). Copyright of the Dissertation is held by the Author.

All rights reserved.

This work is protected against unauthorized copying under Title 17, United States Code
Microform Edition © ProQuest LLC.

ProQuest LLC.
789 East Eisenhower Parkway
P.O. Box 1346
Ann Arbor, MI 48106 – 1346

Thesis
4631
COPY 2



C O N T E N T S

TABLE OF CONTENTS

DECLARATION	i
ACKNOWLEDGEMENTS	ii
DEDICATION	iii
ABSTRACT	iv
INTRODUCTION	v
CHAPTER 1. THE MATHEMATICAL APPROACH TO PHYSIOLOGICAL SYSTEMS.	
1.1. Introduction	1
1.2 Stages in Modelling	2
1.3 Formulation of the Model	3
1.4 Categories of Model	4
1.5 Formulation of Dynamic Models	9
1.6 Formulation of Ordinary Differential Equations	16
1.7 Construction of Block Diagram	22
1.8 Solution of Ordinary Differential Equations	22
1.9 Simulation	29
1.10 "Black-Box" Models	31
1.11 Parameter Estimation	32
1.12 Validation of the Model	33
1.13 Application of Mathematical Models	33
a) Indirect measurement of physiological variables	35
b) Hypothesis testing/experimental design	35
c) Educational role	38
CHAPTER 2. MATHEMATICAL MODELS OF RESPIRATORY GAS TRANSPORT.	
2.1 Introduction	39
2.2 Basic Units	40
2.3 Steady-State Models	44
a) Introduction	44
b) Basic equations	44
c) Steady-state equality of respiratory gaseous nitrogen transport	45
d) Functional compartments in the lung	47
e) Airway convection/diffusion	52
f) Membrane/erythrocyte diffusion	53
g) Distribution component	57

2.4	Breath by Breath Models	78
2.5	Models with Unidirectional Flow Rate	79
2.6	Inspiration/Expiration as an Instantaneous Process	83
2.7	Models with Time-Varying Ventilation (Dynamic Models)	87
2.7b	Development of Dynamic Models	90
2.8	Distributed Models of Gas transport	98
	a) A review of previous models of gas transport in the airways	98
	b) A model of convection and diffusion in pulmonary airways	101
	c) Distributed models of diffusion across the alveolar capillary membrane	109
CHAPTER 3. APPLICATION OF DYNAMIC MODELS OF PULMONARY GAS EXCHANGE TO MEASUREMENT. EXPERIMENTAL AND COMPUTING METHODS.		
3.1	Introduction	112
3.2	Solution of Model Equations	113
	a) Analogue-computation	113
	b) Digital-computation	115
3.3	Experimental System	116
	a) Measurement of gas flow-rate	116
	b) Measurement of partial pressure of gases under study	119
3.4	Experimental Methods	126
	a) Analogue computation	127
	b) Digital computation	128
CHAPTER 4. APPLICATION OF THE TECHNIQUES OF DYNAMIC MODELLING TO THE ANALYSIS OF INERT GAS WASH-OUT TESTS.		
4.1	Introduction	140
4.2	Standard methods of analysis of open-circuit multiple- breath tests of maldistribution of ventilation	141
	a) Rate variables	142
	b) Discrete weighting function	144
	c) The work of Briscoe, Cournand and associates	147
	d) Continuous weighting functions	148
	e) Models with common dead space	150
4.3	Dynamic Modelling Approach	151
	a) Models	151
	b) Parameter estimation	152
	c) Experimental studies	155

4.4	Future Prospects for the Use of Dynamic Models in this Area	166
4.5	The Importance of Taylor Dispersion/A Simulation Study	169
	a) Introduction	169
	b) Simulation studies	170
4.6	Conclusion	181

CHAPTER 5. A DYNAMIC MODEL OF CARBON DIOXIDE TRANSPORT.

5.1	Introduction	183
5.2	Storage of Carbon Dioxide in Lung Tissue	183
5.3	Tissue Stores of Carbon Dioxide	185
5.4	Relationship between the Concentration and Tension of Carbon Dioxide in Blood	187
5.5	Model of Carbon Dioxide Transport	196
5.6	Outline of Experimental Procedure	197
5.7	Parameter Estimation Procedures	199
5.8	Effect of Various Assumptions	215
	a) Lung Volume	215
	b) Dead Space	216
	c) Linear Description of CO ₂ dissociation curve	216
5.9	Measurement of Cardiac Output at Rest	223
5.10	Measurement of Cardiac Output During Exercise	230
5.11	Discussion	234

CHAPTER 6. RECAPITULATION AND PROSPECT. 242

APPENDICES

Appendix 1A	Definition of a derivative	245
Appendix 1B	Construction of ordinary differential equations	245
Appendix 1C	Construction of partial differential equation	246

Appendix 1D	Linearisation of a non-linear equation	248
Appendix 2	Use of an analogue computer	250
1.	Introduction	250
2.	Concept of a machine-unit	250
3.	Analogue computer components	250
4.	Modes of operation	251
5.	Solution of a simple differential equation by analogue computation	251
6.	Amplitude scaling	252
7.	Time scaling	255
8.	Logic capabilities of analogue computers	256
9.	Example of use of analogue computer in solution of a lung model equation	256
Appendix 3	Use of high level simulation language	260
Appendix 4	Simulator for teaching of respiratory gas exchange concepts	263
Appendix 5	Summary of symbols which are used in this thesis	272
Appendix 6	Programme for construction of \dot{V}/\dot{Q} line	279
Appendix 7	Manufacturers of experimental equipment	284
Appendix 8	Software for initial processing of measured data	286
Appendix 9	Parameter estimation methods	297
Appendix 10	Compartmental analysis of \dot{V}/\dot{Q} distribution	300
REFERENCES		302

DECLARATION

This thesis describes research carried out in the Centre for Respiratory Investigation, Glasgow Royal Infirmary, under the supervision of Dr. F. Moran and Professor E.M. McGirr. Certain of the results contained have been presented to learned societies - Physiological Society, Medical Research Society, Scottish Society for Experimental Medicine, Institute of Mathematics and its Applications.

The basic claims to originality are in the development of new methods of assessment of respiratory gas exchange. In particular techniques to analyse gas exchange in non steady-state conditions have been developed. A simulation study of the importance of Taylor dispersion in the lung has also been undertaken. A special purpose analogue computer has been constructed for educational purposes.

ACKNOWLEDGEMENTS

An interdisciplinary thesis of necessity involves people from different disciplines. I have been particularly fortunate in having extremely good colleagues during this work.

I am particularly indebted to Dr. F. Moran. The origins of this project are related to his vision and he, at all times, has been a source of considerable support. I am grateful to Dr. D. Murray-Smith, who has involved himself in those aspects of the work related to parameter estimation. Dr. M. Hooper and Mr. W. Nixon have been interested in the numerical solution of the distributed model which is described in this thesis.

Within the Centre for Respiratory Investigation I am grateful to Dr. R. J. Mills and Mr. W. Gray who have collaborated in the experimental work. The development of on-line computing techniques was achieved by Dr. I. Logan.

I am grateful to my secretaries Miss I. Adams, Miss A. Roy and Mrs. M. Murray.

During my period in this work I have been supported by the Anderson Fund, Glasgow Royal Infirmary and by the Wellcome Trust, to whom I am indebted. I am also extremely grateful to the Scottish Home and Health Department who provided computer facilities.

To Fran

This thesis is dedicated to my wife, who although initially sceptical about a medical graduate becoming involved with mathematics, gave her support unselfishly.

This thesis is concerned with an approach to the assessment of respiratory gas transport in individual subjects, which is based on the techniques of mathematical modelling. The general mathematical modelling approach to a physiological system while similar to that for a physical system is sufficiently different to warrant discussion (Chapter 1). Models have been frequently employed in the study of respiratory gas transport and the different models are reviewed in Chapter 2. A method of characterising these models is suggested. Many of the models consist of simple algebraic equations which describe steady-state conditions. An extension to these models to quantify ventilation-perfusion distribution is presented (Chapter 2 and Appendix 10). The main deficiencies of steady-state models are the restrictions which they impose on experimental conditions both limiting the information content of the experiment and making it difficult to perform tests on certain subjects. A new approach to the measurement of respiratory gas exchange is suggested based on dynamic as opposed to steady-state models and using the techniques of parameter estimation. The necessary experimental and computing techniques have been developed and details are presented in Chapter 3. The feasibility of this approach is proved by application to the study of inert gas wash-out experiments (Chapter 4). While this method of analysis can utilise the within-breath detail of the expired concentration measurements, the physiological mechanisms underlying this aspect of function are not fully clarified. An investigation of one of the relevant mechanism (Taylor diffusion) using a distributed model is also presented in Chapter 4. The techniques of dynamic modelling are applied to the development of a new non-invasive method for the measurement of cardiac output and CO₂ lung volume. (Chapter 5). Models can also be of value for educational purposes and a special simulator of gas transport is presented in Appendix 4.

INTRODUCTION

Many of the applications of mathematical techniques in medicine and physiology are unrelated to the solution of medical problems. This is hardly surprising since the primary motivation of the person who is trained in the physical sciences must be related to his own discipline.

This thesis involves an interdisciplinary approach to the assessment of respiratory gas exchange in human subjects. It is written by a practicing respiratory clinician, who, during the course of the work which is described, became familiar with certain areas of mathematics.

This thesis is directed primarily to the medical reader. The organisation of the thesis is thought to be appropriate to this purpose. (A physical scientist should be able to gain useful information from the text if he has a basic grounding in respiratory physiology). The main literature reviews (Chapter 1 and 2) contain descriptions of the general mathematical modelling approach to physiological systems and detail the methods of mathematical description of respiratory gas exchange which have been employed. The remaining chapters contain therefore literature surveys of the physiological literature related to particular application areas. It is hoped that the mathematical aspects of the work are presented in such a way that they can be understood by the average medical reader. In certain parts of the thesis the units which are used for partial pressure are mmHg, thereby facilitating comparison with other published work.

C H A P T E R 1

THE MATHEMATICAL MODELLING APPROACH
TO PHYSIOLOGICAL SYSTEMS.

1.1. INTRODUCTION

Conventional tests of respiratory gas exchange (see Table 1) which are used widely in clinical practice are carried out under steady-state conditions, i.e. when the ventilation of the subject under test is constant. Such conditions may be difficult to achieve in practice particularly in studying patients who may be distressed. Performance of these tests necessitates collection of expired gas and hence the attachment of experimental equipment to the patient being studied. These tests are more applicable therefore to subjects accustomed to such abnormal breathing conditions, e.g. "trained" subjects in physiological laboratories.

Test	Source of Further Details
Analysis of inert gas wash-out tests	Chapter 4.
Measurement of alveolar-arterial differences	Chapter 2.
Measurement of degree of ventilation-perfusion mismatching (physiological dead space etc).	Chapter 2.
Measurement of transfer factor for carbon monoxide (some methods of)	Chapter 2.
Measurement of cardiac output using Fick principle	Chapter 3.

TABLE 1

Another important disadvantage is that with steady-state tests only a limited part of the patient's total performance can be studied. An analogy is examination of the performance of a car which is limited to study while it is running in a steady-state with a constant speed. More information can be obtained by studying the response to controlled changes in input, thereby inducing transients in the system. There are many examples in engineering practice where analysis of data

collected during transients allows facts to be determined about the system under test which could not be obtained from steady-state studies.

Even with such restrictions steady-state tests may reveal abnormalities at an earlier stage of disease than is possible by other means¹ and may help to distinguish between otherwise similar groups of patients with chronic obstructive airways disease.^{2,3}

Steady-state conditions are necessitated not by the experimental procedures but rather by the methods of mathematical analysis of the data. Such analyses are based on steady-state mathematical models. (These models are described in more detail in Chapter 2.3 of this thesis.) Mathematical methods exist, however, to analyse data collected in non-steady-state conditions.

In this thesis, the foundations are developed of a new approach to the testing of respiratory gas exchange based on dynamic as opposed to steady-state models. The use of such dynamic models removes the necessity of having to establish steady-state conditions in subjects inexperienced in respiratory function testing. Furthermore, the information content of any individual test may be increased since the clinical respiratory physiologist can study the response of the abnormal lung to controlled changes in input.

1.2. STAGES IN MODELLING

In using mathematical models for the study of physiological systems the approach in any particular study is dictated largely by the intended use of the fully developed model. In general, however, the modelling process can be divided into four stages:-⁴

- (1) Formulation of model;
- (2) Simulation;
- (3) Validation of model;
- (4) Application.

1.3. FORMULATION OF THE MODEL

One must first decide the physical structure which will form the basis of the model and then derive the equations which describe its performance, usually employing some initial simplifying assumptions. This approach is widely used in the physical sciences although the term mathematical model is generally avoided.

In writing down even a simple equation to describe the motion of a body falling under the action of gravity we are establishing a mathematical model which will give values for the position and velocity at any point in time. The accuracy of these values depends both on the validity of the laws and on the assumptions which are made concerning the effect of any friction on the falling body.

A similar approach can be applied to physiological systems using a number of simplifying assumptions to reduce the problem to one which can be handled mathematically. These assumptions are often based on intuition rather than on experimental proof, and it is particularly important, in applying mathematical models to physiological systems, to be aware of the assumptions upon which the model is based.

Consider the following model of the kidney. The creatinine clearance measurement which is commonly used in clinical practice is based on a mathematical model of the kidney as a simple filter. The assumptions upon which the mathematical formula for the creatinine clearance is based are:-

- (1) creatinine is neither secreted or reabsorbed in the renal tubules;
- (2) the plasma concentration is constant throughout the day;

(3) the glomerular filtration rate is constant throughout the day;

(4) each nephron has the same glomerular filtration rate;

it is the last of these assumptions which is perhaps least often appreciated by those using the creatinine clearance measurement.

Although the first two assumptions can be verified experimentally,^{5,6,7,8} assumptions (3) and (4) are in a strict sense invalid. In particular assumption (4) will be quite invalid when a pathological process effects the nephrons unequally as in most, if not all, cases of chronic pyelonephritis. The creatinine clearance is in fact a measure of the performance of the 'lumped' system, i.e. considering the kidneys as one uniform organ (Fig. 1) and as such gives an average value of the glomerular filtration rate in the nephrons. 'Lumped models' such as this which disregard differences between the component functional units of an organ or system are used commonly in medicine.

The creatinine clearance illustrates an important principle in the modelling of biological systems; the use of simplifying assumptions which are in a strict sense invalid allows development of a relatively simple mathematical model, which includes the essential features of the system. Hence a relatively simple method of functional assessment is obtained which is of value in clinical practice.

1.4. CATEGORIES OF MODEL

Models can be divided into several categories (see Table 2).

Category of model	Type of mathematical description.	Method of solution of equations.
Steady-state models	Algebraic equations	Simple algebraic manipulation.
Dynamic models:		
(a) Lumped, time-invariant, linear	Ordinary differential equations.	Analytical methods. Graphical methods.
(b) Lumped, time-variant, linear	Ordinary differential equations.	Computer-based methods.
(c) Lumped, non-linear	Ordinary differential equations.	Computer-based methods.
(d) Distributed	Partial differential equations.	Computer-based methods.

TABLE 2

a) Steady-state Models

Steady-state models are used widely in physiology and medicine.

Steady-state models represent conditions in a system only when the variables of the system do not change with time, i.e. they describe a condition of equilibrium. The principal advantage of steady-state models is that they lead usually to systems of algebraic equations which are solved easily.

b) Dynamic Models.

Dynamic models allow change in the system variables with time and are of more general importance and value than the steady-state representation. Dynamic modelling techniques have been applied mostly to the study of physical systems, e.g. industrial chemical processes,⁹ nuclear reactors¹⁰ etc..

In modelling dynamic systems there are quantities which are regarded as INPUTS, i.e. the stimulus to the system, and quantities which are regarded as OUTPUTS, i.e. the actual system response.

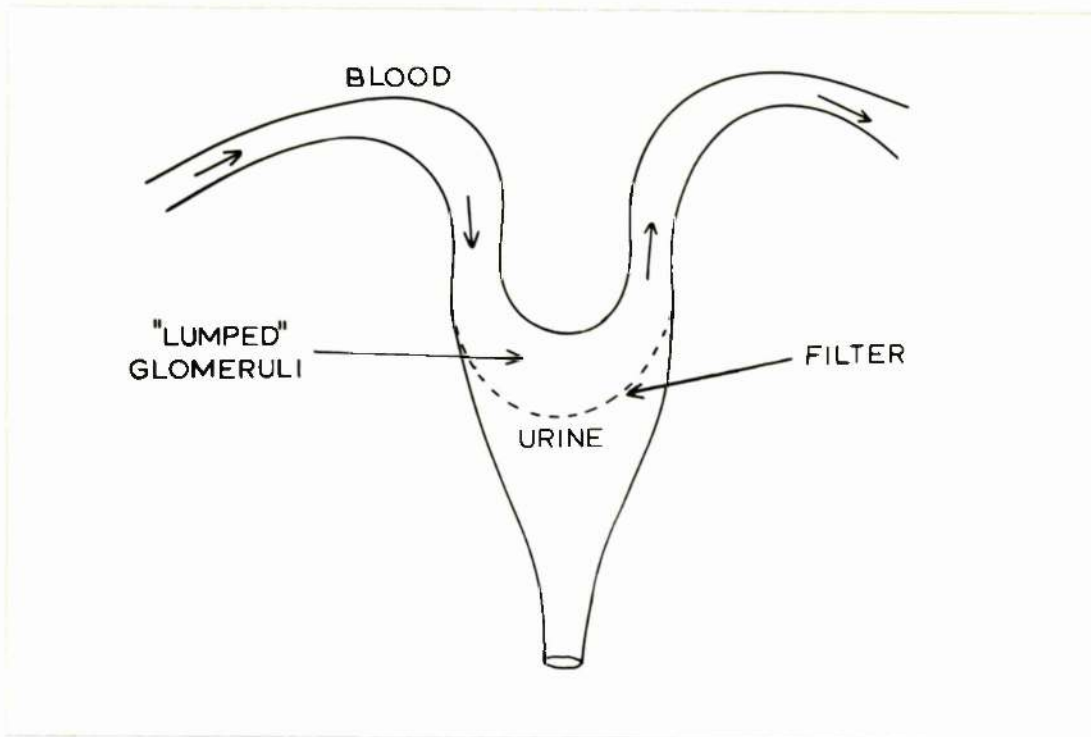


FIGURE 1

Lumped parameter model of the kidney. The glomeruli are represented as a simple filter.

In physiological systems the input and output of the system are in general not defined clearly since the systems are closed. In constructing a model, therefore, of a physiological system one has to decide which variables can be regarded as inputs and which as outputs. Such a decision is based on the intended application of the model and the experimental feasibilities. Thus the same physiological variables may in some circumstances be regarded as an input and in others as an output (see Table 3).

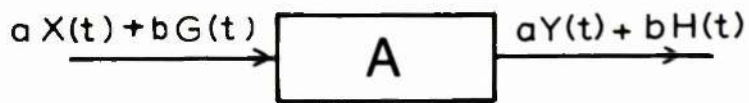
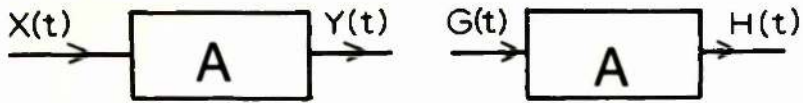
System Under Study	Input Variable	Output Variable
Respiratory gas exchange	Ventilation	Alveolar or arterial partial pressures of oxygen and CO ₂
Respiratory mechanics	Pleural pressure	Ventilation
Respiratory control system	Arterial partial pressures of oxygen and CO ₂	Ventilation

TABLE 3

Certain of the techniques of dynamic modelling are restricted in use to a limited class of systems - those which are regarded as linear and time invariant.

Definition: A linear system is one which obeys the principle of super-position:- the response $y(t)$ of a linear system due to several inputs $x_1(t), x_2(t), \dots, x_n(t)$ acting simultaneously is equal to the sum of the responses of each input acting alone. That is if $y_i(t)$ is the response due to the input $x_i(t)$ then

$$y(t) = \sum_i y_i(t) \quad (\text{see Fig. 2})$$

PRINCIPLE OF SUPERPOSITIONLINEAR SYSTEMFIGURE 2

Diagrammatic representation of the principle of superposition. If an input to a system $X(t)$ induces an output $Y(t)$, and an input $G(t)$ induces an output $H(t)$, then a system is linear if and only if an input $aX(t) + bG(t)$ induces an output $aY(t) + bH(t)$. a & b are arbitrary constants.

Definition; A time invariant system is one in which the observed performance of the system does not depend on the time at which the observation took place.

Physiological systems are often non-linear and time variant, e.g. many biochemical reactions involving enzyme kinetics or saturation phenomena do not satisfy the principle of superposition. In construction of models of physiological systems, however, it is often assumed that the system is linear, i.e. there is IMPLICIT LINEARITY in the model. A typical example of this is the model of peripheral resistance in the vascular system (analogous to Ohm's Law in electric circuit theory).

Linearity should not be assumed but rather the system should be shown experimentally to satisfy the principle of superposition. The experimental proof of superposition involves introducing controlled changes in the input to the system (test signals) (see Fig.3) and observing the subsequent response (see Fig. 4,5).

1.5. FORMULATION OF DYNAMIC MODELS

The variables in a physiological system vary not only with respect to time but also at any instant may have different values at different points within the system (i.e. the independent variables are time and the spatial coordinates). A model of such a system (a DISTRIBUTED PARAMETER MODEL) is described by PARTIAL DIFFERENTIAL EQUATIONS. Distributed parameter models have been used little in physiology. Construction of the partial differential equations of these models is based on the appropriate physical laws and associated equations. (Partial differential equations and their construction is considered in more detail in Appendix 1C).

The mathematical description of the system may be simplified by considering the system as if it consisted of a number of distinct components, at all points within which the variable of interest is considered to be identical at any instant in time. Such a "lumping" process reduces the number of independent variables to one, i.e. time, and leads to what is known as a LUMPED PARAMETER MODEL. Such models are described by systems of ORDINARY DIFFERENTIAL EQUATIONS (O.D.E.) which are an order of magnitude more easily solved than partial differential equations. The distinct components are called COMPARTMENTS. A compartment can thus be defined as an anatomical or conceptual space in which at any instant of time a particular physiological variable is considered to be identical at all points within that space.

In general, therefore, mathematical models of biological systems represent simplifications of reality. Such simplifications have to be chosen carefully since the model must retain the essential features of the system being studied.

Models of physiological systems can be considered at different structural levels. The form of simplification or model reduction depends on which type of model is being considered.

The function of metabolic systems, e.g. albumin, glucose, sodium, potassium etc. is dependent upon a large number of different organ systems. In such models simplification initially takes the form of representing each extremely complex organ system as a single compartment. Even with such "lumping" the model structure is still large. (Fig.6). Further model reduction is based on neglecting those compartments that are thought to have little effect on the system's performance during the time course of the experiment being modelled.

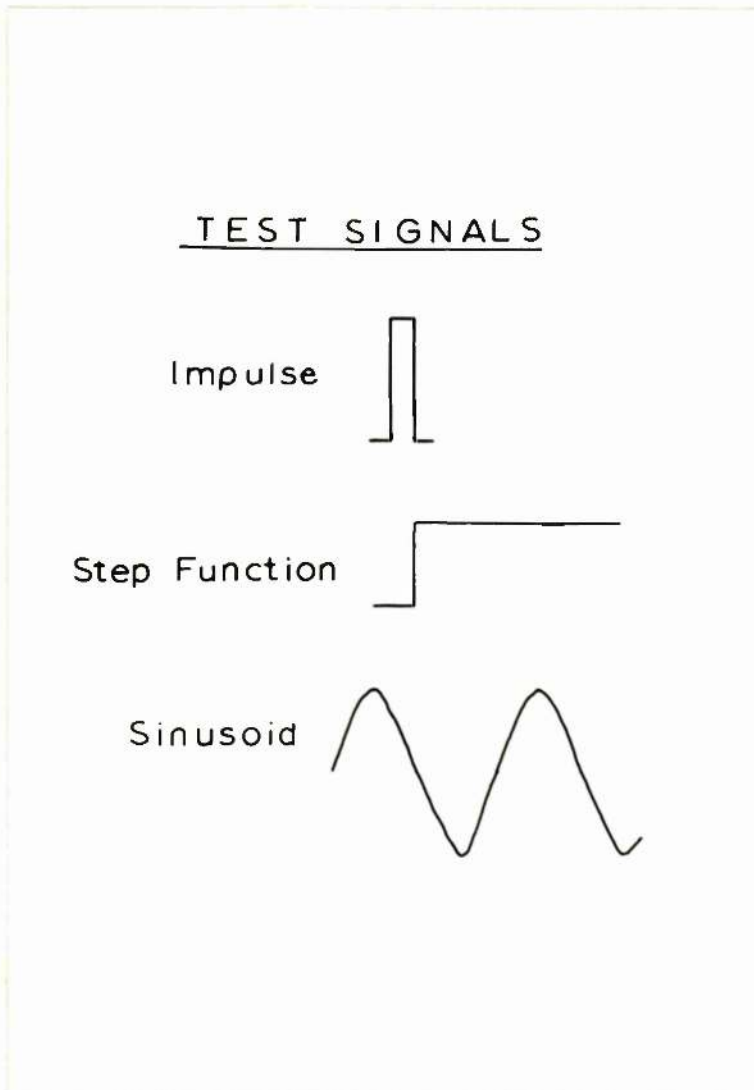


FIGURE 3

Diagrammatic representation of some of the commonly used test signals. The induced time variation in the input follows one of the patterns shown.

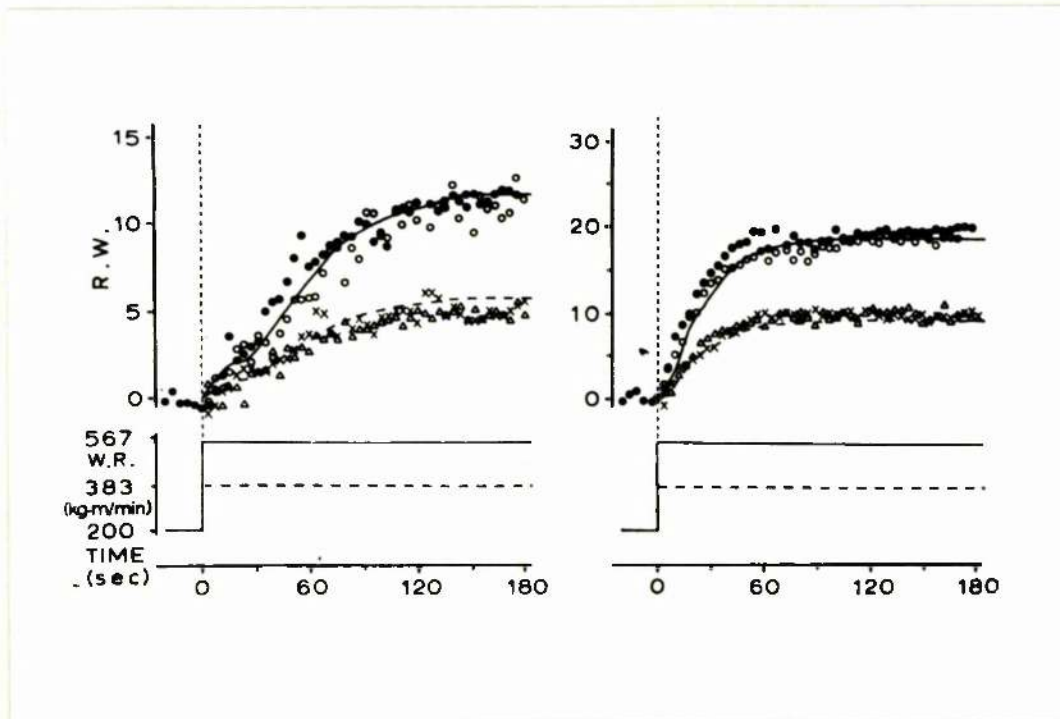


FIGURE 4. a

Responses in ventilation and heart-rate to two different magnitudes of step work load in subject R.W. (from study of Fujihara et al.¹¹) The data at top left of the figure are for change in ventilation (L/min) and on the right for change in heart-rate (beats/min) from initial steady-state values. The step-changes in work load are shown at the bottom of the figure. The continuous and dashed lines through data are the step responses predicted from previously measured responses to impulse stimuli. The system satisfied the principle of superposition. For further details see Fujihara et al.¹¹ (Symbols:- \bullet on-response for large step; \circ off-response for large step; \times on-response for small step; Δ off-response for small step.)

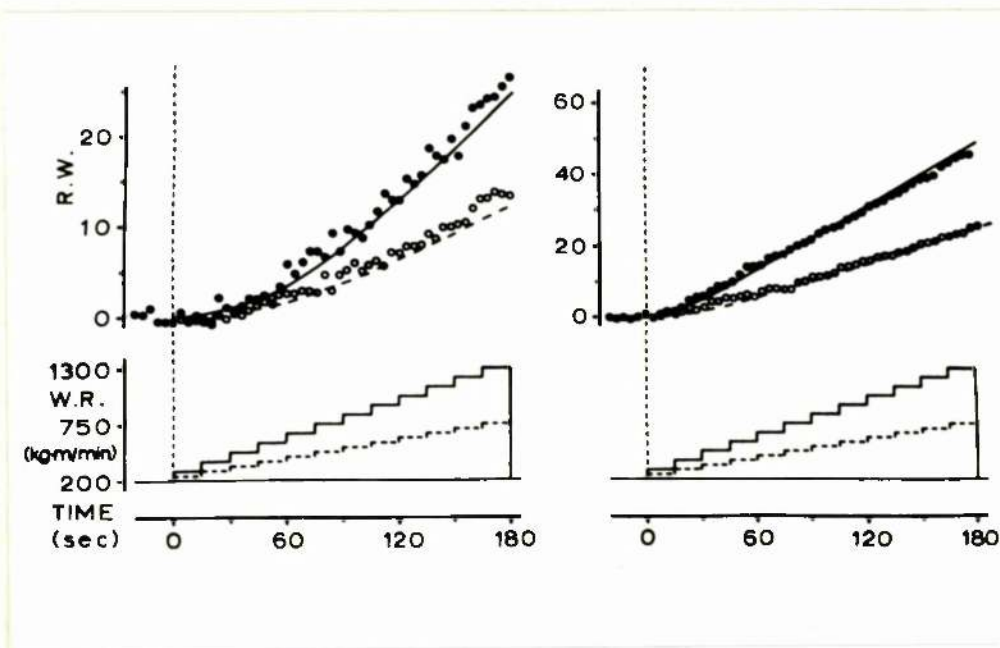


FIGURE 4.b

Similar study to that shown in Figure 4 (from work of Fujihara et al.¹¹) but with response to two different ramp stimuli. (Ramps shown at foot of figure). The data for change in ventilation (L/min) are on the left with change in heart-rate (beats/min) on the right. The lines through the data are ramp responses predicted from measured impulse responses. There is good agreement between measurement and prediction and the principle of superposition is satisfied. (For further details see original publication of Fujihara et al.¹¹)

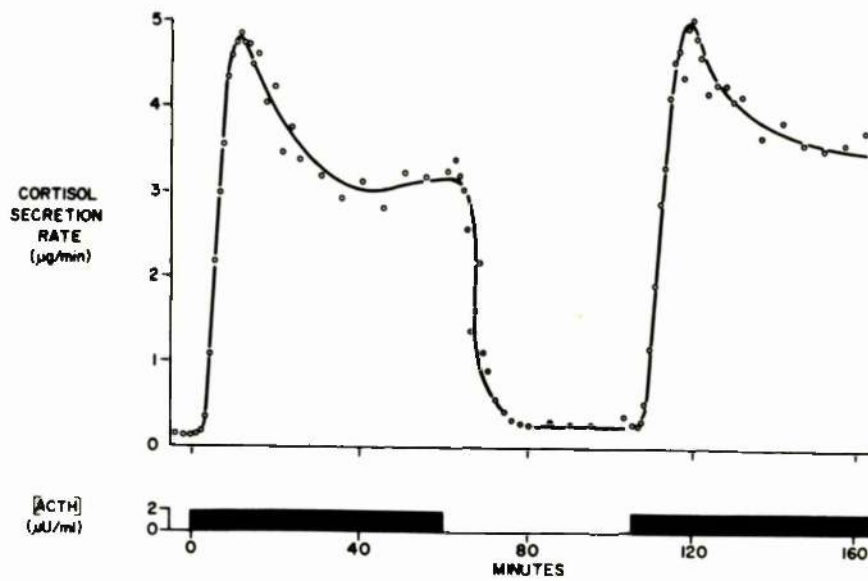


FIGURE 5a

Response of adrenal cortex, as measured in adrenal vein, to a step change in ACTH concentration in adrenal arterial blood. On increasing the ACTH an overshoot in cortisol secretion rate above the final steady-state value is seen. For further details see Li & Urquhart.¹²

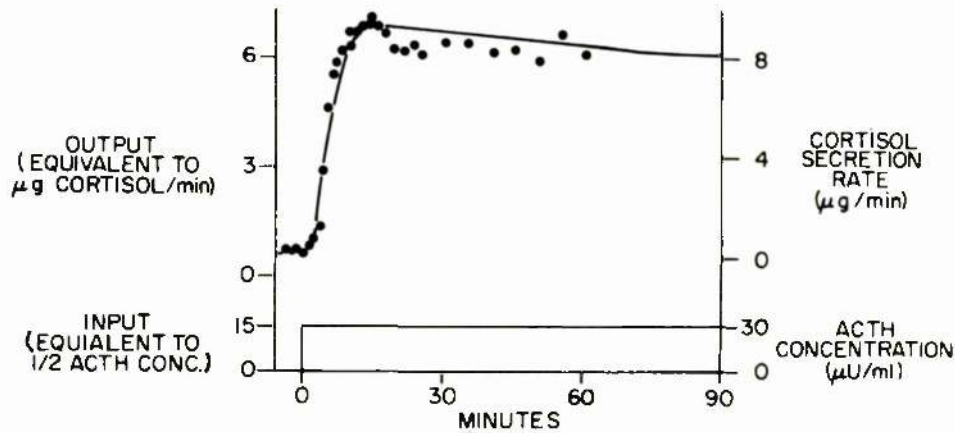


FIGURE 5b

Response of adrenal cortex, as measured in adrenal vein, to much larger step change in ACTH concentration in adrenal arterial blood than that used in experiment, the results of which are demonstrated in Fig.5a. The response does not have the same features, in particular the overshoot is not seen. There is a saturation phenomenon in the performance of the gland. The adrenal cortex is a non-linear system. (For further details see Li & Urquhart.¹²)

If one is interested, however, in studying the function of an individual organ a more detailed model of the system is required. In such a model the organ is considered to consist of a number of components which are often anatomically distinct and have different physiological functions. Such models have been constructed for a large number of different physiological systems such as the cardiovascular system,¹⁴⁻²⁹ respiratory system,³⁰⁻⁴⁹ (excluding here models of gas transport which are considered in detail in Chapter 2), renal system,⁵⁰⁻⁵⁸ metabolic and endocrine systems.⁵⁹⁻⁷⁸ (The references listed are not intended to be an exhaustive list but rather to give the interested reader an introduction to the different subject areas). Models have been used to describe physiological processes at different levels of complexity down to the "unit processes" of biochemistry such as the Krebs cycle and closely related metabolic pathways.⁷⁹⁻⁸³ A special computer language has been developed for the simulation of such complex chemical systems.⁸⁴ In addition to these specific examples there are several more general sources of information related to mathematical modelling of physiological systems.^{4,85-104.}

Once the structure of the lumped parameter model has been decided the equations which describe its performance are derived, usually employing some initial simplifying assumptions. It is seen that in both the stages of formulation of model structure and of derivation of the model equations assumptions are necessitated.

1.6. FORMULATION OF ORDINARY DIFFERENTIAL EQUATIONS

An ordinary differential equation can be regarded simply as an equation containing derivatives. Although a derivative has a precise mathematical definition (see Appendix 1A) a derivative with respect to time represented by the symbol $\frac{d}{dt}$ is in physical terms a rate of change.

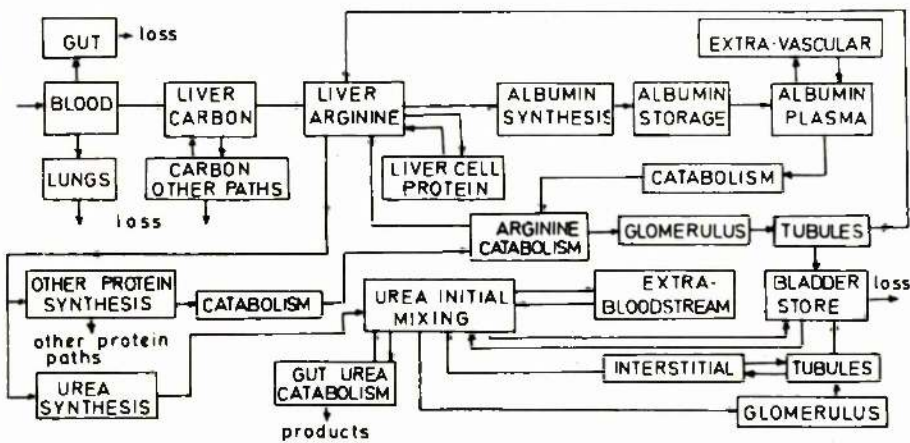


Figure 1 Functional Model of Albumin Metabolism

FIGURE 6

Outline of possible structure for model
of albumin metabolism (From Carson et al¹³).

Ordinary differential equations like dynamic systems are classified into linear and non-linear types, a linear ordinary differential equation being defined as one which is first degree in the dependent variables or their derivatives. Thus the general ordinary linear differential equation, which is illustrated here with the independent variable time (t), has the form

$$\frac{d^n y}{dt^n} + a_1(t) \frac{d^{n-1} y}{dt^{n-1}} + \dots + a_{n-1}(t) y(t) = G(t) \quad (1.1)$$

The input-output relationship of systems described by such equations are linear since the principle of superposition can be shown to be obeyed. There is thus correspondence between the concepts of linearity as applied to systems and to differential equations.

A subclass of the class of linear differential equations are those with constant coefficients. (That is $a_1(t) - a_{n-1}(t)$ in equation 1.1 are replaced with constants $A_1 - A_{n-1}$). Such equations describe linear time-invariant systems. The prominence of this latter class of systems in the theoretical aspects of this subject is not related to their prevalence in real life systems (e.g. most physiological systems are neither linear nor time invariant) but to the fact that linear O.D.E.s with constant coefficients are solved easily mathematically.

In physiological systems the formulation of an ordinary differential equation is often based on mass balance consideration. For example if a compartment X has three inputs of mass ($\dot{I}_1, \dot{I}_2, \dot{I}_3$) and two methods by which mass is lost from X (\dot{O}_1, \dot{O}_2) (See Fig. 7) then the differential equation describing the performance of X is of the form

$$\frac{dM_x}{dt} = \dot{I}_1 + \dot{I}_2 + \dot{I}_3 - \dot{O}_1 - \dot{O}_2 \quad (1.2)$$

where M_x is the mass of the material being studied in X

$\frac{dM_x}{dt}$ is the rate of change of this mass in X

Models of physiological systems may often be formulated using simple principles.

A simple example of this is a differential equation to describe the volume changes in the urinary bladder. Initially we will consider the case when the urethral sphincter is closed. While the urethral sphincter is closed, the volume of urine in the bladder increases as a result of the addition of urine to the bladder from the ureters. Thus the rate of change of the volume of urine in the bladder $\frac{dV}{dt}$ must equal the sum of the flow rates (F_1 and F_2) of urine down each ureter, i.e.:-

$$\frac{dV}{dt} = F_1 + F_2 \quad (1.3)$$

When the urethral sphincter is open there is not only addition of urine to the bladder from the ureters, but also loss of urine down the urethra. As a first approximation we shall assume that the rate of loss of urine down the urethra is directly proportional to the volume of urine in the bladder i.e. the bladder's performance is now described by the equation:-

$$\frac{dV}{dt} = F_1 + F_2 - kV \quad (1.4)$$

Rate of change of volume	=	Addition from ureters	+	Addition from ureters	-	Loss down urethra	(1.4)
-----------------------------	---	--------------------------	---	--------------------------	---	----------------------	-------

(K is constant of proportionality and is positive)

The model could be made more realistic by using a more sophisticated expression for the rate of flow down the urethra which took account of the probable non-linear relationship between the flow rate and bladder volume, and the degree of abdominal musculature activity. In the absence of more precise information this could be modelled

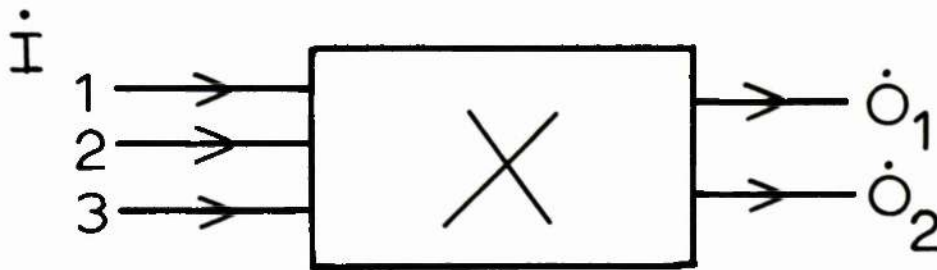


FIGURE 7

Diagrammatic representation of a single compartment (X) with three inputs of mass ($\dot{I}_1, \dot{I}_2, \dot{I}_3$) and two methods by which mass is lost (\dot{O}_1, \dot{O}_2).

at present as an arbitrary function G , when G is a function of volume of urine in the bladder (V), urethral sphincter tone (T), and abdominal musculature activity (M), i.e.:-

$$\frac{dV}{dt} = F_1 + F_2 - G(V,T,M) \quad (1.5)$$

The form of G could only be ascertained by experiment.

If the urethral sphincter remains open (e.g. with a catheter in situ) a steady state will eventually be reached in which the volume of the bladder will be constant as the flow into the bladder is balanced exactly by the flow out. In the steady-state condition there is no change in bladder volume and hence $\frac{dV}{dt}$ is zero. Thus equation (1.4) would simplify to

$$V = \frac{F_1 + F_2}{K} \quad (1.6)$$

It is thus seen as indicated earlier that steady state conditions are described by algebraic equations.

In many circumstances derivation of differential equations is not as simple as the example used would tend to indicate. In such cases the derivation of the differential equation is achieved using the precise mathematical definition of a derivative. (For an illustrative example see Appendix 1B).

Although in general physiological systems are described by non-linear equations, they may often be approximated over a limited range of operation by linear equations. Such linearisation of non-linear equations is e.g. employed in the construction of the differential equations in radioisotope tracer studies. (The linearisation process is presented mathematically in Appendix 1D). Such linearisation is important practically since it converts equations which can only be solved by computer methods to those in which one is able to write down in mathematical terms the exact solution.

1.7. CONSTRUCTION OF BLOCK DIAGRAM

When the complete set of equations describing the system has been established it is possible to express the information contained in the equations in the form of a block diagram. The block diagram is built up from the separate equations describing the system. For example in the bladder example the information contained in equation (1.3) could be represented in block diagram form as in Fig. 8. The diagram can easily be extended to represent equation (1.4) (Fig.9).

Since integration is the mathematical operation which is the inverse of differentiation, by integrating $\frac{dV}{dt}$ with respect to the variable t we obtain the variable V . The operation of integration is represented by a block of type shown in Fig. 10A. Multiplication by a constant is also easily represented (Fig. 10B) and these additional blocks can be combined with the summing element to close the loop and produce a block diagram which contains all the information expressed in the separate equations (Fig. 11).

1.8. SOLUTION OF ORDINARY DIFFERENTIAL EQUATIONS

The solution of an ordinary differential equation, when the independent variable is time, is a function of time. Although mathematical methods, (analytical methods) exist for the determination of the exact nature of this function such methods can be applied only to a restricted class of equations. Linear equations with constant coefficients can always be solved by mathematical means as can some types of linear time-variant or non-linear equations.

The exact solution of a differential equation depends on the state of the system at zero time, i.e. on the INITIAL CONDITIONS.

Of the methods available for analytical solution of O.D.E.s the LAPLACE TRANSFORM method is the most convenient.

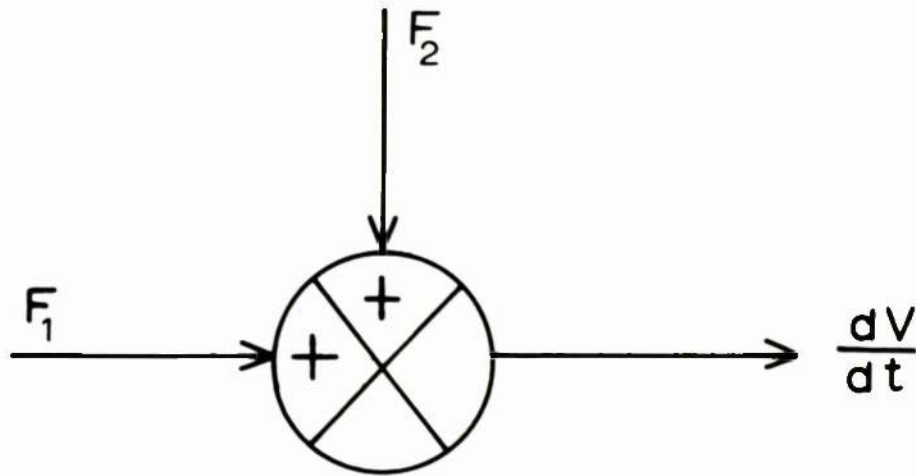


FIGURE 8

Block diagram representing equation 1.3.

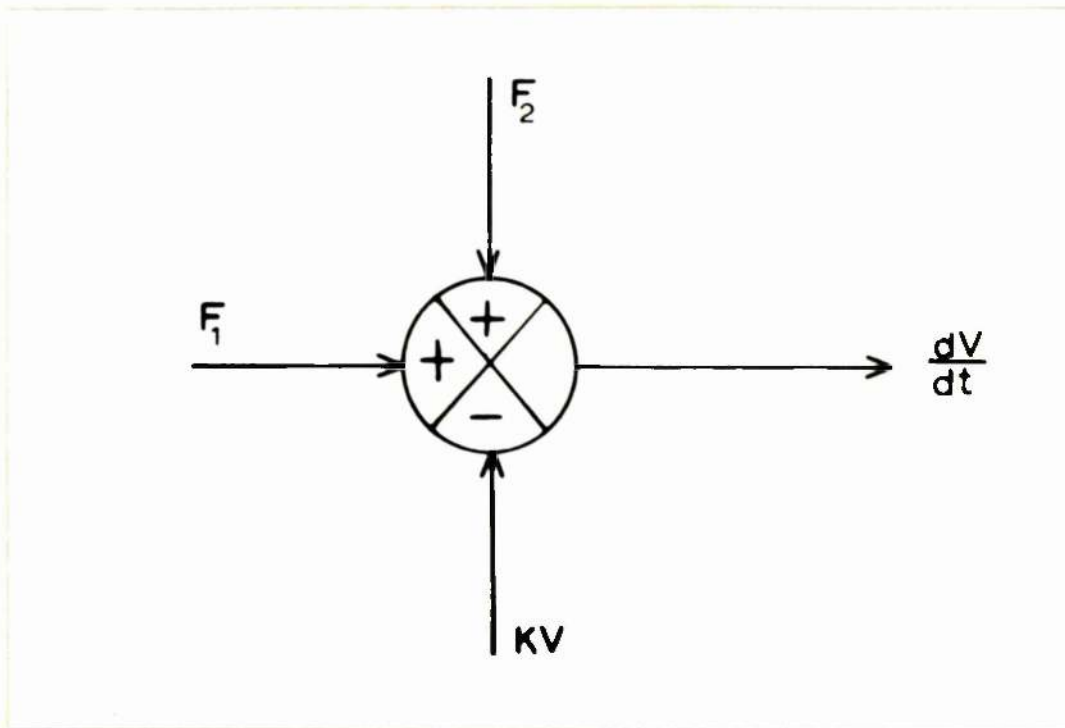


FIGURE 9

Block diagram representing equation 1.4.

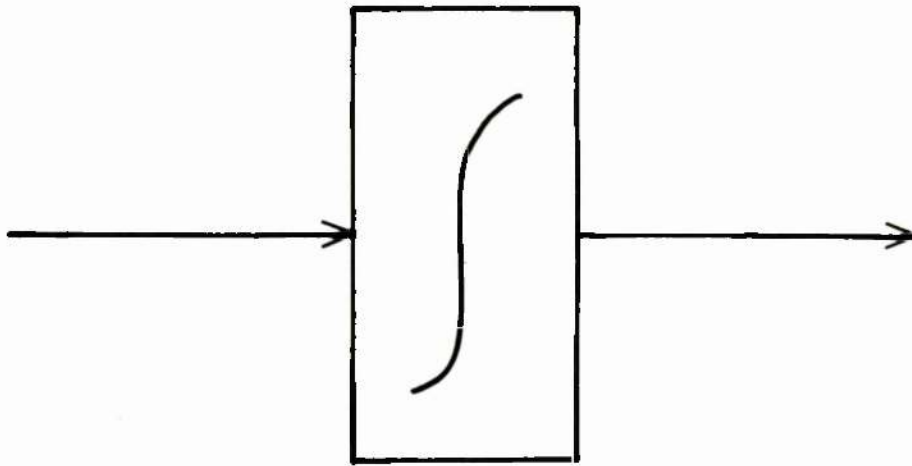


FIGURE 10a

Block diagram representation
for integration with respect
to time.

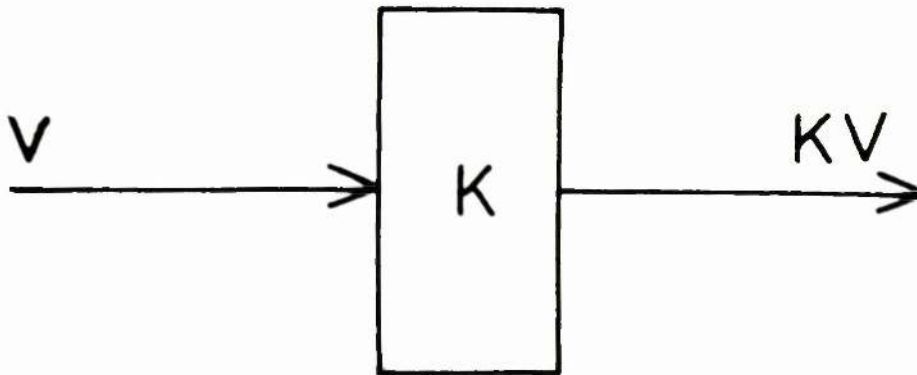


FIGURE 10b

Block diagram representation for
multiplication by a constant (K).

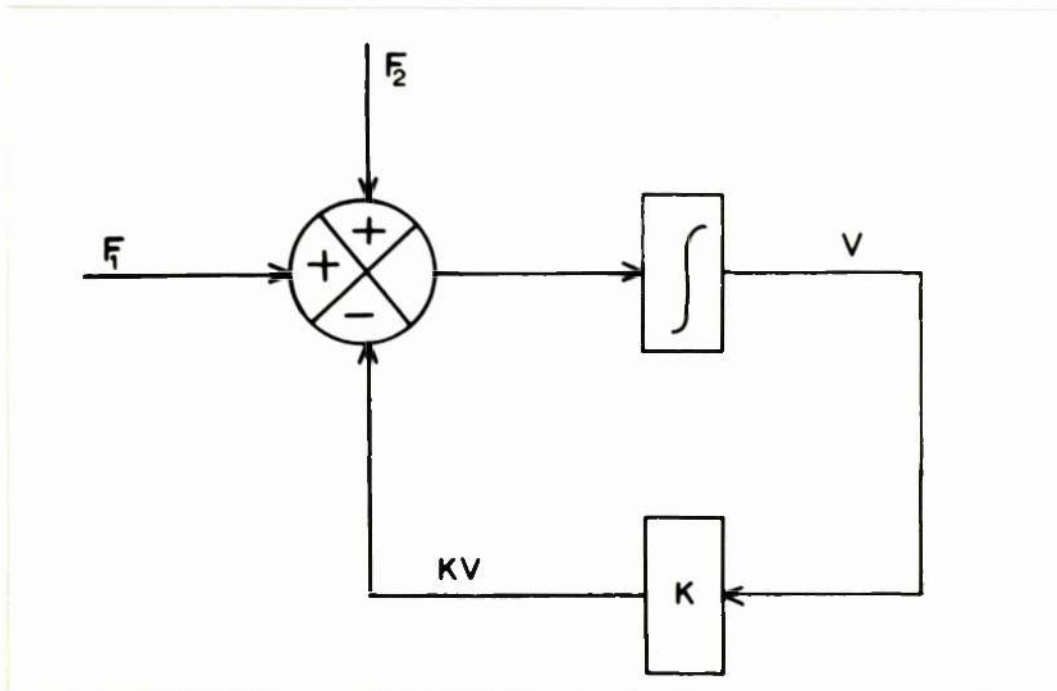


FIGURE 11

In Laplace transformation functions are converted from functions of time to functions of a new variable S (complex frequency) using the conversion formula that given $f(t)$ its Laplace Transform $F(s)$ is

$$f(t) \xrightarrow{\text{LT}} \int_0^{\infty} e^{-st} f(t) dt = F(s)$$

The particular property of the Laplace Transform which is of value in this application is that the Laplace Transform of a derivative $\frac{df}{dt}$ is given by

$$\frac{df}{dt} \xrightarrow{\text{LT}} S F(s) - f(0)$$

It is seen that the initial condition $f(0)$ (the value of the function f at time $t = 0$) appears explicitly in the transform.

Applying this transformation to an O.D.E. allows the solution as a function of s to be obtained easily using the simple rules of algebra. The solution of the equation as a function of time is then found by using the reverse process to Laplace Transformation - the INVERSE LAPLACE TRANSFORM for which several methods exist. Thus for example applying this method to equation (1.4)

$$\frac{dv}{dt} = F_1 + F_2 - kv \quad (1.4)$$

where F_1 and F_2 were constants

$$\begin{aligned} \frac{dv}{dt} &\xrightarrow{\text{LT}} sV(s) - v(0) \\ F_1 &\xrightarrow{\text{LT}} F_1/s \\ F_2 &\xrightarrow{\text{LT}} F_2/s \\ -kv &\xrightarrow{\text{LT}} -kV(s) \end{aligned}$$

i.e. $sV(s) - v(0) = F_1/S + F_2/S - kV(s)$

which becomes

$$V(s) = \frac{F_1 + F_2}{ks} - \frac{(F_1 + F_2)}{k(s+k)} + \frac{v(0)}{(s+k)}$$

and on taking the Inverse Laplace Transform we obtain:-

$$v(t) = \frac{F_1 + F_2}{k} - \frac{F_1 + F_2}{k} e^{-kt} + v(0)e^{-kt} \quad (1.7)$$

The solution contains the exponential function e^{-kt} . Exponential functions arise commonly in the solution of this class of differential equations.

In physical terms the solution of the equation allows us to predict the volume of urine in the bladder at any time t from an arbitrary starting point (when the volume is $v(0)$).

1.9. SIMULATION

In many physiological models, however, analytical methods are not applicable and one has to have recourse to computer based methods of solution.

a) Analogue Computation

For dynamic models the electronic analogue computer is suitable. This differs from the digital computer in that numbers are represented in an analogue machine by a voltage. While the digital computer performs its calculations in a step by step fashion the analogue computer operates in terms of continuous variables and is, therefore, more effective for most types of simulation.

Programming an analogue computer is easy in principle since its operational units (see Table 4) correspond to the elements of a block diagram. One of the operational units is an integrator, which provides the mathematical operation of integration and makes the analogue computer suited to the solution of ordinary differential equations. The interconnections which are required to be made between the units of the computer to obtain a solution of the equations forming the model are represented in a "patch diagram".

COMPONENT	STANDARD SYMBOL	FUNCTION
Potentiometer	<div style="display: flex; justify-content: space-between;"> <div style="text-align: center;"> <u>INPUTS</u> X </div> <div style="text-align: center;">  </div> <div style="text-align: center;"> <u>OUTPUTS</u> $Y = K X$ </div> </div>	Multiplication by a constant
Amplifier	<div style="display: flex; justify-content: space-between;"> <div style="text-align: center;"> X, Z </div> <div style="text-align: center;">  </div> <div style="text-align: center;"> $Y = -(X + Z)$ </div> </div>	Addition, subtraction of variables, or negation of variable
Multiplier	<div style="display: flex; justify-content: space-between;"> <div style="text-align: center;"> X, Z </div> <div style="text-align: center;">  </div> <div style="text-align: center;"> $Y = -(X * Z)$ </div> </div>	Multiplication of variables
Integrator	<div style="display: flex; justify-content: space-between;"> <div style="text-align: center;"> X </div> <div style="text-align: center;">  </div> <div style="text-align: center;"> $Y = - \int X dt$ </div> </div>	Integration of variable with respect to time

TABLE 4

Main components of analogue computer

This diagram will correspond to the block diagram of the system model. There is thus a very direct and useful relationship between the operational units in the analogue simulation and the structure of the model. Most machines of this type have, however, limited facilities for the accurate generation of complex time varying functions and pure time delays.

The deficiencies of the analogue computer can be overcome by using a hybrid computer.¹⁰⁵ The digital computer part of the hybrid system can be utilised for function generation and the simulation of time delays. Analogue computation is considered in greater detail in Appendix 2.

b) Digital Simulation.

Digital computer solution of ordinary differential equations is implemented generally using a mathematical (numerical) technique for integration. A number of these techniques exist¹⁰⁶ and the physiological modeller has the choice of constructing his own programme to implement the method or using a standard software package available on a central computer library.

Particularly useful software packages are high level simulation languages, e.g. C.S.M.P. (continuous system modelling programme).¹⁰⁷ In these languages the programme statements represent the various steps which are required for solution of the model equations, i.e. each statement corresponds to an element in the block diagram (see Appendix 3).

1.10. "BLACK-BOX" MODELS

In certain applications a model of the detailed structure of each component of the system may not be required but rather a mathematical description of its overall performance, i.e. the

relationship between system input and system output.

A commonly used method of describing this relationship is the TRANSFER FUNCTION. This function of the Laplace variable s ($G(s)$) relates system input to system output by the formula

$$\text{TRANSFER FUNCTION } G(s) = \frac{\text{L.T. of system output}}{\text{L.T. of system input}} = \frac{Y(s)}{X(s)}$$

if the initial conditions in the system are zero. One method of obtaining the transfer function is by measurement of the system output after introduction of a standard input into the system whose Laplace transform is known (e.g. impulse, step, or ramp function). Transfer functions can only be obtained for linear time-invariant systems, and this concept has had limited application in physiology (for examples see references 108, 109). It can prove useful in obtaining knowledge of the effect of dynamics of measuring systems on data which have been obtained experimentally.^{110,111}

1.11. PARAMETER ESTIMATION

The performance of any of the types of mathematical models, which have been described, depends upon the numerical values of the constants in the model equations. Such constants or PARAMETERS represent properties of the physiological system being studied.

At its simplest level, if a model is being used in simulation studies, such constants may be assigned appropriate physiological values. Most physiological modelling is of this type.

In applying models to measurement, however, use can be made of the techniques of PARAMETER ESTIMATION.^{112,113,114} In one approach to the experimental evaluation of model parameters (the

so-called model reference approach) the model and system are subjected to the same input and their outputs are compared directly at each instant of time (Fig.12). The discrepancy between the output of the model and the measured output of the system can be expressed as an error function. Minimisation of this error function by appropriate adjustment of model parameters may yield measures of the corresponding physiological quantities.

1.12. VALIDATION OF THE MODEL

The validity of the proposed model and the circumstances in which it can be applied are established by comparing sets of values MEASURED in the real system with values PREDICTED by the model. With dynamic models one uses several forms of test input to cause the system to respond dynamically. Ideally not only should the model and system performance be seen to be in reasonable agreement, but also the estimated parameters of the model should agree with independently made direct measurements of these physiological properties. In many physiological systems this type of validation is not possible since parameter estimation may be the only feasible method of measurement. In such circumstances one should confirm that the same parameter estimates are obtained with different test inputs.

The modelling process as outlined in this chapter is summarised in Figure 13.

1.13. APPLICATIONS OF MATHEMATICAL MODELS

When a model has been constructed and verified experimentally it can be utilised in a number of important ways.

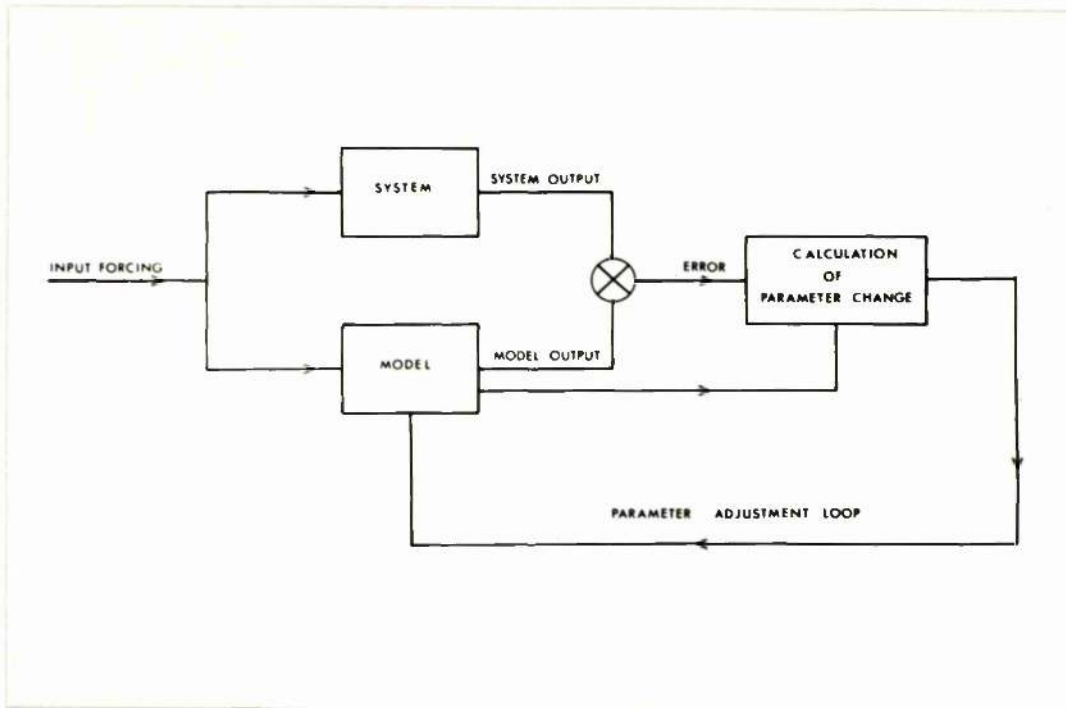


FIGURE 12

Schematic diagram representing the model reference approach to parameter estimation.

1.13. a) Indirect Measurement of Physiological Variables.

The numerical values of the constants which appear in the equations of many of the models of physiological systems are often inaccessible to direct measurement. Techniques for estimation of the parameters of a model may provide, therefore, an indirect method of measurement of physiological quantities.

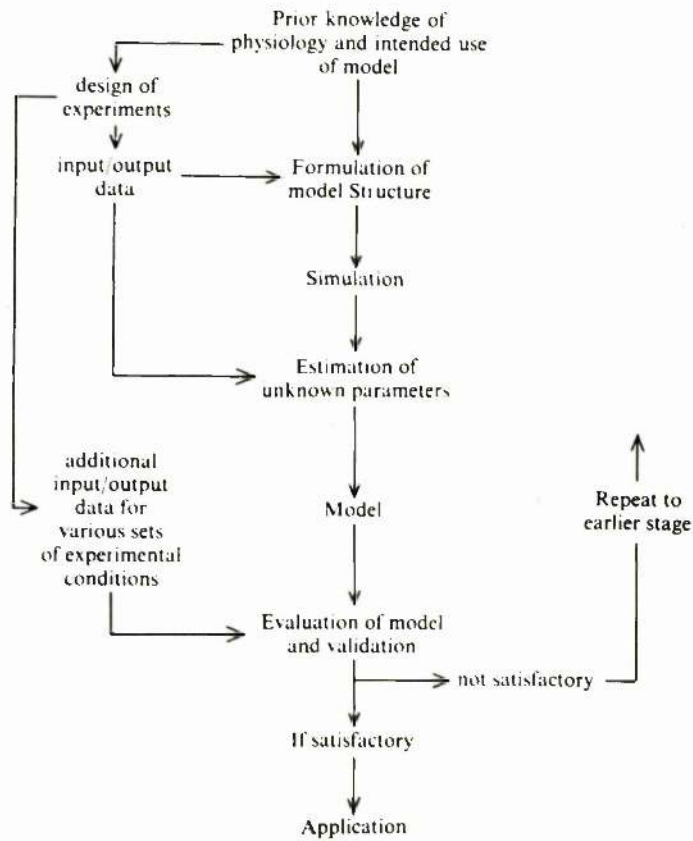
In certain cases parameter estimation by graphical means is possible. This is used particularly in the mathematical models which are the basis of many of the tests in which radio-isotopes are used.

In use of more complex dynamic models simple graphical techniques are not appropriate and computer based methods have to be applied. The application of these methods to models of respiratory gas exchange is considered in this thesis.

b) Hypothesis Testing/Experimental Design.

A hypothesis can be regarded as an "intuitive model" which is generally presented in non-quantitative terms. By converting a hypothesis to the equivalent mathematical model, the experimenter can examine the hypothesis in more detail than is possible without recourse to mathematical description (see Fig. 14a). A critical examination using a mathematical model and the experimental findings together may provide support for the hypothesis or lead to its rejection or modification. Rejection of the hypothesis may lead to the proposal of a new hypothesis or to improvement of the model.

Figure 14b represents the inverse situation in which the hypothesis arises from observation made on the model. The model is thus being used in a predictive fashion and new experiments must be developed to provide the essential supporting evidence.



Flow-chart of modelling process

FIGURE 13

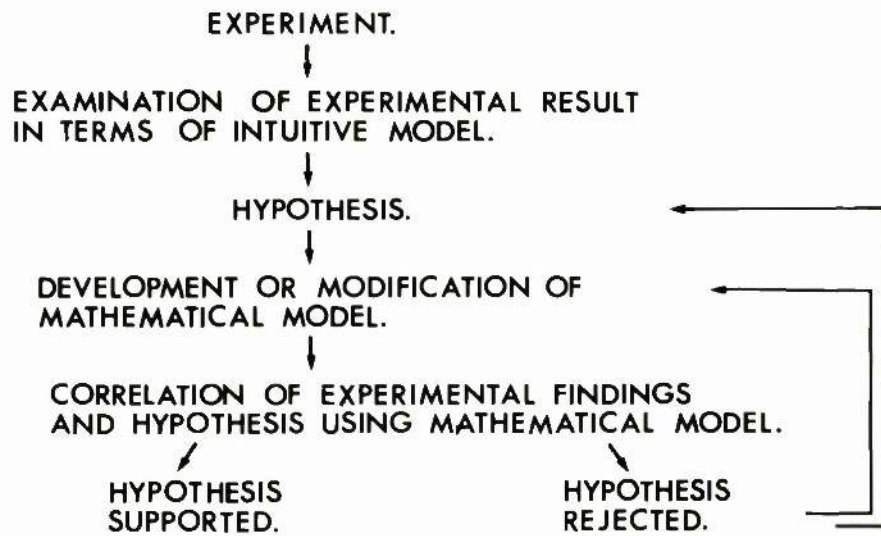


FIGURE 14a

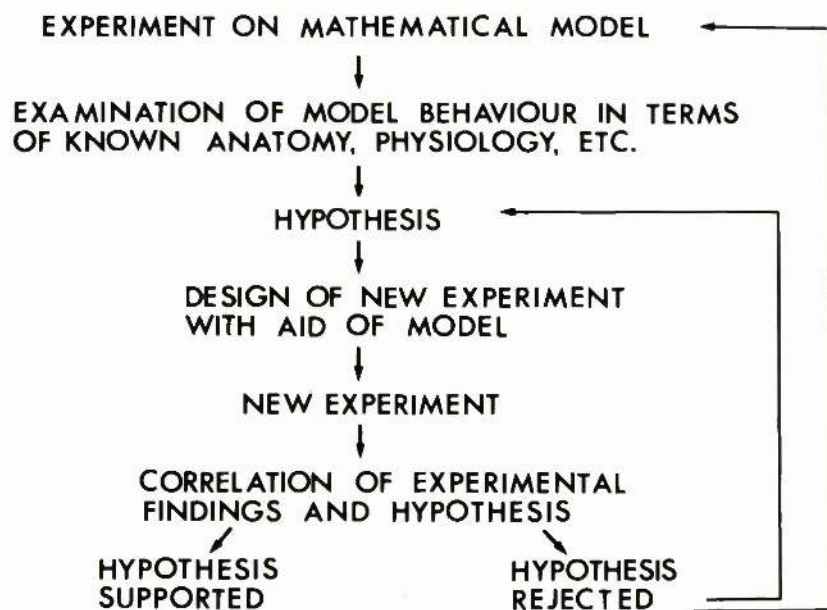


FIGURE 14b

The optimal design of experiment for testing a particular hypothesis may be determined by simulating a number of possible experiments in a system model.

c) Educational Role.

Physiological systems are usually both complex and dynamic; the function of any individual component in the total system may be affected by changes in the others. It is often difficult for the student to understand the overall effect of a change in a single variable. Models of physiological systems can, therefore, be used as an educational aid. Implementation of a model of respiratory gas exchange for this purpose is described in Appendix 4.

CHAPTER 2

MATHEMATICAL MODELS OF RESPIRATORY GAS TRANSPORT.

CHAPTER 2. MATHEMATICAL MODELS OF GAS TRANSPORT

2.1. INTRODUCTION.

There are several different approaches to the construction of mathematical models of gas transport. These approaches can be categorised by the method which is used for mathematical description of ventilation (\dot{V}). Ventilation is a continuous time varying process which contains irregularities due to voluntary effects as well as some small recurring changes in rate and depth.¹¹⁵

Methods vary from those in which time averaged ventilation is used in algebraic equations, to those in which the precise form of ventilation is used in the numerical solution of ordinary or partial differential equations.

The different approaches to construction of models of respiratory gas transport are considered in this chapter and summarised in Table 2.1.

<u>Description of Ventilation</u>	<u>Type of Equation</u>	<u>Method of Solution of Model Equations.</u>
Time-averaged ventilation.	Algebraic equation. Steady-state model.	Algebraic manipulation.
Breath-by-breath tidal volume.	Difference equations.	Algebraic manipulation.
Constant unidirectional flow rate.	Ordinary differential equation.	Analytic solution.
Instantaneous inspiration/expiration with inspiratory & expiratory breath-holds.	Ordinary differential equation.	Analytic solution.
Continuous time-varying \dot{V} .	Ordinary differential equation.	No general analytic solution possible. *
Continuous time-varying \dot{V} & considering events spatially within the lung.	Partial differential equation.	Numerical methods. *

* Computer based methods of solution.

TABLE 2.1.

2.2. BASIC UNITS.

a) Prior to study of the mathematical descriptions of alveolar-capillary gas exchange, familiarity with the standard units and symbols is essential. In the early days of respiratory physiology there was a lack of agreement on appropriate symbols, which adds to the difficulty in understanding the early papers on this subject. This problem was remedied at the 1950 Atlantic City Convention (Pappenheimer, 1950)¹¹⁶ when a standard system of units and symbols was introduced (Table 2.2.).

QUANTITY	SYMBOL	UNITS
Partial pressure	P	mm.Hg. or kilopascal (kPa)
Volume of gas	V	Litre
Fractional concentration	F	Dimensionless
Volume flow rate	\dot{V}	Litre/min.
Concentration of gas species in liquid	C	ml. of gas at STPD/100 ml. of liquid
Solubility in blood	α	Vol. of gas at STPD/Vol. of liquid/Atmosphere of pressure.
<u>SUBSCRIPTS</u>		
UPPER CASE LETTERS (For gas phase)		LOWER CASE LETTERS (For blood phase)
I	Inspired	a Arterial
E	Expired	\bar{v} Mixed venous
A	Alveolar	

TABLE 2.2.

Summary of symbols agreed at Atlantic
City Convention, 1950.¹¹⁶

The equations of alveolar-capillary gas exchange are concerned with the transport of gaseous mass either by convection or diffusion or a combination of both. In the 1950 system amount of gas is represented by a volume expressed at a set condition of temperature, pressure. It has been suggested more recently¹¹⁷ that amount of gas should be expressed in moles and concentration in moles/litre. Although this new system of units is as yet not universally accepted it is probable that it will replace the 1950 system of units. The new system of units is detailed in Table 2.3, and compared with the 1950 system. Since these conventions do not cover all symbols used in this thesis, all symbols are listed for completeness in Appendix 5.

b) Gas Phase:

In the gas phase, concentration in the 1950 system of units is expressed as a fractional concentration F (volume of gas species under consideration/volume of gas medium). The conversion of a fractional concentration to a partial pressure is a simple matter of proportionality as described by Dalton's law. Thus if the fractional concentration of a gas species x is F_x , the total pressure P , the partial pressure exerted by this gas (P_x) is

$$P_x = F_x \cdot P$$

In the new system of units in which amount of a gas is expressed as moles and concentration as moles/litre, the relationship between concentration and partial pressure is defined by the introduction of a capacitance coefficient β which is defined as the increment of concentration (ΔC) per increment of partial pressure (ΔP);

$$\text{i.e. } \beta = \Delta C / \Delta P$$

TABLE 2.3. Comparison of units and symbols as formulated at the Atlantic City Convention, 1950¹¹⁶ and the proposed new system.¹¹⁷ Modified from Piiper et al.¹¹⁷

QUANTITY	ATLANTIC CITY	"NEW" SYSTEM
Amount of gas species.	V, volume (gas)	M, quantity of substance (moles)
Volume of gas species.	V, volume (gas)	V, volume
Transfer rate of gas species.	\dot{V} , volume/time	\dot{M} , quantity/time
Volume flow rate.	\dot{V} , volume/time	\dot{V} , volume/time
Fractional concentration.	F, volume/volume	F, volume/volume
Concentration of gas species in gas phase	-	C, quantity of substance/volume
Concentration of gas species in liquid	$C \frac{\text{volume (gas)}}{\text{volume (liquid)}}$	C, quantity of substance/volume
Solubility in liquid	$\alpha \frac{\text{volume (gas)}}{\text{vol. (liq.) pressure}}$	$\frac{\text{quantity of substance}}{\text{volume (liquid) pressure}}$
Capacitance coefficients		β
blood		β_b $\frac{\text{quantity of substance}}{\text{volume pressure}}$
water		β_w
gas		β_g
Conductance	-	G $\frac{\text{quantity of substance}}{\text{time pressure}}$

β has the units of (moles) (litre)⁻¹ (pressure)⁻¹. The concept can equally be applied if the medium is gaseous or liquid. In the gas phase β will be identical for all ideal gases since from the ideal gas law

$$PV = MRT$$

where P is pressure, V volume, M quantity of substance, R the gas constant, and T absolute temperature;

$$\text{i.e.} \quad \Delta p = \frac{\Delta M}{V} RT$$

$$\text{or} \quad \frac{\Delta C}{\Delta P} = \frac{1}{RT}$$

$$\text{i.e.} \quad \beta = \frac{1}{RT} \text{ for all ideal gases}$$

c) Liquid Phase:

In considering the carriage of gas in a liquid, respiratory physiologists utilise frequently the concept of tension where tension of any gas (x) in a liquid is defined as that partial pressure of x in a gas mixture which if exposed to the liquid would not result in any net exchange of the gas (x). Thus if a gas and liquid mixture are equilibrated the partial pressures of the component are considered identical in the gas and liquid media. The tension of gas in a liquid thus defined is related to concentration. For gases which simply dissolve in the liquid media, this relationship is linear.

In the 1950 system of units, quantity of gas in the liquid is expressed as a volume at STPD and the linear relationship is described by the Bunsen solubility coefficient* (volume of gas at STPD/unit volume of solvent/atmosphere of pressure).

* An alternative coefficient which is used occasionally is the Ostwald coefficient in which the value of gas dissolved is not expressed at STPD but at the conditions of temperature and pressure at which solution took place.

Alternatively if the quantity is expressed in moles then the relationship is described by the capacitance coefficient.

For the two important respiratory gases oxygen and carbon dioxide which combine chemically with blood there is not a simple linear relationship between tension and concentration in blood. The non-linearity of this relationship leads to certain biological advantages but complicates the understanding and mathematical analysis of respiratory gas exchange.

2.3. STEADY-STATE MODELS.

a) Introduction.

In the construction of steady-state mathematical models single values are assigned to expired, alveolar, arterial, and venous partial pressures, tidal volume and minute ventilation. Such models neglect, therefore, any temporal variation in respiratory gas exchange and describe the time-averaged performance of the system. In performing tests which are based on these models some variables are measured continuously and averaged, whereas others are sampled at variable time intervals. The use of such models can, therefore, in theory lead to significant inaccuracies although this problem has been little studied. Nevertheless despite these obvious limitations tests based on steady-state models are used widely.

b) Basic Equations.

The equations of alveolar-capillary gas exchange are all based on the principle of conservation of mass. Thus in considering the transfer of a gas x from the atmosphere to the lung -

$$\dot{M}_x = \dot{V}_I C_{I,x} - \dot{V}_E C_{E,x} \quad (2.1)$$

(moles/unit Amount Amount
time) inspired expired

(All equations are expressed where appropriate in the new system of units.)

In general $\dot{V}_I \neq \dot{V}_E$ because during normal breathing more oxygen is taken up per minute than carbon dioxide produced.

A similar expression as (2.1) describes the transfer of gas between the lung gas and blood:-

$$\dot{M}_x = \dot{Q} (C_{a,x} - C_{\bar{v},x}) \quad (2.2)$$

The equating of equations (2.1) and 2.2) form the basis of the Fick method of measurement of cardiac output.¹¹⁸

In the practical applications of these equations expired ventilation (\dot{V}_E) is measured generally by collection of the expired gas for a known period. Although inspired ventilation could be measured directly it has been standard practice to calculate inspired ventilation from the measured expired ventilation and measured inspired and expired concentrations of nitrogen, using the assumption that in steady-state conditions there is no net transfer of gaseous nitrogen between the lung and atmosphere.

$$\text{i.e. } \dot{V}_I C_{I,N_2} = \dot{V}_E C_{E,N_2} \quad (2.3)$$

$$\text{or } \dot{V}_I = \frac{C_{E,N_2}}{C_{I,N_2}} \dot{V}_E \quad (2.4)$$

(This relationship is known as the Haldane transformation and its validity is considered in the next section.)

c) Steady-State Equality of Respiratory Gaseous Nitrogen Transport.

The assumption that the volume of nitrogen inspired per minute is equal to the volume expired was based originally on the view that gaseous nitrogen was not involved in metabolic processes but was merely a diluent of atmospheric gas. (For history of early work in this area see Dudka et al.¹¹⁹)

The conventional view was challenged by Costa¹²⁰ who proposed that gaseous nitrogen represented an excretory pathway at the end stage of amino-acid metabolism, and found¹²¹ in support

of this assertion that a measured positive nitrogen balance could occur without commensurate gain in body weight.

This work stimulated direct measurement of respiratory nitrogen exchange, in particular by the group in the Human Environment Research Unit, University of Illinois, who demonstrated a small uptake of nitrogen in fasting subjects (mean of 0.027 L/min),¹¹⁹ significant excretion of nitrogen following a protein meal (of the order of 0.1 L/min)¹²² and higher outputs of nitrogen during mild exercise (average 0.217 L/min).¹²³ The magnitude of the nitrogen exchange is such that significant errors would result from use of the Haldane transformation¹²⁴ and led these workers to propose methods to obviate this difficulty.¹²⁵

The size of the measured nitrogen exchange is surprising and approaches in certain conditions the same magnitude as the volume of carbon dioxide excreted. The evidence is moreover conflicting, other workers having demonstrated nitrogen excretion in resting fasting subjects.^{121, 126} There is a large individual variability in the results. The literature has been reviewed by Fox and Bowers¹²⁷ who showed that of the 101 determinations of nitrogen exchange which have been reported in resting fasting man, 44 indicate nitrogen retention and 57 nitrogen production.

The reported results could be due to measurement errors associated with measuring a small difference between large volumes, as was suggested by Herron et al.¹²⁸ The magnitude of the "measured" nitrogen exchange would thus be expected to be higher if the volumes were larger, e.g. during exercise, as is indeed the case. The effect of measurement errors is minimised by reducing the volume fraction of nitrogen in the inspired gas mixture. In an elaborate series of experiments in which subjects breathed a gas

mixture containing 0.15% N_2 for 2.5 - 12 hours the measured nitrogen exchange ranged from -0.003 to +0.008 L/min.¹²⁸ It is thus highly unlikely that the magnitude of the true exchange of gaseous nitrogen is such that significant errors result from use of the Haldane transformation.^{128, 129}

d) Functional Compartments in the Lung.

Equations (2.1) and (2.2) describe the transfer of a gas species (x) between lung gas and atmospheric gas, and lung gas and pulmonary capillary blood respectively. If the pulmonary component of this model is to be considered in more detail it is necessary to study the basic structure of the lung.

As a first approximation the lung can be thought to consist of two types of structure:-

- (1) Conducting airways. A "non-reacting" dead space.
- (2) Alveoli

and a possible "lumped" model structure is illustrated in Fig.2.1. Although this model seems initially a simplification of reality which is too gross to be of value, one can distinguish readily in measured expired concentration data, dead space and alveolar components. Even with such a simplified model structure additional assumptions are necessary to allow formulation of equations, viz.:-

- a) gas flow takes place down the airways with a flat velocity profile, i.e. "plug-flow".
- b) volume change is restricted to the alveolar compartment.
- c) single numerical values can be assigned to the partial pressures in both compartments.

Steady-state equations whose derivation is based on this structure will, therefore, not only represent a time averaged

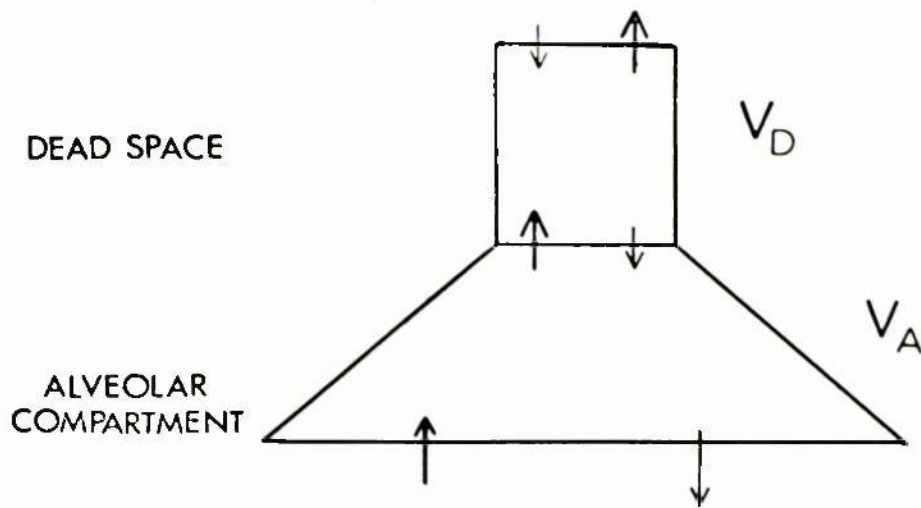


FIGURE 2.1

A simplified lumped parameter model of the lung. The lung is represented as a single dead space compartment with volume V_D , and a single alveolar compartment with volume V_A . Gas transfer takes place between the alveolar compartment and blood stream. The dead space is assumed to be rigid with a compliant alveolar compartment.

mean but also a volume averaged mean (within a lung unit and between the large number of functional units).

The Bohr equation¹³⁰ is one of the frequently used basic equations of alveolar-capillary gas exchange. The equation simply proportions the expired gas mixture between its dead space and alveolar components:

$$\begin{array}{r} V_T C_{E-x} \\ \text{Mixture} \end{array} = \begin{array}{r} V_D C_{I-x} \\ \text{Dead space} \\ \text{component} \end{array} + \begin{array}{r} (V_T - V_D) C_{A-x} \\ \text{Alveolar} \\ \text{component} \end{array} \quad (2.5)$$

and converting to partial pressures we have

$$\begin{array}{r} V_T P_{E-x} \\ \text{Mixture} \end{array} = \begin{array}{r} V_D P_{I-x} \\ \text{Dead space} \\ \text{component} \end{array} + \begin{array}{r} (V_T - V_D) P_{A-x} \\ \text{Alveolar} \\ \text{component} \end{array} \quad (2.6)$$

Another important basic equation is the alveolar air equation. The history of the development of this equation has been presented by Otis¹⁵⁰ and Nunn.¹³¹

In the alveolar compartment of the model illustrated in Figure 2.1 the oxygen and carbon dioxide partial pressures are interrelated. The most simple form of this relationship arises when the subject is breathing 100% oxygen since under these circumstances

$$P_{A O_2} + P_{A CO_2} = P_{I O_2} = B - 47.0 \text{ (mm.Hg)} \quad (2.7)$$

When the subject is breathing air, however, the relationship is more complex and is established by use of the respiratory exchange ratio (R) where R is defined by

$$R = \frac{\dot{V}_{CO_2}}{\dot{V}_{O_2}} = \frac{\text{CO}_2 \text{ output/minute}}{\text{O}_2 \text{ uptake/minute}} \quad (2.8)$$

In the gas phase the transfer from the alveolar compartment is

$$\begin{array}{r} \dot{V}_{CO_2} \\ \text{Expired} \end{array} = \begin{array}{r} \dot{V}_E F_{A CO_2} \\ \text{Expired} \end{array} - \begin{array}{r} (\dot{V}_I - fV_D) F_{I CO_2} \\ \text{Inspired from} \\ \text{atmosphere} \end{array} - \begin{array}{r} fV_D F_{A CO_2} \\ \text{Inspired from} \\ \text{dead space} \end{array}$$

(fractional concentration is used here as it offers certain advantages in derivation of this equation)

likewise

$$\dot{V}O_2 = (\dot{V}_I - fV_D)F_I O_2 + fV_D F_A O_2 - \dot{V}_E F_A O_2$$

In order to simplify these expressions the concept of alveolar ventilation (\dot{V}_A) is introduced where

$$\dot{V}_{A_I} = \dot{V}_I - fV_D$$

$$\dot{V}_{A_E} = \dot{V}_E - fV_D$$

The alveolar ventilation so defined is not the actual volume of gas entering the alveoli but rather the volume of atmospheric gas. The effect of this change of variable is to remove further consideration of dead space volume or concentration.

In the general case $\dot{V}_{A_I} \neq \dot{V}_{A_E}$ since the oxygen uptake is not invariably equal to the carbon dioxide output. In order to negotiate this consideration the standard method of derivation of the alveolar air equation utilises the assumption, which is discussed in the previous section, that there is no net nitrogen exchange.

$$\text{i.e. } \dot{V}_{A_I} F_I N_2 = \dot{V}_{A_E} F_A N_2$$

$$\text{i.e. } \dot{V}_{A_I} = \dot{V}_{A_E} \frac{F_A N_2}{F_I N_2}$$

$$\text{but } F_A N_2 = (1 - F_A O_2 - F_A CO_2)$$

$$F_I N_2 = (1 - F_I O_2 - F_I CO_2)$$

i.e.

$$\dot{V}_{A_I} = \dot{V}_{A_E} \frac{(1 - F_A O_2 - F_A CO_2)}{(1 - F_I O_2 - F_I CO_2)}$$

It is common practice to call \dot{V}_{A_E} alveolar ventilation and delete the subscript E. Thus we have

$$\dot{V}CO_2 = \dot{V}_A F_A CO_2 - \dot{V}_A \frac{(1-F_A O_2 - F_A CO_2)}{(1-F_I O_2 - F_I CO_2)} \cdot F_I CO_2$$

and

$$\dot{V}O_2 = \dot{V}_A \frac{(1-F_A O_2 - F_A CO_2)}{(1-F_I O_2 - F_I CO_2)} \cdot F_I O_2 - \dot{V}_A F_A O_2$$

hence we have

$$R_{GAS} = \frac{F_A CO_2 - \frac{(1-F_A O_2 - F_A CO_2)}{(1-F_I O_2 - F_I CO_2)} \cdot F_I CO_2}{\frac{(1-F_A O_2 - F_A CO_2)}{(1-F_I O_2 - F_I CO_2)} \cdot F_I O_2 - F_A O_2} \quad (2.9)$$

(It should be noted that since R is a ratio, the expression is now independent of the volume of the transport medium).

By algebraic manipulation of the equation and converting where appropriate to partial pressures

$$P_A O_2 = \frac{R P_I O_2 + P_A CO_2 \cdot F_I O_2 (1-R) + P_I CO_2 - P_A CO_2}{F_I CO_2 (1-R) + R} \quad (2.10)$$

A commonly used special case of equation (2.10) occurs when $P_I CO_2 = 0.0$.

In this case the equation reduces to

$$P_A O_2 = P_I O_2 + P_A CO_2 \cdot F_I O_2 \frac{(1-R)}{R} - \frac{P_A CO_2}{R} \quad (2.11)$$

In this derivation of the alveolar air equation the Haldane transformation is used. A form of the alveolar air equation which is not based on the assumption of no net exchange of inert gas was presented by Oszowka & Farhi.¹³² Solution of the equation requires knowledge of the mixed venous partial pressures of inert gases.

As indicated, the derivation of these equations is based on gross simplifications of reality. There are several component processes, involved in the transport of respiratory gases between the atmosphere and arterial blood. Each component may be regarded¹³³ as imparting a resistance to gas transport and

contributing to the overall tension differential between inspired gas and arterial blood i.e. $(I-a)DO_2$ and $(a-I)DCO_2$. Such resistances are accentuated in disease processes. The various components in the overall transport process have been categorised by Hills:¹³³

Airway convection.
Airway diffusion.
Membrane diffusion.
Plasma convection.
Erythrocyte diffusion.
Chemical reaction.

with additional resistances due to

Shunt, i.e. right to left shunting.
Distribution component.

Descriptions of these component processes by means of algebraic equations is considered in the next three sections.

e) Airway Convection/Diffusion.

Transport of gas from the mouth to the alveolar membrane is a complex process. Flow in the larger airways may be turbulent¹³⁴ during periods of peak-flow even at rest, with linear velocities of gas flow in excess of 230 cm/sec and Reynold's numbers of the order of 2000. In the lower airways where gas flow would be expected to be laminar (Reynold's numbers of the order of 10) laminar flow is interrupted at branch points, re-established in the distal airways, and secondary motions occur.¹³⁵ Utilising the anatomical data of Weibel,¹³⁶ and Horsfield & Cumming,¹³⁷ the calculated linear velocities of gas flow in the terminal airways¹³⁸ are such that the main mechanism for transfer of gas to the alveoli is gaseous diffusion.

Such a complex process requires for its description a distributed model. Such models are discussed in Section 2.8 of this chapter, but the complexities are such that a complete

mathematical description of the events is not possible at this time.¹³⁹

In the steady-state approach it is assumed that inspired gas is transported to the alveoli by convection. For carbon dioxide transport

$$\begin{aligned}\dot{V}CO_2 &= \dot{V}_E C_A CO_2 - (\dot{V}_I - fV_D) C_I CO_2 - fV_D C_A CO_2 \\ &= \dot{V}_{A_E} \beta_g P_A CO_2 - \dot{V}_{A_I} \beta_g P_I CO_2\end{aligned}\quad (2.12)$$

and for oxygen

$$\dot{V}O_2 = \dot{V}_{A_I} \beta_g P_I O_2 - \dot{V}_{A_E} \beta_g P_A O_2 \quad (2.13)$$

\dot{V}_{A_I} may be eliminated using the variable R. Since

$$R = \frac{\dot{V}CO_2}{\dot{V}O_2} = \frac{\dot{V}_{A_E} \beta_g P_A CO_2 - \dot{V}_{A_I} \beta_g P_I CO_2}{\dot{V}_{A_I} \beta_g P_I O_2 - \dot{V}_{A_E} \beta_g P_A O_2}$$

$$\dot{V}_{A_I} = \dot{V}_A \frac{P_A O_2 \cdot R + P_A CO_2}{R \cdot P_I O_2 + P_I CO_2} \quad (2.14)$$

In derivation of these equations it is assumed that the concentration of dead space gas which is re-inspired is identical to alveolar gas. Thus application of these equations to individual gas exchange units is equivalent to assuming that each unit has its own separate dead space.

f) Membrane/Erythrocyte diffusion.

The process of diffusion can be described by Fick's Law which states that the flux of a gas species i (\dot{M}_i) across an area of an infinite plane under a concentration gradient $\frac{\partial c_i}{\partial x}$ is given by

$$\dot{M}_i = -A d_i \frac{\partial c_i}{\partial x} \quad (2.15)$$

where d_i is the coefficient of diffusion. This law only applies however to mixtures of two gases, to diffusion of the gas in only

one direction, in one phase and in a steady-state, i.e. when the concentration at each point is constant. When more than two gases are present, as in the lung, the governing equations are the more complex Stefan-Maxwell equations although use of Fick's law does not lead to serious inaccuracies in normal air breathing conditions.¹⁴⁰

Despite the restrictions implicit in equation 2.15 it is the basis of the mathematical description of diffusion across the alveolar-capillary membrane.

For a gas, C can be replaced by partial pressure p such that

$$\dot{M}_i = -Ad_i \beta_i \frac{\partial p_i}{\partial X}$$

and if $\frac{\partial p_i}{\partial X}$ is approximated by $\frac{\Delta P}{X}$ where ΔP is the partial pressure difference between two points which are separated by a distance X , then

$$\dot{M}_i = - Ad_i \beta_i \frac{\Delta P}{X} \quad (2.16)$$

In study of diffusion across the alveolar-capillary membrane ΔP is taken to be the difference in tension between alveolar gas and pulmonary capillary blood and X the thickness therefore of the alveolar-capillary membrane.

Thus for a small length (dl) of an individual pulmonary capillary in a small time dt the flux of a gas species i is given by

$$\frac{SY_i(P_A - P_C)dldt}{X} \quad (2.17)$$

where S is the unit surface area of pulmonary capillary, P_C the tension in that section of pulmonary capillary blood, and $Y_i = d_i \beta_i$.

In studying alveolar-capillary diffusion in man the use of carbon monoxide as the test gas offers advantages because of its

high affinity for haemoglobin (about 220 times that of oxygen), a fact first realised by Bohr.¹⁴¹ If it is assumed that the rate of combination of CO with haemoglobin is instantaneous then equation 2.17 for CO can be written as

$$\frac{SY_{CO}}{X} P_A CO dt \quad (2.18)$$

By assuming that a) the shape and dimensions of capillaries are uniform; b) erythrocytes travel through all capillaries at same rate; c) alveolar PCO is constant; d) resistance to gas transfer across the membrane is constant and uniform along the capillaries, and by integrating along the length of the individual pulmonary capillary and summing with respect to all n pulmonary capillaries then the amount of CO transferred in the lung from alveolar gas to pulmonary capillary blood in small time dt is given by

$$\sum_{j=1}^n \left[\int_0^l \frac{SY_{CO}}{X} P_A CO dl \right] dt$$

i.e.
$$\frac{n l S}{X} Y_{CO} P_A CO dt$$

where l is the length of the pulmonary capillary.

Thus in any unit time the flux of CO across the membrane (\dot{M}_{CO}) is given by

$$\dot{M}_{CO} = \frac{A}{X} Y_{CO} P_A CO \quad (2.19)$$

where A is the alveolar surface area and $n l S = A$.

The constant $\frac{AY_{CO}}{X}$ is known as the diffusing capacity ($D_L CO$) or transfer factor (TF_{CO}). Thus

$$D_L CO = TF_{CO} = \frac{\dot{M}_{CO}}{P_A CO} \quad (2.20)$$

Techniques of measurement of the transfer factor vary in the method used to estimate $P_A CO$. (For details see Forster,¹⁴² Bates et al,¹⁴³ Cotes¹⁴⁴).

Combination of CO with haemoglobin is not an instantaneous process¹⁴⁵ and the diffusing capacity as defined by equation (2.20) can be shown¹⁴⁶ to represent the summed effects of resistance of the pulmonary membrane to diffusion and of the red cells to the uptake of CO. The proof of this (after Roughton & Forster¹⁴⁶) is detailed below. The rate of formation of COHb (v) in the pulmonary capillary at any point depends on the partial pressure of CO in the pulmonary capillary plasma

$$\text{i.e.} \quad v = \theta P_c \text{CO}$$

where θ is a constant which itself depends on oxygen tension.

Equation (2.17) can also be applied to carbon monoxide.

Thus for a small length (dl) of an individual pulmonary capillary in time (dt)

$$\dot{M}_{\text{CO}} = \frac{SY_{\text{CO}}}{X} (P_A \text{CO} - P_c \text{CO}) dl dt$$

Assuming no change of the mass of CO in plasma (<1% of CO is carried in plasma)

$$\frac{SY_{\text{CO}}}{X} (P_A \text{CO} - P_c \text{CO}) dl dt = \theta P_c \text{CO} a dl dt$$

where a is the cross sectional area of the capillary.

Thus

$$P_c \text{CO} = \frac{P_A \text{CO}}{1 + \frac{\theta a X}{SY}}$$

(The subscript CO is omitted after Y).

i.e. for a small length of capillary dl

$$\dot{M}_{\text{CO}} = \frac{SY}{X} P_A \text{CO} \left(1 - \frac{1}{1 + \frac{\theta a X}{SY}} \right) dl dt$$

Integrating along the capillary and summing over all n capillaries

$$\dot{M}_{\text{CO}} = \sum_{j=1}^n \left[\int_0^l \frac{SY P_A \text{CO}}{X} \left(1 - \frac{1}{1 + \frac{\theta a X}{SY}} \right) dl \right] dt$$

$$= \frac{n1SY}{X} P_A CO \left(1 - \frac{1}{1 + \frac{\theta aX}{SY}} \right) dt$$

but $n1S = A$ and $D_M = AY/X$ where D_M is defined to be the membrane component of the diffusing capacity

i.e.

$$\begin{aligned} \dot{MCO} &= D_M P_A CO \left[1 - \frac{1}{1 + \frac{\theta aX}{SY}} \right] dt \\ &= D_M P_A CO dt / \left(1 + \frac{\theta aX}{SY} \right) \\ &= D_M P_A CO dt / \left(1 + \frac{n1SY}{\theta a n1X} \right) \\ &= D_M P_A CO dt / \left(1 + \frac{D_M}{\theta V_c} \right) \end{aligned}$$

when V_c is the volume of the blood in the pulmonary capillaries = $a n1$.

But

$$\dot{MCO} = D_L P_A CO dt \quad (\text{see equation 2.20})$$

$$\text{i.e. } D_L = D_M / \left(1 + \frac{D_M}{\theta V_c} \right)$$

(2.21)

$$\text{i.e. } \frac{1}{D_L} = \frac{1}{D_M} + \frac{1}{\theta V_c}$$

g) Distribution Component.

A similar set of equations to those presented in 2.3.(e) can be developed to describe the transfer of oxygen and carbon dioxide to and from the blood perfusing pulmonary alveoli.

Thus for an individual pulmonary unit (k)

$$\dot{VCO}_{2k} = \dot{Q}_k (C_{\bar{v}} CO_2 - C_{ck} CO_2) \quad (2.22)$$

$$\text{or } \dot{VCO}_{2k} = \dot{Q}_k \left[C_{\bar{v}} CO_2 - f(P_{Ak} CO_2) \right]$$

It is assumed that the end-capillary tension is identical to alveolar partial pressure and related to concentration of carbon dioxide in end-capillary blood by an arbitrary function f . (This notation is preferred to use of a capacitance coefficient for

CO₂ in blood since the latter tends to suggest a constant relationship). The function f is in effect the CO₂ dissociation curve. Computational work has been simplified greatly by provision of standard easily programmed methods both for the CO₂ dissociation curve¹⁴⁷ and oxygen dissociation curve.¹⁴⁸

For oxygen

$$\dot{V}O_{2k} = \dot{Q}_k \left[g(P_{A O_2}) - C_{\bar{v} O_2} \right] \quad (2.23)$$

From equating equations (2.22) and (2.12) and replacing $\dot{V}_{A I}$ by the expression in (2.14)

$$\dot{V}_{AK}/\dot{Q}_K = \frac{C_{\bar{v} CO_2} - f(P_{A CO_2})}{\beta_g P_{AK} CO_2 - \beta_g P_{I CO_2} \frac{(R_K P_{AK} O_2 + P_{AK} CO_2)}{(R_K P_{I O_2} + P_{I CO_2})}}$$

By rearrangement of this equation and replacing R_K by

$$R_K = \frac{C_{\bar{v} CO_2} - f(P_{AK} CO_2)}{g(P_{AK} O_2) - C_{\bar{v} O_2}} \quad (2.24)$$

$$\dot{V}_{AK}/\dot{Q}_K = \frac{1}{\beta_g} \frac{[C_{\bar{v} CO_2} - f(P_{A CO_2})] P_{I O_2} + [C_{\bar{v} O_2} - g(P_{AK} O_2)] P_{I CO_2}}{P_{AK} CO_2 \cdot P_{I O_2} + P_{I CO_2} \cdot P_{AK} O_2} \quad (2.25)$$

In the case where $P_{I CO_2} = 0$ this simplifies to

$$\dot{V}_{AK}/\dot{Q}_K = \frac{1}{\beta_g} \left[\frac{C_{\bar{v} CO_2} - f(P_{AK} CO_2)}{P_{AK} CO_2} \right] \quad (2.26)$$

Such equations are presented in more detail along with graphical representations in the excellent treatise of Rahn & Fenn¹⁴⁹ and by Otis¹⁵⁰.

Thus for any given input conditions in the inspired gas ($P_{I CO_2}, P_{I O_2}$) and in the mixed venous blood ($C_{\bar{v} CO_2}, C_{\bar{v} O_2}$) the

alveolar partial pressures of oxygen and carbon dioxide are determined by \dot{V}_{A_K}/\dot{Q}_K (the ventilation-perfusion ratio). This relationship is best expressed by the ventilation-perfusion line (Fig. 2.2).

Construction of the line^{151,152} is based on the recognition that in a steady state the blood R equals the gas R where the blood R is as defined in equation 2.24 and gas R is calculated from use of the alveolar air equation (2.10).

In manual construction of the line^{149, 153} an R value is chosen and the gas R line which radiates from the inspired gas point is constructed (see Fig. 2.2). The loci of points on this line describe all possible combinations of pO_2 and pCO_2 that could exist in the gas of an alveolus with that R value. The corresponding blood R curve is also drawn, and the point of intersection of these is on the \dot{V}_A/\dot{Q} line.

Non-linearity of the blood R curve (equation 2.24) as a function of pO_2 , pCO_2 makes the problem of identifying the point of intersection of the corresponding blood R curve and gas R line a trial and error procedure. Manual construction of the line for any particular subject is, therefore, tedious and may be inaccurate.

Methods for construction of the line using a digital computer have been described.^{154,132} The first uses a procedure similar to the manual method, in that points on the line are identified by searching along a gas R line for the point of intersection with the corresponding blood R curve. The other method¹³² treats \dot{V}_A/\dot{Q} as the "independent variable". Thus the problem is to find the pO_2 and pCO_2 that are associated with a given \dot{V}_A/\dot{Q} . This is inefficient since it incorporates a search procedure in two-dimensional space.

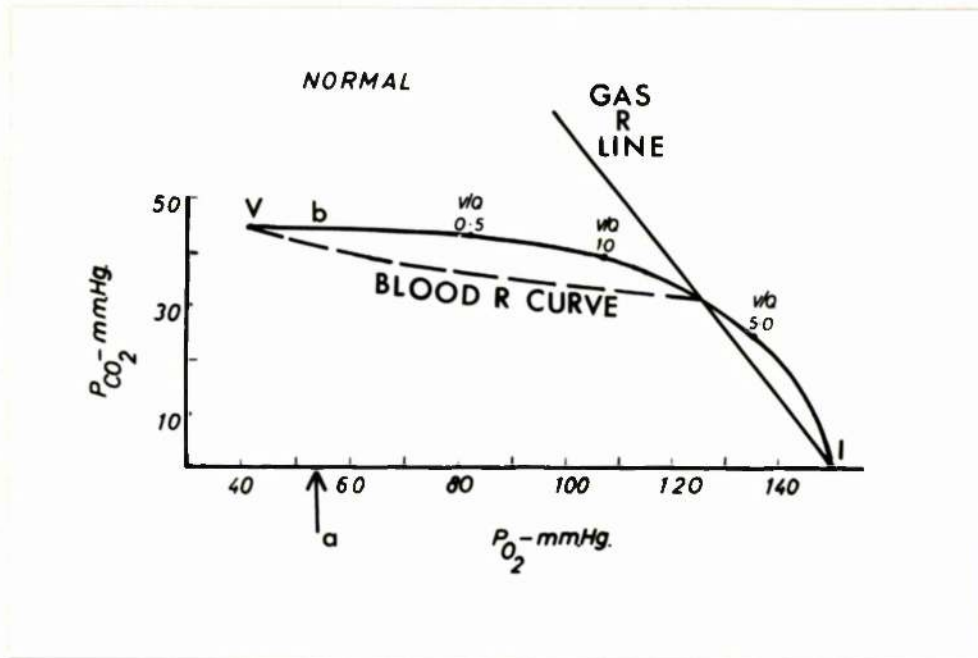


FIGURE 2.2.

Diagrammatic representation of the ventilation-perfusion line. Each point on the line for an individual subject corresponds to a ventilation-perfusion ratio. The line is between the mixed venous point $V (\dot{V}/\dot{Q} = 0)$ and the inspired gas point $I (\dot{V}/\dot{Q} = \infty)$. Points on the line are at the point of intersection between the gas R line and blood R curve. (For more details, see text). In the computer programme described in the text points on the line (b) are identified at specific values of pO_2 (a).

In a computer programme developed by the author, the method is based on eliminating the variable R .¹⁵⁵

By substituting for R in equation 2.10, R as defined in equation 2.24, we obtain a function of $(P_{A O_2}, P_{A CO_2})$ which is equal to zero.

$$P_{A O_2} - \frac{P_{I O_2} a/b + P_{A CO_2} \cdot F_{I O_2} (1 - a/b) + P_{I CO_2} - P_{A CO_2}}{F_{I CO_2} (1 - a/b) + a/b} = 0$$

$$\text{where } a = C_{\dot{V}} CO_2 - f(P_{A CO_2})$$

$$b = g(P_{A O_2}) - C_{\dot{V}} O_2$$

e.g.

$$P_{A O_2} - \frac{P_{I O_2} \cdot a + P_{A CO_2} \cdot F_{I O_2} (b-a) + (P_{I CO_2} - P_{A CO_2}) b}{F_{I CO_2} (b-a) + a} = 0 \quad (2.27)$$

Thus for a defined value of $P_{A O_2}$ the problem of identifying a point on the \dot{V}_A/\dot{Q} line reduces to obtaining the value of $P_{A CO_2}$ which is the root of this equation. The function defined by equation (2.27) has a discontinuity when

$$F_{I CO_2} (b-a) + a = 0$$

Thus for values of $P_{A O_2}$ close to $P_{\dot{V}} O_2$ when b and a will be close to zero, the root of the equation will be close to this discontinuity (see Fig. 2.3). Since most numerical methods of root finding require as starting conditions knowledge of points on either side of the root, the discontinuity presents practical problems in implementation of such methods. This problem has been overcome in the programme which has been developed (see Appendix 6).

Two different numerical methods for root-finding have been investigated - regula falsi,¹⁵⁶ and bisection.¹⁵⁶ (See figs. 2.4 and 2.5 respectively). The bisection method proved to be more efficient than the regula falsi in terms of speed (see Table 2.4).

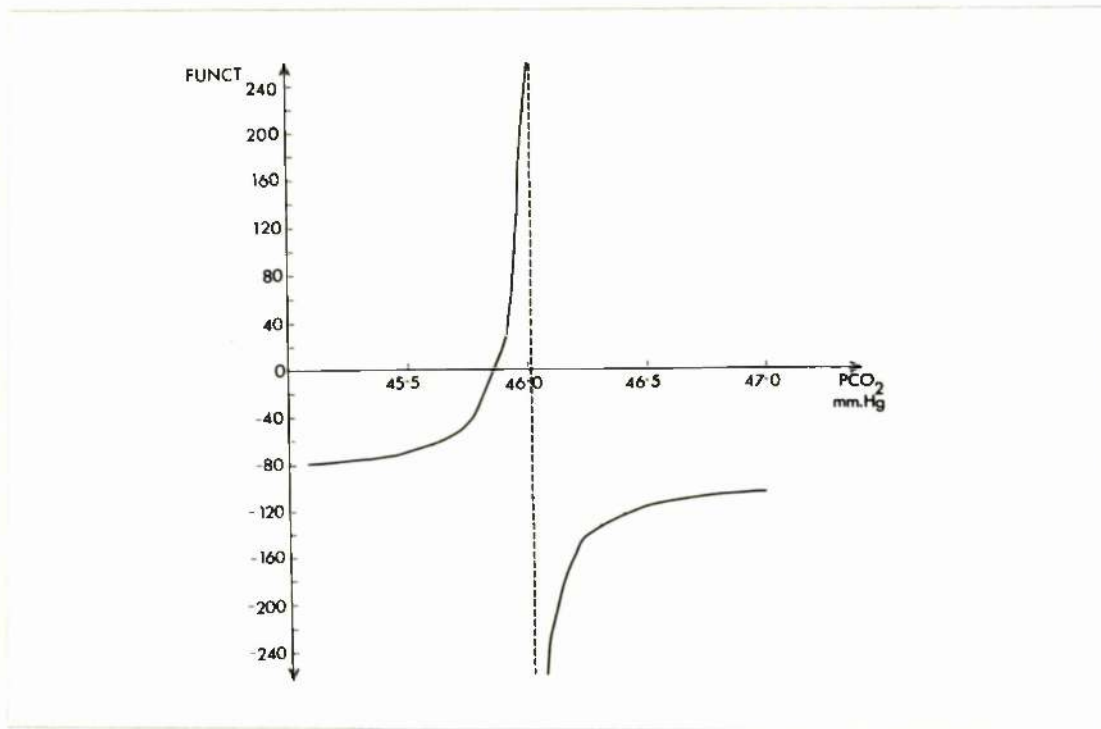


FIGURE 2.3

Graph of function as defined by equation 2.27 at $P_{A}O_2$ of 40.5 mmHg. The $P_{I}O_2$ and $P_{I}CO_2$ used in this calculation were 150.0 and 0.0 respectively with $P_{v}O_2$ of 40.0 and $P_{v}CO_2$ of 46.0. The function has a discontinuity at the pCO_2 marked by the dashed line. The root of the function lies close to the mixed venous pCO_2 .

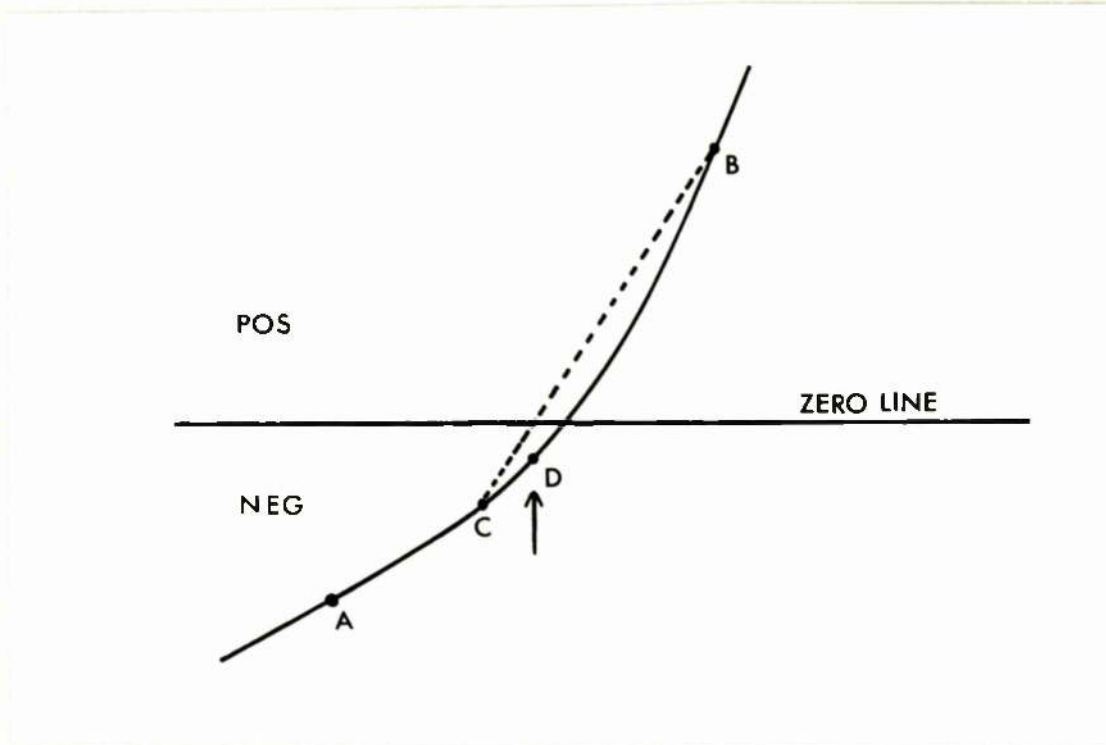


FIGURE 2.4

The method of regula falsi for finding the root of a function. The method is iterative and each iteration begins with points on either side of the root. In the example shown the method is at its second iteration with the two points being B & C. On each iteration the point at which the line between these points cuts the abscissa is identified and the function evaluated at this point. A new point D is thus obtained and one of the previously used points (B or C) is discarded such that the two new points are still on either side of the root. In the example shown C would be discarded and the two points B & D used in the next iteration.

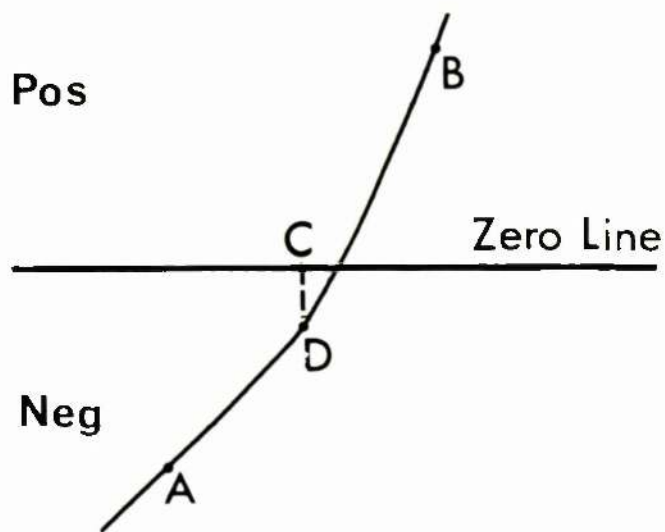


FIGURE 2.5

The bisection method for finding the root of a function. The method is iterative and each iteration begins with points (A & B) on either side of the root. The interval on the abscissa between the points is halved (C) and the function evaluated (D). The original point on the same side of the root as D is discarded (A) and the process repeated with the new points (D & B).

<u>INPUT $P_{A O_2}$</u>	<u>REGULA FALSI</u>		<u>BISECTION</u>	
	<u>Root ($P_{A CO_2}$)</u>	<u>Number of iterations</u>	<u>Root ($P_{A CO_2}$)</u>	<u>Number of Iterations</u>
40.07	43.76	13	43.76	23
71.29	38.60	36	38.60	21
129.69	17.34	73	17.34	15

TABLE 2.4.

In the programme which has been developed a number of points (60, or 100, or 150) on the ventilation-perfusion line equally spaced in terms of $P_{A O_2}$ between $P_{\bar{v} O_2}$ and $P_{I O_2}$ are identified and \dot{V}_A/\dot{Q} calculated. The programme lists these points with associated values of \dot{V}_A/\dot{Q} , $P_{A O_2}$, $P_{A CO_2}$ (in mm.Hg.) and $C_{C O_2}$, $C_{C CO_2}$ (in ml. STPD/100 ml. blood) (See Table 2.5). The programme has the facility for graphing the \dot{V}_A/\dot{Q} line.

In computer models of gas transport the most common application of the ventilation-perfusion line is to obtain values of $P_{A O_2}$, $P_{A CO_2}$ and hence $C_{C O_2}$, $C_{C CO_2}$ associated with a specific \dot{V}_A/\dot{Q} for a specific set of input conditions. In one approach to this problem¹⁵⁷ a time consuming method is used in which given a \dot{V}_A/\dot{Q} , an R value is chosen, the corresponding gas R line searched for the point of intersection with the corresponding blood R curve, \dot{V}_A/\dot{Q} at this point calculated and if not within a specified value from the given \dot{V}_A/\dot{Q} , an updated estimate of R made, and the process repeated.

For this application of the ventilation-perfusion line the author has used interpolation between points identified previously. Such points will be unequally spaced, however, with respect to

\dot{V}_A/\dot{Q}	$P_{A O_2}$	$P_{A CO_2}$	$C_{C O_2}$	$C_{C CO_2}$
0.046	35.08	40.44	15.51	47.75
0.189	39.67	39.65	17.33	47.23
0.319	44.25	38.96	18.79	46.77
0.433	48.84	38.35	19.92	46.39
0.534	53.43	37.81	20.75	46.06
0.627	58.01	37.32	21.36	45.77
0.715	62.60	36.85	21.80	45.50
0.802	67.19	36.38	22.13	45.25
0.894	71.78	35.89	22.39	44.98
0.994	76.36	35.37	22.58	44.71
1.106	80.95	34.81	22.74	44.41
1.236	85.54	34.18	22.86	44.09
1.390	90.12	33.47	22.97	43.71
1.579	94.71	32.66	23.06	43.28
1.816	99.30	31.70	23.14	42.77
2.126	103.88	30.58	23.21	42.16
2.547	108.47	29.22	23.28	41.41
2.855	111.03	28.34	23.31	40.91
3.075	112.57	27.75	23.33	40.57
3.330	114.11	27.12	23.35	40.20
3.626	115.65	26.43	23.37	39.79
3.976	117.19	25.69	23.39	39.35
4.394	118.73	24.88	23.41	38.85
4.902	120.27	24.00	23.43	38.30
5.530	121.81	23.03	23.45	37.68
6.326	123.35	21.97	23.47	36.99
7.366	124.89	20.79	23.49	36.19
8.773	126.43	19.48	23.50	35.28
10.777	127.97	18.02	23.53	34.21
13.837	129.51	16.38	23.55	32.95
19.033	131.06	14.52	23.57	31.42
39.628	132.60	12.41	23.60	29.53
62.032	134.13	9.96	23.63	27.09
193.248	135.16	8.10	23.64	24.95

TABLE 2.5.

\dot{V}_A/\dot{Q} . (In the digital computer programme more points are identified at higher values of \dot{V}_A/\dot{Q} when the difference in \dot{V}_A/\dot{Q} between points equally spaced with respect to $P_{A O_2}$ is larger.) As a result of the unequal spacing of points certain of the commonly used methods of interpolation are inappropriate and Lagrangian interpolation is used.¹⁵⁵ The results of using this approach are illustrated in Table 2.6.

\dot{V}_A/\dot{Q}	Actual PCO_2 (mm.Hg.)	Interpolated PCO_2 (mm.Hg.)	Actual PO_2 (mm.Hg.)	Interpolated PO_2 (mm.Hg.)
0.179	39.71	39.71	39.34	39.34
0.368	38.70	38.70	46.15	46.15
0.628	37.32	37.32	58.06	58.06
1.304	33.86	33.86	87.68	87.68
3.478	26.77	26.77	114.91	114.91
5.488	23.09	23.09	121.71	121.73
9.631	18.81	18.80	127.16	127.18

TABLE 2.6

Comparison of PCO_2 , PO_2 values for a given \dot{V}_A/\dot{Q} obtained by interpolation between sixty points identified on a \dot{V}_A/\dot{Q} line and those obtained directly by an alternative method.

In applying these equations to individual pulmonary units the presence of a common dead space is neglected. In effect the concentration of gas inspired (C'_I) into a pulmonary unit (i) is given by

$$C'_I = C_D V_{D_i} / V_{T_i} + C_I (1 - V_{D_i} / V_{T_i}) \quad (2.28)$$

and leads therefore to a new system of equations. (For details see Ross and Farhi¹⁵⁸.) Since for different pulmonary units V_D/V_T are unequal, the alveolar PO_2 and PCO_2 are not determined, therefore,

by only \dot{V}_A/\dot{Q} .

There is moreover evidence for collateral ventilation in human lungs¹⁵⁹ i.e. gas transfer between adjacent lung regions, and the influence of this on gas exchange in dogs has been studied experimentally^{160, 161} (for a review article on collateral ventilation see Macklem¹⁶²). Collateral ventilation is neglected in the standard analysis of ventilation-perfusion distribution which is presented here but is considered in the computer aided calculations of West.¹⁶³

Steady-state equations are also used to analyse experimental data to obtain information on abnormalities of ventilation-perfusion distribution. The most widely used analysis is the "Riley Analysis" named after its originator.¹⁶⁴ In this method a three compartment alveolar model is used (see Figure 2.6). Expired gas is thus considered to be made up of three components, i.e.

$$\dot{V}_T C_{\bar{E}} = \dot{V}_{D_{ANAT}} C_I + \dot{V}_{D_{ALV}} C_I + (\dot{V}_T - \dot{V}_{D_{ANAT}} - \dot{V}_{D_{ALV}}) C_{IDEAL}$$

and by letting

$$\dot{V}_{D_{PHYSIOL}} = \dot{V}_{D_{ANAT}} + \dot{V}_{D_{ALV}}$$

$$\frac{\dot{V}_{D_{PHYSIOL}}}{\dot{V}_T} = \frac{C_{IDEAL} - C_{\bar{E}}}{C_{IDEAL} - C_I} = \frac{P_{IDEAL} - P_{\bar{E}}}{P_{IDEAL} - P_I} \quad (2.29)$$

Arterial blood is a mixture of two streams - from the shunt and from the ideal compartment, i.e.

$$\dot{Q}_S/\dot{Q}_t = (C_{IDEAL} - C_a)/(C_{IDEAL} - C_{\bar{v}}) \quad (2.30)$$

In application of this method it is assumed generally that P_{aCO_2} is identical to $P_{IDEAL} CO_2$ since a right to left shunt of blood produces little effect on the end-capillary pCO_2 . (The arterio-venous partial pressure difference for CO_2 is relatively small.)

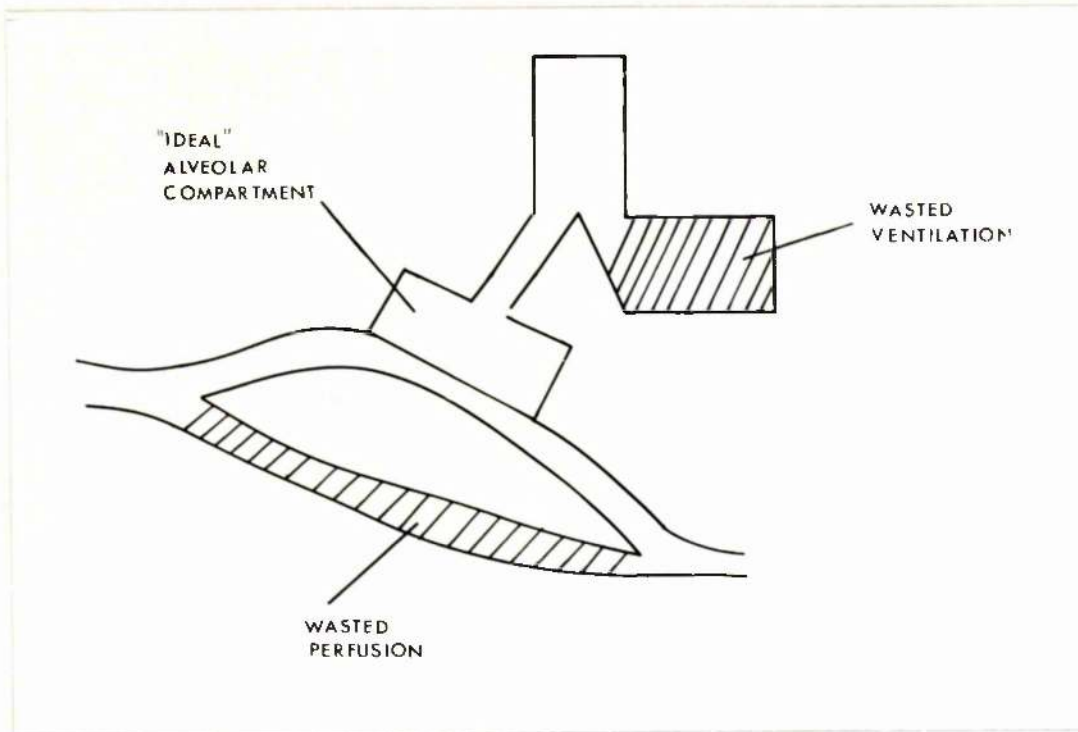


FIGURE 2.6.

Three compartment model of Riley et al.¹⁶⁴
 The model consists of a ventilated and perfused compartment ("ideal" alveolar compartment), a ventilated but unperfused compartment (physiological dead space), and an unventilated and perfused compartment (venous admixture).

Equation 2.29 can thus be used to calculate physiological dead space. Ideal alveolar PO_2 is calculated from the alveolar air equation and substitution of the derived and measured oxygen values in equation 2.30 allows calculation of \dot{Q}_s/\dot{Q}_t (the venous admixture). A more exact approach to the analysis is to regard arterial PCO_2 as only an initial estimate of ideal pCO_2 and to continue to update this estimate to allow for the effects of calculated venous admixture on end-capillary pCO_2 . Such a method of "successive approximations" is implemented easily on a digital computer but makes no appreciable difference to the results unless \dot{Q}_s/\dot{Q}_t is large (>20%).

Although the Riley analysis has proved of clinical value and has been applied widely there are, however, important theoretical limitations. The physiological dead space for carbon dioxide is an underestimate of excess ventilation to units which are relatively overventilated¹⁶⁵ since such units are able to transfer CO_2 relatively well. Furthermore, the formulation of the equations is such that there is direct dependence between the magnitude of the calculated ratios - venous admixture (\dot{Q}_s/\dot{Q}_t) and physiological dead space (V_D/V_T).¹⁶⁶ The calculations are sensitive to small errors in measurement. In the error analysis of Kelman¹⁶⁷ random errors in simulated measured data with 1% coefficient of variation led to estimates of \dot{Q}_s/\dot{Q}_t which ranged from 10 - 28%.

An alternative approach is to consider the lung as if it consisted of a number of compartments in parallel. The minimum number of compartments which can be used is two (see Figure 2.7) and the author has investigated the application of such a model to measurement of ventilation-perfusion distribution using simultaneous

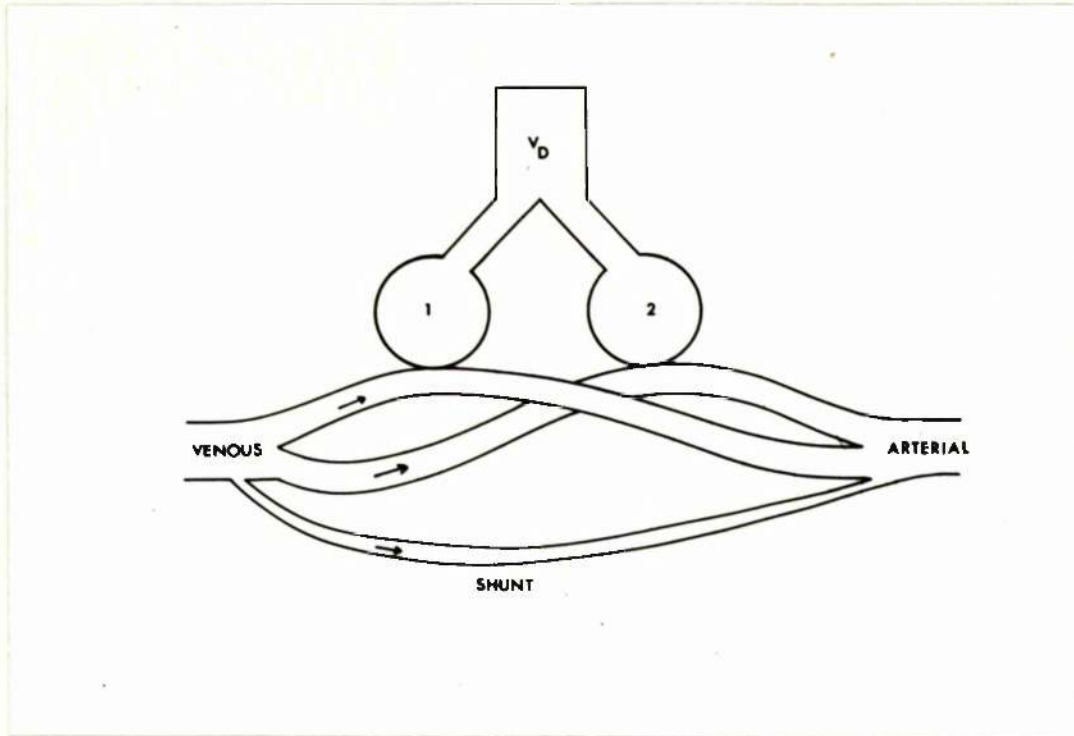


FIGURE 2.7

A model structure with two ventilated and perfused compartments (1 and 2), an anatomical dead space, and a right to left shunt.

analysis of oxygen and carbon dioxide transfer.¹⁶⁸ (See Figure 2.8). The analysis is complicated, however, by the non-linear time varying relationship for oxygen and carbon dioxide between partial pressure and gas concentration in blood, and because of the effect of other factors, e.g. diffusion impairment, on the transport process.

A more profitable approach is to study the exchange of inert gases. Inert gas exchange in an individual pulmonary unit in steady-state conditions can be shown theoretically¹⁶⁹ to be related to the ventilation-perfusion ratio of that unit and to the solubility of the gas. Results obtained from analysis of the overall pulmonary exchange of two inert gases in terms of a two compartment model depend to a large measure on the solubilities of the gases which are used.¹⁷⁰ A more ambitious approach is to use a fifty compartment model¹⁷¹ to analyse the simultaneously measured steady-state exchange of six gases with a wide range of solubilities, thereby obtaining knowledge of the relative distributions of ventilation and perfusion. Such a method would seem likely to yield non-unique results and has stimulated discussions.^{172,173} An example where four different distributions can be obtained from the same set of measured data has been presented.¹⁷⁴ Nevertheless use of data from simultaneous study of exchange of many inert gases must give more information about the relative distribution of ventilation in relation to perfusion.

Ventilation and perfusion may also be maldistributed in relation to diffusing capacity, this representing another source of inefficiency in pulmonary gas transport.^{175,176} Such a distribution effect may lead to errors in the measurement of transfer factor and this problem has been studied theoretically by several

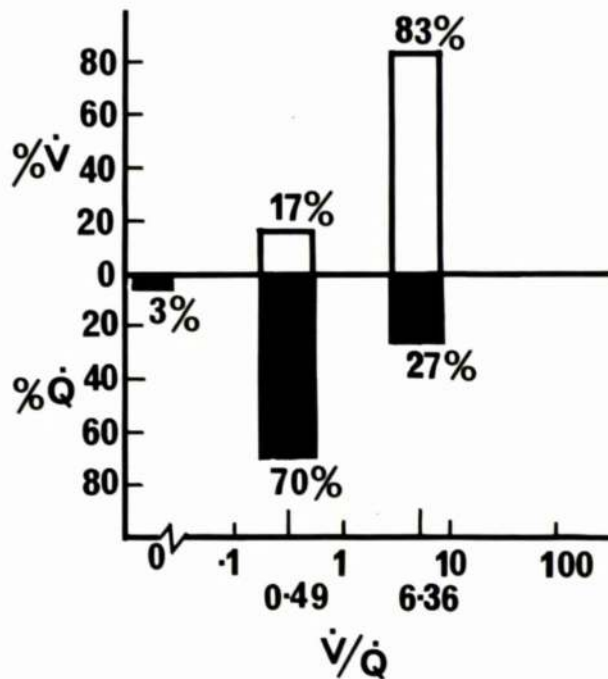


FIGURE 2.8

Application of two compartment model which is shown in Figure 2.7 to the analysis of respiratory gas exchange, for a subject with chronic obstructive airways disease who was in respiratory failure. ($P_{aO_2} = 41.3$ mm.Hg., $P_{aCO_2} = 59.6$ mm.Hg.). The airways obstruction was severe ($FEV_{1.0} = 1.0$ L). The shunt is assumed to be 3% of the cardiac output. The analysis shows that the lung could be considered to consist of two ventilated and perfused compartments with ventilation-perfusion ratios of 0.49 and 6.36 with 17% and 83% of the ventilation and 70% and 27% of the total pulmonary blood flow respectively. The details of the analysis procedure are presented in Appendix 10.

177-182
authors.

In order to quantify the relationship between perfusion and diffusion consider a small length (dl) of capillary (k). For a gas i for which there is a linear relationship between concentration and tension in blood, at any point l along the capillary,

$$\dot{Q}_k B_i [P_i(l + dl) - P_i(l)] = \frac{dl S}{X} d_i B_i (P_{A_i} - P_i(l)) \quad (2.31)$$

where symbols are as defined for equation (2.17)

i.e.
$$\frac{P_i(l + dl) - P_i(l)}{dl} = \frac{S d_i}{X \dot{Q}_k} (P_{A_i} - P_i(l))$$

in the limit as $dl \rightarrow 0$

$$\frac{dP_i}{dl} + \frac{S d_i}{\dot{Q}_k X} P_i = \frac{S d_i}{\dot{Q}_k X} P_{A_i} \quad (2.32)$$

The solution of this equation yields

$$P_i(l) = (P_{V_i} - P_{A_i}) e^{-\frac{S d_i l}{\dot{Q}_k X}} + P_{A_i} \quad (2.33)$$

Thus making the same assumptions as were made for the derivation of (2.19); for a homogenous lung

$$P_i(c) = [P_{V_i} - P_{A_i}] e^{-\frac{D_i}{\dot{B}_i \dot{Q}}} + P_{A_i} \quad (2.34)$$

where $P_i(c)$ is the end-capillary partial pressure, and D_i is defined in Section 2.3(f).

A rearrangement of this equation yields

$$D_i = \dot{Q} \dot{B}_i \log_e \frac{(P_{A_i} - P_{V_i})}{(P_{A_i} - P_{a_i})} \quad (2.35)$$

In the derivation of this equation it is assumed that at any point l along the capillary, P does not vary with time, i.e. it describes a

steady-state condition. For an alternative derivation of the equation, see Piiper et al.¹⁸³

In these equations \dot{Q}_K or \dot{Q} can be replaced by the transit time t_k through a single capillary.

$$\dot{Q}_K = \frac{V_{cK}}{t_k}$$

where V_{cK} is the volume of blood in the capillary or

$$\dot{Q} = \frac{V_c}{t_k}$$

since it is assumed in the derivation of (2.34) and (2.35) that all capillary paths are identical.

For carbon monoxide $P_{\bar{V}}CO = 0$ and thus equation (2.34) reduces to

$$P_c CO = (1 - e^{-D_{CO}/\beta_{CO}\dot{Q}}) P_A CO$$

and $\dot{V}CO = \dot{Q} \beta_{CO} (1 - e^{-D_{CO}/\beta_{CO}\dot{Q}}) (P_A CO)$

If one regards the same process as a purely diffusion limited process, as in equation 2.20

$$\dot{V}CO = D_{app} P_A CO$$

where D_{app} is the apparent diffusing capacity.

Thus

$$\frac{D_{app}}{D} = \frac{1 - e^{-D_{CO}/\dot{Q}\beta_{CO}}}{D_{CO}/\dot{Q}\beta_{CO}} \quad (2.36)$$

For small values of $D_{CO}/\dot{Q}\beta_{CO}$ ($\ll 0.1$) D_{app} is close to the true D (for details of numerical calculations see Piiper & Sikand¹⁷⁸)

which is the case in the normal lung (for a homogenous lung $D_{CO}/\dot{Q}\beta_{CO}$ is approximately 0.01). Thus significant differences between D_{app} and D for carbon monoxide can only result from changes of several orders of magnitudes in the distribution of perfusion to diffusion capacity, as is confirmed by the theoretical

studies of Chinet et al¹⁸² using multicompartment models. This is not the case for the oxygen diffusing capacity^{181,182} although the difference between the apparent and true diffusing capacity is reduced if the oxygen uptake is increased.¹⁸¹

The apparent diffusing capacity for carbon monoxide as measured by steady-state methods is more sensitive to changes in the distribution of ventilation relative to diffusing capacity^{180,182} as is illustrated below.

For a single pulmonary unit j ,

$$\dot{V}_{CO_j} = D_{L_j} P_{A_j}$$

(The subscript CO is omitted for both D_L and P_A in this section).

The apparent diffusing capacity for the whole lung ($D_{L, app}$) is given by :-

$$D_{L, app} = \frac{\dot{V}_{CO_T}}{\bar{P}_A} = \frac{\sum_{j=1}^n D_{L_j} P_{A_j}}{\bar{P}_A}$$

where \bar{P}_A is some weighted mean of the individual P_{A_j} , i.e.

$$\bar{P}_A = \sum_{j=1}^n f(j) P_{A_j}$$

where for all j

$$0 \leq f(j) \leq 1$$

and

$$\sum_{j=1}^n f(j) = 1$$

thus

$$\frac{D_{app}}{D} = \frac{\frac{1}{D} \cdot \sum_{j=1}^n D_{L_j} P_{A_j}}{\sum_{j=1}^n f(j) P_{A_j}} = \frac{\sum_{j=1}^n g(j) P_{A_j}}{\sum_{j=1}^n f(j) P_{A_j}} \quad (2.37)$$

where $g(j)$ is the fraction of the diffusing capacity in the j^{th} unit. Thus differences between D_{app} and D depend on the method of obtaining $\overline{P_A}$.

In practice the measured value is likely to be a mean value weighted with respect to the ventilation of the individual units (i.e. $f(j)$ is the relative ventilation of the j^{th} unit.) For this case for an increase in P_{A_j} the ratio $g(j)$ to $f(j)$ will decrease since for any unit

$$\beta_g f(j) \dot{V}_A \left[P_I \cdot \frac{P_{A_j} N_2}{P_I N_2} - P_{A_j} \right] = g(j) D P_{A_j} \quad (2.38)$$

and

$$\frac{g(j)}{f(j)} = \frac{\beta_g \dot{V}_A}{D} \left[\frac{P_I}{P_{A_j}} \cdot \frac{P_{A_j} N_2}{P_I N_2} - 1 \right] \quad (2.39)$$

Thus the effects of increasing maldistribution of diffusion in relation to ventilation is increasing underestimation of the true diffusing capacity. The magnitude of this effect is illustrated in studies with multi-compartment models.¹⁸²

2.4. BREATH BY BREATH MODELS.

In the steady-state models which have been described in the previous sections temporal variations in respiratory gas transport are neglected. A first approach to considering the time dependence of gas exchange in the lung is to construct models on a breath by breath basis thereby allowing prediction of variables at breath (n) from knowledge of their state at breath (n-1). Thus constancy within one breath cycle is still assumed.

Such an approach has been used particularly in the description of the wash-out of inert gas from the lung, e.g. nitrogen during a period of breathing 100% oxygen. (Such models are considered in greater detail in Chapter 4).

The basic form of this type of model is illustrated in the work of Darling et al,¹⁸⁴ describing the wash-out of nitrogen from the lung, and based on the model structure which is shown in Figure 2.1.

At the start of the wash-out process and at end expiration the mass of nitrogen in the alveolar compartment is given by $V_A C_{A(O) N_2}$ and in the dead space $V_D C_{A(O) N_2}$. Following the subsequent inspiration of oxygen

$$C_{A N_2} = \frac{V_A C_{A(O) N_2} + V_D C_{A(O) N_2} + (V_T - V_D) C_{I N_2}}{V_A + V_T}$$

since $C_{I N_2} = 0$ this becomes

$$C_{A N_2} = \frac{(V_A + V_D) C_{A(O) N_2}}{V_A + V_T}$$

i.e. at the end of the first expiration the alveolar nitrogen concentration $C_{A(1) N_2}$ is given by

$$C_{A(1) N_2} = \frac{V_L}{V_L + (V_T - V_D)} C_{A(O) N_2} \quad (2.40)$$

where $V_L = V_A + V_D$

By assuming that V_A is constant, and that V_T is invariant from breath to breath the alveolar concentration at the end of expiration during the n^{th} breath can be predicted from $C_{A(0)}$ using the relationship

$$C_{A(n)} N_2 = W^n C_{A(0)} N_2 \quad (2.41)$$

where $W = \frac{V_L}{V_L + (V_T - V_D)}$ and is called the alveolar dilution ratio.

The assumption of a constant V_T is an unnecessary simplification but one which reduces the computational task. Its effect on the accuracy of analyses based on such an approach is considered in Chapter 4.

The variable time is thus represented in these models by breath number. Since duration of a breath is itself variable such an approach is not applicable in situations where there are time dependent gas transport processes such as diffusion across the alveolar capillary membrane. These methods have thus limited applicability.

2.5. MODELS WITH UNIDIRECTIONAL FLOW RATE.

In the simulations^{42,44-49} which have been used to study the respiratory control system another approach is adopted and time is considered explicitly as a variable. The lung component of the "controlled plant" is represented commonly by a single compartment ventilated with a constant unidirectional stream of gas and of fixed volume (See Fig. 2.9). Additional simplifications which are employed are:-

- a) The events of the respiratory cycle are ignored.
- b) The dead space is assumed equal to zero.

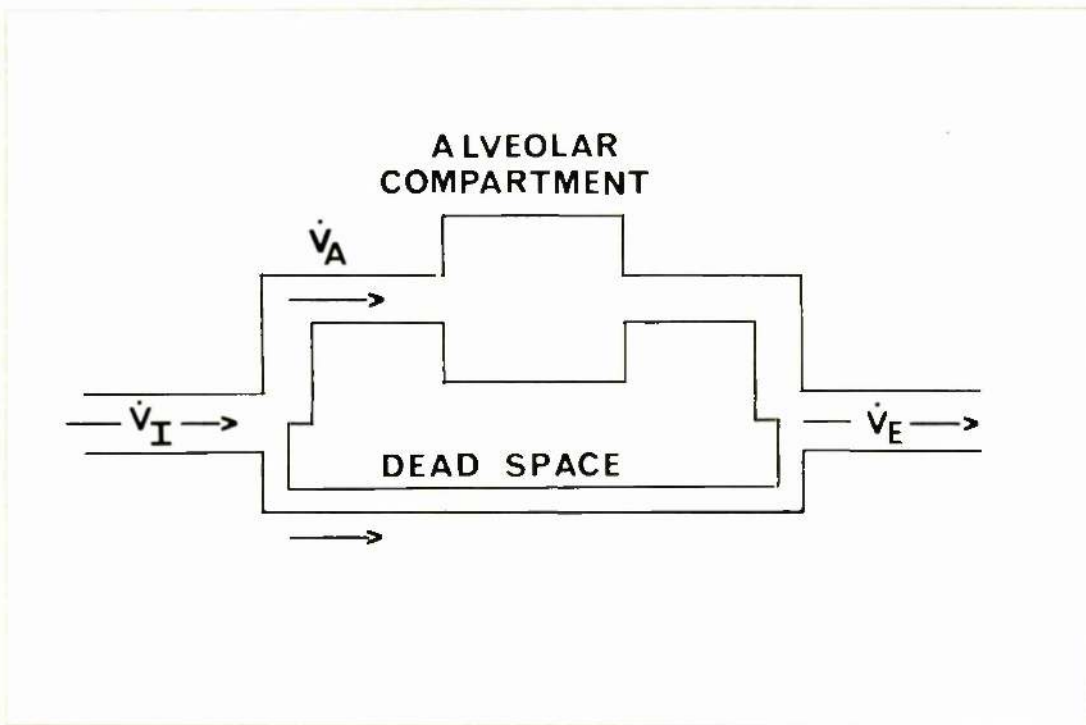


FIGURE 2.9

Model with unidirectional ventilation. The inspired ventilation (\dot{V}_I) is distributed between the alveolar compartment and dead space.

- c) The respiratory exchange ratio (R) is assumed to be constant and equal to one.
- d) Gas tensions in the lung are assumed to be uniform and equal, at every instant, to that of arterial blood and expired gas.

Thus for any gas (x)

$$\frac{d(V_A C_A x)}{dt} = \dot{V}_I C_I x - \dot{V}_E C_A x + \dot{Q}(C_v x - C_a x) \quad (2.42)$$

Rate of change of mass of gas in lung	Addition from atmosphere	-	Loss to atmosphere	+	Addition (or loss) to pulmonary capillary blood.
---	--------------------------------	---	-----------------------	---	--

i.e.

$$\beta g V_A \frac{dP_A x}{dt} = \beta g \dot{V}_I P_I x - \beta g \dot{V}_E P_A x + \dot{Q}(C_v x - f(P_A x))$$

since $\frac{dV_A}{dt} = 0$ (single compartment is assumed to have constant volume).

Assuming $\dot{V}_I = \dot{V}_E = \dot{V}$, we obtain

$$\beta g V_A \frac{dP_A x}{dt} = \beta g \dot{V} (P_I x - P_A x) + \dot{Q} (C_v x - f(P_A x)) \quad (2.43)$$

In the case in which \dot{V} is assumed constant this is a first order differential equation in which the only non-linearity is the function f . Thus for gases which do not react chemically with blood (or for carbon dioxide where a linear approximation to the dissociation curve is used), equation (2.43) is a first order linear, differential equation with constant coefficients of the form -

$$\frac{dP_A}{dt} + K_1 P_A = K_2$$

$$\text{where } K_1 = \frac{\dot{\beta}g\dot{V} + \dot{Q}\beta b}{\beta_g V_A}$$

$$K_2 = \frac{\beta_g \dot{V} P_{I,x} + \dot{Q} C_{\bar{v},x}}{\beta_g V_A}$$

for which a solution can be obtained by analytical methods.

$$P_A x(t) = K_3 + (P_A(0) - K_3) e^{-K_1 t} \quad (2.44)$$

where $P_A(0)$ is the partial pressure in the alveoli at $t = 0$ and

$$K_3 = K_2 / K_1.$$

In such simulations $C_{\bar{v},x}$ is not regarded generally as a constant but is itself obtained by solution of one or more differential equations describing the tissue stores. (Models of tissue stores are considered in more detail in Chapter 5).

Modifications of this approach have obviated the need for assuming that $\dot{V}_I = \dot{V}_E$, by summing the magnitudes of oxygen, carbon dioxide, and nitrogen transport as calculated from such equations in order to obtain a relationship between \dot{V}_I and \dot{V}_E .⁴⁶

Although in the original model of this type it is assumed that the dead space is of zero volume such an assumption is not strictly required since the constant unidirectional ventilation can be alveolar ventilation as defined previously (see Fig. 2.9).

The main advantage of this approach may seem to be that an analytic solution to equation 2.43 is possible. In the simulations of the respiratory control system in which such models have been used, however, other components of the simulation have necessitated use of computer based methods of solution. The equations described have thus been solved using analogue or digital computing techniques.

The simplifications are such that this approach has limited applicability to analysis of experimental data. It neglects, as was pointed out by Yamamoto and Raub¹⁰⁰ that breathing consists of breaths.

The approach has been applied¹⁸⁵ to the analysis of data from nitrogen wash-out experiments. In this case since there is negligible flux of nitrogen across the alveolar-capillary membrane, and the inspired partial pressure of gas is zero. Equation (2.43) reduces therefore to

$$\frac{dP_{A N_2}}{dt} = -\frac{\dot{V}}{V_A} P_{A N_2} \quad (2.45)$$

for which assuming \dot{V} is constant the solution is

$$P_{A N_2}(t) = P_{A(0)} e^{-\dot{V}/V_A t} \quad (2.46)$$

A method of measurement of cardiac output, which is based on parameter estimation¹⁸⁶ applied to this type of model has also been implemented (for more details see Chapter 5).

2.6. INSPIRATION/EXPIRATION AS AN INSTANTANEOUS PROCESS.

In studying diffusion across the alveolar-capillary membrane, models are used in which ventilation is considered to be instantaneous, and uptake of gas to take place in a breath holding period between inspiration and expiration. Such models are applied to the analysis of single-breath experiments. The breath in such experiments contains an inspiratory breath-hold thus reducing the inadequacy of the mathematical description.

The basic equation for this type of model is that derived originally by Krogh¹⁸⁷ which describes the transfer of carbon monoxide from the alveolar compartment of the model structure

represented in Fig. 2.1. For conditions in which there is no mass transport by any mechanism between the alveolar compartment and dead space

$$\frac{dV_A C_A CO}{dt} = -D P_A CO$$

i.e. since $\frac{dV_A}{dt} = 0$

$$\frac{V_A dP_A CO}{dt} = \frac{-D}{\beta_g} P_A CO \quad (2.47)$$

$$\text{thus } P_A(t) CO = P_{A(0)} CO e^{(-D/\beta_g V_A(t))} \quad (2.48)$$

$$\text{and } D = \frac{\beta_g V_A}{t} \log_e \left[\frac{P_{A(0)} CO}{P_A(t) CO} \right] \quad (2.49)$$

Assuming that expiration is instantaneous $P_A(t)$ can be measured directly. If it is also assumed that mixing between inspired and alveolar gas is identical for an inert insoluble gas (helium) and carbon monoxide, then $P_{A(0)} CO$ can be calculated^{188,189} since for instantaneous mixing between inspired and alveolar gas

$$P_{A(0)} CO (V_{A0} + V_T) = (V_T - V_D) P_I CO$$

and

$$P_{A(0)} He (V_{A0} + V_T) = (V_T - V_D) P_I He$$

Since helium is virtually insoluble P_{AHe} is time invariant during the breath hold and hence can be measured directly.

Thus

$$P_{A(0)} CO = P_I CO \frac{P_{AHe}}{P_I He}$$

Application of equation 2.49 to data obtained during a single breath of a gas mixture containing carbon monoxide and helium, the breath containing a long breath hold, allows, therefore, an estimate of D.

The time t in equation 2.49 is the breath-holding time. It was defined originally^{188,189} to be from the start of inspiration until that point on expiration when $P_A\text{CO}$ is measured. The assumption of instantaneous inspiration and expiration leads to errors in the estimation of D which will become more marked if inspiration or expiration is prolonged, leading in the one case to an underestimate and in the other an overestimate of D .¹⁹⁰

An extension of this analysis¹⁹¹ considers the case where inspiration and expiration are not assumed to be instantaneous but rather the inspired or expired ventilatory flow rates are assumed to be constant. Application of the analysis to experimental data gives estimates of D which are unaffected by the duration of inspiration or expiration.

This approach has been extended¹⁹² to the study of steady-state uptake of carbon monoxide. The subjects who were tested had to breathe in time to a metronome with rapid inspirations and expirations which were separated by either inspiratory or expiratory breath-holds.

The single breath method of measurement of transfer factor is also affected by maldistribution since equation 2.49 describes the homogeneous lung. Unlike the steady-state methods of measurement, as described in Section 2.3 (g), the single breath method is affected by maldistribution of inspired ventilation or diffusing capacity in relation to alveolar volume.¹⁷⁸

Models of this type have also been used to study the process of diffusion in the gas phase in the terminal lung unit.¹⁹³ In this work it is assumed that the total resistance to diffusion is located at a boundary in the lung airways, and the presence of a dead space is neglected. There are thus two compartments in

in the model - tidal volume, and alveolar compartment - both of which are treated as being well stirred with uniform concentration. Thus during any breath holding period, for a gas x

$$\dot{M}_x = K_x (P_A^x - P_T^x) \quad (2.50)$$

where K_x is a constant of diffusion and will be equal to $\frac{dx_A}{X}$ where dx is the diffusion constant for the gas, A the area of the boundary, and X the distance over which diffusion takes place. P_T^x is the partial pressure of gas in the tidal volume compartment.

Since the model is used to study inert gas wash-out the inspired gas does not contain any of the gas under study, i.e. $P_I^x = 0$. Thus at any time t after the start of the breath-hold, the mass of gas x in the tidal volume compartment is that which has been transferred from the alveolar compartment,

$$\text{i.e.} \quad V_T \beta_g P_T^x(t) = V_A \beta_g [P_A^x(0) - P_A^x(t)] \quad (2.51)$$

(the subscript x is omitted)

$P_A^x(0)$ is the partial pressure of the gas x in the alveolar compartment at the start of the breath-hold. V_A and V_T are assumed to be constant.

$$\text{Thus} \quad V_A \beta_g \frac{dP_A^x}{dt} = -K_x (P_A^x - P_T^x) \quad (2.52)$$

$$\text{i.e.} \quad \frac{dP_A^x}{dt} = \frac{-K_x}{V_A \beta_g} \left[1 + \frac{V_A}{V_T} \right] P_A^x + \frac{K_x}{V_A \beta_g} \cdot \frac{V_A}{V_T} \cdot P_A^x(0)$$

Solution of this equation gives

$$\frac{P_A^x(t)}{P_A^x(0)} = \frac{V_A}{V_L} + \frac{V_T}{V_L} \left[e - \left[\frac{K_x}{V_A \beta_g} \cdot \frac{V_L}{V_T} t \right] \right] \quad (2.53)$$

where $V_L = V_A + V_T$

$$\text{i.e.} \quad \frac{P_T^x(t)}{P_A^x(0)} = \frac{V_A}{V_T} \cdot \frac{V_T}{V_L} \left[1 - e - \left[\frac{K_x}{V_A \beta_g} \cdot \frac{V_L}{V_T} t \right] \right] \quad (2.54)$$

The authors compared experimental data from the wash-out of helium and sulphur hexafluoride to that predicted by equation 2.54.

2.7. MODELS WITH TIME-VARYING VENTILATION (DYNAMIC MODELS)

In terms of the model structure illustrated in Fig. 2.1, the respiratory cycle can be regarded to consist of three separate stages (Table 2.7) if ventilation is considered, as it is in actuality, as a time varying process.

<u>STAGE</u>	<u>CONDITION</u>
1. Inspiration of dead space gas to alveoli	$\dot{V} \geq 0$ & $\int_{t_I}^t \dot{V}_I dt < V_D$
2. Inspiration of atmospheric gas to alveoli	$\dot{V} \geq 0$ & $\int_{t_I}^t \dot{V}_I dt \geq V_D$
3. Expiration	$\dot{V} < 0$

$t = t_I$ is start of inspiration.

TABLE 2.7

Stages of respiratory cycle. It is assumed that there is "plug-flow" through the dead-space.

From the principle of conservation of mass, it is seen that for a gas which is soluble in blood but does not react chemically with blood

$$\frac{\beta_g d(V_A P_A)}{dt} = S_1 \dot{V}_g \beta_g P_D + S_2 \dot{V}_g \beta_g P_I + S_3 \dot{V}_g \beta_g P_A + \dot{Q}_b \beta_b (P_{\bar{v}} - P_a) \quad (2.55)$$

(For derivation of this equation see Appendix 1B).

If $t = t_I$ defines the start of inspiration

$$S_1 = 1 \text{ for } \dot{V} \geq 0 \text{ and } \int_{t_I}^t \dot{V} dt < V_d; \quad S_1 = 0 \text{ otherwise}$$

$$S_2 = 1 \text{ for } \dot{V} \geq 0 \text{ and } \int_{t_I}^t \dot{V} dt \geq V_D; \quad S_2 = 0 \text{ otherwise}$$

$$\text{and } S_3 = 1 \text{ for } \dot{v} < 0 \quad S_3 = 0 \text{ otherwise}$$

If it is assumed that $P_A = P_a$, that the variation in V_A due to the difference in gas flux to and from the blood can be neglected

(i.e. $\frac{dV_A}{dt} = \dot{V}$) and that at the start of inspiration $P_D = P_A$ then

$$V_A \beta_g \frac{dP_A}{dt} = S \dot{V} \beta_g (P_I - P_A) + \dot{Q} \beta_b (P_v - P_A) \quad (2.56)$$

$$S = 1 \quad \dot{V} \geq 0 \text{ and } \int_{t_I}^t \dot{V} dt \geq V_D; \quad S = 0 \text{ otherwise}$$

For an insoluble gas

$$V_A \frac{dP_A}{dt} = S \dot{V} (P_I - P_A) \quad (2.57)$$

whereas if the gas combines chemically with blood (e.g. oxygen or carbon dioxide) then

$$V_A \beta_g \frac{dP_A}{dt} = S \dot{V} \beta_g (P_I - P_A) + \dot{Q} \left[f_1(P_v) - f_2(P_A) \right] \quad (2.58)$$

where f_1 and f_2 are functions relating partial pressure and concentration in mixed venous and arterial blood respectively.

In the special case of carbon dioxide the relationship between concentration and partial pressure can be approximated by a linear relationship of slope $\beta_b(\text{CO}_2)$ and thus

$$V_A \beta_g \frac{dP_A}{dt} = S \dot{V} \beta_g (P_I - P_A) + \dot{Q} \beta_b(\text{CO}_2) (P_v - P_A) \quad (2.59)$$

In derivation of these basic equations for dynamic models of gas transport it is assumed that for gases which are in solution in lung tissue ¹⁹⁴ that there is identity between the partial pressure of the gas species in lung gas and that in lung tissue. For such gases the V_A in equations 2.56, 2.58, 2.59 is an effective lung volume and includes not only the gas volume contained in alveoli but also the mass of the gas species in pulmonary tissue expressed as an equivalent gas volume. It is also assumed that there is no

difference in partial pressure between end-capillary blood and alveolar gas, that there is plug-flow through the dead space, and that pulmonary capillary blood-flow is constant.

The history of development of such dynamic models is considered in the next section of this chapter, as are modifications to these basic equations.

It should be emphasised that for each system of algebraic equations for steady-state models there is a corresponding system of ordinary differential equations for the equivalent dynamic model. Since in dynamic models ventilation is considered as a cyclic process it may be necessary to make additional assumptions in derivation of the equivalent dynamic equations.

For example for the three compartment model of Riley (Figure 2.6) the equivalent dynamic equation for the "ideal" alveolar compartment is

$$V_1 \beta_g \frac{dP_1}{dt} = S_1 k \dot{V} \beta_g (P_D - P_1) + S_2 k \dot{V} \beta_g (P_I - P_1) + (\dot{Q} - \dot{Q}_s) [f_1(P_{\bar{v}}) - f_2(P_1)] \quad (2.60)$$

when subscript 1 relates to the "ideal" alveolar compartment and k is the fraction of ventilation to this compartment.

In this dynamic model with cyclic ventilation assumptions have to be made about the distribution of dead space gas which is re-inspired. It is here assumed that dead space gas is distributed to the two compartments in proportion to their ventilation.

During expiration gas which enters the dead space passes through it and is expelled to the atmosphere until time $t = t^*$

where $\int_{t_E}^{t^*} |\dot{V}_E| dt = V_T - V_D$

and $t = t_E$ defines the start of expiration. During this phase of the respiratory cycle the partial pressure of gas entering the dead space is

$$P_D(t) = k P_1(t) + (1-k) P_2(t)$$

where subscript 2 relates to the alveolar dead space compartment.

If it is assumed that gas flow through the dead space has a square wave front with no mixing in the dead space then in phase 1 of the next respiratory cycle gas leaving the dead space to enter the alveolar compartment has partial pressure

$$P_D(t) = k P_1(t-\lambda) + (1-k) P_2(t-\lambda) \quad (2.61)$$

where λ is a flow-dependent time delay defined by the equation

$$\int_{t_I}^t |\dot{V}_I| dt = \int_{t_I - \lambda}^{t_I} |\dot{V}_E| dt$$

where $t = t_I$ is the start of inspiration.

Similarly for the alveolar dead space compartment

$$V_2 \frac{dP_2}{dt} = S_1 (1-k) \dot{V} (P_D - P_2) + S_2 \dot{V} (1-k) (P_I - P_2) \quad (2.62)$$

2.7(b). DEVELOPMENT OF DYNAMIC MODELS.

Models such as those described by equations (2.56 - 2.59) were used originally by Chilton & Stacy¹⁹⁵ Chilton et al,¹⁹⁶ and Dubois et al.¹⁹⁷ The term "effective alveolar volume" is introduced by these authors to take account of the gas which is present in lung capillaries and lung tissue in addition to that present in alveolar gas. The authors to a large extent used analytical methods for solution of the model equations. Analytical methods can be applied in certain specialised cases:-

(a) Breath-holding

For breath-holding $\dot{V} = 0$ and

$$V_A \frac{dP_A}{dt} = \frac{\dot{Q}}{\beta_g} \left[f_1(P_{\bar{v}}) - f_2(P_A) \right]$$

For those gases where $C_{\bar{v}} = a + bP_{\bar{v}}$, $C_a = a + bP_a = a + bP_A$

this reduces to

$$\frac{dP_A}{dt} = \frac{\dot{Q}b}{V_A \beta_g} (P_{\bar{v}} - P_A) \quad (2.63)$$

(For the analysis of oxygen transport Chilton et al¹⁹⁶ assumed that C_a is constant i.e. haemoglobin is fully saturated, and that $C_{\bar{v}}$ is constant, thereby simplifying the analysis.)

Equation (2.63) can be solved analytically to give

$$P_A = P_{\bar{v}} - \left[P_{\bar{v}} - P_A(0) \right] e^{-\frac{\dot{Q}b}{V_A \beta_g} t} \quad (2.64)$$

(b) Inspiration (\dot{V} constant) (Phase II of respiratory cycle) ($\dot{V}=K$)

$$V_A \beta_g \frac{dP_A}{dt} = K \beta_g (P_I - P_A) + \dot{Q}b (P_{\bar{v}} - P_A) \quad (2.65)$$

which is of the form

$$\frac{dP_A}{dt} + C_1 P_A = C_2 \quad (2.66)$$

where $C_1 = \frac{K}{V_A} + \frac{\dot{Q}b}{V_A \beta_g}$,

and $C_2 = \frac{K}{V_A} P_I + \frac{\dot{Q}b}{V_A \beta_g} P_{\bar{v}}$

for which the analytical solution is

$$P_A(t) = C_3 + (P_A(0) - C_3) e^{-\frac{(K \beta_g + \dot{Q}b)}{V_A \beta_g} t} \quad (2.67)$$

where

$$C_3 = \frac{K \beta_g P_I + \dot{Q}b P_{\bar{v}}}{K \beta_g + \dot{Q}b} \quad (2.68)$$

A relatively crude numerical method was also employed by Dubois et al.¹⁹⁷

A similar approach has been used by Yamamoto¹⁹⁸ although the equations are formulated as integral equations. Nye¹⁹⁹ used equation 2.58 and a numerical method of solution to investigate the effects of different patterns of ventilation on respiratory gas exchange. Two varieties of model are used, non-homeostatic, in which the mixed venous concentration and alveolar ventilation are fixed, and homeostatic in which the arterial $p\text{CO}_2$ is adjusted to a predetermined value by alteration of tidal volume. Various patterns of breathing were investigated - early vs. late peak expiratory flow, early vs. late peak inspiratory flow, influence of frequency and of relative durations of inspiration and expiration. These exerted minimal effect on the efficiency of gas transport at low levels of oxygen uptake.

With numerical methods of solution of such equations additional refinements to the model can be incorporated.

Murphy^{200,201} considered the case where \dot{Q} is not assumed to be constant but rather pulsatile. \dot{Q} is, therefore represented as a function of time, the form of which is such that there are pulsations in \dot{Q} at the same frequency as the heart beat. The presence of a pulsatile blood flow produces small cardiogenic oscillations in the predicted alveolar partial pressure.

Similar forms of functions have been used in the analysis of Flumerfelt & Crandall²⁰² and Lin & Shir.²⁰³ In these analyses there are more detailed descriptions of flow and diffusion in pulmonary capillaries and they are considered in a later section of this chapter. (Section 2.8 c).

In another more complex model describing alveolar-capillary diffusion²⁰⁴ the author distinguishes between two different physiological mechanisms through which pulsatile blood flow may be mediated - pulse velocity and pulse recruitment. In the former capillary blood volume is constant and the blood velocity through the capillaries is pulsatile, whereas in the latter the velocity is held constant and the capillary volume is varied.

The effect of phase differences between ventilation and blood flow has also been studied²⁰⁵ although in this study it is assumed that they can both be described by sinusoidal functions at the same frequency. In more recent work the description of gas stored in lung tissue and pulmonary capillaries has been improved. In the first place it is possible to consider lung capillary volume independent of lung volume. In the work of Meade et al.,²⁰⁶ this is achieved by making the assumption that mixed venous blood achieves instant equilibrium for carbon dioxide with alveolar gas. (This assumption is not stated explicitly by the authors.) Thus the net transfer of CO₂ from capillaries into alveolar gas in the time Δt is

$$V_c b P_A(t + \Delta t) - V_c b P_A(t) - \dot{Q} b \Delta t [P_{\bar{v}}(t) - P_A(t)]$$

and thus for the alveolar compartment

$$\beta_g (V_A P_A)(t + \Delta t) - \beta_g (V_A P_A)(t) = \Delta t \dot{V}_D \beta_g - V_c b P_A(t + \Delta t) + V_c b P_A(t) + \dot{Q} b \Delta t [P_{\bar{v}}(t) - P_A(t)]$$

Dividing by Δt and taking the limit as $\Delta t \rightarrow 0$ this becomes

$$\beta_g \frac{d(V_A P_A)}{dt} = \beta_g \dot{V}_D - V_c b \frac{dP_A}{dt} + \dot{Q} b (P_{\bar{v}} - P_A)$$

(V_A here is the gas and lung tissue volume).

Expanding the derivative on the left hand side and assuming that

$$\frac{dV_A}{dt} = \dot{V} \quad \text{this becomes}$$

$$\left[V_A + \frac{bV_C}{\beta g} \right] \frac{dP_A}{dt} = \dot{V} (P_D - P_A) + \frac{\dot{Q}_b}{\beta g} (P_{\bar{v}} - P_A)$$

Thus

$$V_{A_{\text{eff}}} = V_A + \frac{bV_C}{\beta g}$$

It is thus evident that this approach produces no change in the analysis and results.

Other workers have not used the assumption of instantaneous equilibrium in the pulmonary capillaries but rather have described explicitly the process of gas transfer between alveolar gas and pulmonary capillary blood. Such models consider partial pressure in the pulmonary capillary as a function therefore not only of time but also of distance along the capillary and are thus discussed more properly in the section on distributed models (Section 2.8c).

Lung tissue has also been considered explicitly in certain models. Yamamoto & Hori²⁰⁷ analysed a model in which the three components - alveolar gas, lung tissue and pulmonary capillary blood - are in series. As a result of the lumped nature of the model it is again necessary to assume that the partial pressure in pulmonary capillary blood is that of arterial blood, i.e. the mass balance equations are

Alveolar Space

$$\beta_g V_A \frac{dP_A}{dt} = \beta_g \dot{V} (P_D - P_A) + K_{AP} (P_{\bar{v}} - P_A) \quad (2.69)$$

Lung Tissue

$$S_P V_P \frac{dP_P}{dt} = K_{AP} (P_A - P_P) + K_{PC} (P_{\bar{v}} - P_P) \quad (2.70)$$

Pulmonary Blood

$$S_C V_{cL} \frac{dP_a}{dt} = S_C \dot{Q} (P_{\bar{v}} - P_a) + K_{PC} (P_P - P_a) \quad (2.71)$$

S represents solubility of the gas under study, K_{AP} , K_{PC} are rate constants, V_{CL} is the pulmonary capillary blood volume, and the subscripts p & c refer to lung tissue and pulmonary capillary blood respectively.

In the model of Hlastala²⁰⁴ the relationship between CO_2 flux between capillary blood and lung tissue ($\dot{V}CO_2$) and CO_2 flux between lung tissue and alveolar gas (\dot{V}^1CO_2) is given by

$$\dot{V}CO_2(i) = \dot{V}CO_2(i) + \frac{V_P CO_2(i) - V_P CO_2(i+1)}{\Delta t} \quad (2.72)$$

where time is divided into small increments (Δt), and the subscript i refers to the ith such increment. The volume of CO_2 in lung tissue ($V_P CO_2$) at any time is defined by

$$V_P CO_2(i) = \frac{P_A CO_2(i) + P_c CO_2(i)}{2} \cdot S_P CO_2 \cdot V_P \quad (2.73)$$

where V_P & S_P are as defined previously, and $P_c CO_2$ the mean pCO_2 in the pulmonary capillaries.

The description of mixing between inspired gas and alveolar gas has also been refined. In the earliest models it is assumed that gas is convected through the dead space with a square wave front. In order to simulate an increased mixing process between inspired and dead space gas Hlastala²⁰⁴ assumes that the partial pressure of the gas which enters the alveoli from the dead space during inspiration

(P_{DA}) is

$$P_{DA}(t) = P_D \text{ for } \int_0^t \dot{V}_I dt < V_D - 50$$

$$P_{DA}(t) = P_D + \frac{P_I - P_D}{100} \left[\int_0^t \dot{V}_I dt - V_D + 50 \right]$$

$$\text{for } V_D - 50 \leq \int_0^t \dot{V}_I dt \leq V_D + 50$$

and $P_{D_A}(t) = P_I$ for $\int_0^t \dot{V}_I dt > V_D + 50$

where P_D is defined to be the partial pressure of gas in the dead space at the end of the previous expiration.

i.e.
$$P_D = \frac{\int_{t^x}^t \dot{V}_E P_A dt}{\int_{t^x}^t \dot{V}_E dt}$$

where t^x is such that $\int_{t^x}^t |\dot{V}_E| dt = V_D$

Such a description corresponds to linear mixing between atmospheric gas and dead space gas from an inspired volume of 50 ml less than the dead space to 50 ml greater than dead space volume.

A more complex description is used by Lin & Cumming.²⁰⁸

Dead space volume is considered to be time variant and alveolar ventilation is thus defined by

$$\dot{V}_A(t) = \dot{V}(t) - \frac{dV_D(t)}{dt} \quad (2.74)$$

The time variation of dead space is obtained from an analysis of a distributed model of gas transport carried out by one of the authors,²⁰⁹ in which concentration of gas in the lung is considered not only as a function of time but also as a function of distance (x) from the mouth. From concentration profiles calculated from use of this model, dead space is defined to be

$$V_D(t) = \int_0^X \frac{C(x,t) - C_A}{C_I - C_A} A(x) dx \quad (2.75)$$

where $A(x)$ is the cross-sectional area of the airways at any point, and X the alveolar-capillary membrane. This definition in essence considers any complex concentration profile in the airways as one in

which there is a sharp boundary between inspired and alveolar gas.

The position of this imaginary boundary is such that the lung

will contain the same total amount of that gas species

$$\text{i.e.} \quad \int_0^X C(x)A(x) dx = \int_0^{x^*} C_I A(x) dx + \int_{x^*}^X C_A A(x) dx$$

where $x = x^*$ represents that boundary.

$$\text{i.e.} \quad \int_0^X C(x)A(x) dx = C_I \int_0^{x^*} A(x) dx + \int_0^X C_A A(x) dx - \int_0^{x^*} C_A A(x) dx$$

$$\text{but} \quad \int_0^{x^*} A(x) dx = V_D$$

and therefore

$$\int_0^X (C(x) - C_A) A(x) dx = V_D (C_I - C_A)$$

thus giving equation (2.75).

The calculations carried out using this approach show that at the start of inspiration $\dot{V}_A(t) = 0$ as $\dot{V}(t) = \frac{dV_D(t)}{dt}$. This is also the case with the more basic models. In late inspiration as $\dot{V}(t)$ falls (a sinusoidal \dot{V} is used) $\dot{V}_A(t)$ may actually exceed $\dot{V}(t)$ since dead space volume is reduced as a result of diffusional processes. The difference this refinement makes to the results is minimal during normal breathing as is seen from the calculations of these authors.

2.8 DISTRIBUTED MODELS OF GAS TRANSPORT.

a) A review of previous models of gas transport in the airways.

In the models which have been discussed so far in this chapter a lumped parameter approach has been employed, but as indicated in Section 2.3 (e) the complex process of gas transport in the airways can only be described by distributed models.

The first approach to this problem was that of Rauwerda²¹⁰ who modelled diffusion in the terminal lung unit, which is represented by a closed cylinder of length 0.7 cm. Diffusion in such a structure occurred rapidly in relation to the breath cycle. This geometric structure is, however, inappropriate as is seen from comparison with the anatomical data of Weibel²¹¹ (see Fig. 2.10). A second model considered by Rauwerda²¹⁰ was a closed truncated cone, the geometry of which is equally inappropriate.

Cumming et al. investigated a number of geometric structures²¹² and found that the result obtained as to the rapidity of diffusion depended on the form of geometry chosen. All models are, however, relatively poor representations of the actual structure (see Fig. 2.10). These workers used convenient mathematical structures, i.e. convenient from the mathematician's view point, and were limited by the use of analytical techniques to solve the diffusion equation.

More appropriate geometric structures have been used more recently (see Fig. 2.10) and computer-based numerical methods for solution of the diffusion equation.²¹³

The first attempt to study simultaneously convection and diffusion is that of Cumming et al.²¹⁴ The diffusion equation is solved numerically, with convection being considered to result in a moving boundary between a region in the airways in which convection is assumed the only transport process and the terminal

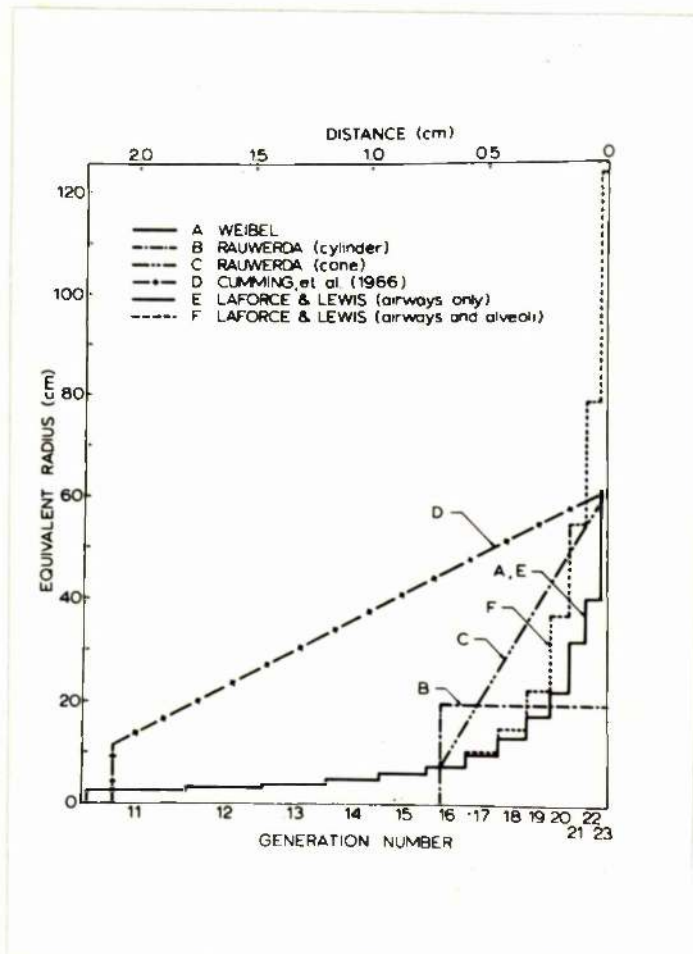


FIGURE 2.10

Comparison of structures of various models, which have been used to describe gas transport in airways, with anatomical data (A) of Weibel.²¹¹ The models shown are those of Rauwerda,²¹⁰ Cumming et al,²¹² and LaForce & Lewis,²¹³ This figure is taken from the review of Chang et Farhi.²²⁴

lung unit in which only diffusional transport occurs.

Equations which have included explicitly both convection and diffusion have been solved numerically but only for limited regions of the bronchial tree. In the work of Paiva²¹⁵ the last thirteen generations of the bronchial tree are modelled with the entry to the model therefore being situated 1.6 cm. from its extremity. Baker et al²¹⁶ modelled conversely the earlier generations of the bronchial tree (0-17) with the volume of generations (18-23) being lumped together into a single well-stirred alveolar compartment. One of the main deficiencies of these analyses is that a constant value for the diffusion coefficient equal to that for molecular diffusion has been used whereas there is strong theoretical and experimental evidence²¹⁷⁻²²¹ that the effective diffusion coefficient varies markedly in the presence of convection (Taylor diffusion). It has been suggested²⁰⁹ that Taylor diffusion is the dominant transport mechanism in generations eight to twelve.

Certain preliminary results for a model of the complete bronchial structure were obtained using an analytical method by Pedley.²²² It is assumed in this analysis that at any point in the bronchial tree the product of total cross-sectional area and the effective diffusion coefficient is constant. Such an assumption is justified on the grounds that it is approximately correct for the extremities of the model (the trachea and twenty-third generation) and there is great uncertainty about the intermediate region due to the complex flow and concentration profiles which are found.¹³⁵ Pedley's analysis has also been

used in the more detailed studies of Davidson.²²³

The deficiencies of these previous analyses have been listed recently in a review by Chang and Farhi²²⁴ (see Table 2.8). The author has developed an analysis which corrects for most of these deficiencies, and the model of gas transport which is employed considers simultaneously convection and diffusion in the entire bronchial tree. In this analysis it is assumed that:-

- a) the lung is a symmetric branching structure;
- b) the airways are compliant, their compliance being proportional to the surface which is alveolated;
- c) radial mixing between the gas in alveolar ducts and alveoli is instantaneous;
- d) the effective diffusion coefficient is enhanced in the presence of convective flow.

The increased mixing due to cardiac action²²⁵ is neglected, as is the detailed anatomy of the terminal lung unit. The latter has been considered in a number of analyses²²⁶⁻²²⁸ which have been restricted to description of events in only the terminal lung unit. This model is presented briefly in this section.

b) A model of convection and diffusion in pulmonary airways.

The lung is represented as a regular dichotomy of airways. Each of the 2^z branches of the z^{th} generation ($0 \leq z \leq 23$) is taken to have identical dimensions, so that the position of any point in the airways is then characterised by its axial distance x from the origin of the trachea. Associated with each axial distance x are the properties of the appropriate generation (such as number of branches, branch diameter, total cross-sectional area of airways and number of alveoli) as given for example by Wiebel²¹¹ or any other morphometric data that is appropriate to a symmetrical

ASSUMPTIONS EMPLOYED IN MATHEMATICAL ANALYSES OF GAS TRANSPORT	
1)	Airways are rigid and have constant volumes.
2)	Flux across the alveolar wall is unimportant.
3)	Diffusion alone is the mechanism for gas mixing in the alveolar region of the lung.
4)	There is a stationary "front" of inspired gas termed by some as a diffusion front.
5)	The diffusion front is a square one, i.e. concentration is initially uniform over the cross section of the front.
6)	Only axial diffusion is significant.
7)	Only two gases are involved in the diffusional process.

TABLE 2.8

branching model. The equations of this model are developed below.

(1) Cross-sectional areas A_A and A_T .

The cross-sectional areas of all the airways at distance x are summed to give a combined airway area $A_A(x,t)$.

Clustered about the terminal airways are alveoli which contribute to the total lung volume. To allow for this a total cross-sectional area $A_T(x,t)$ is introduced, such that the difference $A_T(x,t) - A_A(x,t)$ corresponds to the volume of alveoli in unit length of airway.

To simulate the expansion of the lung during respiration these cross-sectional areas are considered to fluctuate about a mean value $A_{IO}(x)$

$$A_I(x,t) = A_{IO}(x) (1 - f(x)b(t)) \quad (2.76)$$

where $I = A$ (for "airways") or T (for "total"), $b(t)$ is an oscillatory function of time, and $f(x)$ is a "flexibility function". In the simplest form of the model, $b(t)$ may be a sinusoidal function $b_0 \cos \omega t$ with b_0 and ω chosen to give the desired tidal volume and respiratory frequency. The flexibility function $f(x)$ takes account of the varying fractional expansion that occurs at different axial distances x .

The particular form of Equation 2.76 neglects the axial distension during respiration for which there is evidence²²⁹ but to take account of this would require a considerable increase in mathematical complexity, without affecting radically the velocity distribution in the lung. Even with this simplification, there is a lack of experimental evidence on the precise form of $f(x)$.^{229,230} It is, however, expected that expansion of the lung occurs largely in the alveolated region and $f(x)$ is therefore set equal to the

fraction of the airway surface alveolated as given by Weibel²¹¹. This corresponds to putting $f(x) = 0$ for the first sixteen generations after which it increases to 1.0 for the 20th and succeeding generations. Preliminary results suggest that this simulation is relatively insensitive to the precise form of $f(x)$.

(2) Gas partial pressure p.

The transport of a particular gas constituent is considered in terms of its partial pressure $p(x,t)$ varying axially with x and during the breathing cycle with time t . This partial pressure $p(x,t)$ will be the mean value, averaged over any radial variation across a branch.

Variation of pressure p with time occurs due to convection (at velocity $u(x,t)$ through airway area $A_A(x,t)$), due to diffusion (effective diffusion coefficient $D(x,t)$) and due to gas transfer through the alveolar membrane, giving respectively the three terms on the right-hand side of equation (2.77).

$$\frac{\partial}{\partial t} (A_T p) = \frac{-\partial}{\partial x} (A_A u p) + \frac{\partial}{\partial x} (A_A D \frac{\partial p}{\partial x}) - F \quad (2.77)$$

(For derivation of this equation see Appendix 1.C).

To solve the equation for p , all the other quantities appearing need to be specified, as well as the initial conditions $p(x, t = 0)$ and the boundary conditions $p(x = 0, t)$ and $p(x = L, t)$ during breathing, where $x = L$ corresponds to the extremity of the lung model.

(3) Convective flow velocity u.

If it is assumed that the net effect of diffusion, and gas transfer of all the gas constituents present makes a much smaller contribution to the convective flow velocity than the

variation in lung dimensions, then

$$u(x,t) = \frac{1}{A} \int_x^L \frac{\partial A_T}{\partial t} dx \quad (2.78)$$

(4) The effective diffusion coefficient D.

The molecular diffusion coefficients D_{mol} for the respiratory gases in air are known. D_{mol} is, however, only the appropriate diffusion coefficient in the absence of convective flow, whereas in fact during normal breathing, flow velocities of 250 cm/s (and Reynolds numbers of about 2000) are attained. In these circumstances, radial concentration and velocity gradients develop which affect the net axial diffusion rate, as measured relative to the average flow velocity. In conditions of steady laminar flow, for Reynold's numbers up to about 1500, the appropriate diffusion coefficient D is given by the Taylor-Aris equation^{217,218}

$$D(x,t) = D_{mol} + \frac{d^2 u^2}{192 D_{mol}} \quad (2.79)$$

where $d(x)$ is the diameter of the individual airways at axial distance x , and $u(x,t)$ is the convective flow velocity at that instant, averaged across the airway. Both u and d vary, but under typical lung conditions, the second term on the right-hand side of Equation 2.79 (the "radial-diffusion" correction) dominates the first for the first thirteen generations, i.e. for all but the last 1.4 cm of an axial length of about 26 cm.

This form of the effective diffusion coefficient applies only to conditions of steady laminar flow with diffusive equilibrium established. In other situations a more correct form of the expression is

$$D = D_1 + D_2 = D_{\text{mol}} + \alpha \frac{d^2 u^2}{192 D_{\text{mol}}} \quad (2.80)$$

where the added coefficient α in the Taylor-Aris term may be less than 1. In the first place this happens when turbulent flow develops (Reynold's number, $Re > 1500$)²¹⁹ and therefore at brief moments of peak flow during normal breathing when Re approximating 2000 are found in the upper airways, a transitory and spatially limited reduction of α will occur.

The effective diffusion coefficient is also reduced when radial concentration and/or velocity gradients are developing near the start of a tube. The Taylor-Aris theory was originally considered for laminar flow through infinite cylindrical tubes. The necessary extensions to the Taylor-Aris theory have been studied experimentally²¹⁹ and theoretically.^{220,221,231,232} Flint and Eisenklam²¹⁹ showed experimentally that in the laminar flow regime, the effective diffusivity falls below the Taylor-Aris value for flow through tubes of finite length/diameter ratio. This conclusion is supported by the theoretical work of Gill et al. who calculated the dispersion of matter in various circumstances: where the flow velocity is initially zero but develops towards an equilibrium flow pattern,²³¹ where the flow velocity is fluctuating with time,²²⁰ and where initially the concentration varies radially in a non-equilibrium pattern.²²¹ The results are analytically complex, and often involve the sums of infinite series, but when evaluated they support the general conclusion that if a disturbance abolishes the concentration gradient $\frac{\partial p}{\partial v}$, or the velocity gradient $\frac{\partial v}{\partial r}$, then the Taylor diffusivity is initially zero, but rises to its full value as the flow equilibrates. The situation obtaining at bifurcations of lung airways¹³⁵ defies an exact analysis, but the conclusions are expected to be similar. These imply that the coefficient α in equation 2.80 can be considered time dependent being

near zero at a junction, rising linearly with elapsed time from leaving the junction and levelling off to 1.0 as equilibrium is approached.

An alternative empirical form of the effective diffusion coefficient is that obtained by Scherer et al.²³³ from measurement of the dispersion of benzene vapour in a five generation glass reconstruction of the bronchial tree, i.e.

$$D = D_{\text{mol}} + 0.36 \text{ ul (for inspiration)} \quad (2.81)$$

$$D = D_{\text{mol}} + 0.12 \text{ ul (for expiration)} \quad (2.82)$$

The lower value obtained for the effective diffusion coefficient for expiration is thought to be the result of the increased radial mixing which occurs during expiration due to the complex flow patterns produced.¹³⁵

(5) Initial conditions.

The solution of equation (2.77) requires that the initial value of the partial pressure p is specified throughout the lung. If the volume of gas in the lung is distributed over the axial length x from the origin at the trachea, the major part lies in the last few centimetres ($x \sim L$). The initial gas content of the lung expressed as $\int p dV$ will be reasonably correct provided a typical value is given to the partial pressure of gas in the alveoli. With this proviso, the results of the calculation are found to be relatively insensitive to the initial partial pressure distribution assumed. A pressure that is initially uniform at a typical alveolar value is adopted. This is in good agreement with the situation found at the end of one breathing cycle, and the calculations begin at an instant just prior to the start of inspiration.

(6) Boundary conditions.

To specify the solution of equation (2.77) uniquely, the boundary conditions at $x = 0$ and $x = L$ need to be specified:

(a) At $x = 0$. During inspiration, the partial pressure $p(x=0,t)$ is that of the inspired gas. During expiration $p(x = 0, t + \tau)$ is calculated on the basis of information at the previous timestep using the approximation

$$A_T p(x=0, t + \tau) = A_T p(x=0, t) + \tau \frac{\partial}{\partial t} A_T p(x=0, t) \\ = \left[A_T p + \tau \left\{ \frac{\partial}{\partial x} (A_A u p) + \frac{\partial}{\partial x} \left(A_A D \frac{\partial p}{\partial x} \right) \right\} \right] \quad (2.83)$$

where the expression enclosed $[\quad]$ is evaluated at $x = 0$, and time t . The alveolar absorption term in equation (2.77) is negligible near $x = 0$.

(b) At $x = L$. At any point in the model the net flux of gas, G , is given by

$$G(x, t) = A u p - A D \frac{\partial p}{\partial x} \quad (2.84)$$

This is the sum of convective and diffusive terms. At $x = L$, the convective flow velocity u is zero. In order that $G(x = L, t) = 0$ at all times the boundary condition

$$\left(\frac{\partial p}{\partial x} \right)_{x=L} = 0 \quad (2.85)$$

is imposed in all cases.

The equations of this model can be solved using a numerical differencing method. (This aspect of the work has been carried out by my collaborator, Dr. Michael Hooper). Results using this model give insight into the effect of Taylor diffusion. These results are presented as part of the discussion in Chapter 4 of this thesis and are presented elsewhere.⁴⁰¹ The model has also been formulated such that the measured flow velocity at the trachea, i.e. $u(0, t)$ (e.g. obtained from experimental data) can be incorporated directly in the model since the flow velocity at different x may be related to $u(0, t)$ by

$$u(x,t) = u(0,t) \frac{A_{A(0,t)}}{A_A(x,t)} \frac{\int_{x_{To}}^L A_{To}(x') f(x') dx'}{Vf} \quad (2.86)$$

$$\text{where } Vf = \int_0^L A_{To}(x') f(x') dx'$$

$$\text{and } b(t) = b(t=0) - \frac{\int_0^t u(0,t) A_A(0,t) dt}{Vf} \quad (2.87)$$

This will allow direct comparison between experiment and model.

(c) Distributed models of diffusion across the alveolar capillary membrane.

Distributed models have also been applied to the description of gas transfer across the alveolar-capillary membrane. Such models in general describe the homogenous lung and the same assumptions are made as for the derivation of equation (2.19).

For a single capillary path and for a gas for which the relationship between tension and concentration in blood is linear, consider a small length of capillary Δl . For that small length of capillary in a small increment of time Δt :-

Mass change = Addition by blood-flow convection - Loss by blood-flow convection + addition by diffusion.

i.e.

$$\Delta l AC(t+\Delta t, l) - \Delta l AC(t, l) = u(t, l) \Delta t AC(t, l) - u(t, l+\Delta l) \Delta t AC(t, l+\Delta l) + d_{unit} \Delta l \Delta t (P_A - P_C(t, l)) \quad (2.88)$$

where A is the cross-sectional area of capillary

$u(t, l)$ the velocity of blood flow at time t , length l .

d_{unit} the diffusing capacity of the capillary per unit length.

But assuming that all n capillaries are identical (length = L) and that D is distributed uniformly along each capillary then

$$d_{unit} Ln = D$$

$$\text{and } AnL = V_C$$

$$\text{i.d. } \frac{d_{unit}}{A} = \frac{D}{V_C}$$

Thus by dividing equation (2.88) throughout by Δl , Δt and A and taking the limit as $\Delta l \rightarrow 0$ and $\Delta t \rightarrow 0$ we obtain

$$\frac{\partial C}{\partial t} = -u(t) \frac{\partial C}{\partial l} + \frac{(P_A - P_C) D}{V_C} \quad (2.89)$$

or alternatively since $C = \beta_b P_C$

$$\frac{\partial P_C}{\partial t} + u(t) \frac{\partial P_C}{\partial l} = \frac{(P_A - P_C) D}{\beta_b V_C} \quad (2.90)$$

This equation is derived fully by Crandall and Flumerfelt²³⁴ and a method of solution described.

For oxygen and carbon dioxide the equation is complicated not only by the non-linear relationship between tension and concentration, but also by the chemical reaction of these gases in blood. In this case, since

$$\frac{\partial C}{\partial t} = \frac{\partial C}{\partial P} \cdot \frac{\partial P}{\partial t}; \quad \frac{\partial C}{\partial l} = \frac{\partial C}{\partial P} \cdot \frac{\partial P}{\partial l}$$

equation (2.89) can be written

$$\frac{\partial P_C}{\partial t} + u(t) \frac{\partial P_C}{\partial l} = \frac{(P_A - P_C) D}{\left(\frac{\partial C}{\partial P}\right) V_C} \quad (2.91)$$

where D is as defined in equation (2.21).

Since θ is dependent on P_C , D is a function of P_C as was considered originally in the analysis of Staub et al.²³⁵

In most work in this area²³⁴⁻²³⁹ a special case of equation (2.91) is used in which pulmonary-capillary blood flow is considered constant. There will, therefore, be steady-state conditions with concentration at any point in the capillary invariant with time, i.e.

$$u \frac{dc}{dl} = \frac{(P_A - P_C) D}{V_C} \quad (2.92)$$

Alternative forms of this equation are

$$\frac{dc}{dl} = \frac{D}{L} \frac{(P_A - P_C)}{Q} \quad (2.93)$$

($u = \frac{\dot{Q}}{nA}$, $V_C = LnA$) which is identical to equation (2.32) and

$$\frac{dc}{dt} = \frac{(P_A - P_C)}{V_C} \cdot D \quad (2.94)$$

(dl = udt)

Numerical methods of solution have been applied to solution of equation (2.94) for oxygen and carbon dioxide although in earlier work there is reliance on graphical methods.^{240,241,242} The solution for this equation indicates that diffusion impairment has significant effects on both carbon dioxide and oxygen transfer.^{238,239}

The alveolar partial pressure in the equations in this section is considered generally to be constant. It is, however, possible^{202,203} to couple the partial differential equations which describe gas transfer across the alveolar-capillary membrane with the ordinary differential equations which are detailed in section 2.7. The basic dynamic model equation for oxygen (equation 2.58) will become

$$V_A \beta g \frac{dP_A}{dt} = \dot{S}V \beta g (P_I - P_A) - \int_0^L \frac{D}{V_C} (P_A - P_C) Adl \quad (2.95)$$

where the last term describes the total flux of oxygen across the alveolar-capillary membrane.

C H A P T E R 3

APPLICATION OF DYNAMIC MODELS OF PULMONARY GAS
EXCHANGE TO MEASUREMENT

Experimental and Computing Methods

CHAPTER 3. APPLICATION OF DYNAMIC MODELS OF PULMONARY GAS EXCHANGE TO MEASUREMENT /METHODS.

3.1. INTRODUCTION.

With steady-state models the parameters to be measured can be obtained directly by manipulation of the algebraic equations forming the model. For example in measurement of cardiac output (\dot{Q}) using the Fick principle²⁴² \dot{Q} is obtained directly from equation (3.1) after substitution of the measured variables:-

$$\dot{M}O_2 = \dot{Q} (C_aO_2 - C_vO_2) \quad (3.1)$$

With dynamic models such simple substitution is impossible and use must be made of parameter estimation techniques.¹¹²⁻¹¹⁴ One approach (the model reference approach) (see Figure 12, Chapter 1) was considered briefly in Chapter 1.11.

In applying this approach to dynamic models of pulmonary gas exchange, the input of the system is the mass flow rate of the gas species under study which enters the alveolar compartment (i.e. the term \dot{SVP}_I in the equations which were described in Chapter 2.7). One of the outputs of the system is the partial pressure of alveolar gas. Thus the model reference approach can be applied since \dot{V} (flow-rate of gas at the mouth), P_I (partial pressure of inspired gas), and P_A (alveolar partial pressure, which is assumed to be identical to the partial pressure of end expiratory gas) are all measurable directly by non-invasive methods. The lung has thus a particular advantage in this respect since the inputs and outputs to most other physiological systems are inaccessible to measurement.

Comparison of the measured variables with the corresponding model prediction has to be carried out iteratively with different sets of model parameter values. An efficient computational method

for solution of the model equations with input quantities obtained continuously by direct measurement is, therefore, essential.

3.2. SOLUTION OF MODEL EQUATIONS.

In the general case there are no simple analytical solutions for the equations of dynamic models. In certain special cases solutions can be obtained by analytical means, e.g. when $\dot{V} = 0$ (breath-holding), $\dot{V} = \text{constant}$, or $\dot{V} = a+bt$ (linear approximation to ventilatory flow). (See Chapter 2.7b). In order, therefore, to obtain solutions of these equations in the general case in which \dot{V} is a continuously measured quantity, various methods of computer solution have been investigated.

a) Analogue-computation.

The electronic analogue computer, which was described in Chapter 1.9 and in more detail in Appendix 2, provides the simplest method of solution. The circuit diagram for solution of equation (2.57) is shown in Figure 3.1, in which the components are indicated diagrammatically by standard symbols (for details of standard symbols see Table 1.4.) The technique can be applied easily to the solution of equations when the inputs are the electrical signals representing the measured ventilatory flow (\dot{V}) and inspired gas partial pressures (P_I). Furthermore because of the time-scaling facilities of the analogue computer the equations can be solved much faster than real-time. This is particularly useful in this application since the equations of the model have to be solved repetitively with different sets of parameter values.

As discussed in Chapter 1 the analogue computer has certain limitations. Moreover, the expertise required of the operator would be a limiting factor in applying routinely techniques which are based on analogue computation. Digital computer methods have also, therefore, been investigated.

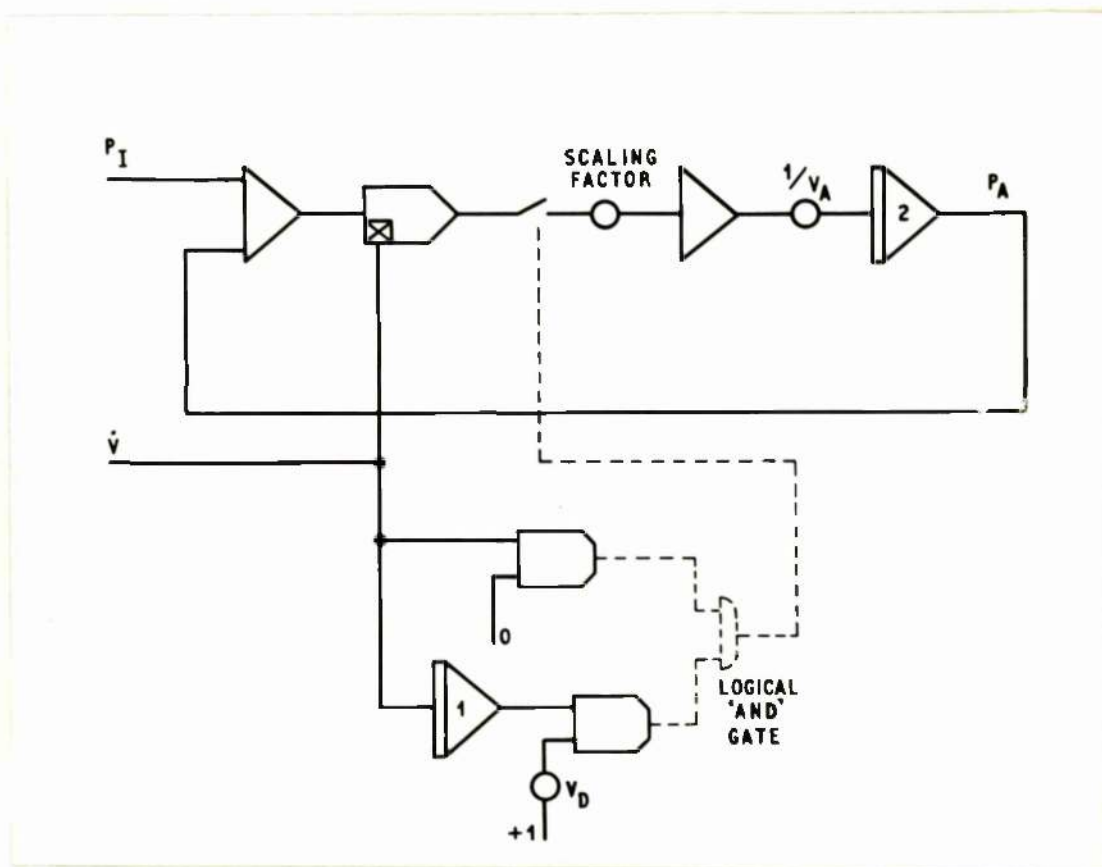


FIGURE 3.1.

"Patch" diagram for solution of equation 2.57.

The symbols are the standard ones for individual components of the analogue computer (See Table 1.4)

b) Digital-computation.

Although a number of standard methods exist for the numerical solution of differential equations, and are readily available in high level simulation languages (see Appendix 3) these require an unacceptably long computation time and for this reason an alternative method of computation has been developed. In the basic dynamic equation for carbon dioxide (2.59) it is the term $\dot{S}V_B(P_I - P_A)$ which presents difficulties in attempting to obtain a solution by analytical methods. If this term is replaced by a constant (K) then a new equation is obtained:-

$$V_{A\beta g} \frac{dP_A}{dt} = -\dot{Q}_b^{\beta}(\text{CO}_2) P_A + \dot{Q}_b^{\beta}(\text{CO}_2) P_{\dot{V}} + K$$

which reduces to

$$V_A \beta \frac{dP_A}{dt} + \dot{Q}_b^{\beta}(\text{CO}_2) P_A = K^1 \quad (3.2)$$

where K^1 is a constant and $= K + \dot{Q}_b^{\beta}(\text{CO}_2) P_{\dot{V}}$.

This latter equation is in a form solved readily by analytical methods. The approach gives rise, therefore to an approximate iterative solution of the form:-

$$P_{A(n+1)} = \frac{K^1}{\dot{Q}_b^{\beta}(\text{CO}_2)} + \left[P_{A(n)} - \frac{K^1}{\dot{Q}_b^{\beta}(\text{CO}_2)} \right] e^{-\frac{\dot{Q}_b^{\beta}(\text{CO}_2)}{V_A \beta g} t} \quad (3.3)$$

where time t is divided into a number of equal intervals and $P_A(n)$ is the P_A at the n^{th} such interval. The value of K (and hence K^1) can be updated at each time step using sampled values of $\dot{V}(t)$ and $P_I(t)$ measured experimentally. The complete response is generated by repeated application of this equation. The accuracy of the solution generated in this way depends upon the sampling interval. It has been shown that in the special case where \dot{V} is simulated by a sinusoidal signal of appropriate amplitude and frequency that a solution accurate to 0.5% after 30 breaths may be obtained using a sampling interval given by $T = 0.01 T_m$ where T_m is the mean period

of a breath. This method shows advantages over the use of a high level simulation language since it is faster in operation and can be implemented on a small computer.

3.3. EXPERIMENTAL SYSTEM.

The experimental system which has been used in this work is shown diagrammatically in Figure 3.2, and the real experimental system is shown in Figure 3.3. The individual components in the system are discussed below.

a) Measurement of gas flow-rate.

In the experiments to be described the subject breathes through a two-way valve-box with small dead space and low resistance (the type and manufacturer of each item of equipment used in this work is shown in Appendix 7).

The inspired and expired flow rates of gas are measured independently by means of pneumotachographs. The voltage outputs from the associated micromanometers are summed electronically using a small analogue computer before input to the computer system. The solution of the equations of these dynamic models requires only the accurate measurement of inspired flow and the identification of zero flow points. There is thus no requirement for accurate measurement of expired flow thereby avoiding the problem of calibration of the expired pneumotachograph.

The inspired pneumotachograph is calibrated daily over the range of flow rates 0 - 2 l/sec, over which it has a linear response. Calibration is carried out by blowing gas through a rotameter and pneumotachograph in series from a vacuum cleaner, the speed of which can be infinitely varied. The calibration of the rotameter was checked by blowing gas through it at several constant flow

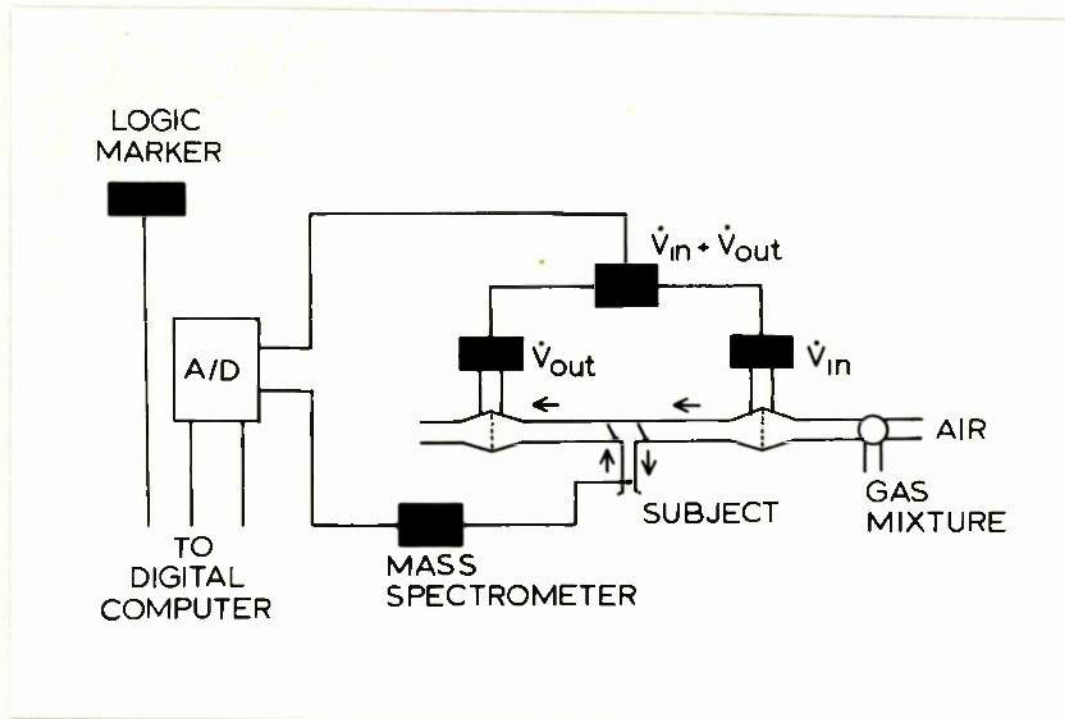


FIGURE 3.2

Schematic diagram of experimental system.

For further details see text.

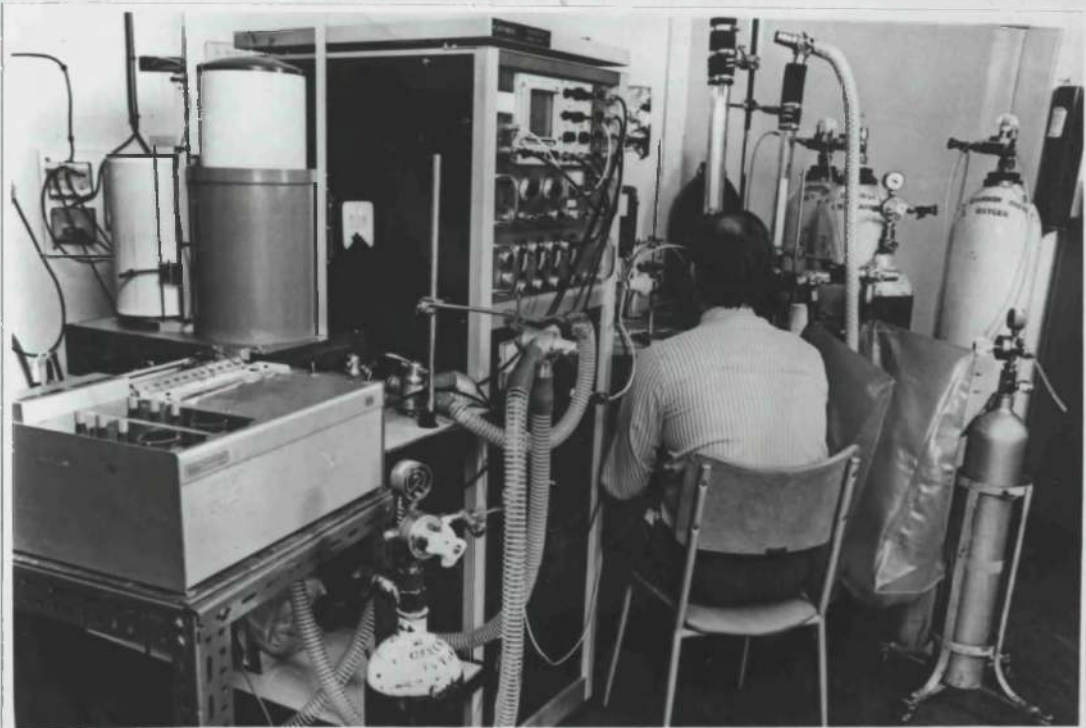


FIGURE 3.3.

The experimental system.
The large instrument on the left is a four channel respiratory mass spectrometer. The cabling on the wall behind this instrument connects the experimental transducers on-line to the computer system in a separate room. The micromanometers are situated on the trolley in front of the subject.

rates and measuring the volume of the effluent gas in a known time by means of a Tissot spirometer of 100 L. capacity.

b) Measurement of partial pressure of gases under study.

Gas concentrations are measured continuously at the mouth using a respiratory mass spectrometer. (In the initial stages of this work an AEI MS4 was used, but in later stages a quadrupole mass spectrometer type MGA 7 (Centronics) has been used).

Transport delays are inherent in high speed gas analysers such as the mass spectrometer which is in contrast to the measurement of respiratory flow which is virtually instantaneous. Reference to the equations of the dynamic models reveals the necessity for simultaneous time correspondence of the respired flow and gas partial pressures. This is achieved by delaying the earlier signals to synchronise all the measured data. In this work typical transport delays are 300 msec for the MS4 and 20 msec for the MGA007 with, in addition, 90% response times of 40 msec and 80 msec respectively.

The delay time and response time of the mass spectrometer are measured daily using a similar method to that described in Cumming and Jones.²⁴³ A gas mixture containing argon is passed through a small metal tube into which the probe of the mass spectrometer is inserted and the partial pressure of argon is measured. A small current is passed from a battery supply through the probe of the mass spectrometer and the metal tube. On abrupt removal of the mass spectrometer from the metal tube a step change in argon concentration is applied at the sample point and the circuit is broken. The output of the mass spectrometer and event marker are displayed on an UV recorder from which the delay time can be measured.

Multi head magnetic tape recorders and electromechanical systems for producing time delays for this application have been described previously.²⁴⁴ Time delays of varying duration are generated easily in the digital computer when digital computation is being used.

For the analogue solution of the equations an analogue simulation of a transport delay has been employed and a fourth-order Padé approximation was chosen²⁴⁵ (for circuit diagram see Figure 3.4) and implemented on a small analogue computer. In order to check that the circuit produced no significant attenuation of the flow signal, a number of experiments were carried out in which comparisons were made between the integrals over the experiment of inspired flow and the delayed flow signal. In these experiments the subject breathed air from a Douglas bag so that the total inspired ventilation during the experiment could be measured and this was compared with inspired ventilation as calculated from integration of the delayed flow signal. The Douglas bag was filled using a known volume of air from a Tissot spirometer prior to the experiment and the remaining air returned to the spirometer on completion of the test. Both the inspired component of the flow signal and the same signal delayed by 300 msec were integrated using an analogue computer. Using the logic facilities and comparators of this computer the integrators were held in the hold mode, i.e. inoperative, during expiration. Experiments were carried out while the subjects were breathing normally and repeated during voluntary hyperventilation. The difference between the total inspired ventilation as measured directly, by means of integration of the flow signal and by integration of delayed flow signal were not significantly different from zero (see Table 3.1(a) and (b)).

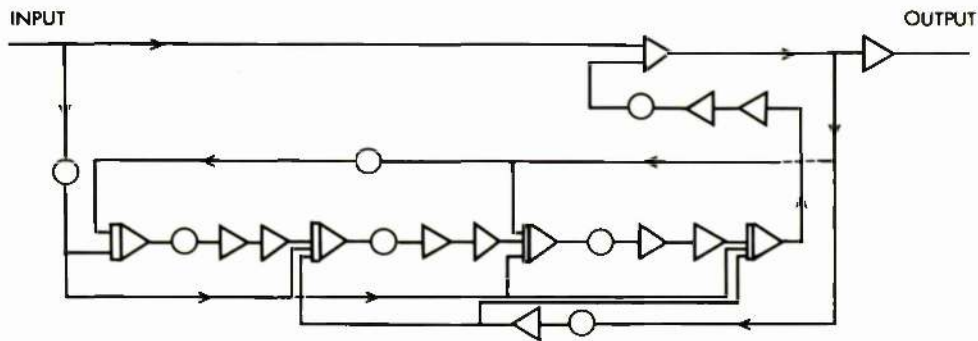


FIGURE 3.4

"Patch" diagram for fourth-order Padé delay circuit, which has been used in this work.

TABLE 3.1.1(a). COMPARISON OF VOLUME INSPIRED (DIRECT MEASUREMENT) WITH THAT CALCULATED BY INTEGRATION OF DELAYED FLOW SIGNAL.

<u>Exp. No.</u>	<u>Resp. frequency</u> <u>/min.</u>	<u>Ventilation (total)</u> <u>Direct Measurement.</u> (litres)	<u>Ventilation (total) calculated</u> <u>from integral of delayed flow.</u> (litres)	<u>% diff.</u>
1	9	16.0	16.2	+1.3%
2	10	16.9	16.5	-2.4%
3	9	17.6	17.8	+1.1%
4	10	18.5	18.5	0.0%
5	15	16.4	16.6	+1.2%
6	29	19.1	18.3	-4.2%
7	30	19.8	19.0	-4.0%

TABLE 3.1(b). COMPARISON OF INTEGRAL OF DELAYED AND UNDELAYED FLOW SIGNAL.

<u>Exp. No.</u>	<u>Resp. frequency</u> <u>/ min.</u>	<u>Ventilation(total) calculated</u> <u>from integral of delayed flow.</u>	<u>Ventilation(total) calculated</u> <u>from integral of undelayed flow.</u>	<u>% diff.</u>
1	8	15.3L	15.3L	0.0%
2	8	19.0L	18.9L	+0.6%
3	18	13.0L	12.7L	+1.9%
4	17	15.4L	15.1L	+1.5%
5	17	9.4L	9.2L	+2.3%
6	19	14.1L	14.1L	0.0%
7	27	13.4L	13.4L	0.0%
8	30	14.6L	14.7L	-0.7%
9	30	15.4L	15.5L	-0.6%
10	32	17.6L	17.7L	-0.6%
11	35	17.5L	17.9L	-2.2%
12	37	13.6L	13.4L	+1.5%
13	39	16.7L	16.6L	-0.6%
14	50	16.5L	16.6L	-0.6%
15	50	16.2L	16.1L	+0.6%

The flow signal and that delayed by 300 msec are shown graphically in Figure 3.5.

For the application of dynamic models it is necessary to obtain, for those gases being studied, the partial pressures of gas at conditions of full saturation with water-vapour at body temperature. The water-vapour pressure at the mouth is continuously variable from the order of 0.80kPa during inspiration to 4.92kPa during expiration.²⁴⁶

It is possible to measure the water vapour pressure at the mouth directly ($P_{m H_2O}$) and thereby calculate the partial pressure of any gas (x) at conditions of full saturation with water-vapour at 37°C ($P_B x$) from the partial pressure as measured at the mouth ($P_m x$)

$$\text{i.e.} \quad P_B x = P_m x \cdot \frac{(B - 6.25)}{(B - P_{m H_2O})} \quad (\text{kPa}) \quad (3.4)$$

This is, however, not an accurate method. In the first instance the respiratory mass spectrometer has different dynamic properties with respect to water vapour than other gases due to the slower transit of water vapour along the sampling tube. Furthermore there is a continuous change in the viscosity of the gas being sampled as a result of the continuous change in water-vapour pressure at the mouth. This leads to alteration in the pressure in the sample chamber and consequently variation of flow into the ion source (for further details see Fowler, 1969).²⁴⁷

An alternative procedure is to manipulate the output data from the mass spectrometer, i.e. the partial pressures of the gases being studied, to obtain their dry gas fractional concentration.

Consider a dry gas mixture containing nitrogen, carbon dioxide, oxygen and argon, the total pressure of the mixture being B, then:-

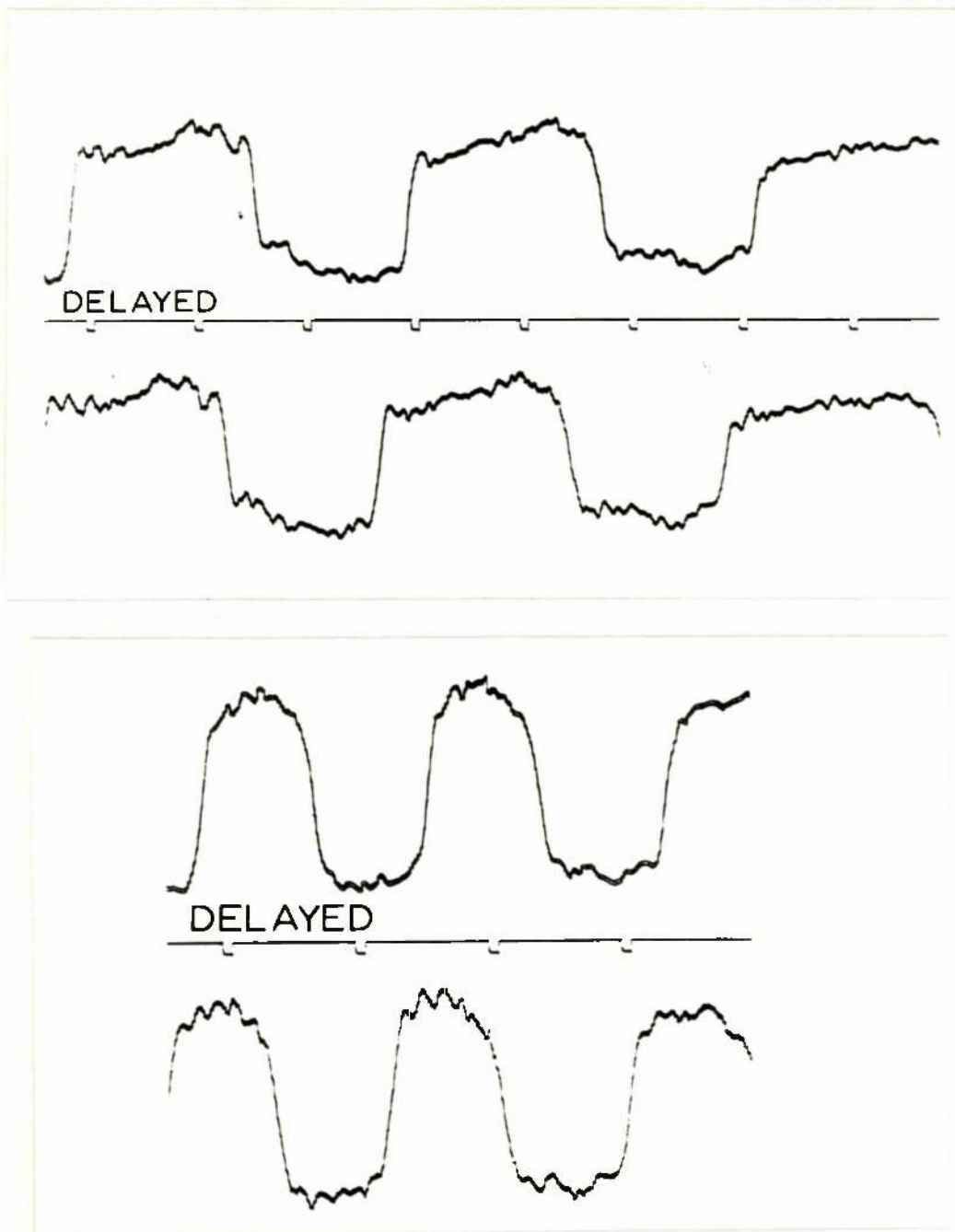


Figure 3.5 (a) and (b)

CAPTION

Comparison of measured flow-rate (\dot{V}) at mouth and that delayed using fourth-order Padé delay circuit, at two different respiratory frequencies. In the middle of the diagrams is a time marker at one second intervals.

$$F_{N_2} + F_{CO_2} + F_{O_2} + F_{AR} = 1.0$$

and

$$P_{N_2} + P_{CO_2} + P_{O_2} + P_{AR} = B$$

If because of changes in the viscosity in the sampling tube the total pressure in the sampling chamber is less (say B^1) then the individual measured partial pressures (P^1_x) will fall

$$\text{i.e. } P^1_{N_2} < P_{N_2}; P^1_{CO_2} < P_{CO_2}; P^1_{O_2} < P_{O_2}; P^1_{AR} < P_{AR}$$

(A similar argument can be applied to saturation of the dry gas mixture with water-vapour, thereby reducing the pressure from B to $(B - PH_2O)$).

The same proportionate fall will occur in each measured partial pressure, since $F_x \cdot B = P_x$ and $F_x \cdot B^1 = P^1_x$

$$\text{i.e. } \frac{P_x}{P^1_x} = \frac{B}{B^1} = K \quad \text{for all gases.}$$

Thus at the new pressure B^1 the following relationship holds for the sum of all the mass spectrometer outputs $\sum P^1_x$:-

$$K \sum P^1_x = \sum P_x = \text{constant}$$

By automatic scaling in the mass spectrometer such that the sum of all the outputs is held constant the mass spectrometer outputs are proportional to $K P^1_x$.²⁴⁸ Thus the output is directly proportional to F_x since

$$F_x = \frac{P^1_x}{B^1} = \frac{P^1_x}{B^1} \cdot \frac{B}{B} = K \frac{P^1_x}{B}$$

The automatic scaling facility is present in the quadrapole mass spectrometer and utilisation of this obviates problems with varying water vapour pressure, allowing direct measurement of F_x and hence P_x at conditions of full saturation with water vapour at 37°C since $P_x = F_x (B - 6.25\text{kPa})$.

The method has however practical difficulties. In the first place the gain on each channel of the mass spectrometer must be set accurately, using a digital voltmeter, so that the output from that channel represents the correct proportion of the total. The total signal available in this mode cannot exceed 10 volts which implies a limitation on the maximum voltage outputs from channels measuring gases in low concentration and hence on the accuracy with which they can be set.

A more flexible approach can be implemented on a digital computer. Using the symbols as before it is seen that:

$$\frac{P^1_X}{P^1_{N_2} + P^1_{CO_2} + P^1_{O_2} + P^1_{AR}} = \frac{F_X \cdot B^1}{F_{N_2} \cdot B^1 + F_{CO_2} \cdot B^1 + F_{O_2} \cdot B^1 + F_{AR} \cdot B^1}$$

$$= F_X$$

Thus measurement of F_X can be obtained without the restriction of ensuring that the gain of individual channels needs to be limited or accurately adjusted. For breathing of atmospheric gas it can be assumed that $F_{AR} = 0.009$ thereby necessitating only the measurement of the other three gases. The summation which is required is carried out digitally after logging by the computer system. This approach has been described previously.²⁴⁹

3.4. EXPERIMENTAL METHODS.

In the experimental work to be described (Chapters 4,5) the standard experiment consists of four distinct phases. Data input to the computer system during the initial phases (zero and calibrate stages) is used for subsequent normalisation of the voltage output from the transducers during the actual test procedure.

The test procedure itself consists of two phases. The onset of the second phase is associated with a step change in the concentrations of the inspired gas mixture.

Subsequent discussion of experimental methods is related to the type of computer system which is used.

a) Analogue computation.

Data from the transducers is recorded on a magnetic-tape loop at a speed of $3\frac{3}{4}$ ips. The electronic sum of the flow signals from the individual pneumotachographs is input to a fourth-order Padé delay circuit on a small analogue computer. The output from this computer is recorded on the tape-loop.

The zero and calibrate phases of the experiment are "marked" on the tape-loop by recording a series of digital logic pulses from a specially constructed multivibrator.

The voltage output of each of the transducers is scaled prior to recording to be in the range 0-1 volt.

The total length of experiment which can be recorded at $3\frac{3}{4}$ ips is of the order of 3 minutes.

For subsequent analysis the recorded data is input to another analogue computer. During replay of the zero and calibrate phases the analogue computer is held automatically inoperative by use of logic facilities in the computer which recognise the presence of the digital logic pulses on the magnetic tape. During this period the operator adjusts potentiometers for the necessary normalisation of the signals. The signals are amplified by the computer to lie in the range 0-10 volts. The tape is replayed at a speed of 30 ips (i.e. x 8 real time).

b) Digital computation.

For digital computation data from the transducers are input on-line to a PDP 11/45 computer system (see Figure 3.6) through analogue-digital convertors. Data are sampled normally at 30 samples/s.

Prior to carrying out any experiment certain basic information is input interactively at a keyboard to the data logging programme (see Figure 3.7).

Communication between the computer system and the experimenter is achieved using a specially constructed interface by means of which the experimenter indicates to the data logging programme which phase of the experiment is current.

In the zero phase of the experiment the computer reads five hundred samples on each input channel of data and outputs the average voltage at the keyboard. Thus:-

READY TO ZERO

CHANNEL	VOLTAGE
FL	-0.388
CR	0.201
OX	0.105
NI	-0.097

DATA OK? OK



Figure 3.6

Picture of the PDP 11/45 computer system, which has been used in this work. The computer is interfaced directly to the experimental system (Fig. 3.3). The cabling which connects the computer to the experimental transducers is seen on the wall to the left of the picture.

```

FILENAME?    TEST1.DAT
PRESSURE?   768.0
TEMP. ?     23.0
M/S DELAYS? 100.0
TIME?      120.0
FREQUENCY? 30.0
CH. 1 = FL
<FL> CAL. LEVEL? 1.0

CH. 2?    CR
<CR> CAL. LEVEL? 4.6

CH. 3?    OX
<OX> CAL. LEVEL? 19.5

CH. 4?    NI
<NI> CAL. LEVEL? 70.1

CH. 5?

NO. LOGGED CHANS. ? 2

DATA OK?   OK

```

Figure 3.7

Interactive dialogue between computer system and operator for input of general information. Responses by computer system are underlined.

The operator has the facility to repeat the zero phase, if this is required.

A similar procedure is implemented when calibrate signals are input to the digital computer. The values obtained during these phases are used by the computer software for subsequent normalisation of the measured data.

During the test procedure normalised sampled data is stored on a temporary disc file. The operator indicates to the software the start of the second phase of the test using the specially constructed interface. This sample number is stored by the programme and is used in later processing of the data. The duration of the experiment is specified by the operator prior to its commencement and is, thereafter, under programme control. After the experiment is completed the data, which is stored on the temporary disc file, is converted to physiological units and scaled into integer form for permanent storage in a file on magnetic tape. Storage in integer form reduces the storage requirements. The scaling factor is different for each measured variable and is specified within the programme. Data in all input channels is synchronised by correcting for the known inherent delay in gas analysis. A number of characteristics of the stored data is contained in the initial record of this file (see Table 3.2). The variables which have been measured are identified by 2 letter identifiers viz. 'FL' for ventilatory flow rate, 'CA' for $p\text{CO}_2$, 'OX' - $p\text{O}_2$, 'NI' - $p\text{N}_2$, 'AR' - partial pressure of argon, 'SU' - partial pressure of sulphur hexafluoride, 'OT' - partial pressure of unspecified inert gas.

TABLE 3.2.

DATE OF EXPERIMENT
 BAROMETRIC PRESSURE
 AMBIENT TEMPERATURE
 SAMPLING FREQUENCY
 NUMBER OF CHANNELS OF INPUT
 TWO LETTER IDENTIFIERS FOR EACH CHANNEL
 SAMPLE NUMBER ASSOCIATED WITH
 CHANGE TO PHASE 2 OF EXPERIMENT.
 TOTAL NUMBER OF SAMPLING PERIODS DURING EXPERIMENT.

Software has also been developed²⁵⁰ for graphing the stored data on an ordinary X/Y recorder. Data is output to the recorder through digital to analogue conversion channels. The software is flexible and allows for either graphing of all measured data (see Figure 3.8) or for more detailed inspection of a portion of the logged data (see Figure 3.9). This last facility is particularly valuable in investigating artifacts in the measured flow data (see Figure 3.10).

Prior to utilising the stored data for parameter estimation it is pre-processed. This software identifies initially the start of each inspiration and expiration and stores the relevant sample numbers for use in the parameter estimation programmes. Recognition of these is complicated by noise in the measured flow signal, some of which is mechanical in origin, being generated by oscillation of the respiratory valves. Problems have also been encountered due to the presence of swallowing. The data is filtered, therefore, prior to pre-processing using a simple low pass filter. The algorithm (see Figure 3.11) which is used for

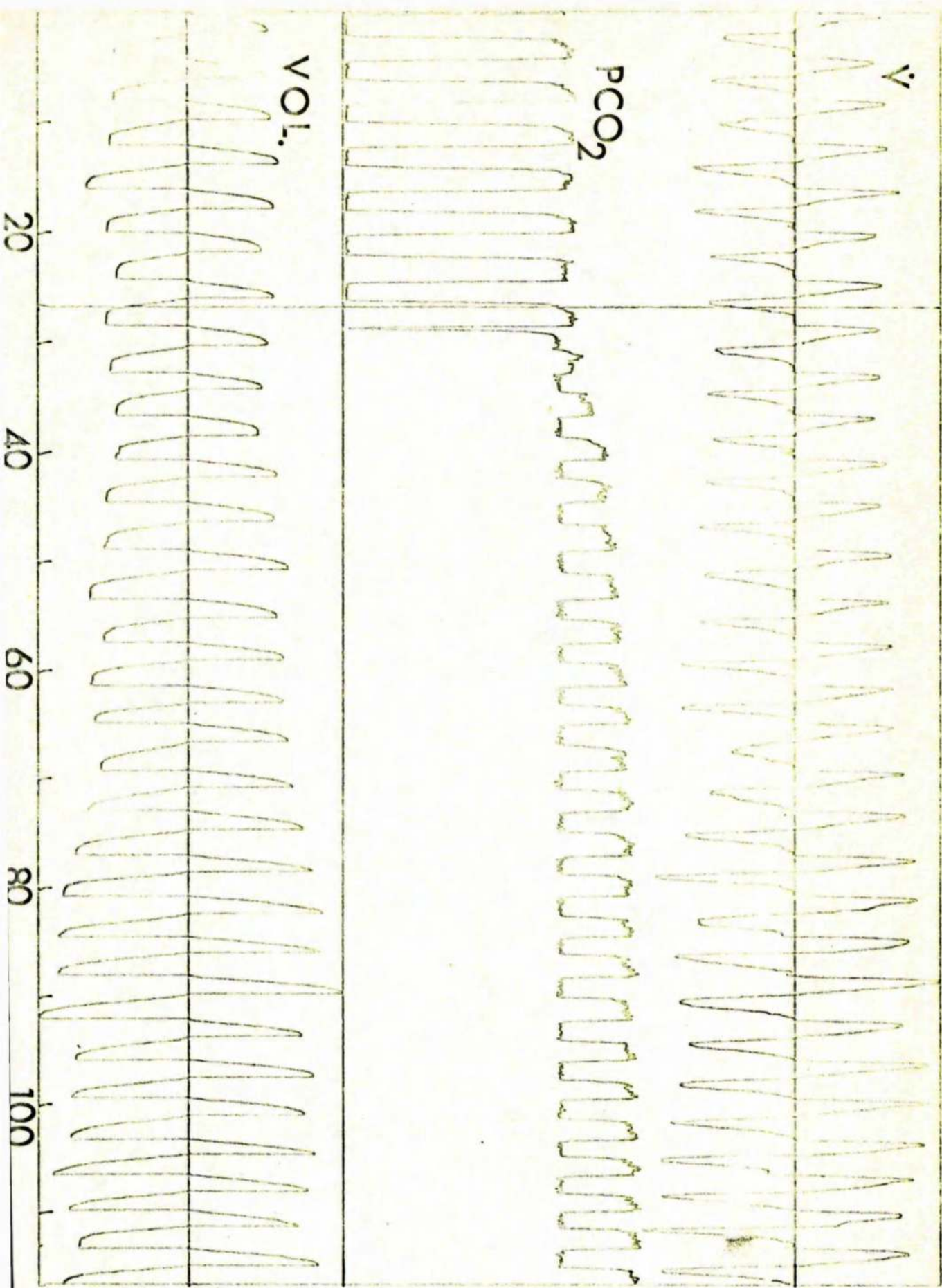


Figure 3.8

Computer graph of measured data (flow and $p\text{CO}_2$).
The volume is calculated by the computer software
from integration of the flow signal (for details see text).

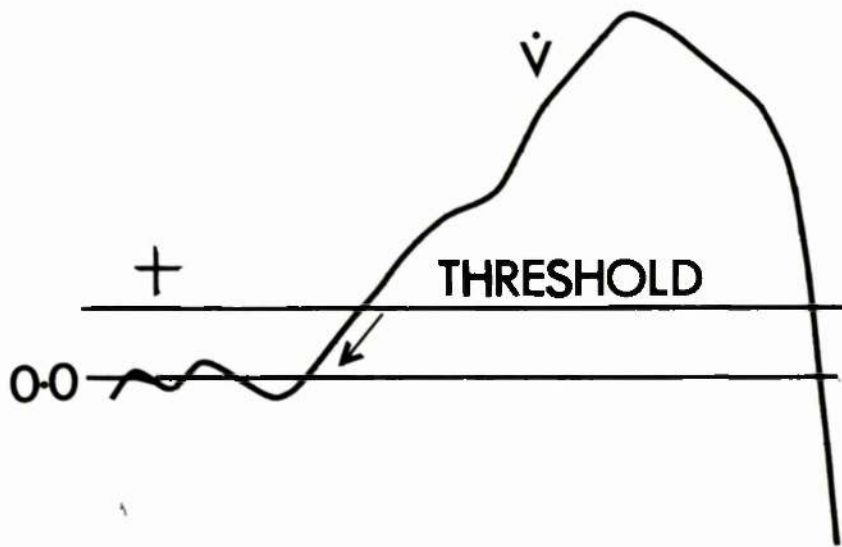


Figure 3.11

Schematic diagram illustrating algorithm for detecting start of breath. The method looks initially for positive "threshold" of 0.15 L/sec. and backtracks to previous zero cross-over. This obviates difficulties caused by noise in flow-signal which would lead to spurious breaths being recognised if only zero cross-overs were identified.

Identification of the start of inspiration and expiration searches initially for "threshold" values (e.g. 0.15 L/sec) and then for the nearest preceding points at which a zero cross-over occurs. The volume inspired and expired in each breath is calculated. The expired flow signal is uncalibrated but the programme carries out a very approximate normalisation of expired flow data by scaling such that the total volume expired in the test is equated with the total volume inspired, using only complete breaths in the calculation. The start of the end-tidal part of each expiration is detected when the integral of expired flow exceeds a volume which is chosen interactively by the experimenter. A suitable initial estimate of this volume is twice the known volume of the anatomical dead space for the subject. (There is experimental evidence²⁵¹ that in normal subjects the dead space is almost cleared completely by this point.) Graphics software is available for the experimenter to check the way in which the programme has detected the end-tidal part of each breath (see Fig. 3.12). The programme creates a separate disc file for each breath containing the end-tidal samples for the gas under study. These files are of course of variable length. This programme which has been written by the author is discussed in more detail in Appendix 8.

Software is also available for extracting from any set of input data a standard experiment, i.e. when the number of breaths in each of the two stages of the tests are defined.

The processed data is analysed subsequently by the parameter estimation software. The analysis programme is particular to a given application. The complete software system is summarised in Figure 3.13.

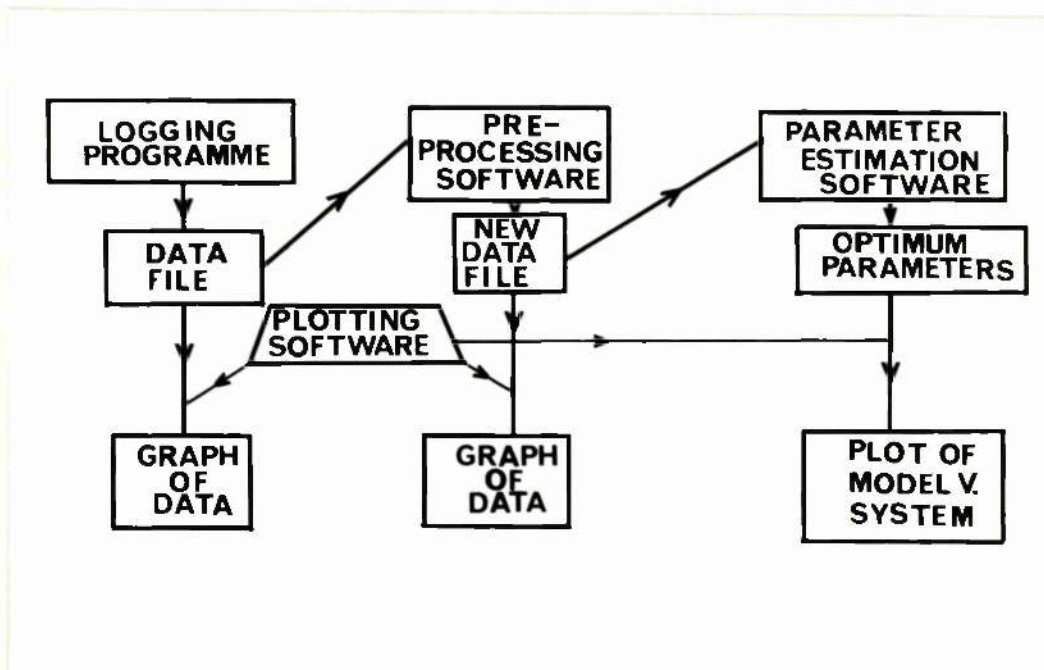


Figure 3.13

Diagram of complete computer software system which has been developed for this work.

CHAPTER 4

APPLICATION OF THE TECHNIQUES OF DYNAMIC
MODELLING TO THE ANALYSIS OF INERT GAS
WASH-OUT TESTS.

CHAPTER 4. APPLICATION OF THE TECHNIQUES OF DYNAMIC MODELLING TO THE ANALYSIS OF INERT GAS WASH-OUT TESTS.

4.1. INTRODUCTION:

Inert gas wash-out tests are used in clinical practice to study and quantify maldistribution of ventilation. (For reviews on early work on this subject see Fowler (1951),²⁵² Bouhuys & Lundin,²⁵³ and Bouhuys.²⁵⁴) In these tests the subject, who is being studied, inspires a gas mixture other than air and the wash-in to or wash-out from the lung of an inert insoluble gas is measured. In the tests which are used commonly^{184,255,256} the inspired gas is pure oxygen and the wash-out of resident nitrogen is studied. Alternatively gas mixtures which contain other inert and relatively insoluble gases, e.g. helium²⁵⁷ or argon²⁵⁸ can be used. The wash-in to the lung or subsequent wash-out from the lung, on returning to breathing air is measured.

The test procedures can be divided into two types:-

- a) Single-breath tests.
- b) Multiple-breath tests.

In the single breath tests the subject inspires only one breath of non-atmospheric gas and the wash-out of inert gas is studied during this breath. In the standard procedure²⁵⁶ the test breath consists of a maximal inspiration of oxygen followed by a maximal expiration. The expired nitrogen concentration is measured continuously. From theoretical considerations it is anticipated that in a normal homogenous lung, the nitrogen concentration during the last part of the expirate (alveolar component) should be constant. This alveolar plateau has, however, a slight slope even in normal subjects.²⁵⁹ The magnitude of this slope is increased in subjects with respiratory disease.²⁵⁹ There has been much discussion

as to the nature of the pathophysiological mechanisms which produce the variation in nitrogen concentration during the last part of expiration. Some workers propose that the main mechanism is asynchronous emptying of different pulmonary units which contain different concentrations of nitrogen, i.e. parallel inhomogeneity.^{254,259,260} Other groups argue, however, that the slope reflects the existence of concentration gradients in the terminal airways (series inhomogeneity)^{212,261}. This debate is considered in more detail in a later section of this chapter (4.4). The value of the single breath tests as an epidemiological tool has been stressed recently^{262,263} since one can obtain simultaneous measurements from this simple test of maldistribution of ventilation, total lung capacity, and closing volume.

The multiple breath tests can be divided into closed-circuit and open-circuit methods. In closed-circuit methods equilibration of an inert gas with lung gas is studied in a closed spirometer system.²⁶⁴ In open-circuit tests the subject breathes a non-atmospheric gas for the duration of the test, and the breath-by-breath fall in nitrogen concentration is studied. There are several methods to analyse data from open-circuit tests. These are discussed in the next section of this chapter.

4.2. STANDARD METHODS OF ANALYSIS OF OPEN-CIRCUIT MULTIPLE-BREATH TESTS OF MALDISTRIBUTION OF VENTILATION.

In the methods of analysis of data from open-circuit tests there are two basic types of variables:-

- a) Rate Variable, which is used to describe the wash-out process in an INDIVIDUAL lung unit.
- b) Weighting Function by means of which the mathematical descriptions of the individual units are combined to give an overall description of the wash-out process in the lung.

a) Rate Variables.

Although there are many different rate variables these can be divided into two different classes. An example of each type of rate variable was given in Chapter 2.4 and Chapter 2.5. In the first group the wash-out process is considered as a function of breath-number, whilst in the other as a function of time. In the derivation of both of these descriptions it is assumed that ventilation is constant. In the application of these analyses to individual pulmonary units it is necessary to make assumptions about the distribution of dead space gas. The problem is simplified by making the assumption that each unit has a separate dead space. Thus the presence of a common dead-space is generally ignored.

Many different forms of rate-variable have been suggested (see Table 4.1). All rate-variables are equivalent, however, if both tidal volume and frequency are constant. This is shown in the work of Rossing²⁶⁵ in which simple formulae are derived translating any one rate variable into any other.

The assumption of constancy of ventilation is unrealistic. It is not possible, however, to obtain a general result to indicate the magnitude of error introduced into data analysis by this simplification. Certain special cases of non-constant ventilation have been studied using simulation methods by Scheid & Piiper.²⁷² The results indicate that at least in the cases studied this assumption does not cause significant errors in the analysis. The problem of ventilation being time variant can be obviated by considering in the analysis that concentration is a function of total volume expired from time $t = 0$, rather than of breath number or of time.^{273, 274}

<u>Rate Variable</u>	<u>Symbol</u>	<u>Formula</u>	<u>Reference</u>
Alveolar Dilution Ratio	W	$W = \frac{VO}{VO + \Delta V}$	Fowler et al. ²⁶⁶ Darling et al. ¹⁸⁴
Specific Tidal Volume	ξ	$\xi = \frac{\Delta V}{VO}$	Gomez ²⁶⁷
(The above are examples of rate variables using the approach described in Chapter 2.4. Those below are related to the approach discussed in Chapter 2.5.)			
Rate Constant	β	$C(t) = C(O)e^{-\beta t}$	Rossing & Danford ²⁶⁸
90% Wash-out Time	M	$C(M) = 0.1 C(O)$	Briscoe & Courmand ²⁶⁹
Turnover Rate	k	$C(t) = C(O)e^{-kt}$	Robertson et al. ¹⁸⁵
Half-time	$X_{1/2}$	$C(X_{1/2}) = 0.5 C(O)$	Van Liew ²⁷⁰
Time-constant	T	$C(t) = C(O)e^{-t/T}$	Nakamura et al. ²⁷¹

TABLE 4.1.

Comparison of rate variables for description of inert gas wash-out from lung. (Modified from Rossing²⁶⁵).

VO is resting volume of unit; ΔV the volume with which it is ventilated per breath; C(t) is the concentration of inert gas in unit at time t and C(O) is the concentration at time t = 0.

The weighting functions which are employed are also of two types - discrete and continuous.

b) Discrete Weighting Function.

With discrete weighting functions the lung is considered to consist of a finite number of units or compartments which are arranged generally in parallel. In the breath to breath models (Chapter 2.4) it was shown that for a single pulmonary unit (i)

$$C_{A_i(n)}^{N_2} = W_i^n C_{A_i(0)}^{N_2} \quad (4.1.)$$

In the work of Fowler et al.²⁶⁶ a two compartment model is used. For the single compartment (i) assuming that there is no common dead space

$$C_{E_i} V_{T_i} = C_{A_i} (V_{T_i} - V_{D_i}) + C_{D_i} V_{D_i}$$

Since in a nitrogen wash-out test $C_{D_i} = 0$

$$C_{E_i} = C_{A_i} \frac{(V_{T_i} - V_{D_i})}{V_{T_i}} \quad (4.2)$$

For a two compartment system

$$C_{E_n} = \frac{V_{T_1} C_{E_1} + V_{T_2} C_{E_2}}{V_{T_1} + V_{T_2}}$$

$$\text{i.e. } C_{E_n} = \frac{V_{T_1}}{V_{T_1} + V_{T_2}} \cdot W_1^n C_{A_1(0)} \cdot \frac{(V_{T_1} - V_{D_1})}{V_{T_1}} + \frac{V_{T_2}}{V_{T_1} + V_{T_2}} \cdot W_2^n C_{A_2(0)} \cdot \frac{(V_{T_2} - V_{D_2})}{V_{T_2}}$$

$$= r_1 W_1^n C_{A_1(0)} + r_2 W_2^n C_{A_2(0)} \quad (4.3)$$

$$\text{where } r_i = \frac{V_{T_i} - V_{D_i}}{\sum_i V_{T_i}}$$

With the small number of parameters a method of graphical analysis is used to determine the values of r_1, W_1, r_2, W_2 . In this method

$\log C_{E_n}$ is plotted against n:-

$$\log C_{\bar{E}_n} = \log (r_1 W_1^n C_{A_1}(0) + r_2 W_2^n C_{A_2}(0)) \quad (4.4)$$

Assuming that $W_2 < W_1$ then the concentration of nitrogen in compartment 1 will fall to a negligible level when there is still significant amounts of nitrogen in compartment 2. During this period of the experiment

$$\begin{aligned} \log C_{\bar{E}_n} &= \log (0 + r_2 W_2^n C_{A_2}(0)) \\ &= n \log r_2 W_2 C_{A_2}(0) \end{aligned}$$

Thus the value for $r_2 W_2$ can be obtained from the slope of a line drawn through the terminal part of the graph. For the earlier part of the experiment, if $r_2 W_2$ is known

$$\log C_{\bar{E}_n} = \log (r_1 W_1^n C_{A_1}(0) + \text{known quantity})$$

and thus $r_1 W_1$ can be obtained similarly. Since at $n = 0$, $W_1^n = W_2^n = 1$ the values of r_1 and r_2 can be obtained from the intercepts of the two linear portions of the graph. (See Fig. 1, Fowler et al²⁶⁶).

The analysis of nitrogen wash-out data is complicated by the transfer of nitrogen from body stores to the atmosphere during the test. The magnitude of the transfer of nitrogen across the alveolar-capillary membrane is small but its importance increases relatively as the nitrogen concentration in the lung falls. Formulae have been given by different authors^{275,276} to correct experimental data for the evolution of tissue nitrogen. It is adequate, however, to consider the correction as being constant.^{266,267}

Other workers have used a similar approach to Fowler et al²⁶⁶ but have modelled the lung with more than two compartments. Parameter estimation methods have been employed. Rossing et al²⁷⁷ found that all curves which are obtained experimentally could be

described adequately with at most four compartments. Attempts by this group to solve for twenty to thirty compartments were unsuccessful as non-unique estimates of parameters were obtained. Hashimoto et al.²⁷⁸ used a six compartment model but added the constraint that each compartment had equal ventilation, i.e.

$\frac{V_T - V_D}{6}$. The problem of parameter estimation reduces, therefore, to finding the volume of each of the six compartments.

Models with the compartments arranged in series will behave identically to the models which have been discussed in this section.¹⁸⁵ Cumming has suggested recently²⁷⁹ that a simple change of variable in the analysis obviates this difficulty. In this work the wash-out curves, now called decay curves, are plotted as the volume of nitrogen remaining in the lung against turnover of original volume. The turnover is defined to be unity when the total ventilation from the start of the test is equal to the lung volume. It is claimed to be possible to identify from decay curves the contributions of parallel and stratified inhomogeneity to the incomplete mixing of inspired gas. On the basis of this work it is proposed that the principal abnormality in chronic obstructive airways disease is stratified inhomogeneity due to impaired gaseous diffusion in the terminal airways.^{279, 280} In simulation studies carried out by J. Lewis in collaboration with the author²⁸¹ the "decay curve" is demonstrated to have limited capability of distinguishing parallel from series model structures.

One of the main limitations of the inert gas wash-out test is the ability to detect units with long time constants, i.e. low ventilation to volume ratios. In the work of Nye²⁸² it is pointed out that to identify such units would need longer experiments than those which are usually conducted and hence greater sensitivity in

the measurement of gas concentration. The analysis of experimental data into discrete compartments will be significantly in error if many such units exist.

The lung in reality consists of a continuum of units each with an associated rate variable. The compartments which are obtained from data analysis are conceptual rather than real entities. The detection of the true nature of the distribution of units by the compartmental approach is limited and many different distributions can be represented adequately by the same two compartment model.

Van Liew²⁸³ demonstrated curves which were made of eight exponential terms but were analysed satisfactorily by a two compartment model.

c) The Work of Briscoe, Cournand and associates.

The discrete compartment analysis of inert gas wash-out data has been applied to the study of disease particularly by Briscoe, Cournand and associates. The basis of this work is analysis of the nitrogen wash-out curve into two components - a slow space and a fast space.²⁸⁴ The work has been extended to consider the relative distribution of perfusion to those two spaces. Initially it was assumed that perfusion is distributed in proportion to lung volume.²⁸⁵ Calculations, of a predicted alveolar-arterial difference for oxygen on the basis of this assumption gave poor agreement in the individual subject between prediction and the measured alveolar-arterial difference.²⁸⁶ A graphical method was substituted to obtain directly the perfusion of each space from the measured arterial O₂ saturation and O₂ consumption.²⁸⁷ On the basis of such studies it has been suggested that results from this method of data analysis revealed differences between patients with pure chronic bronchitis and patients with pure emphysema.^{288, 289} More recent work has, however, failed to

demonstrate such a difference.²⁹⁰ The apparent difference is likely to be due to the fact that cardiac output was not measured directly but assumed to be 5.0 L/min in all subjects.²⁹⁰

The method of analysis has been extended to consider the distribution of the diffusing capacity between the two spaces. Arterial blood gas tensions, oxygen uptake and carbon dioxide output are obtained at different inspired oxygen concentrations (.e.g. air, 24%, 30%) in the subject under test. The method of partitioning the diffusing capacity is a graphical one^{291,292} and is based on the type of equation described in Section 2.8(c). The method has been applied to patients with emphysema²⁹³ and those with the alveolar-capillary block syndrome.²⁹⁴ On the basis of these studies it is suggested that the predominant mechanism causing hypoxaemia in patients with pure emphysema is a low transfer factor in the less ventilated lung spaces.²⁹³

d) Continuous Weighting Functions.

The lung in reality consists of a large number of functional units. For a single pulmonary unit, using the concept of a turnover rate¹⁸⁵ (see Table 4.1)

$$C_{A_i}(t) = C_{A(0)} e^{-k_i t} \quad (\text{it is assumed that for all units } C_{A_i}(0) = C_A(0)).$$

thus

$$V_T C_{\bar{E}}(t) = \sum_{i=1}^n (V_{T_i} - V_{D_i}) C_{A(0)} e^{-k_i t}$$

if the lung consists of N units. By grouping those units together with the same time-constant

$$C_{\bar{E}}(t) = \sum_{k=0}^{\infty} C_A(0) \left(\sum_{n=1}^{M(k)} \frac{V_{T_k} - V_{D_k}}{V_T} e^{-kt} \right)$$

where for each value of k there are M(k) units

$$\text{i.e. } C_{\bar{E}}(t) = \int_0^{\infty} C_A(0) G(k) e^{-kt} dk \quad (4.5)$$

where $G(k)$ is the continuous weighting function or distribution

function and is defined by

$$G(k) = \sum_{M=1}^{M(k)} \frac{V_{T_k} - V_{D_k}}{V_T}$$

The concept of a continuous weighting function can be applied with other forms of the rate variable.

With this approach the problem is to find, for an individual subject, the correct form of $G(k)$.

$G(k)$ may be assumed to have a certain known analytical form. In the work of Rossing et al,²⁷⁷ it is assumed that the distribution function is a gamma distribution and the problem of data analysis reduces, therefore, to finding the three parameters of the distribution. The weighting function which was proposed by Gomez²⁶⁷ can also be shown²⁷⁷ to be a gamma distribution of $\log(1+\xi)$ where ξ is specific tidal volume as defined in Table 4.1. Despite the greater flexibility of the gamma distribution Rossing et al²⁷⁷ suggest that it is easier for most biomedical investigators to interpret parameter values related to a normal distribution, and use a continuous weighting function which is either a single normal distribution or the sum of two such distributions.

Attempts have also been made to obtain $G(k)$ without assuming a definite analytical form.²⁷¹ Equation 4.5 is seen to be the same form of expression which was used to define the Laplace Transform (see Sectn. 1.8) and contains a type of integral known as the Laplace Integral. $G(k)$ can be obtained by inversion of the integral, although inversion by numerical methods is known to be affected by numerical instabilities.²⁹⁵ In the work of Nakamura et al²⁷¹ the

integral is inverted using a limit described by Post²⁹⁶ and Widder²⁹⁷

$$G(K) = \lim_{n \rightarrow \infty} \frac{(-1)^n}{n!} \left(\frac{n}{K}\right)^{n+1} C^{(n)} \left(\frac{n}{K}\right) \quad \text{where}$$

$C^{(n)} \left(\frac{n}{K}\right)$ is the n^{th} derivative of the measured function $C = \frac{C_E(t)}{C_A(0)}$.

In this work²⁷¹ the limit is approximated by taking $n = 1$ whereas in application of the same technique to the study of ventilation-perfusion distribution $n = 5$ is used.²⁹⁸ This method of approach has been studied theoretically in simulation studies by Peslin et al.²⁹⁹ It is shown that using measured data containing noise the limit cannot be evaluated for n greater than 2 because of the necessity for high order numerical differentiation. At low values of n the estimates of the characteristics of trial distributions are poor, e.g. mode underestimated by 50%. The method has limited resolving power in terms of detecting the bimodal nature of trial distributions. For example with $n = 5$ the method will only detect the presence of two distributions if the mean of one is at least 3.7 times the mean of the other. This approach has thus been little used in clinical respiratory physiology.

e) Models with Common Dead Space.

In the models which have been discussed in this chapter, each pulmonary unit is assumed to have an independent dead space. A common dead space was incorporated in the models of Weber and Bouhuys³⁰⁰ and Wise and Defares.³⁰¹ Weber and Bouhuys³⁰⁰ studied a model with continuous unidirectional ventilation and compared model predictions with experimental data both with and without added external dead spaces. A cyclical ventilation model is used, however, by Wise and Defares.³⁰¹ In the work of Nye²⁸² an assessment is made as to the error which is produced in data analysis by neglecting the presence of a common dead space. The error is large when ventilation is minimally maldistributed but becomes of negligible proportions when maldistribution of ventilation is large. The presence of a common dead space tends to reduce the

difference in nitrogen wash-out between different units by slowing the wash-out process in fast spaces and increasing the rate of wash-out in slower spaces.

Attempts to analyse data using models with a common dead space have been made.^{302,303,304} In the work of Paiva and Demeester³⁰² an extremely complex model is used with sixteen compartments and incorporating both common and individual dead spaces. A parameter estimation method is employed but no information is given as to the uniqueness or otherwise of the parameter estimates. The authors comment on the fact that with such a large number of parameters one can adjust a great number of different functions to fit the experimental data. A less elaborate model is used by Saidel et al.³⁰³ The model has five compartments - two "alveolar units" each with a separate dead space and a common dead space. The uniqueness of the parameter estimates which are obtained with this model is not discussed. It has been shown,³⁰⁴ however, that it is not possible with the information available in the nitrogen wash-out test to estimate uniquely the parameters for this five compartment model. It is possible to obtain unique estimates for the parameters of a reduced model with two alveolar units, and a common dead space.³⁰⁴

4.3 DYNAMIC MODELLING APPROACH

a) Models

The dynamic modelling approach to the analysis of inert gas wash-out tests represents an extension to the methods which have been reviewed in this chapter. The basic equation for a single unit is similar to that given in Chapter 2 (equation 2.57)

For a single pulmonary unit i

$$V_{Ai} \frac{dP_{Ai}}{dt} = S_1 K_i \dot{V} (P_D - P_{Ai}) + S_2 K_i \dot{V} (P_I - P_{Ai})$$

$$\text{where } S_1 = 1 \text{ if } K_i \dot{V} \geq 0 \text{ and } \int_0^t K_i \dot{V} dt < V_{Di}$$

$$= 0 \text{ otherwise}$$

$$S_2 = 1 \text{ if } K_i \dot{V} \geq 0 \text{ and } \int_0^t K_i \dot{V} dt \geq V_{Di}$$

$$= 0 \text{ otherwise}$$

Models can be constructed with or without common dead-spaces.

In the case of a multi-compartment model with common dead space P_D can be defined as for the dynamic representation of the Riley model. (Chapter 2, equation 2.61).

i.e.

$$P_D = \sum_i \overline{K_i P_{Ai}} (t-\lambda)$$

where λ is a flow-dependent time delay defined by the equation

$$\int_{t_I}^t |\dot{V}_I| dt = \int_{t_{I-\lambda}}^{t_I} |\dot{V}_E| dt$$

where $t = t_I$ is the start of inspiration.

For dynamic models the weighting factors (K_i) may not be simple constants but rather functions of time to allow for the known phase differences between different pulmonary units consequent to variations in mechanical properties. 260

To test the feasibility of applying this approach to analysis of argon wash-out tests, an experimental study has been carried out in normal subjects. In this study a simple model which describes the homogenous lung has been used.

b) Parameter Estimation

For the homogenous lung

$$V_A \frac{dP_A}{dt} = SV(P_I - P_A) \quad (4.6)$$

and there is only one parameter ($1/V_A$) to be estimated. Use has been made of a method of continuous parameter adjustment.^{306,307} Such methods can only be applied in circumstances where there is a small number of parameters.

The first requirement to apply any parameter estimation method is a measure of goodness of fit between the model prediction and measured response. In the methods which employ continuous parameter adjustment the measure of goodness of fit (criterion function) is the square of the difference between model prediction $Y_m(t, Q)$ and measured response $Y_s(t)$. The process of squaring the difference ensures that the error is always positive and equal weight is, therefore, given to positive and negative errors, i.e.

$$J = e^2(t, Q)$$

where J is the criterion function and

$$e(t, Q) = (Y_s(t) - Y_m(t, Q)) \text{ is the error.}$$

In the analysis of argon wash-out data the criterion function cannot be evaluated continuously but only during the end-tidal part of each breath.

The model prediction $Y_m(t, Q)$ depends on the numerical values for the constants in the model equations. This is represented by Q the vector of parameters. For each parameter q_i a parameter sensitivity can be calculated at each moment of time to give knowledge of the magnitude of the influence of the parameter on the model's response. This is achieved by differentiating the criterion function J with respect to the parameter. Thus

$$\frac{\partial J}{\partial q_i} = 2e \frac{\partial e}{\partial q_i} = -2e \frac{\partial Y_m}{\partial q_i}$$

The partial derivatives $\frac{\partial Y_m}{\partial q_i}$ are known as parameter sensitivity functions.³⁰⁸

The principle of parameter estimation is to adjust the parameters such as to minimise the criterion function. When the error is at a

minimum estimates of the parameters are obtained. In the continuous case adjustment of the parameter is arranged to be proportional not only to the magnitude of error but also to the magnitude of the sensitivity function

$$\text{i.e.} \quad \frac{dq_i}{dt} = -g_i e \frac{\partial y_m}{\partial q_i} \quad (q_i \text{ is an arbitrary gain constant } > 0)$$

For larger values of error the rate of adjustment is high whereas near the optimum setting the error is small and the parameters will, therefore, change more slowly. The gain constant g_i is chosen by a trial and error procedure. Larger values of gain may cause instability while small values of gain may give unacceptably slow convergence.

In the analysis of argon wash-out data there is only one parameter ($1/V_A$) and hence only one parameter sensitivity function. The equation of the basic model is

$$\frac{dP_A}{dt} = \frac{\dot{S}V}{V_A} (P_I - P_A) \quad (4.6)$$

and by differentiating with respect to $1/V_A$ we obtain

$$\frac{d}{d(1/V_A)} \left[\frac{\partial P_A}{\partial t} \right] = \dot{S}V (P_I - P_A) - \frac{\dot{S}V}{V_A} \frac{\partial P_A}{\partial (1/V_A)}$$

(P_A is now considered as a function of t and $1/V_A$)

$$\text{i.e.} \quad \frac{d}{dt} \left[\frac{\partial P_A}{\partial (1/V_A)} \right] = \dot{S}V (P_I - P_A) - \frac{\dot{S}V}{V_A} \frac{\partial P_A}{\partial (1/V_A)} \quad (4.7)$$

$\frac{\partial P_A}{\partial (1/V_A)}$ is the parameter sensitivity function. As a result of the limited capacity of the available on-site analogue computer the second term of the equation was approximated by $M \frac{\partial P_A}{\partial (1/V_A)}$ where M is an arbitrary constant. Such an approximation has been shown using a larger analogue computer not to effect the final estimate of $1/V_A$ but the rate of convergence to the optimum value.

The adjustment of the parameter $1/V_A$ is such that

$$\frac{d}{dt} (1/V_A) = - K_e \frac{\partial P_A}{\partial 1/V_A} \quad (K > 0) \quad (4.8)$$

The three equations, 4.6, 4.7, 4.8 can be solved using an analogue computer. The 'patch' diagram for this solution is shown in Fig. 4.1. The details of derivation of this patch diagram and implementation on an analogue computer are discussed in Appendix 2. The initial value of P_A in the alveolar compartment of the model was such that it corresponded to the measured end-tidal argon partial pressure in the last breath of the wash-in of argon.

c) Experimental Studies

The experimental studies were carried out in twenty-five subjects. All subjects were non-smokers. The anthropometric data of each subject are shown in Table 4.2. In the experiments which were performed the subjects inspired a gas mixture containing approximately 80% argon until equilibrium was reached between the inspired and alveolar concentrations of argon. At this point the subjects returned to breathing room air. The experiments were conducted as described in Chapter 3.4(a). The data were recorded on a magnetic tape loop. Recording of the experimental data was commenced shortly before the end of the period of the wash-in of argon. At the end of the argon wash-out test the subject was asked to expire maximally so that the subject's expiratory reserve volume could be measured. The functional residual capacity was also measured in each subject using the standard closed-circuit helium dilution method.²⁶⁴ A measurement of expiratory reserve volume was obtained at the end of this test.

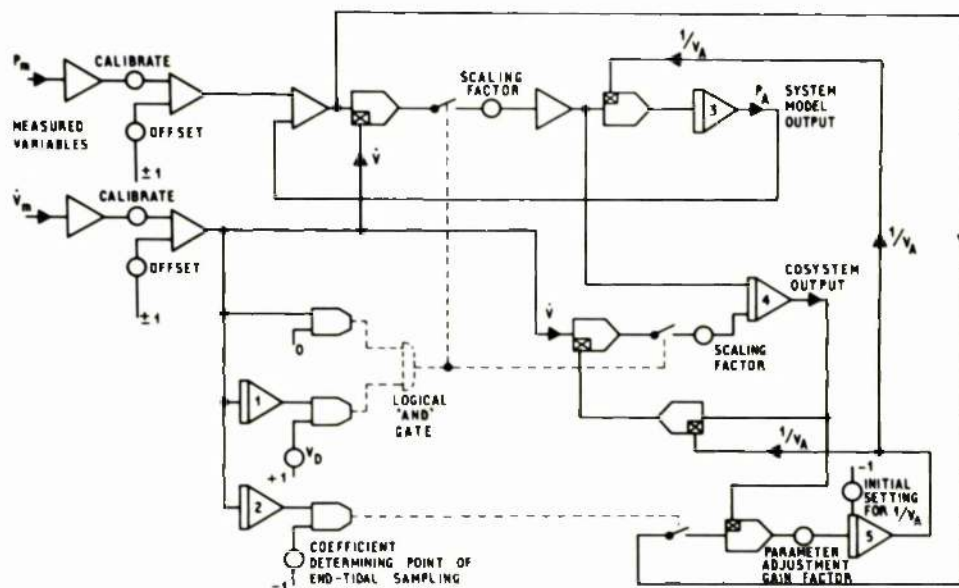


FIGURE 4.1

"Patch" diagram for solution of equations 4.6, 4.7 and 4.8. The value of the parameter $1/V_A$ is obtained as the output of integrator 5. In the diagram shown the condition which is used to detect the end-tidal part of each breath is that $\int \dot{V} dt$ during expiration is greater than an arbitrary volume. This volume is set by the operator using the potentiometer shown.

The experimental data were analysed (see Fig. 4.2) using the parameter estimation method which is described in the previous section and implemented on an analogue computer. (Fig. 4.1). The dead space of the subject was assumed to equal the expected body weight in pounds. (This relationship is demonstrated in the work of Radford³⁰⁹). The agreement between the prediction of alveolar argon partial pressure of a model with the optimum lung volume and measurement is good. (see Fig. 4.3).

There is no significant difference between the estimates of lung volume which are obtained by parameter estimation and those by the closed-circuit helium dilution method after correction to the same end-expiratory volume (see Table 4.3). There is a linear relationship between the results from these methods of measurement. The slope of this relationship is not significantly different from unity (See Fig. 4.4).

The analysis of argon wash-out data using the method of parameter estimation should be unaffected by variation in the ventilation of the subject. This is demonstrated by a study (see Fig. 4.5) in one subject who carried out two argon wash-out tests. In one of these the ventilation was regular but erratic in the other. There is good agreement between model prediction and measurement in both cases and the same result for lung volume was obtained (2.17L and 2.18L respectively).

<u>SUBJECT</u>	<u>SEX</u>	<u>AGE</u>	<u>WEIGHT (lb)</u>	<u>EXPECTED WEIGHT</u>	
1	EM	F	23	127	130
2	MS	F	24	120	121
3	EG	F	24	144	129
4	GB	M	29	152	172
5	FD	M	26	150	160
6	FM	M	42	190	192
7	RJM	M	42	147	140
8	GC	F	19	128	118
9	JMcK	M	23	140	149
10	RMcC	F	40	136	149
11	JDHB	M	54	154	165
12	AS	F	24	136	-
13	ML	F	25	108	125
14	KK	M	29	153	161
15	MK	F	31	113	125
16	AR	F	24	133	132
17	RB	M	28	-	149
18	JW	M	33	147	155
19	JS	F	39	121	130
20	DM	M	10	71	72
21	JS	M	12	77	84
22	AMS	F	13	92	99
23	CW	M	27	152	157
24	JMcE	M	23	168	167
25	JMcK	M	24	145	153

TABLE 4.2

The sex, age, weight and expected weight of each subject who took part in these studies. The expected weight is derived from knowledge of the subject's age, height and sex.³⁰⁵

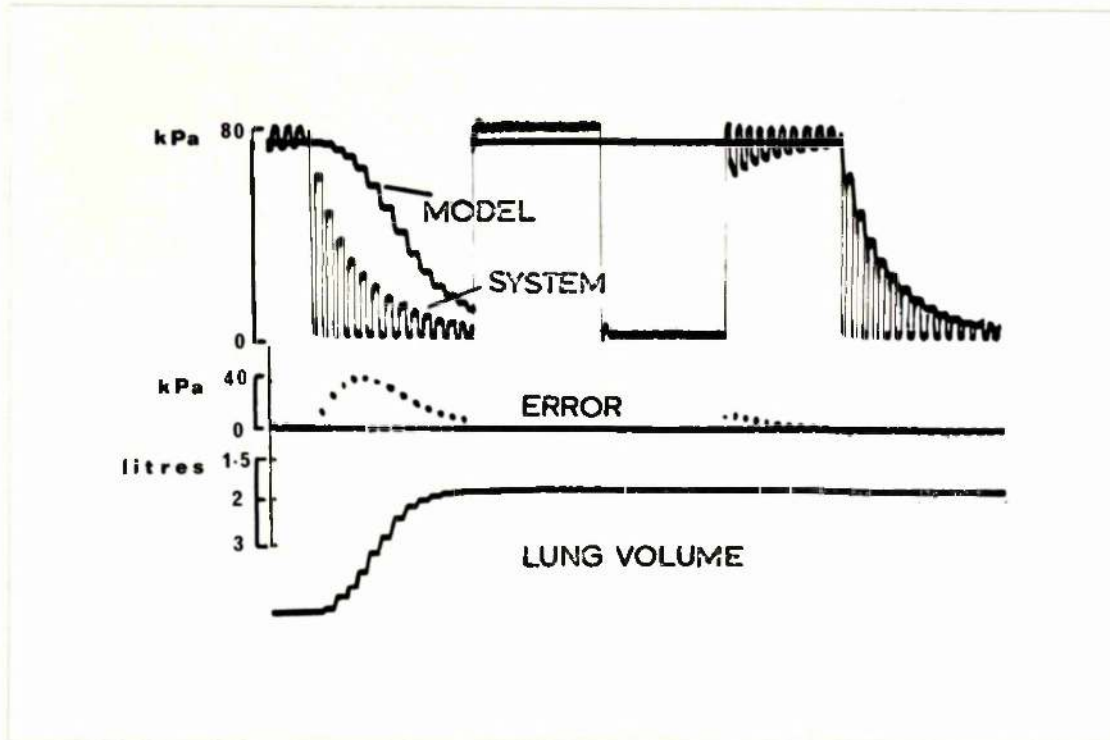


FIGURE 4.2

Outputs from the analogue computer during solution of equations 4.6, 4.7, 4.8. At the top of the figure is the comparison between model prediction of alveolar partial pressure of argon (MODEL) and that measured experimentally (SYSTEM). Since measurement is made at the mouth the model and system should only agree during the end-tidal part of each breath. The end-tidal argon partial pressures show an exponential type decrease during the wash-out. The initial part of the experimental data is from the end of the wash-in during which the model is held in "initial condition" mode. The second line of the figure (ERROR) is the difference between model and system computed during the end-tidal part of each breath. The last line of the figure is the parameter (LUNG VOLUME). Since it is the inverse of lung volume which is the parameter the scale goes from ∞ at the bottom to 1.5L at the top. The value of lung volume is updated on each breath to minimise discrepancy between model and system. The experimental data are recorded on a magnetic tape loop and computation can be repeated. In the example shown the lung volume parameter is such that during the second computation there is good agreement between model and system. The signals between the two sets of data are the zero and calibrate signals.

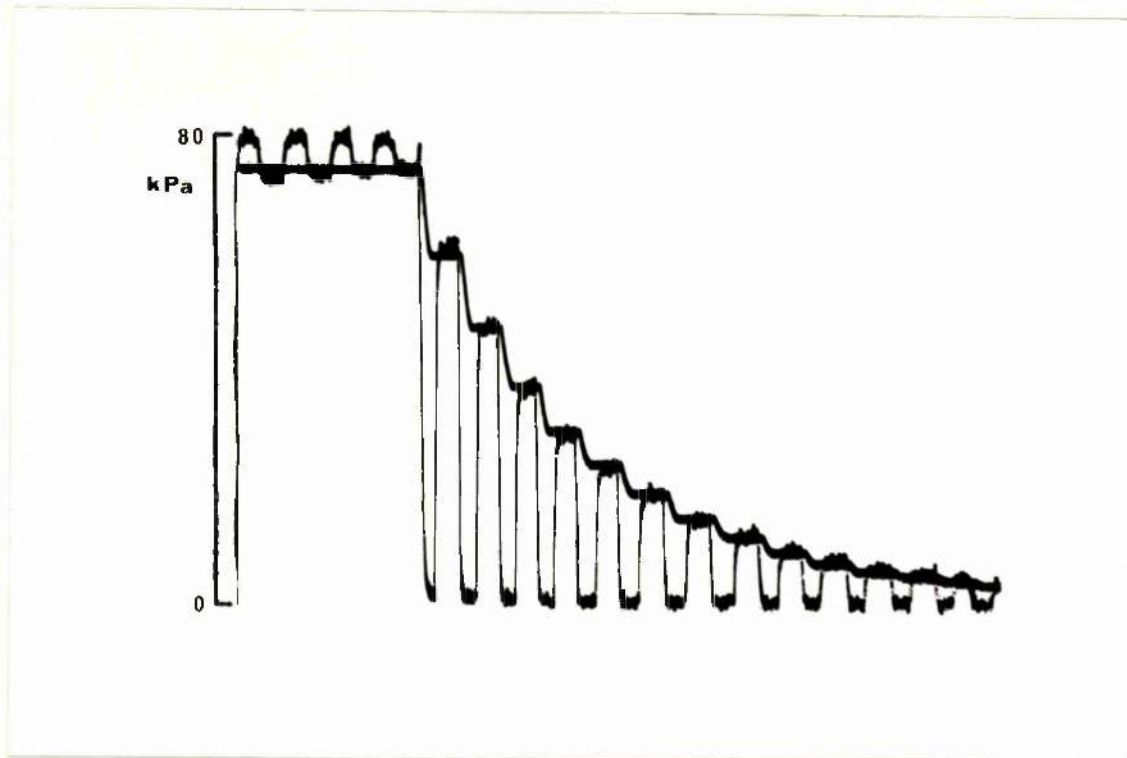


FIGURE 4.3

Comparison of model prediction of alveolar partial pressure of argon during a wash-out with that obtained experimentally, once the parameter ($1/V_A$) is at its optimum value. The measured inspired partial pressure of argon is zero. There is good agreement between model prediction and measurement during the end-tidal part of each breath. The initial part of the record is the end of the period during which argon is washed into the lung. The model is held at an initial alveolar partial pressure until the start of the wash-out.

<u>SUBJECT</u>	<u>FRC MODEL</u>	<u>ERV MODEL</u>	<u>FRC HELIUM</u>	<u>ERV HELIUM</u>	<u>FRC CORRECTED</u>	<u>FRC HELIUM</u>
1 EM	3.39	1.88	3.05	1.72	3.23	3.05
2 SMK	3.05	1.55	2.72	1.41	2.72	2.91
3 EG	3.22	-	3.36	-	3.22	3.36
4 GB	4.16	2.53	4.06	2.32	4.06	3.95
5 FD	4.79	2.05	4.74	2.02	4.76	4.74
6 FM	4.30	2.68	4.86	2.95	4.57	4.86
7 RJM	2.15	0.74	2.21	0.88	2.29	2.21
8 GC	1.70	1.12	1.85	1.01	1.59	1.88
9 JMcK	2.78	1.87	2.94	1.95	2.86	2.94
10 RMcC	3.22	1.88	3.67	1.91	3.25	3.67
11 JDHB	3.03	1.44	3.00	1.55	3.14	3.00
12 AS	2.65	1.30	2.92	1.24	2.59	2.92
13 ML	2.30	1.17	1.83	0.86	1.99	1.83
14 KK	3.67	2.37	3.91	2.73	4.03	3.91
15 NK	2.03	1.03	1.75	0.84	1.84	1.75
16 AR	2.45	1.36	2.55	1.32	2.41	2.55
17 RB	3.46	2.04	3.03	1.85	3.27	3.03
18 JW	3.76	2.29	3.91	2.40	3.87	3.91
19 JS	2.92	1.33	2.89	1.24	2.83	2.89
20 DM	1.48	0.52	1.32	0.44	1.40	1.32
21 JS	1.54	-	1.33	-	1.54	1.33
22 AMS	1.43	1.13	1.65	1.02	1.32	1.65
23 CW	4.60	3.07	4.19	2.92	4.45	4.19
24 JMCE	4.18	1.99	3.39	1.85	4.04	3.39
25 JMcK	3.23	1.93	2.61	1.43	2.73	2.61

TABLE 4.3.

The uncorrected functional residual capacity (FRC) from analysis of argon wash-out (FRC model, column 2) is obtained by addition of the estimated volume of the alveolar compartment (V_A) and pre-set dead space volume. This FRC is corrected to the same end expiratory level (FRC corrected) as that during the measurement of FRC by the closed-circuit helium method. /...

TABLE 4.3. (Caption continued).

The correction is made by subtracting the difference between the measurements of expiratory reserve volume ($ERV_{\text{model}} - ERV_{\text{helium}}$) from FRC model. In subjects in whom a satisfactory measurement of expiratory reserve volume was not obtained, the difference has been assumed to be zero.

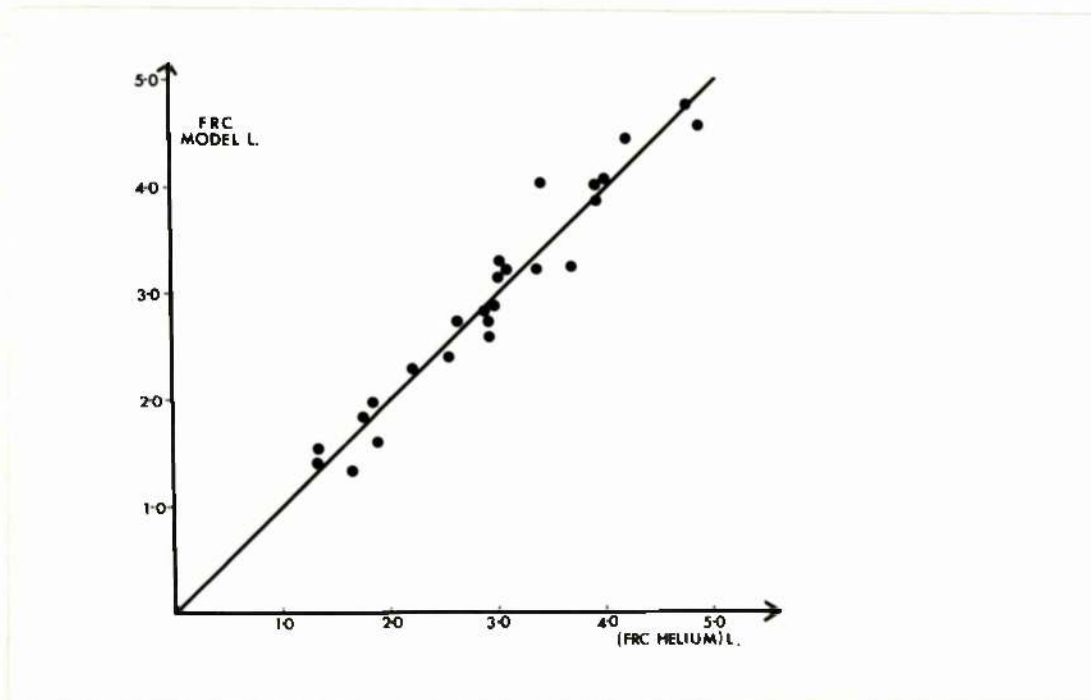


FIGURE 4.4

Comparison of lung volume as estimated by the use of parameter estimation (FRC MODEL) with that obtained by the closed circuit helium dilution method. The line shown is the line of identity.

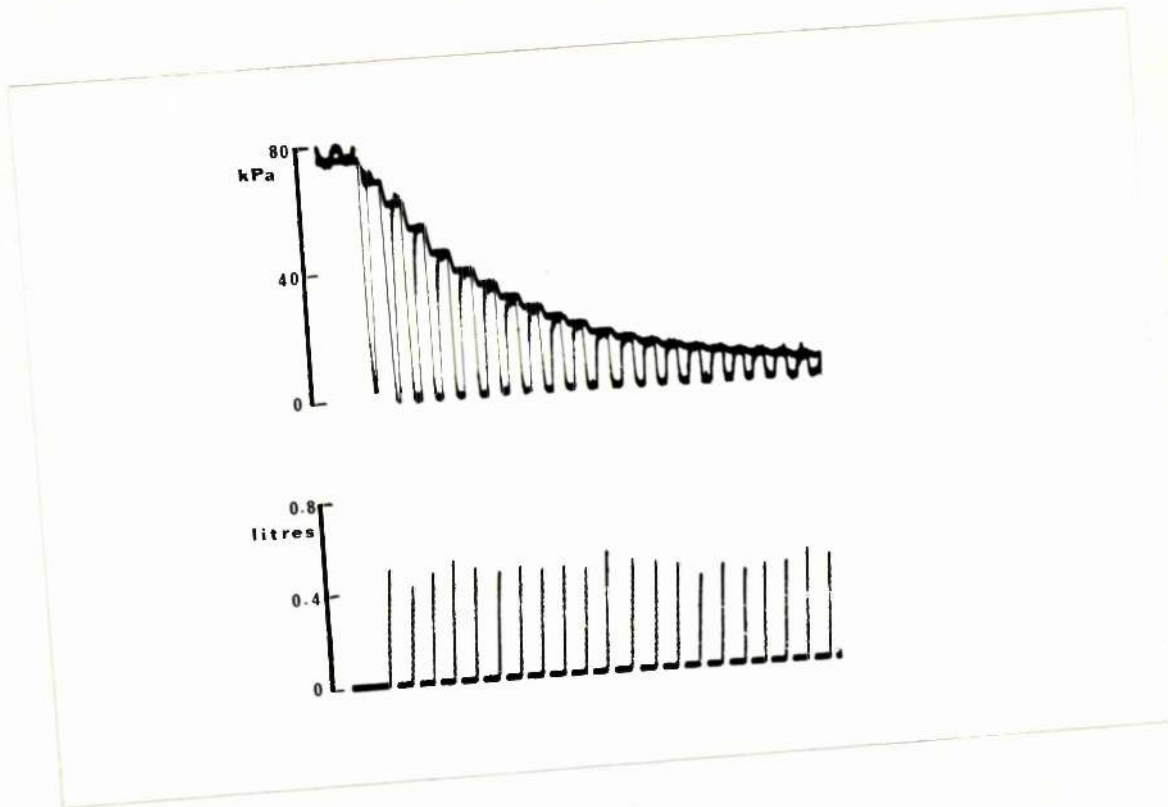


FIGURE 4.5 (a)

For caption see Fig. 4.5 (b)

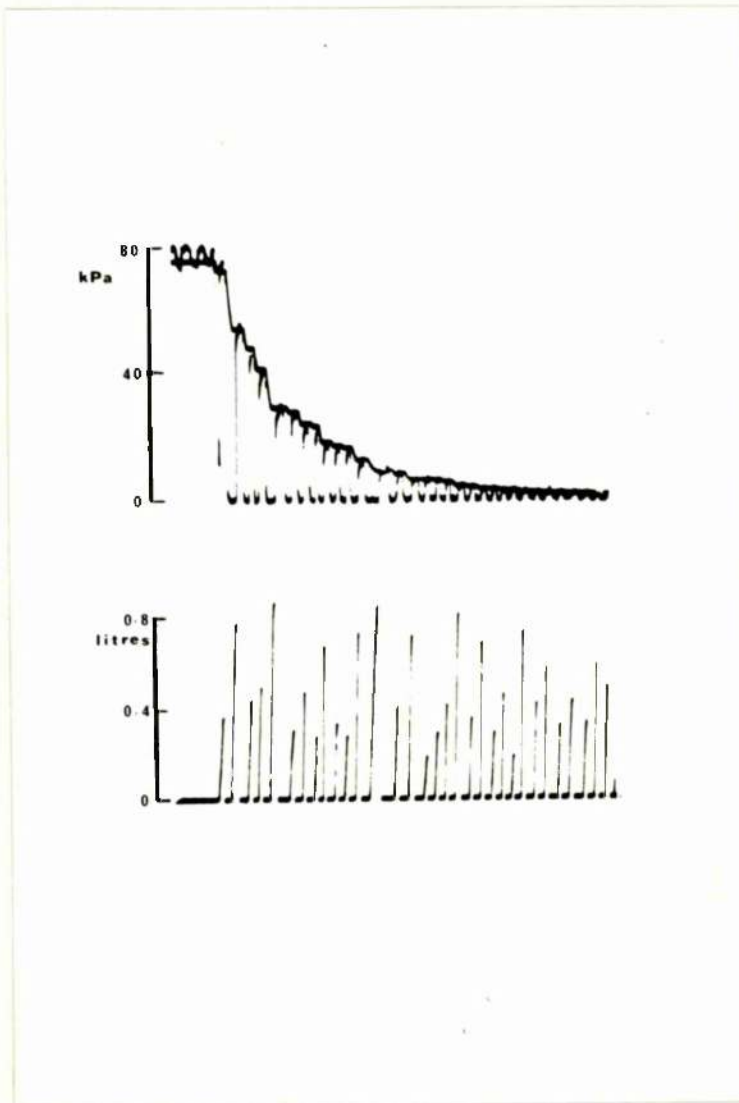


FIGURE 4.5 (b)

Comparison of model prediction and measurement during two argon wash-out experiments in the one subject. (For details of interpretation of records, see caption Fig. 4.3) In these graphs the volume of each breath is also shown, being represented by the height of the spikes at the bottom of the figure. In the first experiment (Fig. 4.5 (a)) the ventilation is relatively constant in contrast to the erratic ventilation in the second experiment (Fig. 4.5 (b)). There is good agreement between model prediction and measurement in both cases and the same result for lung volume was obtained.

4.4. FUTURE PROSPECTS FOR THE USE OF DYNAMIC MODELS IN THIS AREA.

The division of wash-out tests into single-breath, using information within a breath, and multiple-breath, using one data point per breath, is an unnecessary simplification. In multiple-breath tests the changing slope of the alveolar plateau within the individual breaths throughout the test should provide additional information. The dynamic modelling approach will allow utilisation of information within a breath to quantify abnormality. The problem as to what factors are principally responsible for the inconstancy of the alveolar plateau is, however, one of the large unresolved problems in respiratory physiology.

Discussion of this is polarised unnecessarily into a debate between those who propose that "parallel inhomogeneity" is the main mechanism and those who propose "series inhomogeneity". This subject was introduced briefly in the first section of this chapter.

If the slope of the alveolar plateau is to be related to "parallel inhomogeneity", two conditions need to be met:-

- a) the concentration of inert gas is different in different lung units;
- b) these units empty asynchronously, (often called sequential ventilation).

The lung is in reality a highly asymmetric structure. (The asymmetry has been quantified in detailed anatomical studies.¹³⁷) The anatomical asymmetry will lead to condition (a) being fulfilled both due to unequal distribution of dead space gas and unequal distribution of alveolar ventilation. Units can furthermore differ in mechanical properties, i.e. their resistance and

compliance. This will effect both the amplitude and phase of their relative ventilations. This has been studied using mathematical models^{260,35} with related experimental results.³¹⁰⁻³¹²

Differences between the function of different lung regions can be demonstrated experimentally.^{313,314,315,330} This is explained by the effects of gravity leading to less negative pleural pressure at the base of the lung³¹⁶⁻³²¹ and more distended alveoli at the apex.³²² There is also evidence, at least in dogs, of different intrinsic elastic properties in the upper and lower lobes.^{323,324} The different behaviour of the upper and lower lobes is most marked at low lung volumes due to the non-linearity of the pressure volume relationship.^{325,326} Closure of units in the lower zones occurs at low lung volumes.³²⁷⁻³²⁹ The differences in the pattern of ventilation between upper and lower lobes is altered by the inspiratory and expiratory flow-rates.³³³⁻³³⁷ The distribution of inspired gas at low flow rates is determined primarily by the relative compliance of lung regions.^{313,331,332} At high flow rates the relative resistance of different airways is important.

The ventilation to volume ratio difference between upper and lower lobes will not of itself cause inconstancy of the alveolar plateau. There is a need for condition (b) to be satisfied. Sequential ventilation is demonstrable even during tidal breathing but is a small order effect.³³⁸

Much of the slope of the alveolar plateau arises, therefore, from other factors. Significant slopes in inert gas concentration during expiration can be demonstrated in small airways both in man^{315,340} and in dogs.³³⁹ (The latter using a modification of the technique of retrograde catheterisation.³⁴¹) These studies suggest that the inconstancy of the alveolar plateau arises mainly from differences within units subtended by airways whose diameter is less than 3 mm.

The demonstration of significant slopes in small airways does not of itself add weight to either a "parallel" or "series" argument.

For the variation of the alveolar plateau at the mouth to reflect series inhomogeneity it is also necessary for two conditions to be met:-

- (a) gradients in concentration must exist in terminal lung units even at the end of inspiration;
- (b) such gradients must not be abolished by convection during expiration, i.e. they must be demonstrable at the mouth.

Evidence from simulation studies^{212,215,216,226,227} would suggest that condition (a) but not condition (b) is fulfilled.

Supporters of the concept of "parallel inhomogeneity" employ models which assume that gas transport in the airways is solely convective. Supporters of "series inhomogeneity" utilise models which assume equal convection to all lung units.

It is evident both theoretically and experimentally that the truth is unlikely to lie on either side. Indeed in the complex transport in the lung it is impossible to separate so completely the linked processes of convection and diffusion.

The most rational approach to this problem is to construct models which incorporate all mechanisms. This necessitates use of models which combine descriptions of pulmonary mechanics and gas transport. Such "multiple models" are used in the study of cardiovascular problems.^{16,17} The application of more complex models will require increased information content in the experiment. Practical considerations indicate that such models will have to be lumped rather than distributed models. It is, therefore, necessary to consider the importance of the distributed phenomena such as effective diffusion and convection in airways.

4.5 THE IMPORTANCE OF TAYLOR DISPERSION / A SIMULATION STUDY.

a) Introduction.

In Chapter 2.8 a distributed model of gas transport in the airways was described. This model incorporated both convection and Taylor diffusion. The development of lumped parameter models to analyse detailed measurements within a breath will be difficult if Taylor diffusion is an important mechanism.

The existing experimental evidence as to its importance is conflicting. Since in laminar flow diffusion increases with molecular weight (being inversely related to molecular diffusivity) evidence of its presence has been sought with experiments using inert gases of different diffusivities. An increase in the steady-state uptake of carbon monoxide has been demonstrated when a higher density inert gas (sulphur hexafluoride, SF₆ as compared with helium, He) is also present.³⁴⁵ This increase is more marked at higher ventilations. Likewise a larger inspired-arterial pressure difference for oxygen has been demonstrated in dogs when the lighter gas, helium, is substituted for nitrogen.³⁴⁴ The explanation of these results is thought to be enhanced diffusion as a result of Taylor dispersion.

Conversely a number of experiments using gases of different diffusivities indicate the limiting role of molecular diffusion. Sulphur hexafluoride is washed out slower than helium from excised dog lobes¹⁹³ and slower than hydrogen in man.⁴⁰⁰ Single breaths of gas mixtures containing helium and SF₆³⁴² or neon and SF₆³⁴³ indicate that greater amounts of the dense gas are expired in early expiration with increased amounts of the light gas in late expiration. Such differences are abolished by breath holding.

The results from simulation studies using the model which was described in Chapter 2.8 tend to support the view that Taylor

diffusion is relatively unimportant.

b) Simulation Studies.

In these studies a lung model which is based on the data of Weibel²¹¹ is used. Since this data corresponds to a lung at three-quarters of full inflation, the dimensions are scaled to give an equivalent functional residual capacity of 2.4L. The scaling is consistent with physiological studies.²²⁹ The data for the first four generations are not scaled, however, giving a lung model similar to that studied by Paiva.²¹⁵

A sinusoidal flow rate is used in these studies such that the tidal volume is 0.5L and respiratory frequency 15/min. Cardiac output is taken to be 5L/min.

In Figure 4.6 the partial pressure of CO_2 is shown as a function of x every 0.4S during a breathing cycle. Contours are plotted both for the cases in which Taylor diffusion is omitted or incorporated in an unmodified form. This corresponds to the cases in which α in equation 2.80 is set equal to 0 and 1 respectively. The steep pCO_2 pressure gradient is convected towards the alveoli during inspiration (0-2S) and towards the origin of the model during expiration (2-4S). Only during early inspiration (times less than 0.8S) and early expiration (2.0 - 2.8S) does the value of α have any effect on the pCO_2 curves. The convection of the pCO_2 gradient towards the origin of the model during expiration produces the expired concentration curve shown in Figure 4.7. The larger effective diffusion in the upper airways when the Taylor contribution is included produces a small but significant change in the shape of the expirate, but does not cause any significant increase in the amount of CO_2 expired at the end of expiration (less than 3%).

The similar graphs for oxygen are shown in Figures 4.8,4.9.

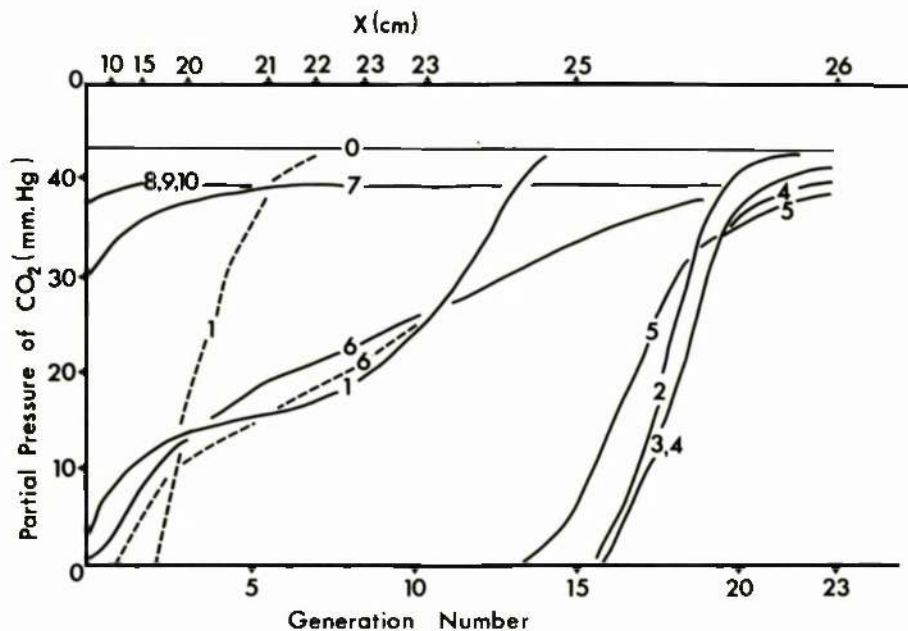


FIGURE 4.6.

Partial pressure profiles of $p\text{CO}_2$ throughout the lung model at ten equally spaced intervals of 0.4 sec during a single breath. Numbers one to five correspond, therefore, to inspiration, and six to ten inclusive are during expiration. The continuous lines are the cases when $\alpha = 1$ and the dotted lines are when $\alpha = 0$. At most times during the breath there is no significant difference between the profiles for $\alpha = 1$ and $\alpha = 0$ in which case only one profile is shown.

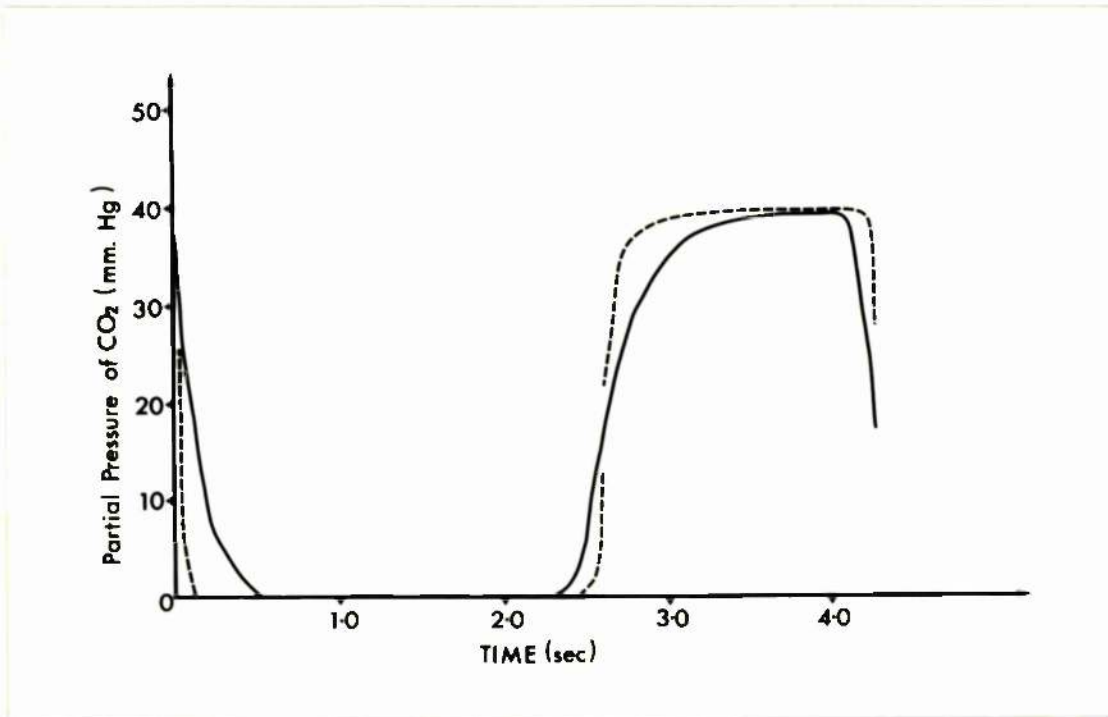


FIGURE 4.7

Comparison of model prediction of $p\text{CO}_2$ at $x = 0$ in the model in the cases in which $\alpha = 1$ (continuous line) and $\alpha = 0$ (dotted line).

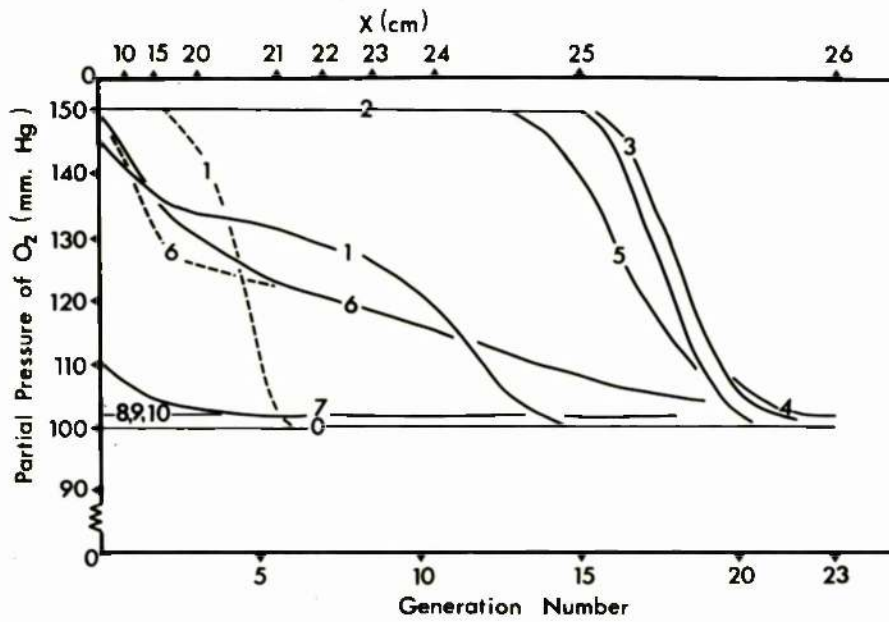


FIGURE 4.8

Profiles of pO_2 throughout the lung during a single breath of atmospheric gas. The symbols are as in Figure 4.6.

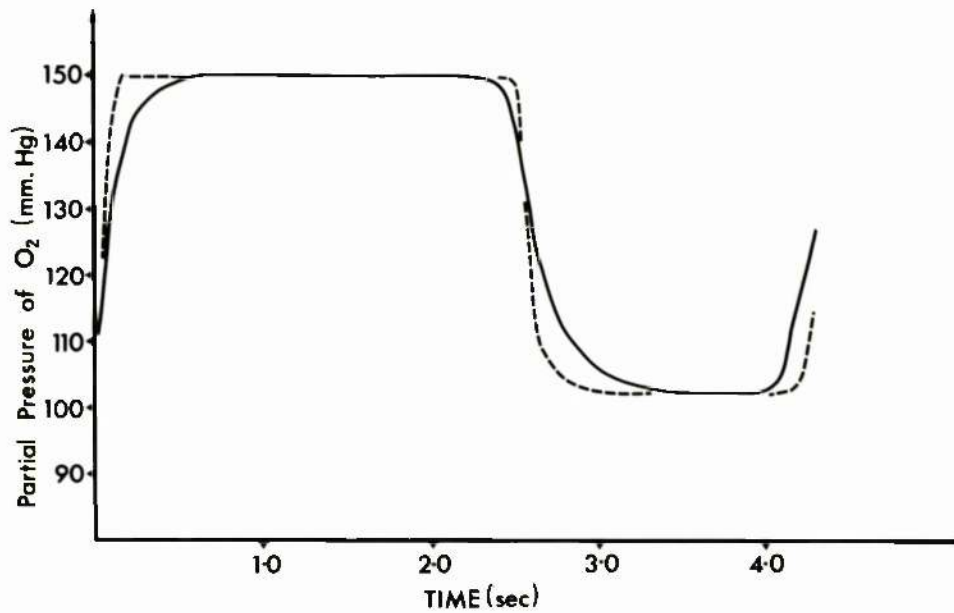


FIGURE 4.9

The model prediction of pO_2 at $x = 0$ during a single breath of atmospheric gas. The dotted curve corresponds to the case when $\alpha = 0$ and the continuous line to $\alpha = 1$.

Again the enhanced diffusion with $\alpha = 1$ produces no increase in the calculated oxygen uptake of the blood.

The results of a simulation of a single breath nitrogen test are shown in Figure 4.10. In this simulation the breath of oxygen is of 0.5L volume. The effect of α is only evident on the partial pressure curves during early inspiration and early expiration. The corresponding effect on the expirate is shown in Figure 4.11. The inclusion of Taylor diffusion does not significantly alter the amount of nitrogen "washed-out" of the lung at end expiration. Thus the value of α has no effect on the calculated volume of the dead space using the Bohr principle.¹³⁰ This is also reported by Lacquet et al.⁴⁰⁰

c) Discussion.

In the simulations which were described in the previous section the inclusion of Taylor diffusion made no significant alteration to gas uptake or output, or to the magnitude of dead space. These simulations are carried out with α of equation 2.80 equal to unity giving therefore the maximum possible effect of Taylor diffusion.

The inclusion of Taylor diffusion does produce certain effects on concentration profiles in the lung during the respiratory cycle. Such effects, are, however, only demonstrable during early inspiration ($t < 0.8S$) and early expiration (2.0- 2.4S). During early inspiration ($t < 0.8S$) the pressure gradients are in the airways where Taylor diffusivity is high. The effects of this high diffusivity on the $p(x,t)$ curve can be seen in Figures 4.6, 4.8, 4.10. During the remainder of inspiration there is no significant difference in the $p(x,t)$ curves for $\alpha = 0$ or 1. Early in expiration (2.0-2.4S in these simulations) the gradients are again in the region in which

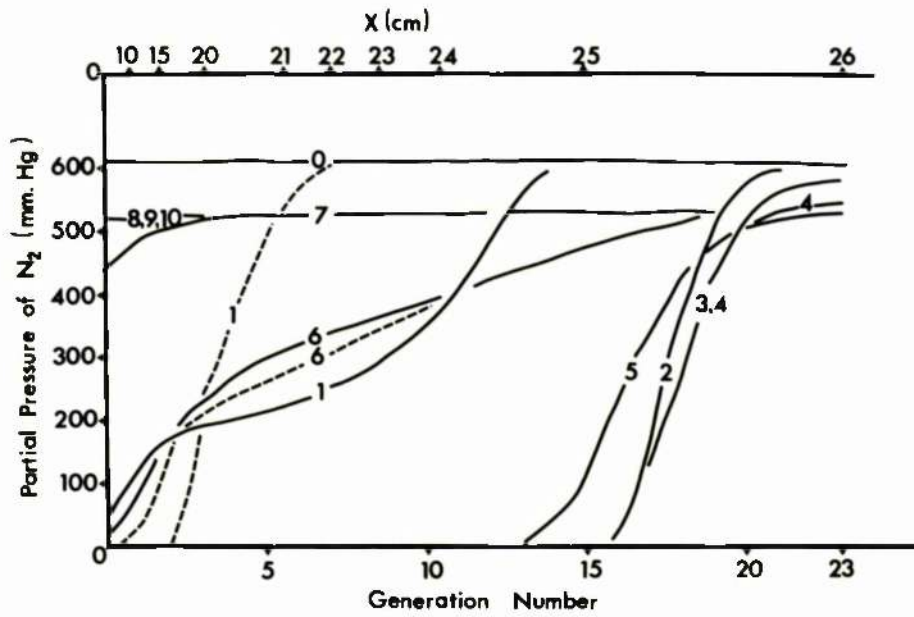


FIGURE 4.10

Partial pressure profiles of pN_2 in the lung during a single breath (tidal volume = 0.5L) of 100% oxygen. The symbols etc are as in Figure 4.6.

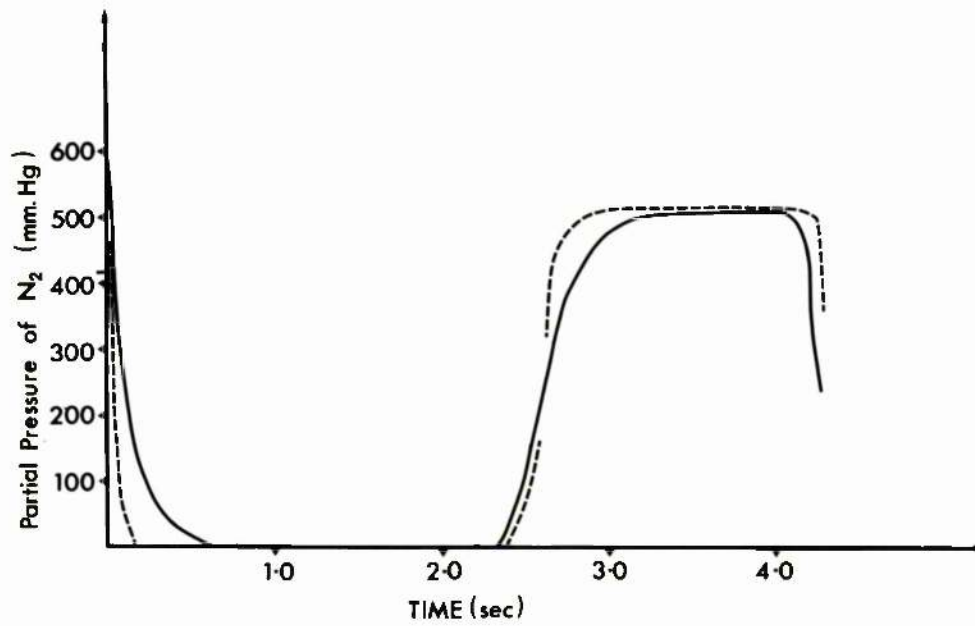


FIGURE 4.11

Comparison of model prediction of p_{N_2} at $x = 0$ during a single breath of 100% O_2 in the cases in which $\alpha = 1$ (continuous line) and $\alpha = 0$ (broken line).

if $\alpha = 1$, the Taylor-Aris diffusivity is high. The resultant effect on the $p(x,t)$ curves can be seen. During the remainder of expiration the gradients have largely been convected out of the lung, and the value of α is not expected to have an effect on the $p(x,t)$ curves.

Quantitative differences in the O_2 , CO_2 and N_2 results are related to the different molecular diffusion coefficients and to the different concentration gradients between inspired and alveolar gas.

The relative lack of effect of Taylor diffusion as compared to its magnitude is explained by:-

- (1) The Taylor-Aris effect, proportional to the square of the flow velocity becomes negligible for generation numbers $Z \geq 12$, since for these generations the flow velocity u is very small. This results in there being a region in the lung where molecular diffusion is the dominant transport mechanism.
- (2) For the upper airways $Z < 12$, the Taylor-Aris diffusivity can be very large at peak flows (e.g. two hundred times larger than molecular diffusivity) but at such times the large flow convects quickly the pressure gradient, through which diffusion operates out of these airways.
- (3) Since the total cross-sectional area of the lung rapidly increases with distance from the trachea after the twelfth generation the flow velocity must decrease rapidly. Thus, during inspiration, gas which is dispersed ahead of the mean convective flow enters initially the region where the flow velocity is low. Thus this gas becomes effectively stationary, whereas the remainder of the inspired concentration front continues to be convected. There is a resultant reduction in the degree of dispersion and an increase in the concentration gradient in this region. Thus although Taylor diffusion alters the concentration profiles in the upper airways, this is not reflected by alterations in the concentration profiles in

the terminal airways. Gas has to be transported across the latter region to enter or be removed from the alveoli. The variation in velocity within the bronchial tree will tend to have the opposite effect during expiration, i.e. increase the degree of dispersion.

The effect of variations in convective velocity at different points on a concentration gradient on the apparent degree of dispersion was neglected by Engel et al.⁴⁰² and by Scherer et al.²³³ who attributed the spread of a gradient to diffusion alone.

It might be expected³⁴⁵ that variations in the tidal volume or breathing frequency will modify the magnitude of the effect of Taylor diffusion since an increase in either of these will increase the flow velocity and hence the Taylor-Aris diffusivity. However, this increased flow velocity will decrease the time that the pressure gradient is in the upper airways and hence the time available for the enhanced diffusion to act. In simulation studies, variations in tidal volume and frequency produce no added effect of Taylor diffusion on overall gas flux as compared to the case with only molecular diffusion.

The main conclusion from these simulations is that Taylor diffusion has little effect on the efficiency of gas exchange. This is contrary to the suggestion of Kvale et al.³⁴⁵ All the experiments which have indicated an important role for Taylor diffusion have measured the relative transfer of gas into the arterial blood in different breathing conditions (e.g. with heavy gas as compared to light gas in the lung). This is in contrast to those experiments which suggest the limiting role of molecular diffusion in which only relatively insoluble gases are studied. It is possible that in the first type of experiment other factors are operative. For example the change in breathing conditions may alter the relative distribution of ventilation-to-perfusion. The

conclusions which are drawn from these simulations will be affected by the validity of the model. The symmetrical nature of the model may be of particular importance. It is conceivable that in pathways with different geometries, for example pathways with shorter transit lengths, Taylor diffusion is more important. It is to be emphasised, however, that the conclusion is reached from simulations in which the effect of Taylor diffusion is maximised ($\alpha=1$).

The main effect of Taylor-Aris diffusion in the lung, therefore, is to alter the distribution of gas in the upper airways ($Z < 12$) relative to molecular diffusion. There is a resultant effect (during expiration) on the partial pressure curve against time at the origin of the model. The distribution of the expirate is affected but not the amount expired. (Note that the integral $\int c_v dt$ gives only the convective contribution to the flux. In the case with $\alpha = 1$ there is a significant diffusive contribution to the total flux at the origin of the model.) Measurements of expired concentration of gases at the mouth resemble more closely the predicted results with $\alpha = 0$. As indicated in Chapter 2 the complex flow conditions in the lung imply that α will be less than 1.0 throughout most of the region in which Taylor diffusivity is operative. The magnitude of α cannot be obtained from mathematical analysis since the problem for the lung is too complex. There is a need for further experimental work both in man and in more realistic structural models than that employed by Scherer et al.²³³ It may be that even the detail of the expired concentration curve is relatively unaffected by Taylor diffusion.

4.6 CONCLUSION

The technique of dynamic modelling has been applied successfully to the analysis of inert gas wash-out experiments. Most methods of analysis of such experiments assume a constant ventilation. Methods which are based on parameter estimation techniques are seen to be applicable even in situations in which the ventilation of the subject is erratic. These studies have been carried out in normal subjects. The alveolar plateau in such subjects is flat, whereas in patients with respiratory disease there is a significant slope. Similar techniques could be applied to such patients by employing averaging techniques over the alveolar portion of the expirate. The time variation of the partial pressure of the expirate throughout the wash-out experiment would seem to present, however, an additional source of experimental information. There is a need for more complex models which incorporate both "parallel" and "series" inhomogeneity to analyse this data. Investigations with a distributed model of gas transport in airways indicates that Taylor diffusion does not produce significant effects on overall gas transport. It may, however, alter the shape of the expired concentration curve. There is a need for further experimental studies to elucidate this role of Taylor diffusion as a step in the development of more complex lumped parameter models. Such models will contain more parameters and hence increase the difficulty of applying parameter estimation methods. Parameter estimation has been applied to the estimation of four parameters in a model of carbon dioxide transport. This is discussed in the next chapter.

CHAPTER 5

A DYNAMIC MODEL OF CARBON DIOXIDE
TRANSPORT.

CHAPTER 5. A DYNAMIC MODEL OF CO₂ TRANSPORT.5.1. INTRODUCTION:

In this chapter the techniques of dynamic modelling are applied to the study of carbon dioxide transport. Carbon dioxide is exchanged between peripheral tissues and the atmosphere. The model which is used is more complex than that for an inert, insoluble gas. The complexities are related to the storage of carbon dioxide in lung tissue, to the peripheral stores of carbon dioxide in other tissues, and to the non-linear relationship between tension and concentration in blood. The structure for the lung component of the model is that which was shown in Fig. 2.1. The equations for a model describing carbon dioxide transport were considered briefly in Chapter 2 (equation 2.59). There are a larger number of parameters in these equations as compared to the model with a single parameter which was discussed in the previous chapter. The problem of parameter estimation is, therefore, more complex.

5.2. STORAGE OF CARBON DIOXIDE IN LUNG TISSUE:

The lung is known to contain more carbon dioxide than could be accounted for by simple solution of CO₂ in pulmonary extravascular water.³⁴⁷ This carbon dioxide is present in several forms - dissolved CO₂, carbonic acid, and bicarbonate. Experimental evidence,^{348,349} which has been obtained by infusion of radio-active labelled bicarbonate and carbon dioxide into the pulmonary artery, suggests that interconversion between the various forms is rapid. The rapidity of the chemical reaction

is related to the presence in the lung of the enzyme, carbonic anhydrase. This enzyme has been demonstrated to be present in blood-free lung tissue.^{350,351} The interconversion between the various forms is altered by administration of a carbonic anhydrase inhibitor.^{348, 352} The pulmonary membrane is thought to be impermeable to bicarbonate.^{348,349} CO_2 diffuses readily through the membrane, combines with water in the lung tissues to form carbonic acid which instantaneously dissociates into hydrogen and bicarbonate ions. The presence of significant amounts of carbon dioxide in the lung, in addition to that present in alveolar gas, buffers the changes in alveolar pCO_2 .³⁵³

The amount of CO_2 in the lungs of man has been measured by Sackner et al,³⁵⁴ using a plethysmographic technique, and by Hyde et al³⁵⁵ using an indicator dilution method with a stable isotope of CO_2 ($^{13}\text{CO}_2$). There is reasonable agreement between the results. The results of these studies have been expressed as the slope of the linear relationship between amount of CO_2 (ml of CO_2 ,STPD) in pulmonary tissue, excluding the amount in the pulmonary capillaries, and the tension of CO_2 (pCO_2 in mmHg). The mean of the results in 5 subjects are 1.32 ml of CO_2 /mmHg and 1.41 ml of CO_2 /mmHg respectively. There is, however, a large variability between individuals in the amount of CO_2 present in pulmonary tissue. In the study of Hyde et al³⁵⁵ values range from 151 to 255 ml of CO_2 (STPD). This variability is not related directly to body-size since the results after standardisation for surface area of each subject vary from 104 ml/m² of surface area to 164 ml/m². One can anticipate that, on average, a subject with a lung volume of 3.0L will have 150 ml of CO_2 in alveolar gas, 200 ml in pulmonary tissue, and 50 ml in

pulmonary capillary blood.

In modelling carbon dioxide transport the "store" of CO_2 in lung tissue can be considered separately from that in lung gas (see Section 2.7b). The process of equilibration, however, between pulmonary gas and surrounding tissue is rapid.³⁵⁶ Studies have been carried out in dogs to quantify this equilibration time^{352,357} using infusions of ether and bicarbonate into pulmonary artery. Ether is used to enable correction of the bicarbonate results for a circulatory delay. The mean time for evolution of 50% of CO_2 from bicarbonate (relative to ether) in these studies is 0.44 sec. Thus the equilibration is sufficiently rapid that for practical purposes equilibrium can be assumed to be instantaneous between alveolar gas and pulmonary tissue. This corresponds to using the concept of an equivalent lung volume,^{195,196,197} which contains components from both lung tissue and lung gas.

5.3. TISSUE STORES OF CARBON DIOXIDE:

There is approximately 100 litres of carbon dioxide stored in an average man.³⁵⁸ The amount of carbon dioxide stored in individual tissues is variable. One of the largest stores of carbon dioxide is in bone, in the form of carbonate.^{359,360} In the early mathematical models of tissue stores⁴⁴ a single homogeneous tissue compartment is used. Experimental studies³⁶¹ of total changes in carbon dioxide stores and arterial pCO_2 during hyper and hypoventilation indicate the presence of multiple tissue compartments with different time constants. Models with multiple tissue compartments were introduced by Farhi & Rahn.³⁵⁸ Each

compartment represents a specific tissue, e.g. muscle, and is considered to be "well-stirred". The parameters for each compartment are its volume, perfusion, CO_2 production, and slope of the dissociation curve relating concentration of carbon dioxide in the tissue to tension. Data for these parameters is given in the original reference,³⁵⁸ although it is incomplete. Tissues with a small perfusion relative to the amount of carbon dioxide stored will show slow dynamic responses to changes in state. This type of model gives reasonable agreement with data from experiments of long duration. There is poor agreement with experimental data^{362,365} from dynamic studies whose duration is less than fifteen minutes.^{358,362,363,36} Changes in arterial and venous pCO_2 are faster than that predicted by this model. These fast changes have led to the concept of an immediate carbon dioxide storage space,³⁶² which was measured using labelled carbon dioxide^{364,11} ($^{14}\text{CO}_2$). Initially it was proposed^{362,364} that the presence of a fast tissue space for carbon dioxide is related to a diffusion barrier between intracellular and extracellular spaces. An alternative hypothesis^{365,366,367} is that CO_2 hydration is slow in certain tissues, particularly muscle. Models which incorporate both mechanisms have been studied.^{366,368} The experimental data³⁶⁵ can be accounted for by either hypothesis.³⁶⁸ There is supporting evidence, however, for the hypothesis that CO_2 hydration is slow. It takes 30 minutes of carbon dioxide inhalation for muscle bicarbonate to increase measurably.³⁶⁹ There are negligible amounts of carbonic anhydrase in muscle.^{365,370} The lack of carbonic anhydrase results in a low slope of the dissociation curve in tissue. Each tissue can thus be considered to have an "effective tissue volume" which is defined as

effective tissue volume = tissue volume $\times \frac{\text{slope of dissociation curve (tissue)}}{\text{slope of dissociation curve (blood)}}$

These more sophisticated models predict the known results as obtained experimentally,^{363,364} Reasonable agreement between model prediction and measurement for short duration experiments is obtained, however, using a single tissue compartment with a small effective tissue volume.³⁶ Such a model structure is used in this chapter since all experiments are of the order of 90 seconds duration following a step change in carbon dioxide concentration in the inspired gas.

5.4. RELATIONSHIP BETWEEN THE CONCENTRATION AND TENSION OF CARBON DIOXIDE IN BLOOD.

The biochemical processes which govern the transport of carbon dioxide in blood are complex (for useful reviews see Davenport,³⁷¹ Roughton,³⁷² Van Slyke.³⁷³). Carbon dioxide is transported in several different forms. It dissolves in plasma and a small amount of this is converted to carbonic acid, which in turn dissociates into hydrogen and bicarbonate ions. The largest fraction of carbon dioxide diffuses into erythrocytes. The enzyme carbonic anhydrase is present in red blood cells in a high concentration. Thus significant amounts of hydrogen and bicarbonate ions are formed here. The hydrogen ions combine with the protein, i.e. haemoglobin, thereby buffering any change in intracellular pH. Bicarbonate ions diffuse from the erythrocytes into plasma since a concentration gradient is established. Electrical neutrality is maintained by a corresponding "shift" of chloride ions into the cells. Carbon dioxide also combines chemically with the amino groups on certain proteins, in particular haemoglobin, to form carbamino compounds,³⁷⁴ i.e.



The relative amounts of carbon dioxide in different chemical forms in blood are shown in Table 5.1.

Total CO ₂ in 1 litre of blood	21.53
<u>Plasma</u>	
Total CO ₂ in plasma	15.94
As dissolved CO ₂	0.71
As bicarbonate ions	15.23
<u>Red Blood Cells</u>	
Total CO ₂ in red blood cells	5.59
As dissolved CO ₂	0.34
As Carbamino compounds	0.97
As bicarbonate ions	4.28

TABLE 5.1.

The distribution of carbon dioxide (mmoles) as transported in one litre of arterial blood. The data are taken from Davenport³⁷¹ The original source of data is Henderson³⁷⁵

The transport of carbon dioxide is linked with the transport of oxygen. For a given pCO₂ more carbon dioxide is carried in blood with a low oxygen content than in blood fully saturated with oxygen. (This difference has become known as the Haldane effect). The biochemical basis is that reduced haemoglobin forms more carbamino-Hb³⁷⁴ and is also a more effective buffer of hydrogen ions.³⁷⁶

There are two main approaches to the mathematical description of the relationship between concentration and tension of carbon dioxide in blood. In one approach a description is developed from the basic physico-chemical equations which are incorporated in a computer subroutine.^{147,377,378} The alternative is to fit a

function to published experimental data which give the relationship between concentration and tension. There is a wide variety of such functions used in simulations of carbon dioxide transport (see Table 5.2).

The main sources of, and the original data are summarised in Table 5.3. The data of Henderson et al³⁸² are derived from studies on the blood of one man (A.V. Bock). The data of Dill et al³⁸³ are published in the form of a nomogram and represent the average of studies in twelve healthy subjects. The data which are presented by Dittmer and Grebe³⁸⁴ are the average of the data in the literature.

Over the range of interest ($30 \leq p\text{CO}_2 \leq 60$ mmHg) the relationship can be approximated by a linear function (see Fig. 5.1 and Table 5.4). There is little difference between the slopes of the straight line fit to different data and at different oxygen saturations (see Table 5.4). The slopes which are shown in Table 5.4 are for oxygen saturations of 95% and 70% corresponding to arterial and mixed venous blood respectively. The intercepts of the linear functions are different for mixed venous and arterial blood (see Table 5.4). This is related to the Haldane effect. This difference is neglected in many of the simulations of carbon dioxide transport.^{94,195,197,198,202,286,380.}

This published data can only be applied to subjects whose biochemical status is similar with respect to several variables, e.g. serum protein, chloride, and bicarbonate concentrations. Indeed, it was appreciated at an early point³⁹⁵ that the relationship between concentration and tension of carbon dioxide in blood is different in different subjects. Of particular importance in

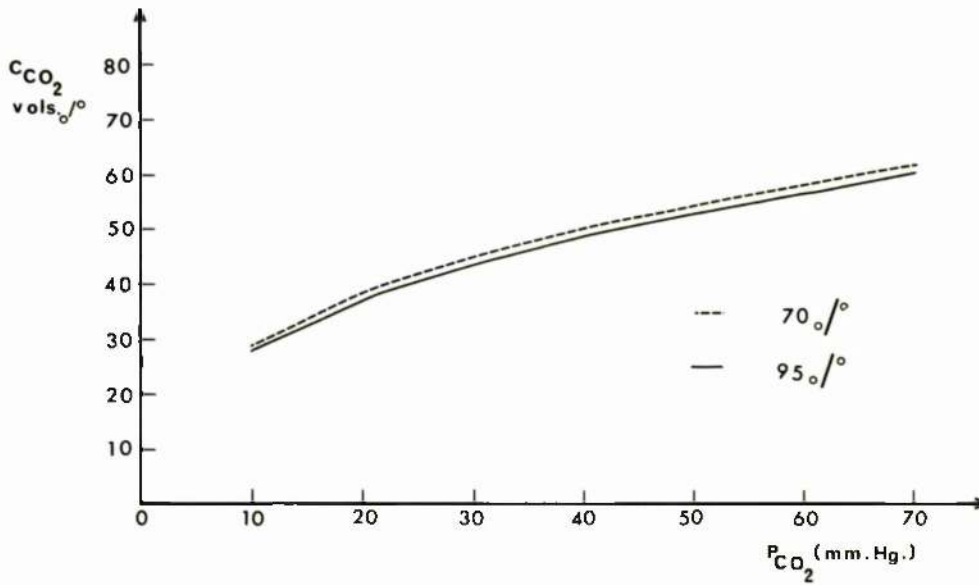


FIGURE 5.1

Graphs showing relationship between carbon dioxide concentration in blood (C_{CO_2} , ml.STPD./100 ml. of blood) and tension (p_{CO_2} , mmHg) at two different oxygen saturations (70 & 95%). Over the range of interest $30 \leq p_{CO_2} \leq 60$ the relationship is seen to be approximately linear.

TABLE 5.2.

<u>Reference</u>	<u>Animal Species</u>	<u>Description</u>
Grodins et al ⁴⁴	Man	$C_{CO_2} = a + bP_{CO_2}$ $b = 0.00425$
Trueb et al ³⁷	Dog	$C_{CO_2} = (0.149 - 0.145S)P_{CO_2}^{0.35}$ $S = \text{Saturation (Oxygen)}$
DuBois et al ¹⁹⁷	Man	$C_{CO_2} = a + bP_{CO_2}$ $b = 0.00425$
Chilton & Stacy ¹⁹⁵	Man	$C_{CO_2} = a + bP_{CO_2}$ $b = 0.00714$
Yamamoto ¹⁹⁸	Man	$C_{CO_2} = a + bP_{CO_2}$ $b = 0.00714$
Lin & Cumming ²⁰⁸	Man	$C_{CO_2} = a + bP_{CO_2}$ $b = 0.0063$
Flumerfelt & Crandall ²⁰²	Man	$C_{CO_2} = 0.01097 -$ $0.0002256P_{CO_2} + 0.000001749P_{CO_2}^2$
Milhorn & Pulley ²³⁷	Man	$C_{CO_2} = \frac{aP_{CO_2} + b(P_{CO_2})^2}{1 + cP_{CO_2}} / 100$ (a,b,c are functions of oxygen saturation)
Visser ³⁷⁹	Man	$C_{CO_2} = 0.3478 + 0.0045 P_{CO_2} -$ $0.065S$ $S = \text{Saturation (Oxygen)}$
Kim et al ³⁸⁰	Man	$C_{CO_2} = a + bP_{CO_2}$ $b = 0.0047$
Meade et al ²⁰⁶	Man	$C_{CO_2} = \frac{P_{CO_2}}{aP_{CO_2} + b}$ $a = 1.255; b = 0.0357$

Different functions which have been employed to relate concentration of carbon dioxide in blood (C_{CO_2} L(STPD)/L) to tension (mmHg), in simulations of carbon dioxide transport.

TABLE 5.3.

Saturation 95%		Saturation 70%		
$p\text{CO}_2$	C_{CO_2} (Henderson et al).	C_{CO_2} (Dill et al)	C_{CO_2} (Dittmer & Grebe)	
10	27.1	NA	27.9	
20	36.8	36.3	37.1	
30	43.3	43.2	43.5	
40	48.3	48.4	48.8	
50	52.5	53.1	53.1	
60	56.5	57.0	57.0	
70	60.0	60.3	60.8	
80	63.3	NA	64.2	
10	28.5	NA	29.2	
20	38.3	38.0	38.4	
30	44.8	44.8	44.9	
40	49.9	50.0	50.2	
50	54.1	54.5	54.5	
60	58.1	58.4	58.4	
70	61.6	62.0	62.3	
80	64.8	NA	65.8	

Carbon dioxide concentration (C_{CO_2} ml/STPD)/100 ml of blood) at different carbon dioxide tensions (mmHg). The data are derived from the nomogram of Dill et al,³⁸³ and by linear interpolation between the published results for completely reduced and completely oxygenated blood of Henderson et al,³⁸² and Dittmer & Grebe.³⁸⁴ Data are given for two different oxygen saturations (70% & 95%). NA indicates that this item of data is not available.

TABLE 5.4.

<u>Saturation 95%</u>			
<u>Source of Data</u>	<u>Slope</u>	<u>Intercept</u>	<u>S.D. of Regression</u>
Henderson et al ³⁸²	0.00432	0.3076	0.6%
Dill et al ³⁸³	0.00461	0.2968	0.9%
Dittmer & Grebe ³⁸⁴	0.00448	0.3044	1.0%
<u>Saturation 70%</u>			
<u>Source of Data</u>	<u>Slope</u>	<u>Intercept</u>	<u>S.D. of Regression</u>
Henderson et al ³⁸²	0.00441	0.3188	0.8%
Dill et al ³⁸³	0.00453	0.3154	0.9%
Dittmer & Grebe ³⁸⁴	0.00451	0.3173	0.9%

The slope and intercept of the linear relationship between carbon dioxide content (L(STPD)/L) and tension (mmHg) over the range 30-60 mmHg. The data from three different sources have been examined, at two different oxygen saturations (70 & 95%). The residual error around the line is small as is demonstrated by the low standard deviation of regression.

causation of this variability is the variability of haemoglobin concentration. The important role of haemoglobin in carbon dioxide transport has been discussed, both in buffering the change in intracellular pH and in the formation of carbamino-Hb. The relationship between concentration of carbon dioxide and tension in blood has a low slope in subjects with anaemia³⁹⁶ and an increased slope in subjects with polycythaemia.³⁹⁷ The effect of haemoglobin concentration on the slope of the linear relationship between concentration and tension has been investigated by Peters et al,³⁹⁸ over a wide range. The oxygen capacity of the bloods which were studied ranged from 2.65 to 28.7 vols% (i.e. haemoglobin concentrations of 1.98G% to 21.42G%). The slope was demonstrated to be related linearly to oxygen capacity of the blood and hence to haemoglobin concentration, i.e.

$$\begin{aligned} \text{Slope L/L/mmHg} &= \frac{0.334 \text{ O}_2 \text{ capacity} + 6.3}{30 \times 100.0} \\ &= \frac{0.448 \text{ Hb. conc.} + 6.3}{30 \times 100.0} \end{aligned}$$

The slopes have been calculated using this relationship for a number of different haemoglobin concentrations and are shown in Table 5.5. For a useful discussion of the effect of biochemical variables on the mathematical description of the carbon dioxide dissociation curve see McHardy.³⁹⁹

TABLE 5.5.

<u>Haemoglobin Concentration</u> G/100 ml of blood	<u>Slope of linear relationship</u> <u>between CCO_2 (L(STPD)/L blood)</u> <u>and PCO_2 (mmHg).</u>
10.0	0.00359
11.0	0.00374
12.0	0.00389
13.0	0.00404
14.0	0.00419
15.0	0.00434
16.0	0.00449
17.0	0.00464

The slope of the linear relationships between carbon dioxide concentration (L(STPD)/L blood) and carbon dioxide tension (mmHg), at several different haemoglobin concentrations. The slopes are calculated from the relationship described by Peters et al.³⁹⁸

5.5. MODEL OF CARBON DIOXIDE TRANSPORT.

The model of carbon dioxide transport which is used in this chapter is based on a lung model with dead space and alveolar compartments (see Fig. 2.1), with the tissues being represented as a single "effective" tissue compartment with volume V_{TC} . It is thus assumed that the dissociation slope for CO_2 in tissues is identical to that in blood. The circulatory delay between the tissues and lung is not modelled. The volume of the alveolar compartment (V_A) is the "equivalent" lung volume. The model is described by two equations, whose form is similar to those described in Chapter 2.7 and derived in Appendix 1.B. i.e.

$$V_A \beta g \frac{dP_A}{dt} = S\dot{V}\beta g(P_I - P_A) + \dot{Q}(f_1(P_{\bar{v}}) - f_2(P_A))$$

$$V_{TC} \frac{d}{dt} (a_{TC} + bP_{TC}) = \dot{M} - \dot{Q}(f_1(P_{\bar{v}}) - f_2(P_A))$$

$$\text{but } f_1(P_{\bar{v}}) = a_{\bar{v}} + bP_{\bar{v}}CO_2 \quad (\text{see section 5.3})$$

$$f_2(P_A) = a_a + bP_A CO_2$$

where b is the slope of the linear relationship between concentration and tension of carbon dioxide. Other symbols as defined in Chapter 2.

i.e.:-

$$V_A \beta g \frac{dP_A}{dt} = S\dot{V}\beta g(P_I - P_A) + \dot{Q}b(P_{TC} - P_A) + \dot{Q}(a_{\bar{v}} - a_a) \quad (5.1)$$

$$V_{TC} b \frac{dP_{TC}}{dt} = \dot{M} - \dot{Q}b(P_{TC} - P_A) - \dot{Q}(a_{\bar{v}} - a_a) \quad (5.2)$$

It is assumed that $P_{TC} = P_{\bar{v}}$.

The equations are solved using the approximate numerical technique which is described in Chapter 3.2(b).

The equations contain a number of unknown parameters, i.e.:-

\dot{Q}	Cardiac output
V_A	Lung volume
\dot{M}	Metabolic production of CO_2
V_{TC}	Tissue volume

In addition values have to be assigned to the initial values of P_A and P_{TC} at time $t = 0$ and to the volume of the anatomical dead space.

Dead space volume³⁸⁵ and $P_A(0)$ are measurable directly. To calculate $P_{TC}(0)$ it is assumed that at time $t = 0$, the tissue compartment is in a steady-state, i.e. $\frac{dP_{TC}}{dt} = 0$. It is not assumed that there is a steady-state in the lung. This does not represent, therefore, a limitation to the experimental procedure.

If $\frac{dP_{TC}}{dt} = 0$ then

$$\dot{M} - \dot{Q}b(P_{TC}(0) - P_A(0)) - \dot{Q}(a_v - a_a) = 0$$

i.e.

$$P_{TC}(0) = \frac{\dot{M}}{b\dot{Q}} - \frac{(a_v - a_a)}{b} + P_A(0) \quad (5.3)$$

Thus a value can be assigned to $P_{TC}(0)$ if $\dot{M}, \dot{Q}, P_A(0)$ are fixed.

The parameter estimation problem is, therefore, to estimate the unknown parameters $\dot{Q}, V_A, \dot{M}, V_{TC}$.

5.6. OUTLINE OF EXPERIMENTAL PROCEDURE.

The experiments which are described in this chapter were carried out in four healthy subjects. The volume of the anatomical dead space for each subject was obtained as described in Chapter 4. All subjects are non-smokers. The physical characteristics of each subject are listed in Table 5.6. Experiments were carried out at rest and during exercise. The experiments which were performed

involve a perturbation so that the dynamic response of the carbon dioxide transport system can be examined. Each experiment consisted of an initial period (30 secs) in which the subject breathed air, followed by a period breathing a gas mixture containing 5% carbon dioxide (90 sec duration). The details of the experimental procedures are considered in later sections of this chapter. The experimental methods were discussed in Chapter 3.

TABLE 5.6.

<u>Subject</u>	<u>Sex</u>	<u>Age</u> (yrs)	<u>Ht.</u> m.	<u>Wt.</u> Kg.	<u>Surface</u> <u>Area</u> m ²	<u>Haemoglobin</u> <u>Concentration</u> g/100 ml.	<u>Functional</u> <u>Residual</u> <u>Capacity</u> L.	<u>Volume</u> <u>Anatomical</u> <u>Dead Space*</u> L.
II	F	23	1.64	68.6	1.75	12.3	1.4	0.150
RMCC	F	43	1.68	59.5	1.67	12.4	3.6	0.175
JU	F	48	1.60	50.9	1.51	14.5	2.2	0.150
WG	M	30	1.82	70.0	1.90	15.4	3.8	0.190

Physical characteristics of the subjects who took part in the studies which are described in this chapter.

* Includes small instrumental dead space.

5.7. PARAMETER ESTIMATION PROCEDURES.

The problem of estimation of four parameters is more complex than the single parameter case, which was discussed in the previous chapter. Continuous parameter estimation techniques^{306,307} are inappropriate and the alternative discrete methods are used.

Discrete methods of parameter estimation involve a criterion function J which is the total error between model prediction and measurement during the complete experiment i.e.

$$J = \int_0^T e^2(t, \underline{Q}) dt$$

where T is the duration of the experiment and

$$e(t, \underline{Q}) = y_s(t) - y_m(t, \underline{Q})$$

is the error, i.e. difference between model prediction $y_m(t, \underline{Q})$ and measurement $y_s(t)$. \underline{Q} is the vector of parameters.

The discrete methods of parameter estimation involve optimisation procedures which adjust the parameter values (\underline{Q}) such as to obtain the minimum of J . There are two different classes of optimisation procedure. Direct search methods involve a search, according to a specified algorithm, to find this minimum. The function J is evaluated at different points in parameter space, i.e. with different values of the parameters. The search procedure moves to a new point such that the value of J is reduced and the search recommenced. Gradient methods carry out a similar procedure but the gradient of the function J is evaluated at each point as well as the function itself. Thus these methods utilise information on the slope of the surface J .

Both types of optimisation method can determine only a local minimum, i.e. a point which is a minimum with respect to its immediate surroundings but not necessarily the overall minimum (global minimum). It is, therefore, useful if it can be established that the function is unimodal, i.e. it has only one minimum over the range of interest

of the parameter values.

Error surfaces are one means of investigating the shape of the function J but can only be used to consider J as a function of two variables. In estimation problems involving a large number of parameters such surfaces allow inspection of the surface J in the plane of two of the parameters. Error surfaces can be drawn as contour plots consisting of contour lines joining points of equal error drawn on a 2 parameter space. Such a plot is generated by calculating the value of J at each point on a grid over the parameter space and using an interpolation technique to find points of equal function value.³⁸⁶ An example of such a surface for the parameter estimation problem which is described in this chapter is shown in figure 5.2. The surface is seen to be unimodal.

Before applying optimisation methods it is useful to obtain information on the effect of individual parameters on the model's performance. This can be achieved by carrying out a number of different simulations of a standard experiment with different values of the parameters. The experiment which has been simulated consists of an initial five breaths of air ($P_I\text{CO}_2 = 0.0$) followed by a step change to an inspired gas such that the inspired partial pressure of carbon dioxide ($P_I\text{CO}_2$) is 21.0 mmHg (2.78kPa). Simulations have been carried out in which each of the parameters ($\dot{Q}, V_A, \dot{M}, V_{TC}$) have been varied in turn over the range of interest with all other parameters fixed. These simulations indicate the effect of cardiac output (Fig. 5.3), lung volume (Fig. 5.4) and metabolic production (Fig. 5.5). The model has a distinct sensitivity to these parameters. There is little interaction between the effects of the parameters. The model's performance throughout the simulation is

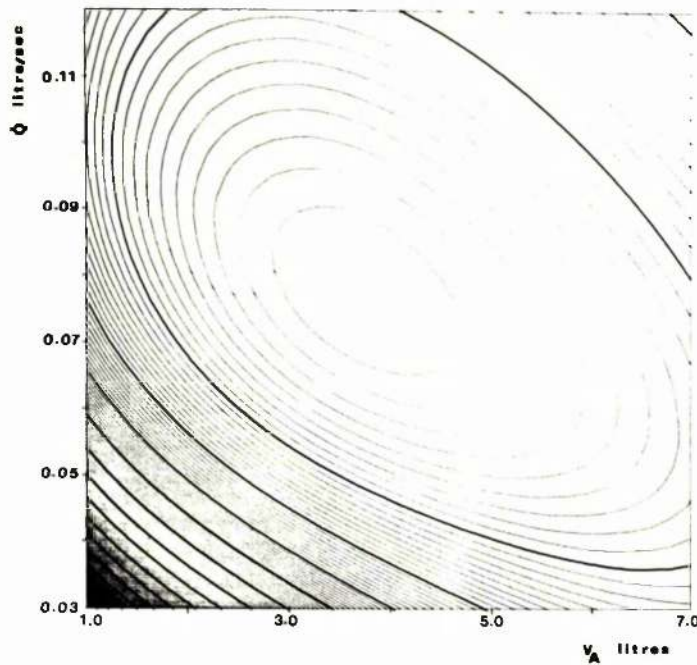


FIGURE 5.2

Error contour plot in the plane of the two parameters \dot{Q} (L/sec) and V_A (L). Each line on the plot represents a line of iso-error. The minimum is at a lung volume of 4.0L and cardiac output 0.08 L/sec. The lines at the periphery of the plot are of higher error. The error contour plot is seen therefore to represent a valley-shaped surface.

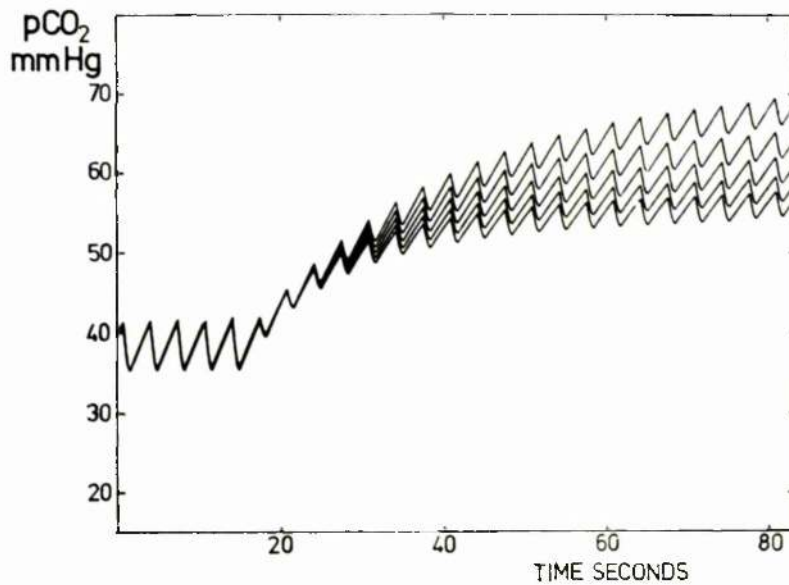


FIGURE 5.3

Demonstration of effect of variations in cardiac output parameter on model's response. The experiment which is simulated consists of an initial period of air-breathing followed by a step-change to breathing gas mixture containing 3% CO_2 . Five different simulations are shown in which the cardiac outputs of the model are 3.5, 4.5, 5.5, 6.5, 7.5 L/min respectively with all other parameters being constant throughout all the simulations. The main effect of the cardiac output parameter is seen to be on the later part of the transient.

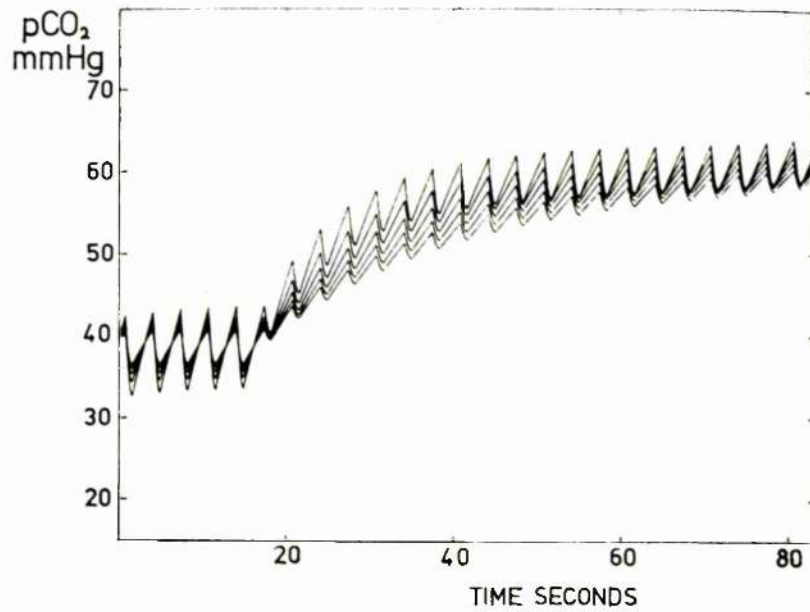


FIGURE 5.4

Demonstration of effect of variations in lung volume parameter on model's response. The same experiment is simulated as for Figure 5.3. Five different simulations are shown in which the lung volumes of the model are 2.5, 3.5, 4.5, 5.5, 6.5L respectively with all other parameters being constant throughout all the simulations. The main effect of this parameter is on the early part of the transient.

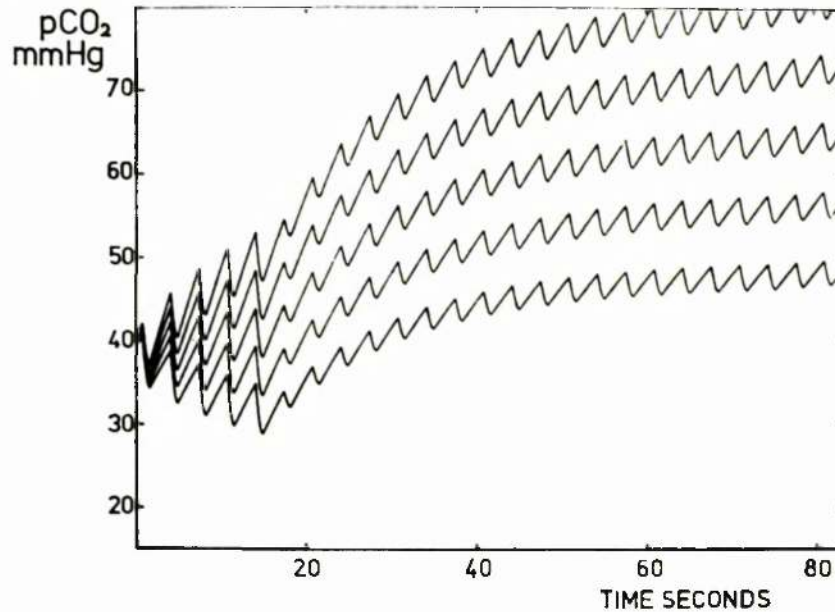


FIGURE 5.5

Demonstration of effect of variations in metabolic production parameter on model's response. The same experiment is simulated as for Figure 5.3. Five different simulations are shown in which the metabolic production is varied from 0.15 L/sec to 0.35 L/sec in increments of 0.05 L/sec with all other parameters being constant throughout all the simulations. Alteration of this parameter affects the entire model response.

affected by the value of metabolic production. The initial part of the transient response to the step-change in inspired $p\text{CO}_2$ is dependent on the value of lung volume. The later part of the transient is sensitive to cardiac output.

Simulations of the model's performance with different values of the tissue volume parameter indicate that the model is much less sensitive to this parameter. Any effect of variation in tissue volume is demonstrated at the end of the transient.

Initially, therefore, parameter estimation has been applied to the estimation of three parameters (\dot{Q}, V_A, \dot{M}) with tissue volume being considered fixed. Investigation of different optimisation procedures as applied to this problem indicates that the two methods (the Rosenbrock method³⁸⁷ and the Davidon-Fletcher-Powell^{388, 389} method) are the most efficient.³⁸⁶ (For useful reviews of optimisation methods see Adby & Dempster,³⁹⁰ Box et al,³⁹¹ Dixon,³⁹² Powell,³⁹³ White³⁹⁴). The Rosenbrock³⁸⁷ method is a direct search method and the Davidon-Fletcher-Powell^{388, 389} is a gradient method. The details of the theoretical basis of these methods and their implementation are presented in Appendix 9.

Optimisation which is carried out with different tissue volumes indicates that the estimates of the other three parameters is dependent on the value of tissue volume (see Table 5.7). There is, furthermore, a distinct minimum in the criterion function at a

TABLE 5.7

Subject	Tissue Volume		Optimum Parameters		Criterion Function
	<u>L</u>	<u>Cardiac Output</u> L/min	<u>Lung Volume</u> L	<u>Metabolic Production</u> L/min	mmHg ²
<u>WG</u>	3.0	7.56	2.03	0.223	0.6225
	4.0	7.40	2.75	0.236	0.4327
	5.0	6.74	3.22	0.241	0.3881
	6.0	6.29	3.62	0.245	0.3850
	7.0	5.88	4.00	0.248	0.3928
	8.0	5.60	4.24	0.249	0.4023
	9.0	5.38	4.52	0.250	0.4110
	10.0	5.21	4.73	0.251	0.4185
	20.0	4.55	5.55	0.254	0.4525
	30.0	4.36	5.78	0.254	0.4631
	40.0	4.29	5.90	0.254	0.4682
<u>Subject</u>					
<u>RMcC</u>	3.0	4.46	4.68	0.197	0.3097
	4.0	3.73	5.67	0.207	0.2662
	5.0	3.24	6.31	0.211	0.2686
	6.0	2.93	6.72	0.213	0.2743
	7.0	2.81	6.91	0.214	0.2791
	8.0	2.67	7.08	0.214	0.2827
	9.0	2.58	7.23	0.215	0.2856
	10.0	2.53	7.32	0.215	0.2879
	20.0	2.32	7.77	0.217	0.2982
	30.0	2.25	7.84	0.218	0.3014
	40.0	2.22	7.90	0.218	0.3030

Effect of tissue volume parameter on estimates of other parameters and on criterion function for experiments which were carried out on subjects WG and RMcC. The experiments were carried out at rest. Each experiment consisted of a period (30 secs) breathing air followed by a step change to a gas mixture containing 5% CO₂. In the simulation of the model's performance, a value of 0.0045 L/L/mmHg is used for b, and a value of 0.0129 L/L for the difference between the intercepts of the linear relationships between CO₂ concentration and tension in mixed venous and arterial blood. The Rosenbrock method of optimisation is used. Variation in tissue volume is seen to affect the estimates of the other three parameters. There is a distinct minimum in the criterion function at a tissue volume of 6.0L for subject WG and 4.0L for subject RMcC. The criterion function is the mean of the square of the differences in mmHg² between model prediction and measurement during the end-tidal part of each breath.

certain tissue volume (see Table 5.7). This minimum in the criterion function occurs at the same tissue volume in different experiments in the same subject at rest (see Table 5.8). The same phenomenon is found in optimising experimental data which are obtained in studies during exercise (see Table 5.9). These results suggest that the information content in the experimental data is sufficient to allow estimation of the four parameters. The input disturbance applied experimentally is not a pure step-function as there are additional random fluctuations due to variations in ventilation.

The criterion function which has been used in these optimisation studies is the integral of the square of the difference between model prediction and measured $p\text{CO}_2$ at the mouth during the end-tidal part of each breath. Thus the information which is obtained experimentally is not just the breath by breath changes in $p\text{CO}_2$ but also the change in $p\text{CO}_2$ within the breath. There is a steeper slope in the alveolar component of the expired concentration record for carbon dioxide as compared to that for an inert insoluble gas (for discussion of the latter, see Chapter 4). This steeper slope is related mainly to the continuing evolution of carbon dioxide from the lung into a reducing lung volume during expiration.²⁰⁶ The slope is steeper during exercise. The model also predicts a slope in the end-tidal $p\text{CO}_2$ and an increase in this slope during exercise. Application of the model to exercise conditions may lead, however, to inappropriate estimates of parameters (see Table 5.10).

TABLE 5.8

<u>Tissue Volume</u>		<u>Optimum Parameters</u>			<u>Criterion Function</u>
<u>L</u>	<u>Cardiac Output</u> <u>L/min</u>	<u>Lung Volume</u> <u>L</u>	<u>Metabolic Production</u> <u>L/min</u>	<u>mmHg²</u>	
<u>Experiment 1</u>					
3.0	5.19	2.69	0.202	0.6109	
4.0	5.25	2.74	0.212	0.2879	
5.0	5.02	2.99	0.219	0.1659	
6.0	4.82	3.28	0.224	0.1252	
7.0	4.65	3.49	0.227	0.1164	
8.0	4.58	3.63	0.230	0.1212	
9.0	4.29	3.85	0.230	0.1280	
10.0	4.23	3.97	0.231	0.1370	
20.0	3.65	4.51	0.233	0.1940	
30.0	3.54	4.72	0.234	0.2174	
40.0	3.54	4.86	0.237	0.2336	
<u>Experiment 2</u>					
3.0	5.71	2.83	0.206	0.7726	
4.0	5.75	2.71	0.214	0.3339	
5.0	5.52	3.03	0.222	0.1800	
6.0	5.26	3.38	0.229	0.1325	
7.0	5.01	3.64	0.232	0.1254	
8.0	4.79	3.89	0.234	0.1331	
9.0	4.63	4.02	0.235	0.1453	
10.0	4.47	4.15	0.236	0.1585	
20.0	3.87	4.81	0.239	0.2399	
30.0	3.74	4.96	0.240	0.2704	
40.0	3.66	5.06	0.240	0.2861	

Effect of tissue volume parameter on estimates of other parameters and on criterion function for two experiments performed on same subject (II) at rest. Experimental details and simulation/optimisation details as in Table 5.7. A minimum in the criterion function occurs at a tissue volume of 7.0L in both cases.

TABLE 5.9

<u>Tissue Volume</u>		<u>Optimum Parameters</u>		<u>Criterion Function</u>
<u>L</u>	<u>Cardiac Output</u> <u>L/min</u>	<u>Lung Volume</u> <u>L</u>	<u>Metabolic Production</u> <u>L/min</u>	<u>mmHg</u> ²
<u>Subject II</u>				
3.0	8.89	4.26	0.628	2.992
4.0	9.58	3.85	0.631	2.196
5.0	9.79	3.83	0.640	1.810
6.0	9.85	3.94	0.651	1.631
7.0	9.64	4.06	0.659	1.553
8.0	9.41	4.14	0.664	1.527
9.0	9.18	4.23	0.668	1.528
10.0	9.05	4.32	0.672	1.542
20.0	7.75	4.89	0.684	1.731
30.0	7.12	5.26	0.687	1.825
40.0	7.07	5.33	0.689	1.873
<u>Subject RMcC</u>				
3.0	7.70	3.54	0.530	2.894
4.0	7.55	3.67	0.541	2.357
5.0	7.19	3.86	0.548	2.177
6.0	6.84	4.11	0.554	2.119
7.0	6.54	4.32	0.558	2.105
8.0	6.30	4.48	0.560	2.106
9.0	6.18	4.58	0.563	2.113
10.0	5.98	4.73	0.564	2.121
20.0	5.41	5.24	0.569	2.181
30.0	5.25	5.40	0.571	2.206
40.0	5.16	5.44	0.570	2.219

Effect of tissue volume parameter on estimates of the other three parameters and on the criterion function for experimental data obtained during exercise in two subjects RMcC and II. Details as in caption for Table 5.7. Exercise was carried out on a bicycle ergometer. A minimum in the criterion function is demonstrated at tissue volumes of 8.0L for subject II and 7.0L for subject RMcC. These values are higher than the corresponding values at rest (see Table 5.7 and Table 5.8). The fit between model prediction and measurement is not as good as that obtained at rest (higher values of criterion function).

TABLE 5.10

	<u>Optimum Parameters</u>			
	<u>Cardiac Output</u> L/min	<u>Lung Volume</u> L	<u>Metabolic Production</u> L/min	<u>Tissue Volume</u> L
Subject WG	6.64	1.62	0.528	2.68
Subject WG	7.67	4.86	0.697	6.23

Same data set but changing criterion function as described in text to the sum of the squares of the differences in "average" end-tidal pCO_2 /breath, gives:-

Parameter estimates for a set of data obtained by measurements on subject WG during exercise. Two different methods of parameter estimation are used. In one the criterion function is the sum of the squares of the differences between model prediction and measurement during the end-tidal parts of all breaths. In the other the criterion function is the sum of the square of the differences between the average end-tidal pCO_2 /breath as predicted by the model and that measured. The first method gives obviously erroneous estimates of the parameters.

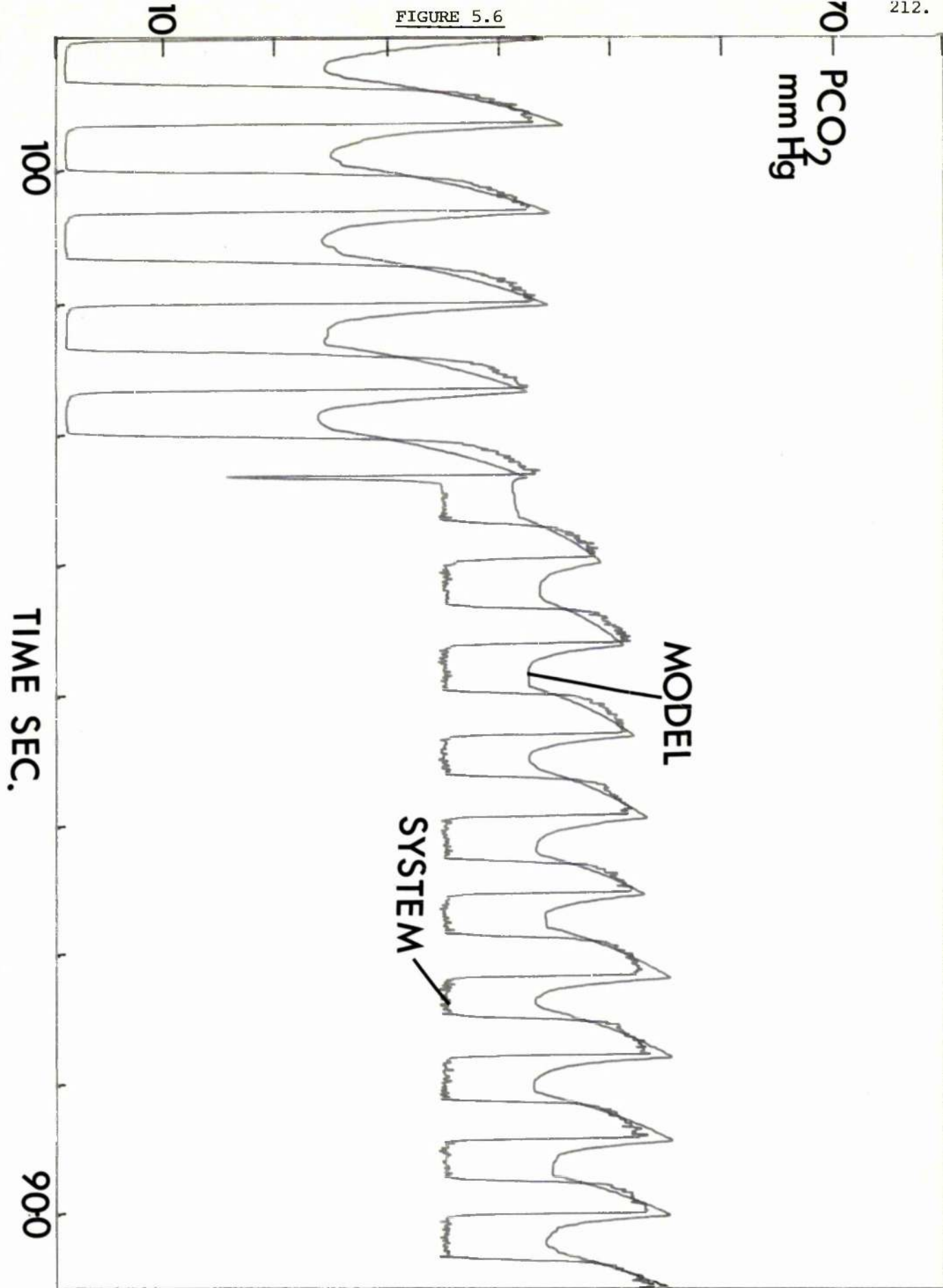
The estimation algorithm is attempting to fit the model to the measured steep slopes in end-tidal pCO_2 (see Fig. 5.6). This leads to a low estimate of lung volume. This problem is overcome if the model's performance is compared with the average pCO_2 during the end tidal part of each breath (see Table 5.10). Thus the criterion function J is

$$J = \sum_{i=1}^n \left[\frac{\sum_{j=1}^{m(i)} pCO_2^S}{m} - \frac{\sum_{j=1}^{m(i)} pCO_2^{model}}{m} \right]^2$$

where there are n breaths in the experiments. m is a function of i (breath number) and is the number of samples measured during the end-tidal part of each breath.

With certain measured data this change in the criterion function produces an insignificant effect on parameter estimates both in studies at rest (Table 5.11(a)) and during exercise (Table 5.11 (b)). In other cases there is a significant difference in the parameter estimates. It is not evident in what way these data sets are different. In view of this uncertainty and the uncertainty as to the mechanisms determining the nature of the expired concentration profile (see Chapter 4) the criterion function which utilises the average end-tidal pCO_2 is used hereafter.

FIGURE 5.6



Comparison of prediction of model with optimum parameters of alveolar pCO₂ and measured pCO₂ at the mouth. The two should be in agreement during the end-tidal part of each breath. For other details see text.

TABLE 5.11(a)

<u>Studies at Rest</u>			<u>Optimum Parameters</u>			
<u>Subject</u>	<u>Experiment</u>	<u>Criterion Function</u>	<u>Cardiac Output</u>	<u>Lung Volume</u>	<u>Metabolic Production</u>	<u>Tissue Volume</u>
			L/min	L	L/min	L
II	1	No averaging	4.78	3.58	0.231	6.44
II	1	Averaging	4.66	3.63	0.230	6.40
II	2	No averaging	4.36	3.48	0.226	6.61
II	2	Averaging	4.36	3.51	0.227	6.73
RMcC	1	No averaging	3.71	5.63	0.207	4.06
RMcC	1	Averaging	3.73	5.42	0.201	3.58
RMcC	2	No averaging	4.13	5.04	0.217	3.73
RMcC	2	Averaging	3.48	5.75	0.216	3.90
WG	1	No averaging	6.59	3.38	0.243	5.39
WG	1	Averaging	5.61	4.85	0.252	7.26

Comparison of parameter estimates as obtained using two different forms of criterion function. The studies were carried out at rest. One form of criterion function involves "averaging" the pCO_2 values during the end-tidal part of each breath before calculation of the square of the difference between model and system. In the simulation of the model's performance a value of 0.0045 L/L/mmHg is used for b , and a value of 0.0129 L/L for the difference between the intercepts of the linear relationships between CO_2 concentration and tension in mixed venous and arterial blood. The optimisation which is used is a combination of the Davidson-Fletcher-Powell method for the initial phase of optimisation followed by a change to the Rosenbrock method.

TABLE 5.11 (b)

Studies on Exercise

<u>Subject</u>	<u>Experiment</u>	<u>Criterion Function</u>	<u>Cardiac Output</u>		<u>Optimum</u>		<u>Parameters</u>	
			<u>L/min</u>	<u>L</u>	<u>Lung Volume</u> <u>L</u>	<u>Metabolic Production</u> <u>L/min</u>	<u>Tissue Volume</u> <u>L</u>	
II	1	No averaging	9.33	4.20	4.20	0.667	8.50	
II	1	Averaging	10.26	3.71	3.71	0.651	7.20	
II	2	No averaging	10.00	3.80	3.80	0.799	9.60	
II	2	Averaging	9.71	3.17	3.17	0.772	8.89	
RMCC	1	No averaging	6.46	4.35	4.35	0.558	7.33	
RMCC	1	Averaging	6.05	4.33	4.33	0.549	7.25	
RMCC	2	No averaging	13.25	4.49	4.49	0.991	9.44	
RMCC	2	Averaging	12.50	6.43	6.43	1.042	11.15	
WG	1	No averaging	6.64	1.62	1.62	0.528	2.68	
WG	1	Averaging	7.67	4.86	4.86	0.697	6.23	

Comparison of parameter estimates as obtained using two different forms of criterion function. The studies were carried out during exercise on a bicycle ergometer. For other details see caption of Table 5.11(a).

5.8. Effect of Various Assumptions.

A number of assumptions have been made both in deriving the equations for the simple model of carbon dioxide transport and implementing parameter estimation techniques. A small number of studies have been conducted to ascertain the likely effect of such assumptions on parameter estimates. These studies are described in this section.

(a) Lung Volume.

In the results which have been presented lung volume has been regarded as a fixed parameter. Thus the variation of lung volume during the respiratory cycle has been neglected. The lung volume increases during inspiration and decreases during expiration:-

For inspiration

$$V_A(t) = V_A(o) + \int_0^t \dot{V} dt - \int_0^t \dot{V}O_2 dt + \int_0^t \dot{V}CO_2 dt$$

where o represents the beginning of inspiration. (A similar expression can be written for expiration). The difference between the last two terms (oxygen uptake and CO₂ output) is small. (Of the order of 5 ml per breath.) Thus

$$V_A(t) = V_A(o) + \int_0^t \dot{V} dt \quad (5.4)$$

During expiration only an approximate measurement of \dot{V} is obtained. (See Chapter 3).

A number of different sets of experimental data have been analysed with $V_A(t)$ fixed and as in equation 5.4, to investigate the importance of incorporating the time variation of V_A . The parameter which is estimated in the case in which V_A is time variant is $V_A(o)$ - the volume of the lung at the start of inspiration. The lung volume of the model is reset to $V_A(o)$

at the start of each breath. Incorporation of the time variation in V_A in the model has only a small effect on parameter estimates both at rest (Table 5.12(a)) and on exercise (Table 5.12(b)).

There is a significant difference in the estimates of lung volume in both cases. Time variation in lung volume is thus incorporated into the model but the relatively small order of its importance is not such that accurate measurement of expired flow is required.

(b) Dead Space.

In applying parameter estimation to this model it is assumed that the volume of the anatomical dead space can either be measured directly³⁸⁵ or estimated from the subject's weight.³⁰⁸ Studies (Table 5.13(a) & (b)) of the effect of variations in dead space volume on parameter estimates indicate that the model is relatively insensitive to this. Any inaccuracies, therefore, in the measurement of dead space volume should not alter significantly the parameter estimates which are obtained.

(c) Linear Description of CO₂ dissociation curve.

A linear description is utilised for both the relationships between the tension of CO₂ and concentration in arterial and venous blood. The relationships have the same slope (b) but different intercepts (a_a and a_v respectively). The parameter estimates are unaffected by a significant alteration in the difference between a_a and a_v . (See Table 5.14(a) and (b)). The estimates of \dot{Q} and V_{TC} are such that the products $\dot{Q} \times b$ and $V_{TC} \times b$ are constant. This is to be expected from the formulation of the equations. Alterations in b have, however, no significant effect on the estimates of the other two parameters.

TABLE 5.12 (a)

STUDIES AT REST

<u>SUBJECT</u>	<u>EXP.</u> <u>NO.</u>	<u>LUNG</u> <u>VOLUME</u>	<u>OPTIMUM PARAMETERS</u>			
			<u>CARDIAC</u> <u>OUTPUT</u> L/min	<u>LUNG</u> <u>VOLUME</u> L	<u>METABOLIC</u> <u>PRODUCTION</u> L/min	<u>TISSUE</u> <u>VOLUME</u> L
II	1	Fixed	4.66	3.63	0.230	6.40
	1	Variable	4.53	3.41	0.226	6.22
II	2	Fixed	4.36	3.51	0.227	6.73
	2	Variable	4.20	3.19	0.221	6.52
RMcC	1	Fixed	3.71	5.63	0.207	4.06
	1	Variable	3.50	5.22	0.198	3.61
RMcC	2	Fixed	3.48	5.75	0.216	3.90
	2	Variable	3.29	5.49	0.213	4.14
WG	1	Fixed	5.61	4.85	0.252	7.26
	1	Variable	5.69	4.47	0.248	6.55
WG	2	Fixed	5.98	5.33	0.229	5.14
	2	Variable	5.92	4.94	0.225	4.95
AVERAGE		Fixed	4.63	4.78	0.227	5.58
		Variable	4.52	4.45	0.222	5.33
AVERAGE DIFFERENCE			0.11	0.33	0.005	0.25
SIGNIFICANCE OF DIFFERENCE BY PAIRED t-test			N.S.	p<0.001	N.S.	N.S.

Comparison of parameter estimates as obtained (a) assuming that lung volume is invariant and (b) that lung volume varies throughout the breath due to ventilation. Data obtained at rest is used in this study. Each experiment consisted of a period of air breathing (30 sec. duration) followed by a step change to breathing a gas mixture containing 5% CO₂ (90 sec. duration). The parameter estimation method used is a combination of the Davidson, Fletcher, Powell & Rosenbrock methods. The estimates have been compared using a paired t-test.

TABLE 5.12 (b)

STUDIES ON EXERCISE

<u>SUBJECT</u>	<u>EXP.</u> <u>NO.</u>	<u>LUNG</u> <u>VOLUME</u>	<u>CARDIAC</u> <u>OUTPUT</u> L/min	<u>LUNG</u> <u>VOLUME</u> L	<u>METABOLIC</u> <u>PRODUCTION</u> L/min	<u>TISSUE</u> <u>VOLUME</u> L
II	1	Fixed	10.26	3.71	0.651	7.20
	1	Variable	10.90	3.09	0.658	6.84
II	2	Fixed	9.71	3.17	0.772	8.89
	2	Variable	10.48	2.70	0.790	8.40
RMcC	1	Fixed	12.50	6.43	1.042	11.15
	1	Variable	12.88	5.59	1.056	10.46
RMcC	2	Fixed	6.05	4.33	0.549	7.25
	2	Variable	6.32	3.57	0.549	6.58
WG	1	Fixed	8.65	5.94	0.946	6.34
	1	Variable	8.79	4.77	0.969	5.74
WG	2	Fixed	7.67	4.86	0.697	6.23
	2	Variable	7.91	4.38	0.725	6.33
AVERAGE		Fixed	9.14	4.74	0.776	7.84
		Variable	9.54	4.02	0.787	7.39
AVERAGE DIFFERENCE			-0.41	0.72	-0.012	0.45
SIGNIFICANCE OF DIFFERENCE BY PAIRED t-test			.005 < p < .01	.001 < p < .005	NS	NS

This is identical study to that presented in Table 5.12(a)
The experimental data used, however, were collected
during exercise on a bicycle ergometer.

TABLE 5.13 (a)

STUDIES AT REST

SUBJECT	EXP. NO.	DEAD SPACE VOLUME	OPTIMUM PARAMETERS			
			CARDIAC OUTPUT	LUNG VOLUME	METABOLIC PRODUCTION	TISSUE VOLUME
		L	L/min	L	L/min	L
II	1	0.130	4.82	3.63	0.237	6.83
	1	0.150	4.66	3.63	0.230	6.40
	1	0.170	4.42	3.57	0.220	6.06
II	2	0.130	4.61	3.46	0.235	7.00
	2	0.150	4.36	3.51	0.227	6.73
	2	0.170	4.10	3.43	0.214	5.85
RMcC	1	0.155	3.92	5.61	0.211	3.91
	1	0.175	3.71	5.63	0.207	4.06
	1	0.195	3.60	5.04	0.189	3.20
RMcC	2	0.155	3.74	5.80	0.226	4.30
	2	0.175	3.48	5.75	0.216	3.90
	2	0.195	3.51	5.76	0.210	3.60
WG	1	0.170	5.88	4.54	0.254	6.80
	1	0.190	5.61	4.85	0.252	7.26
	1	0.210	5.67	4.57	0.254	6.49
WG	2	0.170	5.92	5.21	0.231	5.37
	2	0.190	5.98	5.33	0.229	5.14
	2	0.210	5.86	5.56	0.225	5.01
AVERAGE	$V_D - 0.020$		4.81	4.71	0.232	5.68
	V_D		4.63	4.78	0.227	5.58
	$V_D + 0.020$		4.52	4.65	0.219	5.04
AVERAGE DIFFERENCE	$V_D - 0.020$		0.18	0.07	0.005	0.10
	$V_D + 0.020$		0.11	0.13	0.008	0.54

SIGNIFICANT DIFFERENCES

BY PAIRED t-test

$V_D - 0.20$	N.S.	N.S.	.005 < p < .01	NS
$V_D + 0.20$	N.S.	N.S.	N.S.	.005 < p < .01

Study of the effect of alteration in the volume of anatomical dead space on estimates of the parameters. Parameter estimation was carried out with 3 dead space volumes - the known dead space for the subject (V_D), $V_D - 0.02L$, $V_D + 0.02L$. Data obtained at rest were used in these studies. Whilst this magnitude of alteration in dead space volume produces a change in the parameter estimates, this change is significant only for metabolic production (comparing results for $V_D - 0.20$ & V_D) and tissue volume (comparing results for V_D & $V_D + 0.20$). For the cardiac output parameter, a change in dead space volume of the order of 12% produces a change in the estimate of cardiac output of the order of 3.5%.

TABLE 5.13 (b)

Subject	Exp. No.	Optimum Parameters				
		Dead Space	Cardiac Output	Lung	Metabolic	Tissue
		Volume		Volume	Production	Volume
		L	L/min	L	L/min	L
II	1	0.130	10.22	3.66	0.653	7.26
	1	0.150	10.26	3.71	0.651	7.19
	1	0.170	10.25	3.74	0.646	7.12
II	2	0.130	9.72	3.19	0.778	9.15
	2	0.150	9.71	3.17	0.772	8.88
	2	0.170	9.65	3.22	0.770	9.00
RMcC	1	0.155	12.49	6.13	1.032	10.90
	1	0.175	12.50	6.43	1.042	11.15
	1	0.195	12.53	6.58	1.044	11.20
RMcC	2	0.155	6.11	4.25	0.553	7.82
	2	0.175	6.05	4.33	0.549	7.25
	2	0.195	5.98	4.42	0.548	8.04
WG	1	0.170	8.49	5.73	0.937	6.21
	1	0.190	8.66	5.96	0.947	6.44
	1	0.210	8.76	5.95	0.953	6.36
WG	2	0.170	7.45	4.56	0.687	6.00
	2	0.190	7.67	4.86	0.697	6.23
	2	0.210	7.79	5.00	0.702	6.29
<u>AVERAGE</u>	$V_D - 0.020$		9.08	4.59	0.773	7.89
	V_D		9.14	4.74	0.776	7.86
	$V_D + 0.020$		9.16	4.81	0.777	8.00
<u>AVERAGE DIFFERENCE</u>						
(Compared to V_D)						
	$V_D - 0.020$		0.06	0.15	0.003	0.03
	$V_D + 0.20$		0.02	0.07	0.001	0.14
<u>SIGNIFICANCE OF DIFFERENCES BY</u>						
<u>PAIRED t-test.</u>						
			N.S.	N.S.	N.S.	N.S.

Similar study to that in Table 5.13(a). Data which have been used here were collected during exercise. Alteration of dead space volume has no significant effect on parameter estimates in this case. The magnitude of the alterations in the cardiac output parameter are of a smaller order than at rest. This is related to the larger ventilations of the subjects during exercise.

TABLE 5.14 (a)

SUBJECT	EXP. NO.	$a_v - a_a$ L/L	OPTIMUM PARAMETERS			
			CARDIAC OUTPUT L/min	LUNG VOLUME L	METABOLIC PRODUCTION L/min	TISSUE VOLUME L
II	1	0.0	4.66	3.64	0.230	6.40
	1	0.0129	4.66	3.63	0.230	6.40
II	2	0.0	4.37	3.50	0.227	6.72
	2	0.0129	4.36	3.51	0.227	6.73
RMcC	1	0.0	3.73	5.48	0.201	3.61
	1	0.0129	3.73	5.42	0.201	3.58
RMcC	2	0.0	3.48	5.74	0.216	3.88
	2	0.0129	3.47	5.75	0.216	3.90
WG	1	0.0	5.73	4.78	0.251	6.99
	1	0.0129	5.61	4.85	0.252	7.26
WG	2	0.0	5.76	5.66	0.230	5.35
	2	0.0129	5.98	5.33	0.228	5.14
AVERAGE		0.0	4.62	4.80	0.226	5.49
		0.0129	4.63	4.75	0.226	5.50
AVERAGE DIFFERENCE			-0.01	0.05	0.0	-0.01
SIGNIFICANCE OF DIFFERENCE BY PAIRED t-test			N.S.	N.S.	N.S.	N.S.

Comparison of parameter estimates as obtained (a) neglecting the Haldane effect, $a_v - a_a = 0.0$ and (b) assuming that the difference between the intercepts of the linear functions relating concentration of CO_2 to tension in mixed venous blood (a_v) and arterial blood (a_a) is 0.0129 L CO_2 (STPD)/L. Data obtained at rest are used in this study. Each experiment consisted of a period of air breathing (30 sec. duration) followed by a step change to breathing a gas mixture containing 5% CO_2 (90 sec. duration). The parameter estimation method used is a combination of the Davidon, Fletcher, Powell & Rosenbrock methods. The estimates have been compared using a paired t-test. N.S. is no significant difference.

TABLE 5.14 (b)

SUBJECT	EXP. NO.	$a_v - a_a$ L/L	OPTIMUM		PARAMETERS	
			CARDIAC OUTPUT L/min	LUNG VOLUME L	METABOLIC PRODUCTION L/min	TISSUE VOLUME L
II	1	0.0	10.29	3.73	0.652	7.20
	1	0.0129	10.27	3.73	0.652	7.25
II	2	0.0	9.74	3.17	0.772	8.85
	2	0.0129	9.71	3.19	0.773	8.89
RMCC	1	0.0	12.00	6.43	1.043	11.12
	1	0.0129	12.54	6.41	1.042	11.12
RMCC	2	0.0	5.97	4.38	0.550	7.66
	2	0.0129	6.01	4.35	0.549	7.58
WG	1	0.0	8.72	5.84	0.944	6.28
	1	0.0129	8.66	5.96	0.947	6.44
WG	2	0.0	7.65	4.83	0.696	6.21
	2	0.0129	7.69	4.80	0.696	6.23
AVERAGE		0.0	9.06	4.73	0.776	7.89
		0.0129	9.14	4.74	0.776	7.92
AVERAGE DIFFERENCE			-0.08	-0.01	0.0	-0.03
SIGNIFICANCE OF DIFFERENCE BY PAIRED t-test			N.S.	N.S.	N.S.	N.S.

Identical study to that presented in Table 5.14(a).
Data were collected, however, by measurement
during controlled exercise.

5.9 Measurement of Cardiac Output at Rest

Studies have been carried out in the four subjects while seated. The subjects refrained from drinking tea or coffee for the two hours before the start of the experiment. Prior to the start of the test the subjects were instructed to empty their bladder. Each subject sat quietly for twenty to thirty minutes before measurements were made. The experiment was repeated up to a maximum of six times in each subject.

Each experiment consisted of several phases. The initial phases of the experiment consisted of inputting zero and calibrating signals to the computer system. This was described in detail in Chapter 3. After the subject was connected to the measurement system (see details in Chapter 3) the subject's expired ventilation was collected in a Tissot spirometer for one minute. The expired ventilation was then directed into the room using a valve system and the spirometer emptied. A further two-minute collection of the subject's expirate was performed. Thereafter logging by the computer system of ventilatory flow rate, partial pressures of CO_2 , N_2 and O_2 was commenced. After thirty seconds the subject was switched to breathing a gas mixture containing 5% CO_2 and logging of data was continued for a further 90 secs. Throughout the experiment the subject was connected to an electrocardiogram and the point at which the subject began to breathe the gas mixture containing CO_2 noted. Heart rates were measured over three thirty second periods -

- (a) while breathing air;
- (b) after the start of CO_2 breathing;
- (c) just prior to the end of the experiment.

When the experiment was complete the relevant concentrations of the gas in the Tissot spirometer were measured using the mass spectrometer. The measured data were analysed using the computer software and results obtained

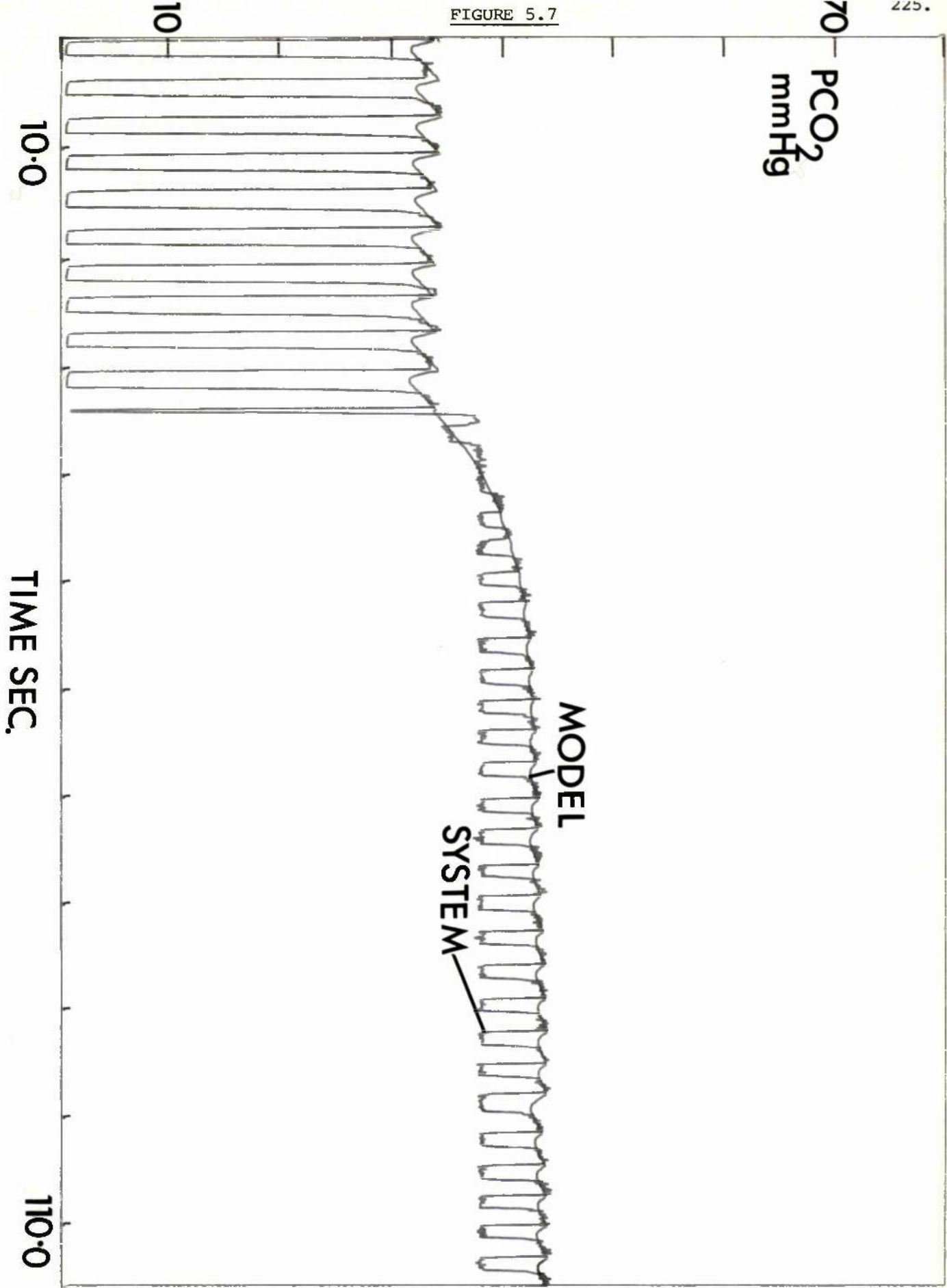
for cardiac output, lung volume, metabolic production, and tissue volume. A graph of the optimised model prediction of $p\text{CO}_2$ as compared to the measured $p\text{CO}_2$ for one of the experiments is shown in Figure 5.7.

The results from these studies are presented in Table 5.15 (a,b,c,d). Each table contains the measured heart-rates during each of the three periods for each experiment. The minute ventilation (\dot{V}_E), carbon dioxide output ($\dot{V}\text{CO}_2$), oxygen uptake ($\dot{V}\text{O}_2$) and respiratory exchange ratios (R) as measured from the collected expired ventilation are shown. The parameter estimates for each of the four parameters are tabulated. The stroke volume is calculated from the cardiac output and heart-rate during the first period.

The cardiac index can be calculated from knowledge of the cardiac output and surface area of each subject. Using the mean of all the measurements the results are:- 2.9 (subject II), 2.7 (subject RMcC), 3.0 (subject JU), and 3.1 (subject WG), (in $\text{l}/\text{min}/\text{m}^2$).

In two of the subjects (II, JU) there is good agreement between the metabolic production as measured by collection of the expired gas and that obtained by parameter estimation. The mean of the differences are $0.014\text{L}/\text{min}$ and $0.009\text{L}/\text{min}$, respectively. There is no significant difference in these results by a paired t-test. In RMcC the mean of the differences is $0.026\text{L}/\text{min}$, but the results are not significantly different. In WG, however, the results from parameter estimation are higher consistently as is confirmed by a paired t-test ($p < 0.001$).

FIGURE 5.7



Comparison of prediction of model with optimum parameters of alveolar pCO₂ and measured pCO₂ at the mouth (system). There is seen to be good agreement during the end-tidal part of each breath.

TABLE 5.15 (a)

SUBJECT II

Laboratory Temperature = 22.5°C.

Run	Heart Rate/min			\dot{V}_E L/min	\dot{V}_{CO_2} L/min	\dot{V}_{O_2} L/min	\bar{R}
	<u>1</u>	<u>2</u>	<u>3</u>				
1.	93	94	90	8.79	0.251	0.249	1.01
2.	98	98	88	7.36	0.223	0.272	0.82
3.	94	92	92	7.18	0.218	0.265	0.82
4.	91	94	92	7.38	0.233	0.294	0.79
5.	-	-	90	6.86	0.215	0.267	0.81
6.	92	96	94	6.47	0.199	0.266	0.75

OPTIMISATION RESULTS

Run	Cardiac Output	(Stroke Volume)	Lung Volume	Metabolic Production	Tissue Volume.
	L/min	ml.	L.	L/min.	L.
1.	5.0	(54)	3.7	0.267	10.7
2.	5.6	(57)	3.3	0.286	12.1
3.	5.3	(56)	3.4	0.228	7.3
4.	4.8	(53)	3.1	0.221	7.5
5.	4.8	(53)*	3.4	0.215	7.1
6.	5.1	(55)	3.2	0.210	6.0
Mean	5.1	(55)	3.4	0.238	8.5
Coeff. of Variation	6.1%	3.0%	6.2%	13.1%	28%

For details see text.* Calculated from measurement of heart-rate during CO₂ breathing.

TABLE 5.15 (b)

<u>SUBJECT RMCC</u>				<u>Laboratory temperature = 24.5°C</u>			
<u>Run</u>	<u>Heart Rate/min</u>			\dot{V}_E <u>L/min</u>	\dot{V}_{CO_2} <u>L/min</u>	\dot{V}_{O_2} <u>L/min</u>	<u>R</u>
	<u>1</u>	<u>2</u>	<u>3</u>				
1.	78	84	82	5.74	0.159	0.191	0.83
2.	76	82	84	6.76	0.175	0.210	0.83
3.	78	82	84	6.82	0.165	0.184	0.90
4.	80	82	86	6.87	0.183	0.206	0.89
5.	78	82	84	7.20	0.194	0.231	0.84

OPTIMISATION RESULTS

<u>Run</u>	<u>Cardiac Output</u> <u>L/min</u>	<u>(Stroke Volume)</u> <u>ml.</u>	<u>Lung Volume</u> <u>L.</u>	<u>Metabolic Production</u> <u>L/min.</u>	<u>Tissue Volume.</u> <u>L.</u>
1.	4.7	(60)	5.6	0.204	4.7
2.	4.0	(53)	5.4	0.204	4.8
3.	5.1	(65)	5.3	0.174	4.5
4.	4.8	(60)	5.1	0.217	4.1
5.	3.9	(50)	5.0	0.209	4.2
Mean	4.5	(58)	5.3	0.201	4.5
Coeff. of Variation	11.6%	10.5%	4.5%	8.1%	6.8%

For details see text.

TABLE 5.15 (c)

SUBJECT J.U.

Laboratory temperature = 23.0°C

Run	Heart Rate/min			\dot{V}_E L/min	$\dot{V}CO_2$ L/min	$\dot{V}O_2$ L/min	R
	<u>1</u>	<u>2</u>	<u>3</u>				
1.	116	106	106	7.79	0.220	0.303	0.73
2.	96	98	100	5.56	0.168	0.235	0.72
3.	96	94	94	5.28	0.172	0.226	0.76
4.	94	94	94	5.75	0.187	0.244	0.77
5.	98	96	96	7.85	0.257	0.285	0.90

OPTIMISATION RESULTS

Run	Cardiac Output	(Stroke Volume)	Lung Volume	Metabolic Production	Tissue Volume.
	L/min	ml.	L.	L/min.	L.
1.	5.9	(51)	3.7	0.264	7.7
2.	3.9	(41)	2.8	0.173	3.4
3.	3.8	(40)	2.8	0.167	3.1
4.	3.7	(39)	3.3	0.195	3.9
5.	5.5	(56)	3.3	0.255	6.6
Mean	4.6	(45)	3.2	0.211	4.9
Coeff. of Variation	23%	16.8%	12.1%	21.8%	42%

For details see text.

TABLE 5.15 (d)

Laboratory temperature = 26.0°C.

<u>Run</u>	<u>Heart Rate/min</u>			\dot{V}_E <u>L/min</u>	\dot{V}_{CO_2} <u>L/min</u>	\dot{V}_{O_2} <u>L/min</u>	<u>R</u>
	<u>1</u>	<u>2</u>	<u>3</u>				
1.	-	88	88	7.05	0.193	0.246	0.79
2.	88	87	88	6.83	0.195	0.275	0.71
3.	87	90	87	6.36	0.193	0.270	0.72
4.	88	88	88	6.77	0.196	0.259	0.76
5.	87	86	86	6.43	0.188	0.275	0.68
6.	86	86	86	6.92	0.197	0.278	0.71

OPTIMISATION RESULTS

<u>Run</u>	<u>Cardiac Output</u> <u>L/min</u>	<u>(Stroke Volume)</u> <u>ml.</u>	<u>Lung Volume</u> <u>L.</u>	<u>Metabolic Production</u> <u>L/min.</u>	<u>Tissue Volume.</u> <u>L.</u>
1.	5.9	(67)	4.5	0.248	6.6
2.	5.5	(63)	3.6	0.225	4.1
3.	5.4	(62)	3.7	0.215	4.0
4.	5.7	(65)	5.1	0.225	5.3
5.	6.7	(77)	5.0	0.226	5.4
6.	6.2	(72)	4.3	0.237	5.2
Mean	5.9	(68)	4.4	0.223	5.1
Coeff. of Variation	8.2%	8.6%	14.4%	4.6%	18.9%

For details see text.

5. 10. Measurement of Cardiac Output During Exercise.

Similar studies have been carried out in three of the subjects during graded exercise on a bicycle ergometer. Collection of the expired ventilation was commenced after the subject had been pedalling for two to three minutes. Heart-rate was not measured during these experiments. The experimental details were as described previously. The results are presented in Table 5.16 (a,b,c).

There is no significant difference by a paired t-test between the results for metabolic production as obtained using parameter estimation and by direct measurement. The mean of the differences between the paired results are 0.01L/^{min.} (subject II), 0.008L/^{min.} (subject RMcC) and 0.039L/^{min.} (subject WG).

The results for cardiac output are as expected correlated with the measured oxygen uptake. The correlation coefficients are 1.00 ($p < 0.001$, subject II), 0.92 ($0.001 < p < 0.01$, subject RMcC), and 0.88 ($0.02 < p < 0.05$, subject WG). For the grouped data the relationship between cardiac output and oxygen uptake can be represented by a line such that

$$\dot{Q} = 4.59\dot{V}O_2 + 5.94$$

TABLE 5.16 (a)Subject IILaboratory Temperature = 27.1°C.

<u>Run</u>	<u>Load</u> kpm/min	\dot{V}_E L/min	$\dot{V}O_2$ L/min	$\dot{V}CO_2$ L/min	<u>R</u>
1.	150	17.02	0.721	0.619	0.86
2.	150	17.81	0.777	0.670	0.86
3.	300	22.91	1.000	0.928	0.93
4.	300	24.00	1.043	0.932	0.89
5.	200	19.29	0.914	0.704	0.77

Optimisation Results

<u>Run</u>	<u>Cardiac</u> <u>Output</u> L/min	<u>Lung</u> <u>Volume</u> L.	<u>Metabolic</u> <u>Production</u> L/min.	<u>Tissue</u> <u>Volume</u> L.
1.	11.1	3.1	0.613	12.1
2.	11.4	3.2	0.676	9.4
3.	13.2	3.1	0.954	8.6
4.	13.5	3.2	0.836	11.0
5.	12.5	3.2	0.776	10.1

For details see text.

TABLE 5.16 (b)

Subject RMcCLaboratory Temperature = 28.0°C.

<u>Run</u>	<u>Load</u> kpm/min	\dot{V}_E L/min	$\dot{V}O_2$ L/min	$\dot{V}CO_2$ L/min	<u>R</u>
1.	100	12.18	0.563	0.445	0.79
2.	100	11.19	0.526	0.426	0.81
3.	150	14.59	0.636	0.547	0.86
4.	150	15.07	0.658	0.558	0.85
5.	250	16.46	0.770	0.662	0.86
6.	250	17.85	0.790	0.668	0.87

Optimisation Results

<u>Run</u>	<u>Cardiac</u> <u>Output</u> L/min.	<u>Lung</u> <u>Volume</u> L.	<u>Metabolic</u> <u>Production</u> L/min.	<u>Tissue</u> <u>Volume</u> L.
1.	7.4	3.9	0.434	7.1
2.	6.9	3.5	0.407	5.5
3.	8.8	4.2	0.507	6.8
4.	7.7	4.0	0.571	7.4
5.	9.2	4.5	0.648	6.2
6.	10.1	4.2	0.693	6.9

For details see text.

TABLE 5.16 (c)

Subject WG Laboratory Temperature = 24.4°C.

<u>Run</u>	<u>Load</u> kpm/min	\dot{V}_E L/min	$\dot{V}O_2$ L/min	$\dot{V}CO_2$ L/min	<u>R</u>
1.	150	13.77	0.690	0.577	0.84
2.	150	-	-	-	0.80
3.	300	16.70	0.926	0.726	0.78
4.	300	18.13	1.009	0.838	0.83
5.	450	20.60	1.202	1.005	0.84
6.	450	22.24	1.329	1.067	0.80

Optimisation Results

<u>Run</u>	<u>Cardiac</u> <u>Output</u> L/min.	<u>Lung</u> <u>Volume</u> L.	<u>Metabolic</u> <u>Production</u> L/min.	<u>Tissue</u> <u>Volume.</u> L.
1.	8.0	1.9	0.533	5.0
2.	7.5	3.4	0.508	4.3
3.	8.2	4.6	0.687	4.5
4.	9.6	3.8	0.753	6.1
5.	9.9	4.9	1.000	6.3
6.	9.8	5.2	1.045	8.6

For details see text.

5.11. DISCUSSION

Application of the techniques of dynamic modelling to the study of carbon dioxide transport leads to a non-invasive method for the measurement of cardiac output and the carbon dioxide lung volume. Other non-invasive methods of measuring cardiac output, which are based on the analysis of gas exchange have utilised generally the Fick principle (see Chapter 3.1).

$$\text{i.e. } \dot{Q} = \frac{\dot{V}_x}{(C_a - C_v)}$$

(For useful reviews see Hamilton,⁴⁰³ Butler,⁴⁰⁴ Farhi & Haab⁴⁰⁵ Guyton, Jones & Coleman⁴⁰⁶).

Methods which have used soluble inert gases^{407, 408} are based on the assumption that, while breathing the foreign gas and during the initial phase of the experiment, C_v is zero. Other variables can be measured directly.

For carbon dioxide C_v has to be estimated by other means. This can be done using a rebreathing procedure in which gas in the lung is equilibrated momentarily with mixed venous blood. $P_v\text{CO}_2$ is obtained either from the exponential change of $P_A\text{CO}_2$ during rebreathing⁴⁰⁹ or from the equilibrium plateau⁴¹⁰ of $p\text{CO}_2$ in the rebreathing bag. Both techniques have been applied to the measurements of cardiac output.⁴¹¹⁻⁴¹⁵ The "plateau method" is said to give more reproducible results.⁴¹⁶ Cardiac output can also be obtained directly from the rate of rise of $p\text{CO}_2$ in the rebreathing bag.⁴¹⁷ Measurements using the rebreathing method are complicated by the fact that equilibrium is not established between venous $p\text{CO}_2$ and alveolar $p\text{CO}_2$.⁴¹⁸ (The so-called upstream difference).

Mixed venous $p\text{CO}_2$ can also be estimated from a breath-holding procedure.³⁸⁰ The theoretical basis is that the magnitude of the Haldane effect is such that when the instantaneous respiratory exchange ratio is 0.32, the mixed venous $p\text{CO}_2$ is equal to the arterial $p\text{CO}_2$.³⁷⁹

This technique has been applied to studies during exercise^{419,420} but is inapplicable at rest.⁴²¹

Techniques involving parameter estimation have also been applied previously in the non-invasive measurement of cardiac output. A model of the type described in section 2.5 of Chapter 2 is used by Maloney.¹⁸⁶ In this technique only one parameter (cardiac output) is adjusted. (Other parameters - tissue volume, metabolic production, CO_2 lung volume, and initial tissue pCO_2 - are fixed.) The experimental data are collected during a steady-state. Sensitivity analysis indicates that the result for cardiac output is dependent on the choice of values for the other parameters, particularly on the choice of initial tissue partial pressure. An incorrect choice of tissue pCO_2 leads to errors in cardiac output estimates of the order of 15%.

A more complex model is employed by Homer and Denysyk³⁷⁸ to predict changes in alveolar pO_2 , pN_2 and pCO_2 . The criterion function which is used is the weighted sum of the differences between model prediction and measurement of pO_2 , pN_2 , pCO_2 . The experiment which is employed is rebreathing of gas mixture containing 15% CO_2 and 15% O_2 , for 30 seconds. The sensitivity studies which are shown in Fig. 5.3 indicate that, for pCO_2 , the model has only a low sensitivity to cardiac output during the first thirty seconds following induction of a transient. Similar studies for oxygen, indicate very low sensitivities to cardiac output during transient states. Nitrogen is virtually insoluble. Thus in this method of measurement results will be determined almost completely by the carbon dioxide component of the model. In the model which is used the dead space is treated as a well-stirred homogenous compartment. The effect of this simplification is not assessed by the authors.

The results which are obtained by the present method are within the expected range for subjects at rest (see Table 5.17). The results which are quoted in this table are for subjects while seated. Differences between subjects are in part related to size differences. Results can be normalised by calculating the cardiac index (cardiac output/surface area) although use of this ratio has been criticised by Tanner⁴²² on theoretical grounds. Although there is still significant variability between subjects sixty-one percent of the results for cardiac index from the studies which are shown in Table 5.17 lie between 2.5 and 3.5 L/min/m². Thus the results which have been obtained by this non-invasive method are in good agreement with published data.

In assessing the reproducibility of measurement of cardiac output by the type of experiment which has been described, there is a significant biological component in the measured variability. This is most obvious in the results for J.U. In the first experiment both the heart-rate and cardiac output are high. This may be related to anxiety. After the fifth experiment the subject stated that she had felt uncomfortable during the test and both the measured cardiac output and minute ventilation were increased.

Previous studies of reproducibility of measurement of cardiac output by the standard Fick method have assessed reproducibility by comparing the results of duplicate measurements. The results are expressed as the mean and standard deviation of the differences between the two measurements. Analysis of the present data using both the results at rest and exercise show comparable reproducibility to the Fick method (see Table 5.18). In the study of Selzer and Sudrann⁴²⁹ reproducibility is expressed as the relative error, i.e. the difference between the two measurements/average of the two

TABLE 5.17

<u>Reference</u>	<u>No. of Subjects</u>	<u>Sex</u>	<u>Age (Range)</u>	<u>Cardiac Output</u> Mean (Range) L/min	<u>Surface Area</u> Mean (Range) $\frac{m^2}{2}$	<u>Cardiac Index</u> Mean (Range) L/min/m ²
423 Donald et al	10	7F, 3M	19-59	5.9(4.4-8.7)	1.59(1.41-1.88)	3.7(.0-5.1)
424 Bevegård et al	6	6M	20-28	6.2(4.0-8.2)	1.98(1.72-2.15)	3.2(2.0-4.8)
425 Stenberg et al	8	7M, 1F	20-39	4.8(3.4-6.1)	1.84(1.70-1.99)	2.6(1.8-3.3)
426 Bevegård et al	7	7M	21-40	5.9(4.5-7.0)	1.92(1.76-2.12)	3.1(2.3-3.5)

Published data for measurement of cardiac output
in normal subjects while seated.

measurements. The mean relative error in this study was 8.6%. If the data from our new method of measurement is analysed in this way the mean relative error is 7.6%, i.e. slightly better than the Fick method.

The measurements of cardiac output during exercise show as expected a correlation with the oxygen uptake. The linear relationship which is demonstrated between cardiac output and oxygen uptake is similar to that obtained in other studies (see Table 5.19).

The estimates of metabolic production which have been obtained by parameter estimation agree in all but one set of data with those obtained independently. The explanation for the discrepancy with this set of data is not clear. There is no evidence that during parameter estimation a local and, therefore, false minimum was detected. The metabolic productions as obtained by steady-state gas collection seem low for a subject of this size.

The estimated carbon dioxide lung volumes for all subjects are as expected greater than the corresponding inert gas lung volume. At rest the comparable figures are 3.4L and 1.4L for subject II, 5.3L and 3.6L for subject RMCC, 3.2L and 2.2L for J.U., 4.4L and 3.8L for subject WG. These estimates are lower than would be expected from the data of Hyde et al.,³⁵⁵ and Sackner et al.³⁵⁴ This may be related to the assumption of instantaneous equilibrium between alveolar gas and lung tissue.

The estimates for tissue volume show, as would be expected from the relatively low sensitivity, the highest coefficient of variation. The estimates are, however, of the correct order of magnitude as compared to published data.³⁶⁴ The fast space for carbon dioxide can be related to the extracellular fluid space³⁶⁴ with a volume of 17.0L. This is composed on average of 5.0L of

TABLE 5.18

<u>References</u>	<u>No. of duplicate measurements</u>	<u>Conditions</u>	<u>Mean Difference L/min</u>	<u>Standard Deviation of Differences</u>
Present Work	17	Rest/Exercise	0.04	0.63
Donald et al ^{423*}	10	Rest	0.36	0.49
Thomasson ⁴²⁷	17	Rest	0.22	0.65
Holmgren et al ⁴²⁸	17	Rest	0.53	0.89
Holmgren et al ⁴²⁸	27	Exercise	0.43	0.82

Comparison of reproducibility of new non-invasive method of measuring cardiac output with published data for Fick method.

* Analysis of results for normal subjects in this paper.

blood and 12.0L of water. Thus if the dissociation slope of the tissue compartment is assumed to be 0.0045 L/L/mmHg its volume should be

$$V_{TC} = \frac{5.0 \times 0.0045 + 12.0 \times 0.0007}{0.0045} = 6.87L$$

The estimates of tissue volume which have been obtained are 8.5 (II), 4.5 (RMCC), 4.9 (JU), and 5.1 (WG). (in litres).

TABLE 5.19

<u>Reference</u>	<u>Age</u> <u>yr.</u>	<u>No.</u>	<u>Sex</u>	<u>Cardiac Output</u> <u>Regression Equation</u> <u>L/min</u>
Astrand et al ⁴³⁰	19-33	11	F	$\dot{Q} = 5.48 + 5.34 \dot{V}O_2$
Astrand et al ⁴³⁰	21-30	12	M	$\dot{Q} = 4.34 + 5.22 \dot{V}O_2$
Bevegard et al ⁴²⁶	23-41	10	M	$\dot{Q} = 4.63 + 5.75 \dot{V}O_2$
		9	F	$\dot{Q} = 7.61 + 5.28 \dot{V}O_2$
Donald et al ⁴³¹	21-52	16	(M,F)	$\dot{Q} = 6.93 + 5.34 \dot{V}O_2$
Holmgren et al ⁴³²	16-40	14	M	$\dot{Q} = 6.93 + 5.74 \dot{V}O_2$
Holmgren et al ⁴³²	16-25	4	F	$\dot{Q} = 6.34 + 6.17 \dot{V}O_2$
Julius et al ⁴³³	18-34	18	(m,F)	$\dot{Q} = 4.2 + 6.3 \dot{V}O_2$
Reeves et al ⁴³⁴	19-44	10	M	$\dot{Q} = 3.95 + 5.88 \dot{V}O_2$

Published data for relationship between cardiac output and oxygen uptake during submaximal exercise. The data is taken from Altman & Dittmer.⁴³⁵

CHAPTER 6

CONCLUDING REMARKS.

The starting point of the work described in this thesis was the belief that current methods of analysing respiratory gas exchange could be improved by improving the techniques of mathematical treatment of measured data.

The initial work was an extension of the available methods for studying ventilation-perfusion distribution. (See Chapter 2). There are existing methods based on studies with inert gases, but an attempt was made to base the work on the more readily available data for oxygen and carbon dioxide transport. The analysis is complicated by the need to incorporate the oxygen and carbon dioxide dissociation curves, so that it was necessary to develop an efficient method for construction of the ventilation-perfusion line for the individual subject. The analysis itself was empirical in type and was based on finding the point of correspondence between the minima of two error criterion functions (see Appendix 10). The method was used to analyse data collected during steady-state studies.

It became clear that the limitations of this approach included difficulties in establishing steady-state conditions, particularly in dyspnoeic subjects, and the restricted information content imposed by the steady state conditions was developed. This was based on dynamic models consisting of ordinary differential equations rather than the more familiar algebraic equations of steady-state models. Both analogue and digital computing methods were applied to the solution of these equations. Experimental methods for application of these techniques were developed together with the necessary computer software (see Chapter 3). The software, which incorporates facilities for synchronisation of the measured data, breath detection, and detection of the end-tidal sections, is of general use for on-line studies with a

respiratory mass spectrometer. A complete set of graphics facilities is included.

The feasibility of this new approach to measurement was shown by application of the technique to analysis of argon wash-out experiments (Chapter 4). It was demonstrated that the parameter estimates obtained were well correlated with independent measurements of the same variable, even when erratic breathing patterns occurred.

The dynamic modelling technique was also applied to study of carbon dioxide transport (Chapter 5). In this model there were four parameters to be estimated, equivalent to lung volume, cardiac output, metabolic production of carbon dioxide and "tissue volume". Sensitivity studies and other evidence, e.g. error contour plots, suggested that the parameter estimates obtained were likely to be unique. Standard methods of parameter estimation were employed. (The optimal methods of parameter estimation for this particular problem have been investigated.³⁸⁶) Studies of optimisation results with different assumptions in the model indicated that the parameter estimates were relatively insensitive to certain of these assumptions.

The estimates of cardiac output obtained were of the correct magnitude both at rest and on exercise. The reproducibility of the method was comparable to that of the standard Fick method. Thus a new simple non-invasive method of measurement of cardiac output was developed.

In application of these methods to measurement it was necessary to use the average end-tidal partial pressure. Thus the full potential of this new approach was not realised since the within-breath detail of the expired concentration measurements was not exploited. The patho-physiological mechanisms which determine the expired concentration curve are not known at this time. As a first step

to investigating this a simulation study of the importance of Taylor dispersion in the airways was carried out (Chapter 4).

Although in this thesis a number of new techniques of measurement have been developed, there are considerable possibilities for further expanding this approach. Since the available information content in experiments is increased it should be possible to identify parameters for more complex model structures. The first obvious step is characterisation of the way in which gas is handled within the lung itself (since gas transfer into blood is ignored in this step). A number of available insoluble gases is suitable for this experimental work. At a further stage, models will have to be developed which incorporate both pulmonary mechanics and gas transport.

The dynamic modelling approach can be extended to the study of other aspects of respiration. A particularly fruitful area would seem to be the study of the respiratory control system: currently available techniques of assessment of respiratory control ignore the dynamic aspects of controller function. They are, moreover, applicable only to linear systems which the respiratory control system is not.

Models can also be used for educational purposes. Because the model should demand no special computing ability of the student, a special purpose analogue computer operated by dialled controls, has been built. Although digital computation is more flexible students may find interaction with the digital computer tedious if it involves typing. The current availability of micro-processor technology will enable construction of special purpose simulators with more elaborate models than have been used here, incorporating, for example, gas exchange, mechanics and control.

A P P E N D I C E S

APPENDIX 1A.DEFINITION OF DERIVATIVE.

The derivative of a function f of the independent variable time t at a time t_0 is defined to be the limit of

$$\frac{f(t_0 + \Delta t) - f(t_0)}{\Delta t} \quad \text{as } \Delta t \text{ tends to zero.}$$

APPENDIX 1B.CONSTRUCTION OF ORDINARY DIFFERENTIAL EQUATION.

Equation 2.55 can be derived using the definition of a derivative as given in Appendix 1A. The mass of a gas species i which is present in the alveolar compartment of the lung model illustrated in Fig. 2.1, at time $t = t_0$ during phase 2 of the respiratory cycle (as defined in Table 2.7), is

$$M(t_0) = V_A(t_0) C_A(t_0)$$

and at time $t = t_0 + \Delta t$ when Δt is a small increment

$$M(t_0 + \Delta t) = V_A(t_0) C_A(t_0) + \Delta t \dot{V} C_I(t) + \Delta t \dot{Q} (C_{\bar{v}} - C_a)$$

$$\text{i.e.} \quad \frac{M(t_0 + \Delta t) - M(t_0)}{\Delta t} = \dot{V} C_I(t) + \dot{Q} (C_{\bar{v}} - C_a)$$

and taking the limit as $\Delta t \rightarrow 0$ this becomes

$$\frac{dM}{dt} = \dot{V} C_I(t) + \dot{Q} (C_{\bar{v}} - C_a)$$

and hence since $M(t) = V_A(t) C_A(t)$ and $C_A = \beta \frac{P_A}{g}$ etc

$$\beta \frac{d(V_A P_A)}{dt} = \dot{V} \beta \frac{P_I}{g} + \dot{Q} \beta_b (P_{\bar{v}} - P_a)$$

Partial differential equations can be derived similarly.

For a function f of two variables (x, t) the partial derivative of

the function with respect to x , $\frac{\partial f}{\partial x}$ is defined as

$$\frac{\partial f}{\partial x} = \lim_{\Delta x \rightarrow 0} \frac{f(x_0 + \Delta x, t_0) - f(x_0, t_0)}{\Delta x} \quad \text{and}$$

the partial derivative with respect to t , $\frac{\partial f}{\partial t}$ is

$$\frac{\partial f}{\partial t} = \lim_{\Delta t \rightarrow 0} \frac{f(x_0, t_0 + \Delta t) - f(x_0, t_0)}{\Delta t}$$

To derive equation 2.77 which describes gas transport in the airways consider a small section of airway as demonstrated in Fig. I. At time t_0 let the mass of gas in a small segment of length Δx be $M(t, x)$. Then the mass present at time $t + \Delta t$, $M(t + \Delta t, x)$ is given by

$$M(t + \Delta t, x) = M(t, x) + u(t, x)A_A(t, x)C(t, x) \Delta t - u(t, x + \Delta x)A_A(t, x + \Delta x)C(t, x + \Delta x) \Delta t - \left[\frac{\partial C}{\partial x} A_A D \right] (t, x) \Delta t + \left[\frac{\partial C}{\partial x} A_A D \right] (t, x + \Delta x) \Delta t - F^* \Delta x \Delta t$$

where

$u(t, x)$ is the velocity of gas flow at length x in the model

and time t .

$A_A(t, x)$ is the cross-sectional area of airways.

D is the diffusion coefficient.

F^* is a function describing transfer of gas across the alveolar-capillary membrane per unit length per unit time.

but

$$M(t + \Delta t, x) = \Delta x A_T(t + \Delta t, x) c(t + \Delta t, x)$$

$$M(t, x) = \Delta x A_T(t, x) C(t, x)$$

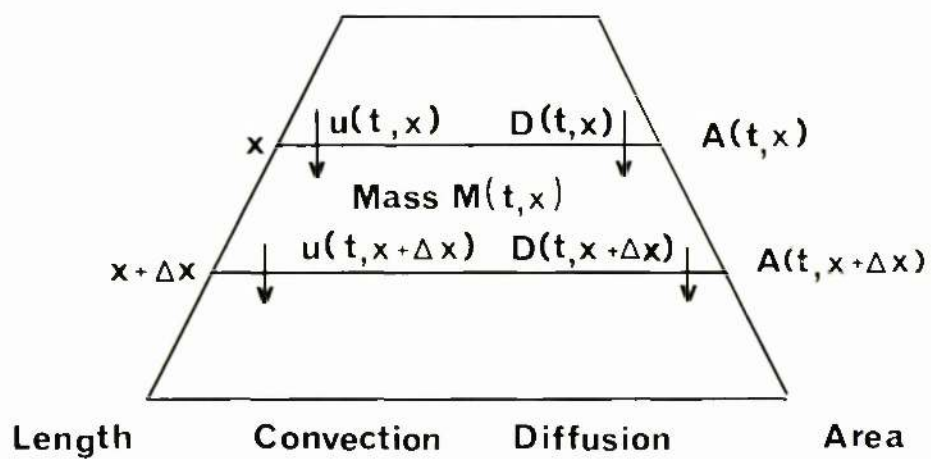


FIGURE I

Three small segments of airways of length Δx .
The symbols etc. are explained in text.

where

A_T is the cross-sectional area of airways plus alveoli.

By forming

$$\frac{M(t+\Delta t, x) - M(t, x)}{\Delta t} \quad \text{and taking the limit as}$$

$\Delta t \rightarrow 0, \Delta x \rightarrow 0$ we obtain

$$\frac{\partial}{\partial t}(A_T C) = -\frac{\partial}{\partial x}(A_A u c) + \frac{\partial}{\partial x}(A_A D \frac{\partial C}{\partial x}) - F^*$$

but $C = \beta_g P$ and if $F = F^*/\beta_g$

$$\frac{\partial}{\partial t}(A_T P) = \frac{\partial}{\partial x}(A_A u p) + \frac{\partial}{\partial x}(A_A D \frac{\partial P}{\partial x}) - F$$

APPENDIX 1D. LINEARISATION OF A NON-LINEAR EQUATION.

The operation of many non-linear systems can be described approximately by linear differential equations with constant coefficients provided that the description is only applied to a very limited range of the system's performance.

The linearisation process is based on Taylor Series expansion. For a function f of time t which fulfills the mathematical conditions of continuity and differentiability the function f can be represented over a limited region from $t = t_0$ by

$$f(t) = f(t_0) + \frac{df(t_0)}{dt} \cdot (t-t_0) + \frac{d^2f(t_0)}{dt^2} \frac{(t-t_0)^2}{2!} \dots \dots \frac{d^n f(t_0)}{dt^n} \frac{(t-t_0)^n}{n!} \dots$$

$$\dots \dots \dots + R_n$$

where R_n is the remainder

$$\text{As } n \rightarrow \infty \quad R_n \rightarrow 0.$$

For the non-linear equation describing the

motion of a pendulum

$$\frac{d^2\theta}{dt^2} + (g/l) \sin\theta = 0$$

where l is the length of the pendulum, and g is the acceleration of gravity, and θ is the angle of the pendulum from the vertical.

For a small operating range around $\theta = 0$ this becomes

$$\frac{d^2\theta}{dt^2} + (g/l) \sum_{n=0}^{\infty} \frac{\theta^n}{n!} \left(\frac{d^n}{d\theta^n} (\sin \theta) \Big|_{\theta=0} \right) = 0$$

i.e.
$$\frac{d^2\theta}{dt^2} + (g/l) \left[\theta - \frac{\theta^3}{3!} \dots \dots \dots \right] = 0$$

Approximating with only the first term of the expansion we obtain the linear equation

$$\frac{d^2\theta}{dt^2} + (g/l)\theta = 0 \quad \text{which is valid over a small}$$

operating range around $\theta = 0$.

1. Introduction.

The use of an analogue computer was considered briefly in Chapter 1. The practical details of its use are considered in more detail in this section. (Most of the standard texts on this subject require prior knowledge of electronics.)

2. Concept of a Machine-Unit.

In using analogue computers it is necessary to scale all voltages to lie inside a certain defined range, which is specific to the computer (commonly ± 10 volts). It is more convenient for practical scaling purposes, however, to consider this as scaling all variables to lie between +1 to -1, where +1 is defined to be a MACHINE-UNIT. This not only allows the user to consider problems numerically, rather than in voltages, but also the solution which is developed for a particular problem is also applicable immediately to other analogue computers, where one machine unit may correspond to different voltage levels, e.g. 100 volts, 10 volts, 1 volt.

3. Analogue Computer Components.

As indicated in Chapter 1, the analogue computer has a number of distinct components, each one of which carries out a specific function. In order to programme the computer, the components have to be linked by wires (patch-cords) in a pre-determined way. The main components were considered in Chapter 1 (see Table 1.4).

4. Modes of Operation.

The analogue computer has four modes of operation, which are controlled by the operator using panel mounted controls.

These modes are detailed below:-

<u>Mode</u>		<u>Output of Integrators</u>	<u>Function</u>
Potentiometer Setting (P.S.)		Zero	For manually setting potentiometers to the required values.
Initial condition	(I.C.)	Starting values of variables.	For setting problem to initial status.
Hold	(H)	Output is held constant.	For "freezing" operation of computer so that current status of problem can be examined.
Operate	(O.P.)	Required solution.	Integrators are made to operate and the solution of the differential equation obtained.

5. Solution of a Simple Differential Equation by Analogue Computation.

As indicated in Chapter 1 the main application of the electronic analogue computer is in the solution of ordinary differential equations.

Consider the following simple equation:-

$$\frac{d^2v(t)}{dt^2} + K_1 \frac{dv(t)}{dt} + K_2 v(t) = A$$

where K_1, K_2, A are constant. At zero time (i.e. $t = 0$) $v(t) = 1, \frac{dv(t)}{dt} = 0$.

A patch diagram, which describes the required linkages between the computational components, must be developed to programme the problem. To aid development of the patch diagram, the equation should be reformulated with the highest order derivative on the left hand side:-

$$\frac{d^2V(t)}{dt^2} = -K_1 \frac{dV(t)}{dt} - K_2V(t) + A.$$

The derivative terms in the equation are removed using integrator units; thus, for example, if the input to an integrator is

$$\frac{d^2V(t)}{dt^2} \text{ its output will be } \frac{-dV(t)}{dt}.$$

The equation can be solved with the "patch" illustrated in Figure II. The values of $V(t)$ and $\frac{dV}{dt}(t)$ at zero time are set as initial conditions on the integrators. The solution $V(t)$ is obtained as an output of the appropriate integrator.

6. Amplitude Scaling.

Problem variables must be normalised so that they fall within the range ± 1 machine unit. This normalisation or scaling of variables presents a problem in analogue computation, but it is a problem which is overcome easily if a systematic approach is employed. The most logical approach is to establish equality, for any problem variable x , between one machine unit (computer maximum) and the maximum possible value of the variable x_{\max} .

i.e.

$$x_{\text{normalised}} = \frac{x}{(x_{\max})}$$

The equations are rewritten in terms of these new normalised variables. It is more convenient to normalise the equations describing the performance of individual amplifiers in the patch (the so-called decomposed equations) rather than the differential equations themselves.

For the decomposed equations for integrators

$$\frac{d}{dt} (\text{amplifier output}) = \text{algebraic sum of inputs}$$

and for summers

$$-(\text{amplifier output}) = \text{algebraic sum of inputs}$$

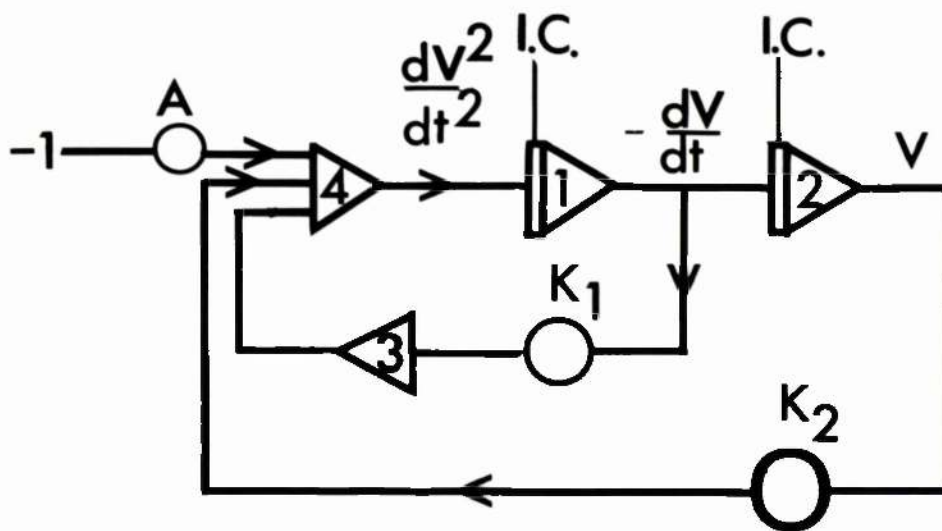


FIGURE II

Patch diagram for solution of equation described in text. Standard symbols (see Table 1.4) are used. The solution (V) is obtained as the output of one of the integrators.

In the example of the previous section the "unscaled" patch diagram (Fig. II) contains 4 amplifiers. The decomposed equations for each amplifier are:-

$$1) \quad -\frac{d}{dt} \left[\frac{dV(t)}{dt} \right] = \frac{d^2 V(t)}{dt^2}$$

$$2) \quad -\frac{d}{dt} [V(t)] = -\frac{dV}{dt}$$

$$3) \quad -K_1 \frac{dV(t)}{dt} = -K_1 \frac{dV(t)}{dt}$$

$$4) \quad -\frac{d^2 V(t)}{dt^2} = K_1 \frac{dV(t)}{dt} + K_2 V(t) - A$$

and on normalising these equations assuming that the maximum values are

$$\frac{d^2 V(t)}{dt^2}_{\max} = 10 ; \quad \frac{dV(t)}{dt}_{\max} = 10 ; \quad V_{\max} = 100$$

we obtain:-

$$1) \quad -\frac{d}{dt} \left[\frac{dV}{dt} \right]_{\text{norm}} \times 10 = \left[\frac{d^2 V}{dt^2} \right]_{\text{norm}} \times 10$$

$$2) \quad -\frac{d}{dt} [V]_{\text{norm}} \times 100 = -\left[\frac{dV}{dt} \right]_{\text{norm}} \times 10$$

$$3) \quad -K_1 \left[\frac{dV}{dt} \right]_{\text{norm}} \times 10 = -K_1 \left[\frac{dV}{dt} \right]_{\text{norm}} \times 10$$

$$4) \quad -\left[\frac{d^2 V}{dt^2} \right]_{\text{norm}} \times 10 = K_1 \left[\frac{dV}{dt} \right]_{\text{norm}} \times 10 + K_2 [V]_{\text{norm}} \times 100 - A.$$

where $[]_{\text{norm}}$ represents a normalised variable.

This reduces to the final form of the normalised or so called MACHINE EQUATIONS.

Amplifier No.

Machine Equation

1.
$$-\frac{d}{dt} \left[\frac{dv}{dt} \right]_{\text{norm}} = \left[\frac{d^2v}{dt^2} \right]_{\text{norm}}$$
2.
$$-\frac{d}{dt} [v]_{\text{norm}} = \frac{-1}{10} \left[\frac{dv}{dt} \right]_{\text{norm}}$$
3.
$$-K_1 \left[\frac{dv}{dt} \right]_{\text{norm}} = -K_1 \left[\frac{dv}{dt} \right]_{\text{norm}}$$
4.
$$-\left[\frac{d^2v}{dt^2} \right]_{\text{norm}} = -K_1 \left[\frac{dv}{dt} \right]_{\text{norm}} + 10K_2 [v]_{\text{norm}} - \frac{A}{10}$$

The maximum values of each of the variables, which are used in this normalisation process, may be estimated in many cases from knowledge of the physical problem or differential equation solution.

The recommended approach in the absence of such knowledge, is to carry out trial simulations on a digital computer, e.g. using a high level simulation language, to ascertain the likely numerical range of the variables.

7. Time-scaling.

A great advantage of the analogue computer is that the duration of the computation can be altered by the user. This is unlike the digital computer where the computational time depends only on the capabilities of the particular computer. The variable time in the equations (t) can be replaced by a new variable $T = Bt$, and solution of the reformulated equations can either accelerate or slow down the simulation depending on choice of the constant B .

8. Logic Capabilities of Analogue Computers.

Modern analogue computers provide logic facilities for controlling the mode of operation of individual units or of the entire computer. The logic in an analogue computer is standard binary logic which is based on the concepts of Boolean Algebra. Thus logic variables have only two states, either on or off, (1 or 0). Logic variables are distinct from problem variables.

The logic area of the analogue receives inputs from various sources which are monitoring the problem's status in a preset way, operates on such logic, and produces logic information to control the operation of the computer.

The main logic inputs to the logic area are (a) from signals from outwith the analogue computer; (b) from a "clock" in the computer at pre-set times and (c) from comparators. Comparators are components which compare the relative magnitude of two problem variables (x, y). If $x \gg y$ the logic output is on (1) and if $x < y$ the logic output is 0. The analogue computer has a number of components which operate only on logic variables:-

<u>Unit</u>	<u>Function</u>
And gate	Logic output is one if and only if both inputs to the and gate are one.
Or gate	Logic output is one if either of inputs is one.
Complement	Logic output is the opposite of input.
Monostable	Logic output is "held" unaltered for pre-set time after input to this unit has changed.
Differentiator	Unit recognises changes in logic states.

9. Example of Use of an Analogue Computer in Solution of a Lung Model Equation.

In Chapter 4 the application of a continuous parameter

estimation method to the analysis of inert gas wash-out experiments was discussed. The equations to be solved on the analogue computer were

$$\frac{dP_A}{dt} = \frac{S\dot{V}}{V_A} [P_I - P_A] \quad (a)$$

$$S = 1 \text{ for } \dot{V} \geq 0 \text{ \& } \int_0^t \dot{V} dt \geq V_D$$

$$S = 0 \text{ otherwise}$$

$$\frac{d}{dt} \left[\frac{\partial P_A}{\partial 1/V_A} \right] = S\dot{V} \left[P_I - P_A \right] - \frac{SM}{V_A} \frac{\partial P_A}{\partial 1/V_A} \quad (b)$$

$$\frac{d(1/V_A)}{dt} = -Ke \frac{\partial P_A}{\partial 1/V_A} \quad (c)$$

Following the procedure outlined in this Appendix, the first step is preparation of the unscaled patch diagram (Fig. 4.1 with scaling factor = 1). In this patch logic is generated to obtain S in the equations; to control individually the mode of the integrator which is integrating \dot{V} ; to control the mode of operation of all the integrators collectively; and to sample the difference between model and system only during the last part of the expiration. The variable S can be generated by opening (S=0) and closing (S=1) a relay (see Fig. 4.1). The operation of this relay is controlled by logic output from a comparator. This comparator compares the integral of inspired flow during each respiratory cycle with the pre-set dead space volume. Thus the integrator which is integrating the flow signal is controlled to operate only during the inspired phase of the respiratory cycle and to reset to zero during expiration. The phase of the respiratory cycle is determined by another comparator.

Since the experimental data has to be computed iteratively the operation of the computer is controlled such that it computes only during the actual experiment. This is achieved by generating

logic external to the computer. A rapid series of electronic pulses, which are sensed by a differentiator/monostable unit, is recorded on the magnetic tape to mark the zero and calibrate section, of the experiment. The error function e is generated by closing a relay during the last part of expiration. This period of the respiratory cycle is recognised when two conditions are satisfied; $\dot{V} < 0$ (by a comparator) and a pre-set time has elapsed from the start of expiration. (A comparator and monostable in series are used to monitor for this latter condition)

For amplitude scaling of these equations the following problem variables have to be scaled \dot{V} , P_A , $\frac{\partial P_A}{\partial l/V_A}$, l/V_A , e , and the measured partial pressure of argon. The following maximum values are used:-

\dot{V}	2L/sec
P_A	$P_A \text{ max kPa}$
$\frac{\partial P_A}{\partial l/V_A}$	$P_A \text{ max}$
l/V_A	1 L
e	$P_A \text{ max kPa}$
Measured argon partial pressure	$P_A \text{ max kPa}$

Since the data is input to the computer at eight times the speed at which it was recorded, the computer time $T = 1/8t$ where t is real time. Substituting these values into equations (a), (b), (c) we obtain

$$\frac{d(P_A)_{\text{norm}}}{d8T} \cdot P_{A_{\text{max}}} = \frac{S(\dot{V})_{\text{norm}} \times 2.0}{(V_A)_{\text{norm}}} \times \left[P_I - P_A \right]_{\text{norm}} \times P_{A_{\text{max}}}$$

$$\frac{d}{d8T} \left[\frac{\partial P_A}{\partial 1/V_A} \right]_{\text{norm}} \cdot P_{A_{\text{max}}} = S(\dot{V})_{\text{norm}} \times 2.0 \times \left[P_I - P_A \right]_{\text{norm}} \times P_{A_{\text{max}}} - \frac{SM}{(V_A)_{\text{norm}}} \times \left[\frac{\partial P_A}{\partial 1/V_A} \right]_{\text{norm}} \times P_{A_{\text{max}}}$$

$$\frac{d}{d8T} (1/V_A)_{\text{norm}} = -K(e)_{\text{norm}} \left[\frac{\partial P_A}{\partial 1/V_A} \right]_{\text{norm}} \cdot P_{A_{\text{max}}} \cdot P_{A_{\text{max}}}$$

i.e. the equations become in their scaled form

$$\frac{d(P_A)_{\text{norm}}}{dT} = \frac{16.0 \times Sx(\dot{V})_{\text{norm}}}{(V_A)_{\text{norm}}} \times (P_I - P_A)_{\text{norm}} \quad (d)$$

$$\frac{d}{dT} \left[\frac{\partial P_A}{\partial 1/V_A} \right]_{\text{norm}} = 16.0 \times Sx(\dot{V})_{\text{norm}} \times (P_I - P_A)_{\text{norm}} - \frac{SM^*}{(V_A)_{\text{norm}}} \left[\frac{\partial P_A}{\partial 1/V_A} \right]_{\text{norm}} \quad (e)$$

$$\frac{d}{dT} (1/V_A)_{\text{norm}} = -K^* e \left(\frac{\partial P_A}{\partial 1/V_A} \right)_{\text{norm}} \quad (f)$$

where $K^* = K \times 8 \times (P_{A_{\text{max}}})^2$. K is an arbitrary constant chosen by trial and error. M^* is $8 \times M$.

Thus the main effect of scaling is to introduce an arbitrary scaling factor 16.0 into equations (d) and (e). This scaling factor is represented on the patch diagram (Fig. 4.1) and is obtained using a potentiometer set at 0.16 and altering, as is possible, the "gain" on the associated amplifier such that the output of the amplifier is x100 the input.

APPENDIX 3. USE OF HIGH LEVEL SIMULATION LANGUAGE.

A number of high level simulation languages exist which are relatively simple to programme. One of the most widely used languages is CSMP (Continuous System Modeling Program) which was developed by the IBM corporation. These languages enable users to solve sets of ordinary differential equations simply. The program statements are related closely to the formulation of the equations. The language provides users with a number of functions which can be called in the programme, e.g. integration. CSMP has several numerical integration routines - fixed step Runge-Kutta; Simpson's; trapezoidal; fifth-order Milne predictor-corrector; fourth order variable step Runge-Kutta.

In CSMP the programme consists of three sections:-

- Initial All statements in the initial section are executed prior to the simulation.
- Dynamic Simulation section.
- Terminal All statements in the terminal section are executed only at conclusion of the simulation.

The parameter values for the simulation are set in the programme. The programme has the facility to assign new values to the parameters and to repeat the simulation. The compiler sorts the problem statements in the dynamic section into the order which is required for numerical solution of the equations. The program outputs the solution as a plot on a line printer of the chosen variable against sample number.

A listing of a programme to solve a differential equation which describes the wash-out of an inert gas from the lung is shown.

The equation is

$$\frac{dP_A}{dt} = \frac{S\dot{V}}{V_A} (P_I - P_A)$$

(equation 2.57 & 4.6)

$$S = 1 \quad \dot{V} > 0 \quad \& \quad \int_0^t \dot{V} dt \geq V_D$$

= 0 otherwise.

The descriptions on each line are to aid the reader and are not part of the programme.

PROGRAMME

TITLE	ARGON MODEL	
PARAMETER	VA = (3.5, 5.0, 6.5)	Allows 3 runs of programme with 3 different values of V_A (L)
INCON	IPA = 600.0	Initial condition for P_A .
INCON	IVOL = 0.0	Initial condition for $\int \dot{V}$.
CONSTANT	PI = 0.0	Value of P_I .
CONSTANT	VT = 0.5, F = 15.0	Sets values for tidal volume and respiratory frequency.
CONSTANT	VD = 0.150	Sets volume of dead space.
INITIAL	W = 2.0 * 3.412 * F / 60.0 A = W * VT / 2.0	Calculates appropriate amplitude and frequency for sinusoidal ventilation.
DYNAMIC		Dynamic section contains solution of equation.
	VDOT = A * SINE (0.0, W, 0.0)	Sinusoidal ventilation, \dot{V}
	VOL = INTGRL (IVOL, VDOT)	$VOL = \int \dot{V} dt$
	SO = COMPAR (VOL, VD)	SO = 1 VOL \geq V_D .
	SP = COMPAR (VDOT, 0.0)	SP = 1 VDOT \geq 0.0.
	S = AND (SO, SP)	Generates S.
	CALC = S * VDOT * (PI - PA) / VA	Forms R.H.S. of equation.
	PA = INTGRL (IPA, CALC)	Obtains P_A .

No need for terminal section.

TIMER DELT = 0.02, FINTIM = 6000.0, OUTDEL = 10.0

Sets:- Time step for calculation (DELT).
Total length of simulation (FINTIM).
Time step for print/plotting (OUTDEL).

LABEL ALVEOLAR PARTIAL PRESSURE OF ARGON.

Label for plot on line printer.

PRTPLOT (PA)

Causes print/plotting of sampled
values of P_A .

END

STOP

ENJOB.

APPENDIX 4 SIMULATOR FOR EDUCATIONAL USE.

The observation and manipulation of the performance of an adequate model of a complex physiological system may give students greater insight into physiology than can be obtained by more standard methods of teaching. Respiratory gas exchange is such a complex process which students find difficult to comprehend completely; in particular they often find difficulty in understanding the ventilation-perfusion concept. (See Chapter 2).

The main reason for this difficulty is that students have to consider simultaneously several inter-related physiological variables:- ventilation, dead space volume, perfusion; inspired gas concentrations and partial pressures; alveolar, arterial, mixed venous partial pressures and related gas contents which in the case of carbon dioxide and oxygen involve complex inter-dependent non-linear relationships with the associated partial pressures; respiratory exchange ratio, oxygen uptake, carbon dioxide output.

A model which simulates ventilation-perfusion distribution in the lung must have a minimum of two compartments so that ventilation can be maldistributed in relation to perfusion. A model (Fig. II) therefore, which has a common dead space, two ventilated and perfused compartments, and a right to left shunt has been used to simulate gas exchange for educational purposes. In addition the model structure may or may not contain a single tissue compartment.

Equations of the Model.

In the case where no tissue compartment is included the equations of the model are:-

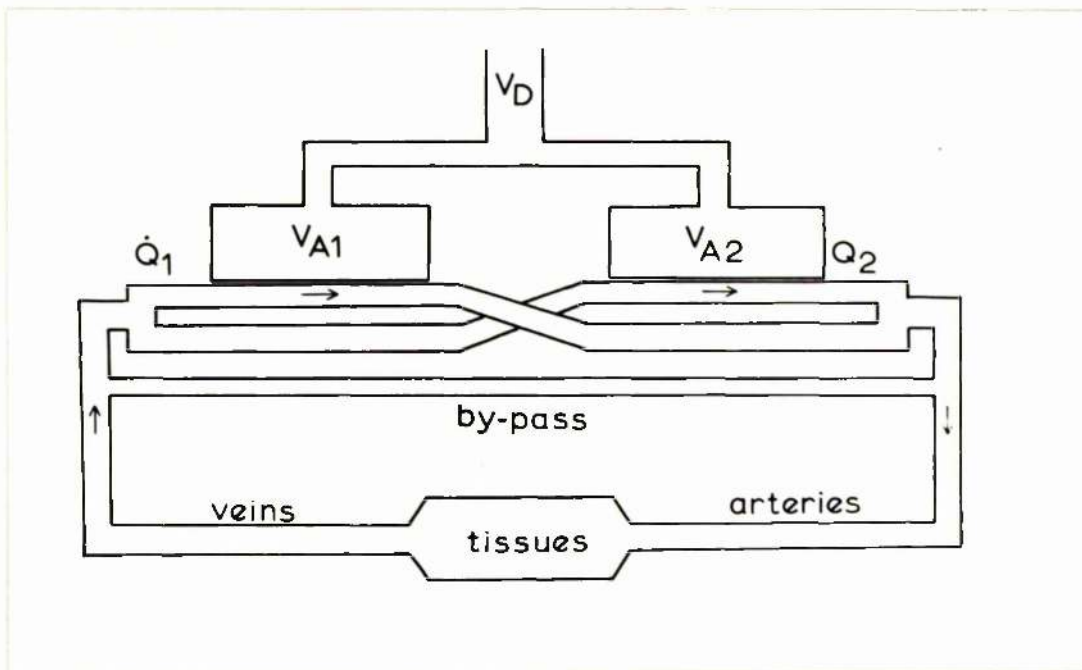


FIGURE III

Model structure on which the simulator is based. The model consists of two ventilated and perfused compartments with volumes V_{A1} and V_{A2} , and blood flows \dot{Q}_1 and \dot{Q}_2 . There is a right to left shunt (by-pass). The anatomical dead space has volume V_D . The tissues are represented by a single tissue compartment.

Alveolar Compartment 1.

$$V_{A_1} \frac{dP_{A_1}}{dt} = S_1 k \dot{V} [P_D - P_{A_1}] + S_2 k \dot{V} [P_I - P_{A_1}] \\ + \dot{Q}_1 \frac{\beta b}{\beta g} [f_1(P_{\bar{v}}) - f_2(P_{A_1})]$$

$$\text{where } S_1 = 1 \quad \dot{V} \geq 0 \text{ \& } \int_0^t \dot{V} dt < V_D$$

$$= 0 \quad \text{otherwise}$$

$$S_2 = 1 \quad \dot{V} \geq 0 \text{ \& } \int_0^t \dot{V} dt \geq V_D$$

$$= 0 \quad \text{otherwise}$$

f_1 = function relating mixed venous partial pressure to mixed venous gas content

f_2 = function relating end-capillary partial pressure to end-capillary content.

(It is here assumed that there is equality between end capillary and alveolar partial pressure.)

Symbols as in remainder of thesis, and are summarised in Appendix 5.

The subscript 1 refers to compartment 1.

Alveolar Compartment 2.

$$V_{A_2} \frac{dP_{A_2}}{dt} = S_1 (1-k) \dot{V} (P_D - P_{A_2}) + S_2 (1-k) \dot{V} (P_I - P_{A_2}) + \dot{Q} \frac{\beta b}{\beta g} [f_1(P_{\bar{v}}) - f_2(P_{A_2})]$$

Arterial blood.

$$f_2(P_a) = \frac{\dot{Q}_1 f_2(P_{A_1}) + \dot{Q}_2 f_2(P_{A_2}) + \dot{Q}_s f_1(P_{\bar{v}})}{\dot{Q}_1 + \dot{Q}_2 + \dot{Q}_s}$$

when \dot{Q}_s is flow rate through right to left shunt.

Mixed Alveolar Gas.

$$P_{\bar{A}} = kP_{A_1} + (1-k)P_{A_2}$$

thus allowing calculation of the alveolar-arterial difference for the gas under study ($P_{\bar{A}} - P_a$).

In the case where a tissue compartment is included the equations are almost identical, except that P_v is replaced by P_{Tc} , (circulatory time delay between tissues and lung is not included) and an equation for the tissue compartment is added:-

$$V_{Tc} \frac{df_3(P_{Tc})}{dt} = \dot{M} - \dot{Q}_1 \left[f_1(P_{Tc}) - f_2(P_{A_1}) \right] - \dot{Q}_2 \left[f_1(P_{Tc}) - f_2(P_{A_2}) \right]$$

when f_3 = function relating partial pressure in tissue compartment to gas content.

An analogue computer solution of these equations presents no particular difficulties and the "patch" diagram is shown in Figure IV.

For educational purposes the model simulation should be interactive, so that the student can alter the model's performance directly and observe immediately the effect of this change. Communication between the student and simulation should be simple. In the simulations used for teaching in industrial practice, e.g. flight-deck simulation, the student is completely unaware that there is a computer, and the man-machine interface is an exact replica of the flight-deck.

The model of respiratory gas exchange for teaching purposes is implemented therefore using a specially constructed simulator (see Figure V). This incorporates a special purpose analogue computer.*

* Construction of this was completed by an electronics technician, Mr. E. Miller.

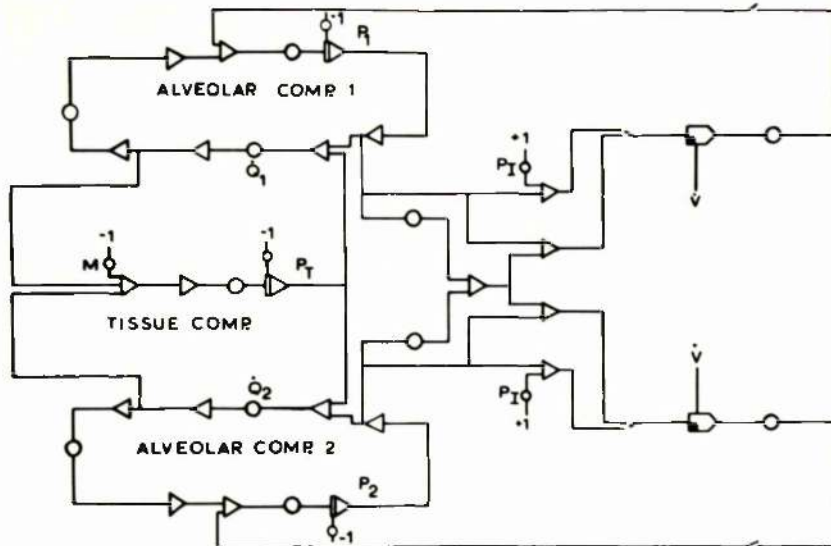


FIGURE IV

"Patch" diagram for solution of equations for simulator. The symbols are the standard ones (see Table 1.4). The patch has 3 integrators - one for alveolar compartment 1, one for alveolar compartment 2, and one for the tissue compartment. In this form of the model it is assumed that $f_1 = f_2 = f_3 = f$. $f(PCO_2) = a + bPCO_2$ where a and b are constants.

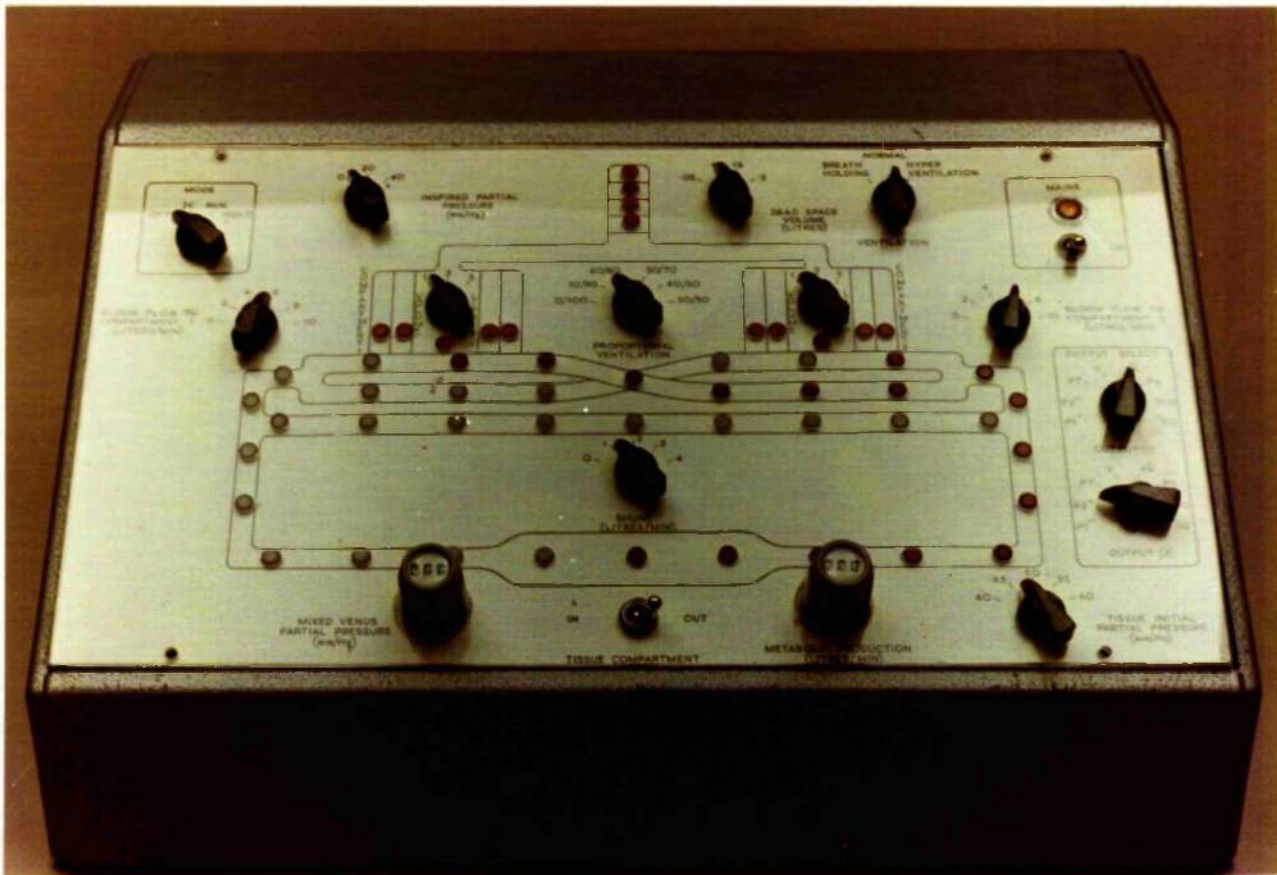


FIGURE V

Picture of simulator. The front panel has a diagram of the model lung. The controls are calibrated in physiological units. The simulator can be attached to an oscilloscope or chart recorder for observation of the temporal changes in $p\text{CO}_2$.

The design of the simulator embodies the following features:-

1. It is constructed from readily available low cost components, which achieve an accuracy of 1%.
2. It is compact and suitable for desk-top operation.
3. Use of the simulator does not require knowledge or skill in analogue computation.
4. All controls are easily identified and calibrated in appropriate physiological units. The controls are placed at anatomically appropriate positions on a drawing of the model, similar to Figure III which forms part of the front panel of the machine. Rotary switches are used for all the controls which are associated with representation of the parameter values apart from the continuously variable controls for metabolic production and mixed venous tension.
5. Time scaling is used to solve the equations in a time much faster than real time ($\times 10$). By this means the student can observe more quickly the effect of changing model parameters. The ventilation is, therefore, simulated by a sine wave generator, the frequency of which is ten times real time (i.e. 3 Herz).
6. The outputs from the computer are continuous electrical signals which show the time variation in model variables using an oscilloscope or chart recorder. Two output channels are available, each output having sufficient positions to provide zero & 50 mm. of Hg. CO_2 tension calibrating signals, and a choice of the CO_2 tension in each of the alveolar compartments, mixed alveolar CO_2 tissue tension and arterial tension.

7. One parameter in the simulation is fixed and the student cannot alter this (V_{Tc}); in addition the rate of breathing is constant although the depth can be varied. The values of the remaining parameters are under the control of the student

The student can observe by using this simulator both dynamic and steady-state aspects of gas exchange. In particular the effect of changes on perfusion and ventilation on alveolar and arterial pressures can be studied (see Figure VI). The mechanism of production of an alveolar-arterial difference for carbon dioxide can be investigated.

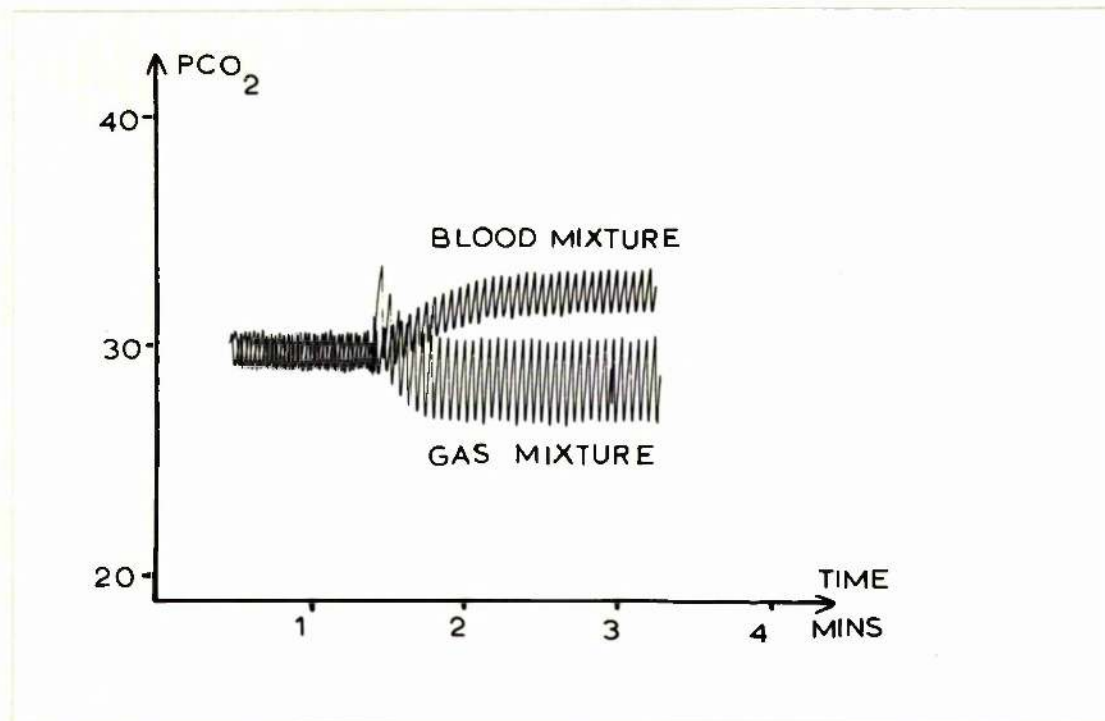


FIGURE VI

Graph of $p\text{CO}_2$ output from simulator of arterial $p\text{CO}_2$ (blood mixture) and of mixed alveolar $p\text{CO}_2$ (gas mixture). In the initial part of the record the two alveolar compartments have equal blood flows and ventilations. In the later part of the record one compartment is hyperventilated relative to the other. The development of an arterial-alveolar difference for CO_2 is seen. There is a slight switching transient at the point at which the parameter values have been changed.

APPENDIX 5.

SUMMARY OF SYMBOLS WHICH ARE USED IN THIS THESIS.CHAPTER 1

F_1	Flow rate of urine down one ureter.
F_2	Flow rate of urine down other ureter.
$G(V,T,M)$	Arbitrary function describing flow of urine down urethra. This function is a function of volume of bladder (V), urethral sphincter tone (T) and tone of abdominal musculature (M).
\dot{I}_1 etc.	Flux of mass into compartment X.
M_x	Mass of material in compartment X.
\dot{O}_1 etc.	Flux of mass from compartment X.
$x_i(t)$	Input to system.
$y_i(t)$	Output of system in response to input $x_i(t)$.
$y(t)$	Overall system output.

CHAPTER 2/3

Several symbols in these chapters are subscripted. The subscripts are listed separately. Greek symbols which are used are also listed separately. The symbols which are used are where appropriate the standard ones in use in respiratory physiology. Otherwise the symbols are taken from the original publications. A small number of symbols are used consequently at different parts of these chapters for different variables. This is clearly identified in text and in this list. The appropriate page numbers are given for more than one usage of a symbol.

Symbols Continued (Chapter 2/3)

a	Cross-sectional area of individual pulmonary capillary.
A	Area of membrane through which diffusion occurs. Cross sectional area of pulmonary capillary (page 100).
A(x)	Cross sectional area of airways.
$A_A(x,t)$	Cross sectional area of airways (excluding alveoli).
$A_T(x,t)$	Cross sectional area of airways (including alveoli).
b	Slope of dissociation curve for CO ₂ .
b(t)	Oscillatory function of time.
B	Barometric pressure.
C	Concentration of gas species. Moles/L.
d	Diameter of individual pulmonary airway.
d_i	Diffusion coefficient of gas species (i).
d_{unit}	Diffusing capacity of capillary per unit length.
D(x,t)	Effective diffusion coefficient of gas in airways.
D_{app}	Apparent diffusing capacity of lung (as calculated assuming that lung is homogenous).
D_L	Diffusing capacity of lung.
D_M	Membrane component of pulmonary diffusing capacity.
D_{mol}	Molecular diffusion coefficient.
f	Frequency of breathing.
f(x)	Flexibility function describing compliance of airways.
f_1	Function relating concentration to partial pressure of a gas species in venous blood.
f_2	Function relating concentration to partial pressure of a gas species in arterial blood.
$f(P_A CO_2)$	Function relating concentration of carbon dioxide in arterial blood to alveolar partial pressure.
F	Fractional concentration of gas species. L/L.

Symbols Continued (Chapter 2/3)

$g(j)$	Fraction of pulmonary diffusing capacity in j^{th} unit.
$g(P_{A O_2})$	Function relating concentration of oxygen in arterial blood to alveolar partial pressure.
G	Conductance of gas species.
K	Constant of diffusion between tidal volume and alveolar compartments. (page 78).
K_{AP}	Rate constant of transfer of gas species between alveolar gas and pulmonary tissue.
K_{PC}	Rate constant of transfer of gas species between pulmonary tissue and pulmonary capillary blood.
l	Length of individual pulmonary capillary.
L	Termination of model of pulmonary airways.
M	Quantity of an individual gas species.
\dot{M}	Flux of an individual gas species.
n	Number of pulmonary capillaries.
P	Partial pressure of gas.
\bar{P}_A	Mean "alveolar" partial pressure.
\dot{Q}	Pulmonary capillary blood flow.
\dot{Q}_s	Blood flow through right to left shunt.
\dot{Q}_t	Total pulmonary capillary blood flow.
R	Respiratory quotient. Gas constant (page 43).
S	Unit surface area of pulmonary capillary. Switch function defining stage 2 of respiratory cycle (page 80).
S_1	Switch function defining "phase 1" of respiratory cycle.
S_2	Switch function defining "phase 2" of respiratory cycle.
S_3	Switch function defining expiration.
S_c	Slope of dissociation curve relating concentration to partial pressure in pulmonary capillary blood.

Symbols Continued (Chapter 2/3)

S_P	Slope of dissociation curve relating concentration to partial pressure in pulmonary tissue.
t_E	Start of expiration.
t_I	Start of inspiration.
t_K	Transit time through individual pulmonary capillary.
T	Absolute temperature.
T_F	Transfer factor of lung.
$u(x,t)$	Velocity of gas flow in airways.
$u(t)$	Velocity of blood flow along pulmonary capillary.
V	Volume.
V_C	Volume of blood in pulmonary capillaries.
V_{CL}	Volume of blood in pulmonary capillaries.
V_D	Dead space volume.
V_{DALV}	Volume of "alveolar" dead space
V_{DANAT}	Volume of anatomical dead space.
$V_{DPHYSIOL}$	Volume of physiological dead space.
V_T	Tidal volume.
\dot{V}	Flow rate of gas.
\dot{V}_{CO_2}	Carbon dioxide transfer per unit time.
\dot{V}_{O_2}	Oxygen transfer per unit time.
$\dot{V}^1_{CO_2}$	Flux of carbon dioxide between lung tissue and alveolar gas in unit time.
\dot{V}_{CO_T}	Total amount of carbon monoxide transferred into blood in unit time.
w	Alveolar dilution ratio.
x	Thickness of pulmonary-capillary membrane. Alveolar-capillary membrane (page 88).
x^*	Boundary between inspired and alveolar gas.
y	For individual gas this equals $d_i \beta_i$.

Symbols Continued (Chapter 2/3)Greek Symbols.

α	Solubility of gas species. Coefficient for Taylor-Aris effective diffusion term (page 97).
β	Capacitance coefficient for gas species ($\Delta C/\Delta P$).
θ	Rate of formation of carboxyhaemoglobin per unit time per unit plasma tension.

Subscripts.

a	Arterial.
A	Alveolar Airway - referring to Area.
A_E	Alveolar (expired) (Applied to ventilation).
A_{eff}	Effective alveolar (refers to volume) (page 86).
A_I	Alveolar (inspired) (Applied to ventilation).
b	Blood.
B	At conditions of full saturation with water vapour at 37°C (refers to partial pressure).
C	Pulmonary capillary blood.
\bar{c}	For mean (partial pressure) in pulmonary capillaries.
D	Dead space gas.
DA	Refers to gas passing from dead space to alveoli during inspiration.
E	Expired gas.
\bar{E}	Mixed expired gas.
g	Gas.
i	Individual gas species.
I	Inspired gas.
$\cdot I$	Gas inspired into individual pulmonary unit.
IDEAL	Ideal compartment.
j	Individual pulmonary unit.

Symbols Continued (Chapters 2/3)

k	Individual pulmonary unit.
L	Lung.
m	Mouth.
P	Pulmonary tissue.
T	Tidal volume compartment. Total cross sectional - refers to airway area (page 94).
\bar{v}	Mixed venous.
x	Individual gas species.
(o)	Breath zero / or time zero $t = 0$.
(1)	Breath one.
(n)	Breath n.
1	Compartment 1.
2	Compartment 2.

Abbreviations for individual gases.

AR	Argon.
CO	Carbon monoxide.
CO ₂	Carbon dioxide.
HE	Helium.
H ₂ O	Water Vapour.
N ₂	Nitrogen.
O ₂	Oxygen.

CHAPTER 4

Many of the symbols which are used in this chapter are similar to those used in Chapters 2 and 3. Additional symbols, redefinition of symbols, subscripts are listed below.

C	Compliance of individual unit.
e	Error function.
$e(t, \underline{Q})$	Error function.
G(k)	Continuous weighting function.
J	Criterion function.
K	Turnover rate.
M	90% wash-out time.
q_i	Individual parameter.
\underline{Q}	Vector of parameters.
T	Time constant.
$X_{1/2}$	Half-time.
$y_m(t, \underline{Q})$	Model output.
$y_s(t)$	System output (measured).

Greek Symbols.

β	Rate constant.
ξ	Specific tidal volume.

Subscripts.

i	Single pulmonary unit.
---	------------------------

CHAPTER 5

Most symbols as in rest of thesis.

a_a	Intercept of linear relationship between CO_2 concentration and tension in arterial blood.
$a_{\bar{v}}$	Intercept of linear relationship between CO_2 concentration and tension in mixed venous blood.
\dot{M}	Metabolic production.
T	Duration of experiment.

Subscript TC is for tissue compartment.

APPENDIX 6. PROGRAMME FOR CONSTRUCTION OF \dot{V}/\dot{Q} LINE.

The listing of the principal subroutines of a programme for construction of the ventilation-perfusion line using the method which was described in Chapter 2.3(f). The programmes are written in Fortran but there are some non-standard features due to the programmes being written for the Egtran compiler. The main part of the programme (the listing for which is not given) carries out calculation of minute ventilation, oxygen uptake, etc. from measured input data.

The construction of the \dot{V}/\dot{Q} line is carried out in subroutine SVQ. In this form of the routine 150 points on the line are identified, 75 of these being spaced equally between $P_{\bar{V}}O_2$ and 110.0 (mmHg) and 75 between 110.0 and $P_I O_2$. Evaluation of the function whose root is sought is carried out in subroutine FUNCT. The subroutine SVQ includes facilities for obtaining the root by either bisection or regula falsi methods. Much of the initial part of this subroutine is to obviate the difficulty which is produced by the discontinuity in the function. The calculated values of \dot{V}_A/\dot{Q} , $P_A CO_2$, $C_C O_2$, $C_C CO_2$ along with $P_A O_2$ are stored in an array.

These values can be graphed subsequently if required. In this version of the routine the inspired PO_2 , PCO_2 are calculated to allow for the effects of rebreathing of dead space gas.

EGTRAN COMPILER MARK NO. 302 DATE 07/03/73 TIME

SUBROUTINE SVQ

```

DIMENSION V(7),Y(30),VQ(150,5)
PUBLIC VQ,VDANAT,VOLST,BLOG1,BLOG2,Y,V,11,0,CVC02,CV02,
1SHUNT,PA02, KK
EQUIVALENCE(VDS,VDANAT),(VDOT,VOLST),(M,I),(PAL,PA02)
1,(Y1,BLOG1),(Y2,BLOG2)
PRINT 101
101 FORMAT(3HSVQ)
PH1=Y(30)
PH2=Y(28)
PETC02=Y(9)*(V(4)-47.0)/100.0
IF(PETC02.LE.0.001)PETC02=Y(17)
PET02=Y(10)*(V(4)-47.0)/100.0
IF(PET02.LE.0.01)PET02=PAL
PI02=Y(2)*(V(4)-47.0)/100.0

```

C
C
C CALCULATE NUMBER OF BREATHS/MINUTE
C

NB=Y(4)/Y(5)

C
C CORRECT FOR DEADSPACE AND COMPUTE INSPIRED PCO2
C

PI02=(PI02*(VDOT-NB*VDS)+NB*VDS*PET02)/VDOT

PIC02=(NB*VDS*PETC02)/VDOT

WRITE(2,10)PI02,PIC02

10 FORMAT(6H PI02=,F7.3,10X,7H PIC02=,F7.3)

PVC02=(Y(21)+Y(24))/2.0

PV02=(Y(22)+Y(25))/2.0

K=2

STEP=(110.0-PV02)/75.0

PA02=PVC02

DO 100 KK=1,149

IF(PA02.GT.110.0)STEP=(PI02-110.0)/75.0

11 PA02=PA02+STEP

IF(PA02.GT.PI02)GOTO 150

A=PIC02

J=1

B=PVC02-3.0

C
C WE WILL TEST OUR UPPER STARTING VALUE FOR ROOT FINDING
C

C
C IF K IS 1 WE ARE USING A METHOD OF FALSE POSITION. IF K IS 2 WE ARE
C USING A METHOD OF BISECTION
C

C
C TEST THAT B IS NOT THE ROOT
C

CALL FUNCT(B,PA02,PH1,PH2,PI02,PIC02,AID)

FUNCTB=AID

BABS=ABS(FUNCTB)

IF(BABS.LT.0.0001)GO TO 28

C
C TEST TO SEE IF FUNCTION EVALUATED AT B IS POSITIVE
C

IF(FUNCTB.LT.0.001)GO TO 12

GO TO 14

C
C FUNCTION NOT POSITIVE, B INCREASED UNTIL IT IS POSITIVE
C

12 DO 13 I=1,300

B=B+0.1

CALL FUNCT(B,PA02,PH1,PH2,PI02,PIC02,AID)

FUNCTB=AID

C
C TEST THAT WE HAVE NOT HIT THE ROOT

BABS=ABS(FUNCTB)

IF(BABS.LT.0.0001)GO TO 28

```

IF(FUNCTB.GT.0.001)GO TO 16
13 CONTINUE
WRITE(2,450)B,FUNCTB
450 FORMAT(15H STEP UP FAILED,10X,2F10.3)
GO TO 90
C
C TEST THAT B IS NOT VERY LARGE
14 IF(FUNCTB.LT.150.0)GO TO 16
IF(K.EQ.2)GO TO 16
C
C FUNCTION POSITIVE AND LARGE ,B REDUCED UNTIL FUNCTION SMALLER
DO 18 I=1,200
B=B-0.1
CALL FUNCT(B,PA02,PH1,PH2,PI02,PICO2,AID)
FUNCTB=AID
C
C TEST THAT WE HAVE NOT HIT THE ROOT
BABS=ABS(FUNCTB)
IF(BABS.LT.0.0001)GO TO 28
C
IF(FUNCTB.LT.150.0)GO TO 17
C
18 CONTINUE
WRITE(2,7000)B,FUNCTB
7000 FORMAT(17H STEP DOWN FAILED,10X,2F10.3)
GO TO 90
17 IF(FUNCTB.GT.0.001) GO TO 16
TEST THAT WE HAVE NOT OVER-STEPPED
IF(FUNCTB.LT.-0.001)GO TO 35
16 CALL FUNCT(A,PA02,PH1,PH2,PI02,PICO2,AID)
FUNCTA=AID
21 X=FUNCTA*FUNCTB
IF(X.GT.0.0)GO TO 40
IF(K.EQ.2)GO TO 22
C=B-(B-A)*FUNCTB/(FUNCTB-FUNCTA)
GO TO 24
22 C=A+(B-A)/2.0
24 CALL FUNCT(C,PA02,PH1,PH2,PI02,PICO2,AID)
D=AID
F=ABS(D)
IF(F.LE.0.0001)GO TO 30
TEST=FUNCTA*D
IF(TEST.GT.0.0)A=C
IF(TEST.LT.0.0)B=C
IF(TEST.GT.0.0)FUNCTA=D
IF(TEST.LT.0.0)FUNCTB=D
J=J+1
IF(J.GT.250)GO TO 50
GO TO 21
28 PACO2=B
GO TO 32
30 PACO2=C
32 PHX=PH(PACO2,PH1,PH2,Y1,Y2)
CALCULATE CO2 AND O2 CONTENTS
C
C
NUM=1
CALL CONTO(PA02,PACO2,PHX,V(5),V(7),NUM,SATRN,VALUE)
SATO2=SATRN
CAO2=VALUE
NUM=0
CALL CONTO(PA02,PACO2,PHX,V(5),V(7),NUM,SATRN,VALUE)
CACO2=VALUE
A=8.63

```

C
C
C

```

COMPUTE V/Q
RVQ=A*((CVC02-CAC02)+(CA02-CV02)*(P1C02/P102))/(PAC02-PA02*P1C02/P
1102)
GO TO 80
35 WRITE(2,600)B,FUNCTB
600 FORMAT(31H OVER-STEPPED FUNCTION NEGATIVE,5X,2F10.4)
GO TO 90
40 WRITE(2,60) PA02
GO TO 90
50 WRITE(2,70) PA02
GO TO 90
60 FORMAT(10H ERROR 1 ,F7.3)
70 FORMAT(10H ERROR 2 ,F7.3)
80 WRITE(2,500)RVQ,PA02,PAC02,CA02,CAC02,KK,K,J
500 FORMAT(5X,5F10.4,4X,13,4X,11,18)
JL=KK+1
VQ(1,1)=0.0
VQ(1,4)=PV02
VQ(1,5)=PVC02
VQ(JL,1)=RVQ
VQ(JL,2)=CA02
VQ(JL,3)=CAC02
VQ(JL,4)=PA02
VQ(JL,5)=PAC02
90 CONTINUE
100 CONTINUE
150 CONTINUE
RETURN
END

```

```

EGTRAN COMPILER      MARK NO. 302      DATE 07/03/73
SUBROUTINE FUNC(Z,PA02,PH1,PH2,P102,P1C02,AID)
DIMENSION V(7),Y(30)
PUBLIC CVC02,CV02,BLOG1,BLOG2,Y,V,11
EQUIVALENCE(Y1,BLOG1),(Y2,BLOG2)
PHZ=PH(Z,PH1,PH2,Y1,Y2)
NUM=1
CALL CONTO(PA02,Z,PHZ,V(5),V(7),NUM,SATRN,VALUE)
SAT02=SATRN
CZ02=VALUE
NUM=0
CALL CONTO(PA02,Z,PHZ,V(5),V(7),NUM,SATRN,VALUE)
CZC02=VALUE
IF(CZ02-CV02.EQ.0.0) CZ02=CZ02+0.000001
R=(CVC02-CZC02)/(CZ02-CV02)
F1C02=P1C02/(V(4)-47.0)
F102=P102/(V(4)-47.0)
X=F1C02*(1.0-R)+R
IF(X.EQ.0.0)X=0.000001
AID=PA02-(R*P102-Z+P1C02+(Z*(1.0-R)*F102))/X
RETURN
END

```

EGTRAN COMPILER MARK NO. 302 DATE 07/03/73 TIME

```

C
C   SUBROUTINE CONTO(PCO2,PHX,HB,PCV,NUM,SATRN,VALUE)
C
C   THIS SUBROUTINE CONVERTS PO2 TO CONTENT IF NUM 1, OR PCO2 TO CONTENT IF
C   THE SATURATION IS RETURNED IN SATRN AND THE CONTENT IN VALUE
C   THE SUBROUTINE IS AN AMALGAMATION OF TWO SEPARATE FUNCTIONS ORIGINATED
C   BY KELMAN
C
  DIMENSION V(7)
  PUBLIC V
  TEMP=37.0
  A1=-8.532229E3
  A2=2.121401E3
  A3=-6.707399E1
  A4=9.359609E5
  A5=-3.134626E4
  A6=2.396167E3
  A7=-6.710441E1
10  X=PO2*10.0**((0.024*(37.0-TEMP)+0.40*(PHX-7.4)+0.06*(1.6021
  | -ALOG10(PCO2)))
  SATRN=100*(X*(X*(X*(X+A3)+A2)+A1))/(X*(X*(X*(X+A7)+A6)+A5)+A4)
15  IF(NUM.EQ.0)GO TO 20
  VALUE=(1.39*SATRN*HB)/100.0+0.003*PO2
  GO TO 30
20  P=7.4-PHX
  PK=6.086+0.042*P+(38.0-TEMP)*(0.00472+0.00139*P)
  TEMP=37.0-TEMP
  SOL=0.0307+0.00057*TEMP+0.00002*TEMP**2
  DOX=0.590+0.2913*P-0.0844*P**2
  DR=0.664+0.2275*P-0.0938*P**2
  D=DOX+(DR-DOX)*(1.0-SATRN/100.0)
  CP=SOL*PCO2*(1.0+10.0**((PHX-PK))
  CC=D*CP
  PCV2=PCV*0.01
  VALUE=(PCV2*CC+(1.0-PCV2)*CP)*2.22
30  RETURN
  END

```

APPENDIX 7.

List of equipment which has been used in these studies:-

Tissot Spirometer 100 litre recording spirometer.

Made by:- G.Plant & Son,
Harborne, Birmingham 17.
(No longer available).

Analogue Computers. TR20 and EAL 380.

Made by:- Electronic Associates Ltd.,
Victoria Road,
Burgess Hill, Sussex.

Pneumotachographs. Disposable Flowhead Type Fl.

Made by:- Mercury Electronics Ltd.,
Pollock Castle Estate,
Newton Mearns, Glasgow.

Micromanometers. Type MDC Range 0.5"Wg.

Made by:- Furness Controls Ltd.,
Beeching Road South,
Bexhill-on-sea, Sussex.

Tape Recorder. 8-channel Six-speed
FM and Digital Recorder
Type MR 1200.

Made by:- Epsylon Research & Development Co. Ltd.,
Central Way,
Feltham, Middlesex.

Schofander Micro Gas Analyser Type ES 34.

Made by:- W.G. Flaig & Sons Ltd.,
Exelo Works,
Margate Road,
Broadstairs, Kent.

Bicycle Ergometer Type AM 368.

Made by:- Elema-Shönander AB,
Stockholm, Sweden.

Lung Volume Spirometer.

Made by:- C.F.Palmer Ltd.,
High Wycombe,
Buckinghamshire.
(No longer available).

Mass Spectrometers.

(1) M.S.4

Made by:- A.E.I. Ltd.,
Manchester.

(2) Centronics MGA 007.

Made by:- 20th Century Electronics Ltd.,
New Addington,
Croydon.

Digital Computer.

PDP 11/45.

Made by:- Digital Equipment Company,
Maynard,
U.S.A.

APPENDIX 8 SOFTWARE FOR PRE-PROCESSING OF MEASURED DATA.

In this appendix programme listings are given for the Fortran programme to pre-process the experimental data (see Figure 3.13) The version of the programme shown here is specific to a data set in which only pCO_2 and ventilatory flow have been measured. Synchronisation of the data to compensate for the inherent time delay in the mass spectrometer is carried out in the data logging programme. The main programme - NSTCO2 - reads the data from the file which is created by the logging programme and stores the data in separate disc files related to each of the measured variables. The flow data are filtered and corrected to BTPS conditions. This programme has the facility for plotting the measured data (programme PLTDAT). In the routine NNORM the sample numbers associated with the start of each inspiration and expiration are determined and stored in a disc file (IBRB.DAT). The volume and minute ventilation of each breath are determined. The expired flow is normalised approximately by calculating a correction factor such that the total volume inspired during the experiment is equal to the total volume expired. The sample numbers associated with the start and end of the end-tidal section on each breath are calculated as described in the text and stored in the disc file (EBRB.DAT). The important general information about this data file are stored in the file INDX.DAT. The measured pCO_2 values are normalised to BTPS conditions using the routine NFILE.

```

C   NST002
C
C   DIMENSION IA(60), ICARB(60), IFLOW(60), NAME(3)
C   1, NTEMP(120)
C   BYTE DATE(9), DATEFIL(15)
C   COMMON/AREAR2/BAR, TEMP, FSRM, NCHAN, NAME, NSWI, NSAM, KB
C   COMMON/AREAR3/NREAD
C   DATA NOP, NIP, NPRIN/1, 1, 0/
C   KB=6
C
C***  READ IN NAME OF DATA FILE.
C   WRITE (6, 500)
C 500  FORMAT('0'/'#NAME OF DATA FILE (CSI FORMAT) ? ')
C   READ (6, 501) (DATEFIL(I), I=1, 14)
C 501  FORMAT(14R1)
C   DATEFIL(15)='0'
C   CALL ASSIGN(7, DATEFIL, 0, IERR1)
C   READ(7) (DATE(I), I=1, 9), BAR, TEMP, FSRM, NCHAN, (NAME(I), I=1, NCHAN)
C   1, NSWI, NSAM, FMM
C   PR20=1.42*TEMP-11.4
C SET UP CONSTANTS FOR FILTERING FLOW
C   P=EXP(-10.0/FSRM)
C   Q=1.0-P
C
C
C   WE SET UP FILES ON DISC
C
C   CALL SETFIL(1, 'FLOW.DAT', IER2, 'DC', 0, 0, "233, 2)
C   DEFINE FILE 1(120, 60, U, IVAR1)
C   CALL SETFIL(2, 'UCARB.TMP', IER5, 'DC', 0, 0, "233, 2)
C   DEFINE FILE 2(120, 60, U, IVAR5)
C
C WE READ JUST NUMBER OF DATA POINTS(NPTS) TO MAKE THIS MULTIPLE OF 60
C
C   NSAM1=NSAM
C 100  NPTS=NSAM*NCHAN
C   NPTS=NPTS-MOD(NPTS, 60)
C
C WE CALCULATE NUMBER OF RECORDS AND MAKE THIS MULTIPLE OF NCHAN
C
C   NREC=NPTS/60
C   NREC=NREC-MOD(NREC, NCHAN)
C   NREAD=NREC/NCHAN
C   NPTS=NREC*60
C   NSAM=NPTS/NCHAN
C   KILL=1
C
C
C
C WE READ DATA FROM DATA FILE IN BLOCKS OF NCHAN NUMBERS OF RECORDS
C AND BUILD UP TEMPORARY ARRAY
C
C   DO 240 JM=1, NREAD

```

```
DO 140 JK=1,NCHAN
  READ(7,ERR=767)(IA(I),I=1,60)
  KILL=KILL+1
  DO 130 JI=1,60
    J=JI+60*(JK-1)
130 NTEMP(J)=IA(JI)
140 CONTINUE
C
C WE BUILD UP ARRAYS "FLOW" ETC. FROM NTEMP
C
  J=1
  K=2
  DO 150 IN=1,60
    IFLOW(IN)=NTEMP(J)
    J=J+NCHAN
    ICARB(IN)=NTEMP(K)
150 K=K+NCHAN
C FILTER FLOW DATA
  DO 152 I=2,60
152 IFLOW(I)=IFIX(P+FLOAT(IFLOW(I-1))+Q+FLOAT(IFLOW(I)))
C
C WE NOW NORMALISE FLOW TO BTFS
  DO 154 I=1,60
154 IFLOW(I)=IFIX((FLOAT(IFLOW(I))*(BAR-PH20)+310.0)
  1/(BAR-47.0)+(273.0+TEMP)))
C
C WE NOW OUTPUT ARRAYS TO DISC
C
155 WRITE(1,IM)(IFLOW(L),L=1,60)
165 WRITE(2,IM)(ICARB(L),L=1,60)
240 CONTINUE
C
C WE NOW CLOSE THE FILES
C
  REWIND 7
  END FILE 7
  REWIND 1
  END FILE 1
  REWIND 2
  END FILE 2
230 CONTINUE
  WRITE(KB,332)
232 FORMAT('/#CHECK PRINT?')
  READ(KB,333)NCK
233 FORMAT(A2)
  IF(NCK.EQ.'YE')NPRIN=1
237 CONTINUE
  IF(NPRIN.NE.1)GO TO 241
  WRITE(S,329)(DATFIL(I),I=1,14)
229 FORMAT('0 FILE NAME ',3X,14A1/1X,28(' '))
241 CALL MNORM(FMX,NOP,NIP,NPRIN,DATFIL)
  IF(NOP.EQ.0.OR.NIP.EQ.0)GO TO 700
650 CONTINUE
  GO TO 770
700 CONTINUE
```

```

WRITE(KB, 704)
704 FORMAT('NEW RUN ?')
READ(KB, 333)NRUN
IF(NRUN.EQ.'NO')GO TO 707
CALL DELX(NOP, NIP, 0)
NPRIN=1
NIP=1
NOP=1
GO TO 337
707 CONTINUE
CALL DELX(NOP, NIP, 1)
750 WRITE(KB, 8004)
8004 FORMAT('DATA PLOT?')
READ(KB, 333)NPLOT
IF(NPLOT.NE.'YES')GO TO 770
CALL RUNX(OR, PLYDAT)
757 WRITE(S, 1)KILL NSAM1
1 FORMAT('FAILURE ON READ', I4, 'NSAM=', I6)
770 CONTINUE
END

```

SUBROUTINE DELX(NOP, NIP, INT)

REWIND 1

END FILE 1

REWIND 2

END FILE 2

CALL DELETE('DC:IBRS.DAT')

IF(INT.EQ.0)GO TO 5

CALL DELETE('DC:FLOW.DAT')

CALL DELETE('DC:UCRS.TMP')

5 IF(NIP.EQ.0)GO TO 10

REWIND 3

END FILE 3

CALL DELETE('DC:ESRS.DAT')

10 CONTINUE

RETURN

END

SUBROUTINE NNORM(FMX, NCP, NIP, NPRIN, DATFIL)

C
C

```

BYTE DATFIL(15)
REAL MINVEN
INTEGER EBR, TOTBR, RBR
DIMENSION EBR(50, 2), IER(50, 2), NAME(3), RBR(50, 2)
DIMENSION IHLP(20)
COMMON/AREP2/BR, TEMP, FSRM, NCHAN, NAME, NSWI, NSAM, KB
COMMON/AREP3/NREAD
DATA LP, FLMAX/5, 0, 0/
J=1
NC=0
LEWI=0
CONST=1. 0
SUM1=0. 0
SUM2=0. 0
IHEL=1
WRITE(6, 0)
8 FORMAT(' #THRESHOLD=? X, XX')
READ(6, 9) THRES
9 FORMAT(F4, 2)
IF(NPRIN, NE, 1)GO TO 15
WRITE(LP, 513)THRES
513 FORMAT(' THRESHOLD=', F4, 2, ' L/SEC')

```

C
C
C
C

WE OBTAIN SAMPLE NUMBER ASSOCIATED WITH START OF EACH BREATH

```

WRITE(LP, 10)
10 FORMAT(' @***BREATH NO. ***SAMPLE(INSP)***SAMPLE(EXP)***TIDAL VOL(IN
1SP)***MIN VEN***DUR. OF BREATH***' /1X, 12(' - '), 3X, 12(' - '), 3X, 11('
2 - '), 3X, 15(' - '), 3X, 8(' - '), 3X, 14(' - '))
15 CONTINUE
CALL SETFIL(1, 'FLOW.DAT', IERR, 'DC', 0)
DEFINE FILE1(7200, 1, U, IVARA)

```

C
C
C
C

NC IS ACTIVATOR AND IF 1 WE SEARCH FOR INSPIRATORY
THRESHOLD AND IF 0 WE LOOK FOR START OF EXPIRATION
CALCULATE THRESHOLD

```
ITHRES=IFIX(THRES*10000. 0/FMX)
```

C

```

DO 400 JK=1, NSAM
READ(1, JK)IFSAM
IF(IFSAM, LT, -ITHRES)NC=1
IF(NC, NE, 1)GO TO 400
IF(IFSAM, LT, ITHRES)GO TO 400

```

C
C
C

AT THIS POINT WE HAVE CROSSED THRESHOLD &BACKTRACK TO FIND ZERO

```

DO 300 L=1, 200
LB=JK-L
READ(1, LB)IFSAM

```

IN 005.13

00:44:34

13-AUG-76

PAGE

2

```

      IF(IFSAM.LE.0)GO TO 370
350 CONTINUE
C
C   AT THIS POINT WE HAVE FOUND START OF INSPIRATION
C   WE ENTER VALUE IN IER AND DEACTIVATE SEARCH UNTIL EXPIRATION.
C
370 IER(J,1)=LB
      J=J+1
      NC=0
400 CONTINUE
      TOTER =J-2
      CALL SETFIL(2,'IBR.DAT',IERB,'DC',0,0,'233,2')
      DEFINE FILE 2(50,2,U,IVRSS)
      KTOT=TOTER+1
      T=1.0/FSAM
C
C   WE NOW OBTAIN INSPIRED TIDAL VOLUMES
C
C
C
      DO 210 JZ=1,TOTER
        ISTART=IER(JZ,1)+1
        IEND=IER((JZ+1),1)
        VOL=0.0
        DO 200 LZ=ISTART,IEND
          MZ=LZ+1
          READ(1,LZ)IFSAM1
          READ(1,MZ)IFSAM2
          FLOW1=(FLOAT(IFSAM1)+FRK)/30000.0
          IF(FLOW1.GT.FLMAX)FLMAX=FLOW1
190  FLOW2=(FLOAT(IFSAM2)+FRK)/30000.0
          VOL=VOL+(FLOW1+FLOW2)*T/2.0
          IF(IFSAM2.LT.0)GO TO 202
200  CONTINUE
202  SUM1=SUM1+VOL
          VOL=VOL+1000.0
          IVOL=IFIX(VOL)
C
C   WE SET UP FIRST COL RBR FOR TIDAL VOL
C
210  RBR(JZ,1)=IVOL
C   SET UP SECOND COLUMN OF RBR FOR MINUTE VENTILATION
C
      DO 220 I=1,TOTER
        MINVEN=(FLOAT(RBR(I,1)))/((IBR((I+1),1)-IBR(I,1))*T)
1+00.0
        RBR(I,2)=IFIX(MINVEN/10.0)
220  CONTINUE
C
C
C   WE NOW OBTAIN START SAMPLE NUMBERS FOR EXPIRATION AND STORE IN
C   SECOND COL OF IER
C
C
      J=1
      NC=0

```

```

      ISTART=IBR(1,1)
      DO 250 JK=ISTART,NSAM
      READ(1,JK)IFSAM
      IF(IFSAM.GT.ITHRES)NC=1
      IF(NC.NE.1) GO TO 250
      IF(IFSAM.GT.-ITHRES)GO TO 250
      DO 230 L=1,200
      LB=JK-L
      READ(1,LB)IFSAM
      IF(IFSAM.GE.0)GO TO 240
230  CONTINUE
240  IBR(J,2)=LB
      J=J+1
      NC=0
250  CONTINUE
      DO 251 I=1,KTOT
251  WRITE(2,I)(IBR(I,J),J=1,2)

```

C
C
C
C

WE NOW CALCULATE EXPIRED VOLUMES AND THE TOTAL EXPIRED VOLUME

```

252  DO 300 JZ=1,TOTBR
      ISTART=IBR(JZ,2)+1
      IEND=IBR(JZ+1,2)
      IF(JZ.EQ.TOTBR)IEND=NSAM
      VOL=0.0
      DO 260 LZ=ISTART,IEND
      MZ=LZ+1
      READ(1,LZ)IFSAM1
      READ(1,MZ)IFSAM2
      FLOW1=(FLOAT(IFSAM1)+FMX)*CONST/30000.0
      IF(ABS(FLOW1).GT.FLMAX)FLMAX=ABS(FLOW1)
      FLOW2=(FLOAT(IFSAM2)+FMX)*CONST/30000.0
      VOL=VOL-(FLOW1+FLOW2)*T/2.0
      IF(LSWI.EQ.1)GO TO 254
      IF(IFSAM2.GT.0)GO TO 280
      GO TO 260
254  IF(LZ.EQ.IEND.OR.IFSAM2.GT.0)GO TO 422
      IF(VOL.LT.EVST)GO TO 260
      EBR(JZ,1)=LZ

```

C
C
C
C

WE HAVE FOUND WHERE DEAD SPACE HAS BEEN EXPIRED AND LOOK FOR END OF END TIDAL SECTION

```

      DO 255 MN=LZ,IEND
      READ(1,MN)IFSAM
      IF(IFSAM.GT.-300)GO TO 258
      IF(MN.GE.IEND)GO TO 1198
255  CONTINUE
258  EBR(JZ,2)=MN-4
      GO TO 300
260  CONTINUE
280  SUM2=SUM2+VOL
      VOL=VOL+1000.0
      IVOL=IFIX(VOL)
      DUER=(FLOAT(EBR(JZ+1,1))-FLOAT(EBR(JZ,1)))*T

```

```

TV=FLOAT(BBR(JZ,1))/1000.0
VEN=FLOAT(BBR(JZ,2))/100.0
IF(VEN.GT.3.0)GO TO 290
NIP=0
IHELP(IHEL)=JZ
IHEL=IHEL+1
WRITE(KB,287)JZ
287 FORMAT('0MIN. VENTILATION LESS THAN 3.0L ON BREATH ',I4)
290 IF(NPRIN.NE.1)GO TO 300
WRITE(LP,13)JZ,IBR(JZ,1),IBR(JZ,2),TV,VEN,DUBR
13 FORMAT(' ',6X,I2,10X,I4,11X,I4,9X,F5,3,13X,F5,2,9X,F4,1)
300 CONTINUE
IF(NIP.EQ.1)GO TO 319
JAND=IHEL-1
DO 316 I=1,JAND
WRITE(LP,313)
313 FORMAT('1FLOW DATA FOR CHECKING THRESHOLD LEVEL'/1X,38(' '))
WRITE(LP,314)IHELP(I)
314 FORMAT('0BREATH NUMBER',4X,I4)
JON=IBR(IHEL(I),1)-15
JUN=IBR(IHEL(I),1)+15
DO 318 JIN=JON,JUN
READ(1,JIN)IFSAM
FLOW=(FLOAT(IFSAM)+FMX)*CONST/30000.0
WRITE(LP,315)JIN,FLOW
315 FORMAT(' SAMPLE NUMBER=',I5,10X,'FLOW=',F6,3)
IF(JIN.NE.IBR(IHEL(I),1))GO TO 316
WRITE(LP,3437)
3437 FORMAT(' ',15(' '),10(' '),15(' '))
316 CONTINUE
GO TO 300
319 CONTINUE
IF(LSWI.EQ.1)GO TO 428
C
C WE OBTAIN APPROXIMATE CALIBRATING FACTOR FOR EXPIRED
C PNEUMOTACHOGRAPH FROM COMP. OF INSP. & EXP. VOLS.
C
CONST=SUM1/SUM2
LSWI=1
C
C IF FLOW IS PRESENT IN INPUT WE OBTAIN SAMPLE NUMBERS FOR END
C TIDAL SAMPLES
C IF(NPRIN.NE.1)GO TO 75
C
WRITE(LP,70)
70 FORMAT('1 ',24X,'+++END TIDAL SECTIONS+++'/,25X,24(' '))
WRITE(LP,90)
90 FORMAT('0 BREATH NUMBER',3X,' START SAMPLE PARTIAL PRESSURE END
1 SAMPLE PARTIAL PRESSURE')
75 CONTINUE
CALL SETFIL(3,'EBRS.DAT',IERZ,'DO',0.0,"233,2)
DEFINE FILE 3/50,2,U,IVRRZ)
WRITE(KB,1000)
1000 FORMAT('ENTER VOLUME OF EXP. FOR END TIDAL (X.XXX) = ')
1010 READ(KB,1010)EVET
1010 FORMAT(F5,3)

```

N VGS 13 00:44:24 12-AUG-76 PAGE 5

```

C
C   GO TO 252
C
C   ERROR MESSAGES FROM FAILURES IN END TIDAL SECTION
C
C   422 CONTINUE
C     WRITE(KB, 4000)JZ
C   4000 FORMAT('0CALCULATED EXPIRED VOLUME LESS THAN TWICE DEAD SPACE ON
C     1BREATH', I3)
C     NOP=0
C     GO TO 800
C
C
C   1198 WRITE(KB, 1200)JZ
C   1200 FORMAT('0NO STRAT OF EXPIRATION FOUND ON BREATH', I3)
C     NOP=0
C     GO TO 800
C   428 CONTINUE
C
C
C   WE NOW OUTPUT EBR TO DISC
C
C     DO 429 I=1, TOTBR
C   429 WRITE(2, I)(EBR(I, K), K=1, 2)
C     REWIND 1
C     REWIND 2
C     REWIND 3
C     END FILE 1
C     END FILE 2
C     END FILE 3
C
C
C   430 CONTINUE
C   WE NORMALISE ALL CHANNELS TO STPS
C
C   CARBON DIOXIDE SECTION
C     IF(NPRIN, NE, 1)GO TO 433
C
C     WRITE(LP, 3001)
C   3001 FORMAT('0CARBON DIOXIDE', /, 14(' '))
C   433 CONTINUE
C     CALL SETFIL(2, 'UCARB, TMP', IERI, 'DC', 0)
C     DEFINE FILE 2(120, 50, U, IVAR1)
C     CALL SETFIL(3, 'CARB, DAT', IERJ, 'DC', 0, 0, '233, 2')
C     DEFINE FILE 3(120, 50, U, IVARJ)
C     CALL MFILE(NREAD, BAR, 400, 0, TOTBR, EBR, NPRIN)
C     CALL DELETE('0C:UCARB, TMP')
C   550 CALL SETFIL(8, 'INDX, DAT', IERU, 'DC', 0)
C     WRITE(8)BAR, TEMP, PSAM, NCHAN, (NAME(I), I=1, NCHAN), NSWI, NSAM, TOTBR,
C     1FLMAX, (DATEIL(I), I=1, 15)
C
C     REWIND 9
C     END FILE 9
C
C
C   OUTPUT EBR TO DISC
C     CALL SETFIL(1, 'EBR, DAT', IERY, 'DC', 0, 0, '233, 2')

```

M 986.12

88.44.34

13-AUG-76

PAGE

```
DEFINE FILE 1(50, 2, U, IVARY)
00 750 I=1, TOTSR
750 WRITE(1, I) (RBR(I, K), K=1, 2)
REWIND 1
END FILE 1
800 CONTINUE
RETURN
END
```

I 005. 13

00:49:20 13-AUG-76 PAGE 1

```

SUBROUTINE NFILF(NRERO, BAR, CORR, TOTBR, EBR, NPRIN)
INTEGER TOTBR, EBR
DIMENSION NWAT(60), NGRS(60), NEWG(60), WAT(60), GASNEW(60), GAS(60)
DIMENSION EBR(50, 2)
LP=5
DO 20 I=1, NRERO
  READ(2, I) (NGRS(L), L=1, 60)
  DO 15 JK=1, 60
    GAS(JK)=FLOAT(NGRS(JK))/CORR
    GASNEW(JK)=(BAR-47. 0)/BAR+GAS(JK)
15  NEWG(JK)=IFIX(GASNEW(JK)+CORR)
20  WRITE(3, I) (NEWG(L), L=1, 60)
  DO 30 I=1, TOTBR
    LREM1=MOD(EBR(I, 1), 50)
    LREM2=MOD(EBR(I, 2), 60)
    NREC1=(EBR(I, 1)-LREM1)/50+1
    NREC2=(EBR(I, 2)-LREM2)/60+1
    IF(LREM1 NE. 0)GO TO 22
    LREM1=50
    NREC1=NREC1-1
    GO TO 24
22  IF(LREM2 NE. 0)GO TO 24
    LREM2=60
    NREC2=NREC2-1
24  READ(3, NREC1) (NGRS(L), L=1, 60)
    READ(3, NREC2) (NEWG(L), L=1, 60)
    GAS1=FLOAT(NGRS(LREM1))/CORR
    GAS2=FLOAT(NEWG(LREM2))/CORR
25  FORMAT(' ', 5X, I3, 11X, I5, 10X, F4, 1, ' (MM. HG. )', 7X, I5, 7X, F4, 1, ' (MM. HG
1. )')
    IF(NPRIN NE. 1)GO TO 35
30  WRITE(LP, 25) I, EBR(I, 1), GAS1, EBR(I, 2), GAS2
35  CONTINUE
    REWIND 2

```

```

0024          REWIND 3
0035          END FILE 2
0036          ENDFILE 3
0037          RETURN
0038          END

```

APPENDIX 9. PARAMETER ESTIMATION METHODS.

Parameter estimation methods work by proceeding in an iterative manner improving the estimates of the parameters at each step. The improvement is such that the error criterion function is reduced. Thus at any step a new estimate of parameters (\underline{a}_{k+1}) is obtained from the old estimate (\underline{a}_k):

$$\underline{a}_{k+1} = \underline{a}_k + \lambda_k \underline{d}_k$$

when \underline{d}_k represents the direction in which the parameters are changed and λ_k the distance or amount by which they are changed. \underline{a}_k etc are vectors and contain elements therefore of all the parameters to be estimated.

In order to implement parameter estimation methods it is necessary to scale the parameters so that they are numerically similar. This is achieved for any single parameter α by the relationship

$$\alpha_{SC} = \frac{\alpha - \alpha_{\min}}{\alpha_{\max} - \alpha_{\min}}$$

where α_{SC} is the scaled version of α which is an element in the vector \underline{a} . α_{\min} and α_{\max} are the minimum and maximum possible value of the parameter as determined in this case by physiological considerations.

There are two main methods used in this thesis. The first of these (the Rosenbrock method³⁸⁷) is a direct search method. The method operates by taking step lengths $\Delta S_1, \Delta S_2, \dots, \Delta S_n$ along each of a set of n orthonormal direction vectors $\underline{S}_1, \underline{S}_2, \dots, \underline{S}_n$ in turn. (The initial choice of these vectors is the "coordinate" vectors for the multidimensional parameter space). From the initial estimate of parameters \underline{a}_0 a new estimate is obtained (\underline{a}_1) where

$$\underline{a}_1 = \underline{a}_0 + \Delta S_1 \underline{S}_1$$

If the error function at \underline{a}_1 is less than at \underline{a}_0 the new estimate of \underline{a}_1 is retained and the step is termed a success. On the next search along this direction the size of the step is increased such that

$$(\Delta S_1)_{\text{new}} = 3.0 \Delta S_1$$

However, if the error is greater, \underline{a}_1 is rejected and the step is termed a failure. On the next search in this direction the size of the step length is reduced, i.e.

$$(\Delta S_1)_{\text{new}} = 0.5 \Delta S_1$$

This process is repeated until there are consecutive failures in all n directions.

At this point a new estimate of parameters is current $(\underline{a})_{\text{new}}$. A new set of n "axes" are calculated centred on this point. The first of these corresponds to the direction between the initial \underline{a} and $(\underline{a})_{\text{new}}$. This set of "axes"-orthonormal vectors - are obtained using the Gram-Schmidt orthonormalisation relationships, details of which are found in textbooks of linear algebra.

The second method which has been used is the Davidon-Fletcher-Powell method.^{388,389} This method is a gradient method and calculates the new direction of search from knowledge of the gradient of the error surface at any step. The mathematical details of the method are based on Taylor series expansion for a function of several variables.

For a function of several variables $(a_1 - a_n)$

$$J(\underline{a} + \underline{\Delta a}) = J(\underline{a}) + \sum_{j=1}^n h_j \left(\frac{\partial J}{\partial a_j} \right)_a + \frac{1}{2} \sum_{j=1}^n \sum_{k=1}^n h_j h_k \left(\frac{\partial^2 J}{\partial a_j \partial a_k} \right) \dots$$

$$\text{where } \underline{\Delta a} = (h_1 - h_n)$$

In matrix notation

$$J(\underline{a} + \underline{\Delta a}) = J(\underline{a}) + \underline{g}^T \underline{\Delta a} + \frac{1}{2} \underline{\Delta a}^T \underline{H} \underline{\Delta a} \dots$$

where \underline{g} is the gradient vector and \underline{H} the Hessian matrix of second derivatives.

For a quadratic function in which \underline{H} is constant at all points on the surface it can be shown that

$$\underline{\Delta a} = - \underline{H}^{-1} (\underline{a}) \underline{g}(\underline{a})$$

Applying this result leads to a procedure of the form

$$\underline{a}_{k+1} = \underline{a}_k - \lambda_k \underline{H}_k^{-1} \underline{g}_k$$

where the value of λ_k is determined by searching according to a suitable algorithm along the direction $-\underline{H}_k^{-1} \underline{g}_k$ for a minimum.

Clearly in this method the inverse of the matrix of second derivatives \underline{H}^{-1} has to be obtained. In the Davidon-Fletcher-Powell method an iterative procedure is developed in which an improved approximation to \underline{H}^{-1} is obtained at each iteration.

APPENDIX 10 COMPARTMENTAL ANALYSIS OF \dot{V}/\dot{Q} DISTRIBUTION.

This appendix describes the method of analysis of ventilation-perfusion distribution which is based on the model structure shown in Figure 2.7.

For both oxygen and carbon dioxide the arterial blood composition can be considered to consist of three components, i.e. from the right to left shunt, from compartment one, and from compartment 2.

i.e.

$$\begin{aligned}\dot{Q}_1 C_1 \text{CO}_2 + \dot{Q}_2 C_2 \text{CO}_2 &= \dot{Q} C_a \text{CO}_2 - \dot{Q}_s C_v \text{CO}_2 \\ \dot{Q}_1 C_1 \text{O}_2 + \dot{Q}_2 C_2 \text{O}_2 &= \dot{Q} C_a \text{O}_2 - \dot{Q}_s C_v \text{O}_2\end{aligned}$$

where C is the concentration of oxygen or carbon dioxide and \dot{Q} is blood flow. Subscripts refer to compartment 1(1) compartment 2(2) the right to left shunt (S) arterial blood (a), and mixed venous blood (\bar{v}). The quantities on the right hand side of these equations can be measured directly. (In the example shown in Figure 2.8 \dot{Q} was measured by the dye dilution method, \dot{Q}_s assumed to be 3% of cardiac output, and $P_a \text{O}_2$, $P_a \text{CO}_2$ measured simultaneously. By converting $P_a \text{O}_2$, $P_a \text{CO}_2$ into the corresponding concentrations ($C_a \text{O}_2$, $C_a \text{CO}_2$) using the standard computer subroutines,^{147, 148} $C_v \text{O}_2$ and $C_v \text{CO}_2$ can be calculated by application of the Fick principle since $\dot{V} \text{O}_2$ and $\dot{V} \text{CO}_2$ were also measured).

Thus

$$\begin{aligned}\dot{Q}_1 C_1 \text{CO}_2 + \dot{Q}_2 C_2 \text{CO}_2 &= K_1 \\ \dot{Q}_1 C_1 \text{O}_2 + \dot{Q}_2 C_2 \text{O}_2 &= K_2\end{aligned}$$

where K_1 and K_2 are known.

If arbitrary values are assigned to the ventilation perfusion ratio of the two compartments (\dot{V}_1/\dot{Q}_1 and \dot{V}_2/\dot{Q}_2 , $\dot{V}_1/\dot{Q}_1 < 1.0$, and $\dot{V}_2/\dot{Q}_2 > 1.0$) $C_1 \text{CO}_2$, $C_1 \text{O}_2$, $C_2 \text{CO}_2$ and $C_2 \text{O}_2$ can be obtained from the

ventilation-perfusion line for that subject. The equations can then be solved to yield \dot{Q}_1 and \dot{Q}_2 . \dot{V}_1 and \dot{V}_2 can also be obtained since the ventilation-perfusion ratios of two compartments are known.

It must be the case however that

$$\dot{Q}_1 + \dot{Q}_2 = \dot{Q} - \dot{Q}_s$$

and

$$\dot{V}_1 + \dot{V}_2 = \dot{V}$$

Where \dot{V} is the measured total ventilation of the two compartments.

Thus two error functions can be defined:-

$$e_1 = (\dot{Q} - \dot{Q}_1 - \dot{Q}_2 - \dot{Q}_s)$$

and

$$e_2 = (\dot{V} - \dot{V}_1 - \dot{V}_2)$$

By evaluating the two error functions with large numbers of values of \dot{V}_1/\dot{Q}_1 and \dot{V}_2/\dot{Q}_2 it is found that for low values of \dot{V}_1/\dot{Q}_1 minima in e_1 and e_2 can be demonstrated. These minima are small and are either zero or close to zero. The minima do not occur however at the same value of \dot{V}_2/\dot{Q}_2 . By increasing \dot{V}_1/\dot{Q}_1 a point is reached at which the minimum in each of the error functions is at the same value for \dot{V}_2/\dot{Q}_2 . This is taken to be the solution. For higher values of \dot{V}_1/\dot{Q}_1 one or other of the error functions does not show a distinct minimum, i.e. with values on either side of a minimum.

REFERENCES

REFERENCES

1. LEVINE, G., E., Housley, P. MacLeod, P.T. Macklem (1970).
Gas exchange abnormalities in mild bronchitis and asymptomatic asthma.
New Eng. J. Med., 282: 1277 - 1282.
2. MORAN, F., A.R., Lorimer, G. Boyd, R.J. Mils, (1968)
Alveolar and blood gas relationships during hyperventilation in emphysema and bronchitis (P).
Thorax, 23: 569
3. JONES, N.L. (1966)
Pulmonary gas exchange during exercise in patients with chronic airway obstruction.
Clin. Sci., 31: 39-50.
4. PACK, A.I., D.J. Murray-Smith (1972).
Mathematical models and their applications in medicine.
Scot. Med. J., 17: 401-409.
5. MILLER, B.F., A.W. Winkler (1968).
The renal excretion of endogenous creatinine in man. Comparison with exogenous creatinine and inulin.
J. Clin. Invest., 17: 31-40.
6. STEINITZ, K., H. Türkand, (1940).
The determination of the glomerular filtration rate by the endogenous creatinine clearance.
J. Clin. Invest., 19: 285-298.
7. BROD, J., J.H. Sirota, (1948).
The renal clearance of endogenous "creatinine" in man.
J. Clin. Invest., 27: 645-654.
8. CAMARA, A.A., K.D. Arn, A. Reimer, L.H. Newburgh (1951).
The twenty-four hourly endogenous creatinine clearance as a clinical measure of the functional state of the kidneys.
J. Lab. Clin. Med. 37: 743-763.
9. GUSTAVSSON, I. (1973).
Survey of applications of identification in chemical and physical processes in Identification and System Parameter Estimation, Eykhoff, P. (Editor), North Holland Publishing Co., American Elsevier Publishing Co.
10. OLSSON, G. (1973).
Modelling and identification of nuclear power reactor dynamics from multivariable experiments, in Identification and System Parameter Estimation. Eykhoff, P. (Editor) North Holland Publishing Co., American Elsevier Publishing Co.

11. FUJIHARA, Y., J.R. Hildebrandt, J. Hildebrandt. (1973).
Cardiorespiratory transients in exercising man. I. Tests of
superposition.
J. Appl. Physiol. 35: 58-67.
12. LI, C.C., J. Urquhart (1969).
Modelling of adrenocortical secretory dynamics. in Concepts
and Models of Biomathematics. Heinmets, F. (Editor)
Marcel Dekker Inc., New York.
13. CARSON, E.R., L. Finkelstein. (1973).
Problems of identification in metabolic systems. in Identification
of System Parameter Estimation. Eykhoff, P. (Editor). North
Holland Publishing Co., American Elsevier Publishing Co.
14. BENEKEN, J.E.W. (1965).
A mathematical approach to cardiovascular function.
Ph.D. Thesis, Institute of Medical Physics, Utrecht, Netherlands.
15. BENEKEN, J.E.W., B. de Wit (1967).
A physical approach to haemodynamic aspects of the human
cardiovascular system. in Physical Bases of Circulatory Transport,
pg. 1-45. (Ed) Reeve, E.B., Guyton, A.C. (Saunders, W.B., Philadelphia.)
16. BENEKEN, J.E.W., V.C. Rideout (1968).
Use of multiple models in cardiovascular system studies:
Transport and perturbation methods.
IEEE Trans. Bio-Med. Eng. 15: 281-289.
17. DICK, D.E. (1968).
A hybrid computer study of major transients in the canine
cardiovascular system.
Ph.D. Dissertation, University of Wisconsin, Madison.
18. DONDERS, J.J.H., J.E.W. Beneken (1971).
Computer model of cardiac muscle mechanics.
Cardiovasc. Res. Suppl. 1: 34-50.
19. GRODINS, F.S. (1959).
Integrative cardiovascular physiology: A mathematical synthesis
of cardiac and blood vessel hemodynamics.
Quart. Rev. Biol. 34: 93-116.
20. GUYTON, A.C., T.G. Coleman, H.J. Granger (1972).
Circulation: Overall Regulation.
Annual Reviews of Physiology, 34: 13-46.
21. McLEOD, J. (1966).
PHYSBE, a physiological simulation benchmark experiment.
Simulation, 7: 324-329.

22. MORENO, A.H., A.I. Katz, L.D. Gold. (1969).
An integrated approach to the study of the venous system with steps towards a detailed model of the dynamics of venous return to the right heart.
IEEE Trans. Bio-Med. Eng. 16: 308-324.
23. PICKERING, W.D., P.N. Nikiforuk, J.E. Merriman. (1969).
Analogue computer model of the human cardiovascular control system.
Medical and Biological Engineering, 7: 401-410.
24. SIMS, J.B. (1970).
A hybrid computer-aided study of parameter estimation in the systemic circulation system.
Ph.D. Dissertation, University of Wisconsin, Madison.
25. SIMS, J.B. (1972).
Estimation of arterial system parameters from dynamic records.
Computer & Biomed. Res., 5: 131-147.
26. SYNDER, M.F. (1969).
Hybrid computer simulation of the human systemic venous system.
Ph.D. Dissertation, University of Wisconsin, Madison.
27. SYNDER, M.F., V.C. Rideout. (1969).
Computer simulation studies of the venous circulation.
IEEE Trans. Bio-Med. Eng. 16: 325-334.
28. WARNER, H.R. (1962).
Use of analogue computers in the study of control mechanisms in the circulation.
Fed. Proc. 21: 87-91.
29. WESSELING, K.H., B. de Wit, J.E.W. Beneken. (1973).
Arterial haemodynamic parameters derived from non-invasively recorded pulse waves, using parameter estimation.
Med. Biol. Eng. 11: 724-731.
30. COLLINS, R.E., R.W. Kilpper, D.E. Jenkins, (1967).
A mathematical analysis of mechanical factors in the forced expiration.
Bull. Math. Biophys. 29: 737-752.
31. JACKSON, A.C., H.T. Milhorn, Jnr. (1973).
Digital computer simulation of respiratory mechanics.
Comput. & Biomed. Res. 6: 27-56.
32. JODAT, R.W., J.D. Horgan, R.L. Lange. (1966).
Simulation of respiratory mechanics.
Biophys. J. 6: 773-785.

33. SHEEHAN, R.M. (1969).
A "sluice" model of the circulation in lungs with shunts.
Comput. & Biomed. Res. 2: 385-410.
34. FRY, D.L. (1968).
A preliminary model for simulating the aerodynamics of the
bronchial tree.
Comput. & Biomed. Res. 2: 111-134.
35. PEDLEY, T.J., M.F. Sudlow, J. Milic-Emili. (1972).
A non-linear theory of the distribution of pulmonary
ventilation.
Resp. Physiol. 15: 1-38.
36. LONGOBARDO, G.S., N.S. Cherniack, I. Staw. (1967).
Transients in carbon dioxide stores.
IEEE Trans. Bio-Med. Engr. 14: 182-191.
37. TRUEB, T.J., N.S. Cherniack, A.F. D'Souza, A.P. Fishman (1971).
A mathematical model of the controlled plant of the respiratory
system.
Biophys. J. 11: 810-834.
38. MAPELSON, W.W. (1964).
Inert gas-exchange theory using an electric analogue.
J. Appl. Physiol. 19: 1193-1199.
39. MAPELSON, W.W. (1973).
Circulation-time models of the uptake of inhaled anaesthetics
and data for quantifying them.
Brit. J. Anaesth. 45: 319-333.
40. ZWART, A., N.Ty Smith, J.E.W. Beneken. (1972).
Multiple model approach to uptake and distribution of
halothane. The use of an analog computer.
Comput. & Biomed. Res. 5: 228-238.
41. COWLES, AL., H.H. Borgstedt, A.J. Gillies. (1973).
A simplified digital method for predicting anaesthetic
uptake and distribution.
Comput. Biol. Med., 3: 385-395.
42. DEFARES, J.G., H.E. Derksen, J.W. Duyff. (1960).
Cerebral blood flow in the regulation of respiration.
Acta. Physiol. Pharmacol. Neerl. 9: 327-360.
43. DUFFIN, J. (1972).
A mathematical model of the chemoreflex control of ventilation.
Respir. Physiol. 15: 277-301.
44. GRODINS, F.S., J.S. Gray, K.R. Schroeder, A.L. Norins, R.W. Jones.
(1954).
Respiratory responses to CO₂ inhalation. A theoretical study
of a non-linear biological regulator.
J. Appl. Physiol. 7: 283-308.

45. GRODINS, F.S., G. James (1963).
Mathematical models of respiratory regulation.
Ann. N.Y. Acad. Sci. 109: 852-868.
46. GRODINS, F.S., J. Buell, A.J. Bart (1967).
Mathematical analysis and digital simulation of the respiratory control system.
J. Appl. Physiol. 22: 260-276.
47. LONGOBARDO, G.S., N.S. Cherniack, A.P. Fishman (1966).
Cheyne-Stokes breathing produced by a model of the human respiratory system.
J. Appl. Physiol. 21: 1839-1846.
48. MILHORN, H.T.Jr., R. Benton, R. Ross, A.C. Guyton (1965).
A mathematical model of the human respiratory control system.
Biophys. J. 5: 27-46.
49. MILHORN, H.T. Jr., W.J. Reynolds, G.H. Holloman, Jr. (1972).
Digital simulation of the ventilatory response to CO₂ inhalation and CSF perfusion.
Comput. & Biomed. Res. 5: 301-314.
50. ABBRECHT, P.H., N.W. Prodanly (1971).
A model of the patient-artificial kidney system.
IEEE Trans. Bio-Med. Engr. 18: 257-264.
51. BIGELOW, J.H., J.C. de Haven, M.L. Shapley (1973).
Systems analysis of the renal function.
J. Theoret. Biol. 41: 287-322.
52. CANTRAINED, F.R.L., P. Bergmann, M. Geens, A. Lenaers, K. Jank, H. Cleempoel (1972).
A new model for quantitative description of the nephrogram.
Comput. Biomed. Res. 5: 41-58.
53. DEEN, W.M., C.R. Robertson, B.M. Brenner (1972).
A model of glomerular ultrafiltration in the rat.
Amer. J. Physiol. 223: 1178-1183.
54. FURUKAWA, T., S. Takasugi, M. Inoue, H. Inada, F. Kajiya, H. Abe (1974).
A digital computer model of the renal medullary counter-current system.
Comput. & Biomed. Res. 7: 213-229.
55. JACQUEZ, J.A., B. Carnahan, P. Abbrecht. (1967).
A model of the renal cortex and medulla.
Math. Biosci. 1: 227-261.

56. KELMAN, R.B. (1962).
A theoretical note on exponential flow in the proximal part of the mammalian nephron.
Bull. Math. Biophys. 24: 303-317.
57. MERLETTI, R. (1972).
Computer simulation and analysis of the physiology and pathology of the body fluids and comparison of results with physiological data.
Ph.D. Dissertation, The Ohio State University.
58. MERLETTI, R., H.R.Weed, S.A.Garson, (1973).
Analysis and simulation of renal function. In Regulation and Control in Physiological Systems, pg. 442-449.
Ed. A.S. Iberall, A.C. Guyton, Instrument Society of America, Pittsburgh.
59. ACKERMAN, E., L.C. Gatewood, J.W. Rosevear, G.D. Molnar (1965).
Model studies of blood-glucose regulation.
Bull. Math. Biophys. (Special Issue) 27: 21-36.
60. ATKINS, G.L. (1971).
Investigation of some theoretical models relating the concentrations of glucose and insulin in plasma.
J. Theoret. Biol. 32: 471-494.
61. BERMAN, M., E. Hoff, M. Barandes, D.V.Becker, M. Sonnenberg, R. Benua, D.A. Koutras (1968).
Iodine Kinetics in man - a model.
J. Clin. Endocr. Metab. 28: 1 - 14.
62. CARSON, E.R., L. Finkelstein (1970).
Dynamics and control of chemical processes in man.
Measurement and Control 3: T157-T167.
63. CERASI, E. (1971).
An analogue computer model for the insulin response to glucose infusion.
Simulation 16/17: 243-255.
64. CHARETTE, W.P., A.H. Kadish, R.Sridhar (1969).
Modelling and control aspects of glucose homeostasis. In Hormone Control Systems. Ed. E. B.Stear, A.H. Kadish.
Math. Biosci. Supplement 1: 115-149.
65. DANZIGER, L., G.L. Elmergreen (1957).
Mathematical models of endocrine systems.
Bull. Math. Biophys. 19: 9-18.
66. DISTEFANO, J.J. (1969).
A model of the normal thyroid hormone glandular secretion mechanism.
J. Theoret. Biol. 22: 412 -417.

67. DISTEFANO, J.J., R.F. Chang (1971).
Computer simulation of thyroid hormone binding, distribution,
and disposal dynamics in man.
Amer. J. Physiol. 221: 1529-1544.
68. FOSTER, R.O. (1970).
Dynamics of blood sugar regulation.
M.Sc. Thesis, Massachusetts and Institute of Technology.
69. GATEWOOD, L.C., E. Acherman, J.W., Rosevear, G.D. Molnar,
T.W. Burns (1968).
Tests of a mathematical model of the blood-glucose regulatory
system.
Comput. & Biomed. Res. 2: 1-14.
70. GATEWOOD, L.D., E. Acherman, J.W. Rosevear, G.D. Molnar (1968).
Simulation studies of blood-glucose regulation: effect of
intestinal glucose absorption.
Comput. & Biomed. Res. 2: 15-27.
71. GRODSKY, G.M. (1972).
A threshold distribution hypothesis for packet storage of
insulin and its mathematical modelling.
J. Clin. Invest. 51: 2047-2059.
72. MATTHEWS, C.M.E. (1957).
Theory of tracer experiments with ¹³¹I labelled plasma proteins.
Phys. Med. Biol. 2: 36-53.
73. ROSTON, S. (1959).
Mathematical representation of some endocrinological systems.
Bull. Math. Biophys. 21: 271-282.
74. SCRINIVASAN, R., A.H. Kadish, R. Sridhar (1970).
A mathematical model for the control mechanism of free fatty
acid-glucose metabolism in normal humans.
Comput. & Biomed. Res. 3: 146-165.
75. COBELL, C. (1975).
Modeling, identification and parameter estimation of bilirubin
kinetics in normal, haemolytic and Gilbert's states.
Comput. & Biomed. Res. 8: 522-537.
76. THOMPSON, H.E., J.D. Horgan, E. Delfs (1969).
A simplified mathematical model and simulations of hypophysis-ovarian
endocrine control system.
Biophys. J. 9: 278-291.
77. URQUHART, J., C.C.Li (1969).
Dynamic testing and modeling of the adrenocortical secretory
function.
Ann. N.Y. Acad. Sci. 156: 756-778.

78. YATES, F.E., R.D. Brennan (1969).
Study of the mammalian adrenal glucocorticoid system by computer simulation.
In Hormone Control System, Ed. E.B. Stear, A.H. Kadish., Math. Biosci. Supplement 1: 20-87.
79. GARFINKEL, D. (1971).
Simulation of the Krebs cycle and closely related metabolism in perfused rat liver. I. Construction of a model.
Computers & Biomed. Res. 4: 1-17.
80. GARFINKEL, D. (1971).
Simulation of the Krebs cycle and closely related metabolism in perfused rat liver. II. Properties of the model.
Comput.&Biomed. Res. 4: 18-42.
81. ACHS, M.J., J.H. Anderson, D. Garfinkel (1971).
Gluconeogenesis in rat liver cytosol. I. Computer analysis of experimental data.
Comput.&Biomed. Res. 4: 65-106.
82. ANDERSON, J.H., M.J.Achs, D. Garfinkel (1971).
Gluconeogenesis in rat liver cytosol. II. Computer simulation of control properties.
Comput.&Biomed. Res. 4: 107-125.
83. GARFINKEL, D. (1969).
Simulation of glycolytic systems. In Concepts and Models of Biomathematics. Ed. F. Heinmets, pg. 1-74.
Marcel Dekker, Inc., New York.
84. GARFINKEL, D. (1968).
A machine-independent language for the simulation of complex chemical and biological systems.
Comput.&Biomed. Res. 2: 31-44.
85. DEFARES, J.G., I.N. Sneddon (1973).
An Introduction to the Mathematics of Medicine and Biology (2nd Edition).
North Holland Publishing Company, Amsterdam, London.
86. ATKINS, G.L. (1969).
Multi-compartment Models for Biological Systems.
Methuen, London.
87. BERMAN, M. (1963).
Formulation and testing of Models.
Ann. N.Y. Acad. Sci. 108: 182-194.

88. BELLMAN, R., K.J. Astron (1970).
On structural identifiability.
Math. Biosci. 7: 329-339.
89. BLESSER, W.B. (1969).
A Systems Approach to Biomedicine.
McGraw Hill Book Company, New York, London.
90. CLYNES, M. (Editor) (1969).
Rein control, or unidirectional rate sensitivity, a
fundamental dynamic and organising function in biology.
Ann. N.Y. Acad. Sci. 156: 627-968.
91. GRODINS, F.S. (1963).
Control Theory and Biological Systems.
Columbia University Press, New York.
92. HEINMETS, F. (Editor) (1969).
Concepts and Models of Biomathematics.
Marcel Dekker, Inc., New York.
93. MESAROVIC, M.D. (Editor) (1968).
Systems Theory and Biology.
Springer, Berlin.
94. MILHORN, H.T. Jr. (1966).
Applications of Control Theory to Physiological Systems.
Saunders, Philadelphia.
95. MILSUM, J.H. (1966).
Biological Control Systems Analysis.
McGraw-Hill, New York.
96. RIGGS, D.S. (1963).
The Mathematical Approach to Physiological Problems.
Williams and Wilkins, Baltimore.
97. RIGGS, D.S. (1970).
Control Theory and Physiological Feedback Mechanisms.
Williams and Wilkins, Baltimore.
98. ROBERTSON, J.S. (1957).
Theory and use of tracers in determining transfer rates
in biological systems.
Physiol. Rev. 37: 133-154.
99. STEAR, E.B., KADISH, A.H. (Editors) (1969).
Hormonal control systems.
Math. Biosci. Suppl. 1.
100. YAMAMOTO, W.S., RAUB, W.F. (1967).
Models of the regulation of external respiration in mammals.
Problems and promises.
Comput. & Biomed. Res. 1: 65-104.

101. IBERALL, A.S., Guyton, A.C. (Editors) (1973).
Regulation and Control in Physiological Systems.
Instrument Society of America, Pittsburgh.
102. BEKEY, G.A. (1973).
Parameter estimation in biological systems: a survey
in Identification and Systems Parameter Estimation.
Editor P. Eykhoff, North Holland Publishing Company -
American Elsevier Publishing Co.
103. JOHNSON, L.E. (1974).
Computers, models and optimisation in physiological
kinetics.
CRC Critical Reviews in Bioengineering (February) 2: 1-37.
104. TOATES, F. (1975).
Control Theory in Biology and Experimental Psychology.
Hutchison Educational, London.
105. BEKEY, G.A., Karplus, W.J. (1968).
Hybrid Computation.
John Wiley & Sons, Inc., New York, London.
106. DORN, W.S., McCracken, D.D. (1972).
Numerical Methods with Fortran IV Case Studies.
John Wiley & Sons, Inc., New York, London.
107. SPECKHART, F.H., Green, W.L. (1976).
A guide to using C.S.M.P.
Prentice-Hall, Inc., Englewood Cliffs, N.J.
108. COULAM, C.M., Warner, H.R. Marshall, H.W., Bassingthwaighte, J.B.
(1967).
A steady-state transfer function analysis of portions of the
circulatory system using indicator dilution techniques.
Comput. & Biomed. Res. 1: 124-138.
109. SUGA, H., Oshima, M. (1971).
Measurement of the transfer function of the carotid sinus
pressure control system with its feedback loop physiologically
closed.
Med. & Biol. Engineering 9: 147-150.
110. BJURSTEDT, H., Karlsson, H., Linnarsson, D., Wigertz, O. (1970).
Pulmonary capillary-to-radial artery transfer functions as
estimated in man during rest and exercise.
Report. Lab. Aviat. Naval Med., Karol. Inst., Stockholm. (Aug).
111. WIGERTZ, O. (1971).
Dynamics of respiratory and circulatory adaptation to muscular
exercise in man. A systems analysis approach.
Acta. Physiol. Scand. (Supplement). No. 363.

112. ÅSTRÖM, K.J., Eykhoff, P. (1971).
System identification - a survey.
Automatica 7: 123-162.
113. EYKHOFF, P. (1974).
System Identification
J. Wiley and Sons, Ltd., London.
114. GRAUPE, D. (1972).
Identification of Systems.
Van Nostrand Reinhold Co., New York.
115. PRIBAN, I.P. (1963).
An analysis of some short-term patterns of breathing in man
at rest.
J. Physiol. 166: 425-434.
116. PAPPENHEIMER, J. et al. (1950).
Standardisation of definitions and symbols in respiratory
physiology.
Fed. Proc. 9: 602-605.
117. PIIPER, J., Dejours, P., Haab, P., Rahn, H. (1971).
Concepts and basic quantities in gas exchange physiology.
Resp. Physiol. 13: 292-304.
118. FICK, A. (1870).
Ueber die Messung des Blutquantums in den Hertzventrikeln. S.B.
Phys. Med. Ges. Wurzburg, 16-17.
119. DUDKA, L.T., Inglis, H.J., Johnson, R.E., Pehinski, K.M.,
Plowman, S. (1971).
Inequality of inspired and expired gaseous nitrogen in man.
Nature 232: 265-267.
120. COSTA, G. (1960).
Hypothetical pathway of nitrogen metabolism.
Nature, 188: 549-552.
121. COSTA, G., Ullrich, L., Kantor, F., Holland, J.F. (1968).
Production of elemental nitrogen by certain mammals including man.
Nature 218: 546-551.
122. CISSIK, J.H., Johnson, R.E., Rokosch, D.K. (1972).
Production of gaseous nitrogen in human steady-state conditions.
J. Appl. Physiol. 32: 155-159.
123. CISSIK, J.H., Johnson, R.E., Hertig, B.A. (1972).
Production of gaseous nitrogen during human steady state exercise.
(Abstract) Physiologist 15: 108.

124. CISSIK, J.H., Johnson, R.E. (1972).
Myth of nitrogen equality in respiration: its history and implications.
Aerospace Med. 43: 755 - 758.
125. CISSIK, J.H., Johnson, R.E. (1972).
Regression analysis for steady-state N₂ inequality in O₂ consumption calculations.
Aerospace Med. 43: 589-591.
126. MUYSERS, K. (1970).
Gibt es eine Stickstoffabgabe über die menschliche Lunge?
Pflugers Arch. 317: 157 - 172.
127. FOX, E.L. Bowers, R.W. (1973).
Steady-state equality of respiratory gaseous N₂ in resting man.
J. Appl. Physiol. 35: 143-144.
128. HERRON, J.M., Saltzman, H.A., Hills, B.A., Kylstra, J.A. (1973).
Differences between inspired and expired minute volumes of nitrogen in man.
J. Appl. Physiol. 35: 546-551.
129. WILMORE, J.H., Costill, D.L. (1973).
Adequacy of the Haldane transformation in the computation of exercise VO₂ in man.
J. Appl. Physiol. 35: 85-89.
130. BOHR, C. (1891).
Ueber die Lungenathmung.
Skand. Arch. Physiol. 2: 236-268.
131. NUNN, J.F. (1971).
Applied Respiratory Physiology with Special Reference to Anaesthesia.
Butterworths, London.
132. OLSZOWKA, A.J., Farhi, L.E. (1969).
A digital computer program for constructing ventilation-perfusion lines.
J. Appl. Physiol. 26: 141 - 146.
133. HILLS, B.A. (1974).
Gas transfer in the lung.
Cambridge University Press.
134. WEST, J.B., Hugh-Jones, P. (1959).
Patterns of gas flow in the upper bronchial tree.
J. Appl. Physiol. 14: 753-759.
135. SCHROTER, R.C. Sudlow, M.F. (1969).
Flow patterns in models of the human bronchial airways.
Resp. Physiol. 7: 341-355.

136. WEIBEL, E.R. (1963).
Morphometry of the human lung.
Springer, Berlin.
137. HORSFIELD, K., Cumming, G. (1968).
Morphology of the bronchial tree in man.
J. Appl. Physiol. 24: 373-383.
138. HORSFIELD, K., Cumming, G. (1968).
Functional consequences of airway morphology.
J. Appl. Physiol. 24: 384-390.
139. SAFFMAN, P.G. et al. (1969).
General discussion. A mathematical treatment of dispersion in
flow through a branching tree. in Circulatory and Respiratory
Mass Transport, Ciba Foundation Symposium., J. & A. Churchill Ltd.
London.
140. CHANG, H.K., Tai, R.C., Farhi, L.E. (1975).
Some implications of ternary diffusion in the lung.
Resp. Physiol. 23: 109-120.
141. BOHR, C. (1919).
Ueber die spezifische Tätigkeit der Lungen bei der respiratorischen
Gasaufnahme und ihr Verhalten zu der durch die
Alveolarwand stattfindenden Gasdiffusion.
Skand. Arch. Physiol. 22: 221-280.
142. FORSTER, R.E. (1957).
Exchange of gases between alveolar air and pulmonary capillary
blood: pulmonary diffusing capacity.
Physiol. Rev. 37: 391-452.
143. BATES, D.V., Macklem, P.T., Christie, R.V. (1971).
Respiratory Function in Disease.
W.B. Saunders, Co. Philadelphia/London/Toronto.
144. COTES, J.E. (1975).
Lung Function Assessment and Application in Medicine.
3rd Edition. Blackwell Scientific Publications, Oxford.
145. ROUGHTON, F.J.W. (1945).
Kinetics of the reaction $\text{CO} + \text{O}_2\text{Hb} \rightleftharpoons \text{O}_2 + \text{COHb}$ in human blood at
body temperature.
Amer. J. Physiol. 143: 609-620.
146. ROUGHTON, F.J.W., Forster, R.E. (1957).
Relative importance of diffusion and chemical reaction rates
in determining rate of exchange of gases in the human lung,
with special reference to true diffusing capacity of pulmonary
membrane and volume of blood in the lung capillaries.
J. Appl. Physiol. 11: 290-302.

147. KELMAN, G.R. (1967).
Digital computer procedure for conversion of $p\text{CO}_2$ into blood CO_2 content.
Respir. Physiol. 3: 111-115.
148. KELMAN, G.R. (1966).
Digital computer subroutine for the conversion of oxygen tension into saturation.
J. Appl. Physiol. 21: 1375-1376.
149. RAHN, H., Fenn, W.O. (1955).
A Graphical Analysis of the Respiratory Gas Exchange.
Am. Physiol. Soc., Washington.
150. OTIS, A.B. (1964).
Quantitative relationships in steady-state gas exchange.
in Handbook of Physiology. Section 3: Respiration.
Editors, W.O. Fenn & H. Rahn.
151. RAHN, H. (1949).
A concept of mean alveolar air and the ventilation-bloodflow relationships during gas exchange.
Amer. J. Physiol. 158: 21-30.
152. RILEY, R.L., Cournand, A. (1949).
'Ideal' alveolar air and analysis of ventilation-perfusion relationships in the lungs.
J. Appl. Physiol. 1: 825-847.
153. WEST, J.B. (1965).
Ventilation/Blood Flow and Gas Exchange.
Blackwell Scientific Publications, Oxford.
154. KELMAN, G.R. (1968).
Computer program for the production of O_2 - CO_2 diagrams.
Resp. Physiol. 4: 260-269.
155. PACK, A.I., Emery, B., Moran, F. Murray-Smith, D.J. (1974).
Computer models of gas exchange processes in pulmonary ventilation. in Ventilatory and Phonatory Control Systems.
Editor, B. Wyke, Oxford University Press, London.
156. HAMMING, R.W. (1971).
Introduction to Applied Numerical Analysis.
McGraw-Hill Book Co., New York.
157. WEST, J.B. (1969).
Ventilation-perfusion inequality and overall gas exchange in computer models of the lung.
Respir. Physiol. 7: 88-110.

158. ROSS, B.B., Farhi, L.E. (1960).
Dead-space ventilation as a determinant in the ventilation-perfusion concept.
J. Appl. Physiol. 15: 363-371.
159. HENDERSON, R., Horsfield, K., Cumming, G. (1968/69).
Intersegmental collateral ventilation in the human lung.
Resp. Physiol. 6: 128-134.
160. LINKSKOG, G.E., Bradshaw, H.H. (1934).
Collateral respiration: the chemical composition and volume of the collaterally respired gases.
Am. J. Physiol. 108: 581-592.
161. FLENLEY, D.C., Welchel, L., Macklem, P.T. (1972).
Factors affecting gas exchange by collateral ventilation in the dog.
Resp. Physiol. 15: 52-69.
162. MACKLEM, P.T. (1971).
Airway obstruction and collateral ventilation.
Physiol. Rev. 51: 368-436.
163. WEST, J.B. (1971).
Gas exchange when one lung region inspires from another.
J. Appl. Physiol. 30: 479-487.
164. RILEY, R.L., Cournand, A. (1951).
Analysis of factors affecting partial pressures of oxygen and carbon dioxide in gas and blood of lungs: theory.
J. Appl. Physiol. 4: 77-101.
165. FARHI, L.E. (1966).
Ventilation-perfusion relationship and its role in alveolar gas exchange. in *Advances in Respiratory Physiology*.
Editor: C.G. Caro. Edward Arnold (Publishers) Ltd., London.
166. WORKMAN, J.M., Penman, R.W.B., Bromberger-Barnea, B., Permutt, S., Riley, R.L. (1965).
Alveolar dead space, alveolar shunt, and transpulmonary pressure.
J. Appl. Physiol. 20: 816-824.
167. KELMAN, G.R. (1972).
Errors in Riley analysis.
Brit. J. Anaesth. 44: 433-436.
168. MORAN, F., Pack, A.I. (1973).
Measurement of ventilation-perfusion distribution.
Proc. Roy. Soc. Med. 66: 975-977.
169. FARHI, L.E. (1967).
Elimination of inert gas by the lung.
Resp. Physiol. 3: 1-11.

170. YOKOYAMA, T., Farhi, L.E. (1967).
Study of ventilation-perfusion ratio distribution in the anesthetized dog by multiple inert gas washout.
Resp. Physiol. 3: 166-176.
171. WAGNER, P.D., Saltzman, H.A., West, J.B. (1974).
Measurement of continuous distributions of ventilation-perfusion ratios: theory.
J. Appl. Physiol. 36: 588-599.
172. THAM, M.K. (1975).
Letter to Editor. J. Appl. Physiol. 38: 950.
173. TEPLICK, R., Snider, M.T. (1975).
Letter to Editor. J. Appl. Physiol. 38: 951-952.
174. OLSZOWKA, A.J. (1975).
Can \dot{V}_A/\dot{Q} distributions in the lung be recovered from inert gas retention data.
Resp. Physiol. 25: 191-198.
175. PIIPER, J. (1961).
Variations of ventilation and diffusing capacity to perfusion determining the alveolar-arterial O_2 difference: theory.
J. Appl. Physiol. 16: 507-516.
176. PIIPER, J. (1961).
Unequal distribution of pulmonary diffusing capacity and the alveolar-arterial pO_2 differences: theory.
J. Appl. Physiol. 16: 493-498.
177. FORSTER, R.E., Fowler, W.S., Bates, D.V. (1954).
Considerations on the uptake of carbon monoxide by the lungs.
J. Clin. Invest. 33: 1128-1134.
178. PIIPER, J., Sikand, R.S. (1966).
Determination of D_{CO} by the single breath method in inhomogeneous lungs: theory.
Resp. Physiol. 1: 75-87.
179. STAUB, N.C. (1963).
Alveolar-arterial oxygen tension gradient due to diffusion.
J. Appl. Physiol. 18: 673-680.
180. JOHNSON, R.L., Miller, J.M. (1968).
Distribution of ventilation, blood flow, and gas transfer coefficients in the lung.
J. Appl. Physiol. 25: 1-15.
181. PIIPER, J. (1969).
Apparent increase of the O_2 diffusing capacity with increased O_2 uptake in inhomogeneous lungs: theory.
Resp. Physiol. 6: 209-218.

182. CHINET, A., Micheli, J.L., Haab, P. (1971).
Inhomogeneity effects on O₂ and CO pulmonary diffusing capacity estimates by steady-state methods. Theory. Resp. Physiol. 13: 1-22.
183. PIIPER, J., Canfield, R.E., Rahn, H. (1962).
Absorption of various inert gases from subcutaneous gas pockets in rats. J. Appl. Physiol. 17: 268-274.
184. DARLING, R.C., Cournand, A., Richards, D.W. Jr. (1944).
Studies on the intrapulmonary mixture of gases V. Forms of inadequate ventilation in normal and emphysematous lungs, analysed by means of breathing pure oxygen. J. Clin. Invest. 23: 55-67.
185. ROBERTSON, J.S., Siri, W.E., Jones, H.B. (1950).
Lung ventilation patterns determined by analysis of nitrogen elimination rates: use of the mass spectrometer as a continuous gas analyser. J. Clin. Invest. 29: 577-590.
186. MALONEY, J.C. (1971).
A new non-invasive technique for estimation of cardiac output from respiratory models and measurement. Ph.D. Thesis, University of California.
187. KROGH, M. (1915).
Diffusion of gases through the lungs of man. J. Physiol. 49: 271-300.
188. FORSTER, R.E., Fowler, W.S., Bates, D.V. and Van Lingen, B. (1954).
The absorption of carbon monoxide by the lungs during breathholding. J. Clin. Invest. 33: 1135-1145.
189. FORSTER, R.E., Cohn, J.E., Briscoe, W.A., Blakemore, W.S., Riley, R.L. (1955).
A modification of the Krogh carbon monoxide breathholding technique for estimating the diffusing capacity of the lung: a comparison with three other methods. J. Clin. Invest. 34: 1417-1426.
190. OGILVIE, C.M., Forster, R.E., Blakemore, W.S., Morton, J.W. (1957).
A standardised breath holding technique for the clinical measurement of the diffusing capacity of the lung for carbon monoxide. J. Clin. Invest. 36: 1-17.
191. JONES, R.S., Meade, F. (1961).
A theoretical and experimental analysis of anomalies in the estimation of pulmonary diffusing capacity by the single breath method. Quart. J. Exp. Physiol. 46: 131-143.

192. FILLEY, G.F., Bigelow, D.B., Olson, D.E. Lacquet, L.M. (1968).
Pulmonary gas transport. A mathematical model of the lung.
Amer. Rev. Resp. Dis. 98: 480- 489.
193. OKUBO, T., Piiper, J. (1974).
Intrapulmonary gas mixing in excised dog lung lobes studied
by simultaneous washout of two inert gases.
Resp. Physiol. 21: 223-239.
194. SACKNER, M.A., Feisal, K.A., Dubois, A.B. (1964).
Determination of tissue volume and carbon dioxide
dissociation slope of the lungs in man.
J. Appl. Physiol. 19_ 374-380.
195. CHILTON, A.B., Stacy, R.W. (1952).
A mathematical analysis of carbon dioxide respiration in man.
Bull. Math. Biophys. 14: 1-18.
196. CHILTON, A.B., Barth, D.S., Stacy, R.W. (1954).
A mathematical analysis of oxygen respiration in man.
Bull. Math. Biophys. 16: 1-14.
197. DUBOIS, A.B., Britt, A.G., Fenn, W.O. (1952).
Alveolar CO₂ during the respiratory cycle.
J. Appl. Physiol. 4: 535- 548.
198. YAMAMOTO, W.S. (1960).
Mathematical analysis of the time course of alveolar CO₂.
J. Appl. Physiol. 15: 215-219.
199. NYE, R.E. Jr. (1970).
Influence of the cyclical pattern of ventilatory flow on
pulmonary gas exchange.
Resp. Physiol. 10 321-337.
200. MURPHY, T.W. (1966).
Rand Corp. Memo. RM-4833-NIM.
201. MURPHY, T.W. (1969).
Modeling of lung gas exchange - mathematical models of the
lung: the Bohr model, static, and dynamic approaches.
Math. Biosciences. 5: 427-447.
202. FLUMERFELT, R.W., Crandall, E.D. (1968).
An analysis of external respiration in man.
Math. Biosciences, 3: 205-230.
203. LIN, K.H., Shir, C.C. (1974).
A numerical model of oxygen uptake in the human lung during a
respiratory cycle.
Math. Biosciences. 19:319-342.

204. HLASTALA, M.P. (1972).
A model of fluctuating alveolar gas exchange during the respiratory cycle.
Resp. Physiol. 15: 214-232.
205. SUWA, K., Bendixen, H.H. (1972).
Pulmonary gas exchange in a tidally ventilated single alveolus model.
J. Appl. Physiol. 32: 834-841.
206. MEADE, F., Pearl, N., Saunders, M.J. (1967).
Distribution of lung function (\dot{V}_A/\dot{Q}) in normal subjects deduced from changes in alveolar gas tensions during expiration.
Scand. J. Res. Dis. 48: 354-365.
207. YAMAMOTO, W., Hori, T. (1971).
Phasic air movement model of respiratory regulation of carbon dioxide balance.
Comput. Biomed. Res. 3: 699-717.
208. LIN, K.H., Cumming, G. (1973).
A model of time-varying gas exchange in the human lung during a respiratory cycle at rest.
Resp. Physiol. 17: 93-112.
209. WILSON, T.A., Lin, K.H. (1970).
Convection and diffusion in the airways and the design of the bronchial tree. in Airway Dynamics, Edited by A. Bouhuys, Charles C. Thomas, Springfield, Illinois, U.S.A.
210. RAUWERDA, P.E. (1946).
Unequal ventilation of different parts of the lung and determination of cardiac output.
Thesis. Gronigen State University, Netherlands.
211. WEIBEL, E.R. (1963).
Morphometry of the Human Lung.
Springer, Berlin.
212. CUMMING, G., Crank, J., Horsfield, K., Parker, I. (1966).
Gaseous diffusion in the airways of the human lung.
Resp. Physiol. 1: 58-74.
213. LaFORCE, R.C., Lewis, B.M. (1970).
Diffusional transport in the human lung.
J. Appl. Physiol. 28: 291-298.
214. CUMMING, G., Horsfield, K., Preston, S.B. (1971).
Diffusion equilibrium in the lung examined by nodal analysis.
Resp. Physiol. 12: 329-345.

215. PAIVA, M. (1973).
Gas transport in the human lung.
J. Appl. Physiol. 35: 401-410.
216. BAKER, L.G., Ultman, J.S., Rhoades, R.A. (1974).
Simultaneous gas flow and diffusion in a symmetric airway system: a mathematical model.
Resp. Physiol. 21: 119-138.
217. TAYLOR, G. (1953).
Dispersion of soluble matter in solvent flowing slowly through a tube.
Proc. Roy. Soc. London, Ser. A. 219: 186-203.
218. ARIS, R. (1956).
On the dispersion of a solute in a fluid flowing through a tube.
Proc. Roy. Soc. London, Ser. A. 235: 67-77.
219. FLINT, L.F., Eisenklam, P. (1970).
Dispersion of matter in transitional flow through straight tubes.
Proc. Roy. Soc., London. Ser. A. 315: 519-533.
220. GILL, W.N., Sankarasubramanian, R. (1970).
Exact analysis of unsteady convective diffusion.
Proc. Roy. Soc. London, Ser. A. 316: 341-350.
221. GILL, W.N., Sankarasubramanian, R. (1971).
Dispersion of a non-uniform slug in time-dependent flow.
Proc. Roy. Soc. London, Ser. A. 322: 101-117.
222. PEDLEY, T.J. (1970).
A theory for gas mixing in a simple model of the lung.
AGARD Conference No. 65 (NATO). (Paper 27).
223. DAVIDSON, M.R. (1973).
Flow and oxygen transport in lung airways.
Ph.D. Thesis, University of Queensland, Australia.
224. CHANG, H.K., Farhi, L.E. (1973).
On mathematical analysis of gas transport in the lung.
Resp. Physiol. 18: 370-385.
- 225a. ENGEL, L.A., Menkes, H., Wood, L.D.H., Utz, G., Joubert, J., Macklem, P.T. (1973).
Gas mixing during breath holding studied by intrapulmonary gas sampling.
J. Appl. Physiol. 35: 9-17.

- 225b. ENGEL, L.A. Wood, L.D.H., Utz, G., Macklem, P.T. (1973).
Gas mixing during inspiration.
J. Appl. Physiol. 35: 18-24.
226. CHANG, H.K., Cheng, R.T., FARHI, L.E. (1973).
A model study of gas diffusion in alveolar sacs.
Resp. Physiol. 18: 386-397.
227. PAIVA, M. (1974).
Gaseous diffusion in an alveolar duct simulated by a digital computer.
Computers and Biomedical Research. 7: 533-543.
228. DAVIDSON, M.R., Fitzgerald, J.M. (1972).
Flow patterns in models of small airway units of the lung.
J. Fluid. Mech. 52: 161-177.
229. HUGHES, J.M.B., Hoppin, F.G., Mead, J. (1972).
Effect of lung inflation on bronchial length and diameter in excised lungs.
J. Appl. Physiol. 32: 25-35.
230. MARSHALL, R., Holden, W.S. (1963).
Changes in calibre of the smaller airways in man.
Thorax, 18: 54-58.
231. GILL, W.M., Ananthakrishnan, V., Nunge, R.J. (1968).
Dispersion in developing velocity fields.
AICHE J. 14: 939-946.
232. CHATWIN, P.C. (1970).
The approach to normality of the concentration distribution of a solute in a solvent flowing along a straight pipe.
J. Fluid. Mech. 43: 321-352.
233. SCHERER, P.W., Shendalman, L.H., Greene, N.M., Bouhuys, A. (1975).
Measurement of axial diffusivities in a model of the bronchial airways.
J. Appl. Physiol. 38: 719-723.
234. CRANDALL, E.D., Flumerfelt, R.W. (1967).
Effects of time-varying blood flow on oxygen uptake in the pulmonary capillaries.
J. Appl. Physiol. 23: 944-953.
235. STAUB, N.C., Bishop, J.M. Forster, R.E. (1962).
Importance of diffusion and chemical reaction rates in O_2 uptake in the lung.
J. Appl. Physiol. 17: 21-27.
236. VISSER, B.F., Maas, A.H.J. (1959).
Pulmonary diffusion of oxygen.
Phys. Med. Biol. 3: 264-272.

237. MILHORN, H.T.Jr., Pulley, P.E.Jr. (1968).
A theoretical study of pulmonary capillary gas exchange and venous admixture.
Biophys. J. 8: 337-357.
238. HIASTALA, M.P. (1973).
Significance of the Bohr and Haldane effects in the pulmonary capillary.
Resp. Physiol. 17: 81-92.
239. WAGNER, P.D., West, J.B. (1972).
Effects of diffusion impairment on O₂ and CO₂ time courses in pulmonary capillaries.
J. Appl. Physiol. 33: 62-71.
240. BOHR, C. (1909).
Über die spezifische Tätigkeit der Lungen bei der Respiratorischen Gasaufnahme und ihr Verhalten zu der durch die Alveolarwand stattfindenden.
Gasdiffusion. Scand. Arch. Physiol. 22: 221-280.
241. FARHI, L.E., Riley, R.L. (1957).
Graphic analysis of moment-to-moment changes in blood passing through the pulmonary capillary, including a demonstration of three graphic methods for estimating the mean alveolar-capillary diffusion gradient (Bohr integration).
J. Appl. Physiol. 10: 179-185.
242. BRIEHL, R.S. Fishman, A.P. (1960).
Principles of the Bohr integration procedure and their application to measurement of diffusing capacity of the lung for oxygen.
J. Appl. Physiol. 15: 337-348.
243. CUMMING, G., Jones, J.G. (1966).
The construction and repeatability of lung nitrogen clearance curves.
Resp. Physiol. 1: 238-248.
244. LEEMING, M.N., Howland, W.S. (1969).
Time delay technique in respiratory instrumentation.
Resp. Physiol. 7: 399-402.
245. HOLST, P.A. (1969).
Pade approximations and analog simulations of time delays.
Simulation 12/13: 277-290.
246. GREEN, I.D., NESARAJAH, M.S. (1968).
Water vapor pressure of end-tidal air of normals and chronic bronchitics.
J. Appl. Physiol. 24: 229-231.

247. FOWLER, K.T. (1969).
The respiratory mass spectrometer.
Phys. Med. Biol. 14: 185-199.
248. SCHEID, P.H., SLAMA, H., PIIPER, J. (1971).
Electronic compensation of the effects of water vapor in
respiratory mass spectrometry.
J. Appl. Physiol. 30: 258-260.
249. DAVIES, E.E., HAHN, H.L. SPIRO, S.G., EDWARDS, R.H.T. (1974).
A new technique for recording respiratory transients at the
start of exercise.
Resp. Physiol. 20: 69-79.
250. LOGAN, I. and Pack, A. (1976).
A software system including graphics for on-line mass
spectrometer experiments. (In preparation).
251. MARTIN, C.J., TSUNODA, S., YOUNG, A.C. (1974).
Lung emptying in diffuse obstructive pulmonary syndromes.
Resp. Physiol. 21: 157-168.
252. FOWLER, W.S. (1951).
Intrapulmonary distribution of inspired gas.
Physiol. Review. 32: 1 - 20.
253. BOUHUYS, A. & LUNDIN, G. (1959).
Distribution of inspired gas in lungs.
Physiol. Rev. 39: 731-750.
254. BOUHUYS, A. (1964).
Distribution of inspired gases in the lungs. in Handbook
of Physiology, Section 3. Respiration.
Edited by W.O. Fenn and H. Rahn,
American Physiological Society, Washington, D.C.
255. DARLING, R.C., COURNAND, A., RICHARDS, D.W. Jr. (1940).
Studies on the intrapulmonary mixture of gases. III. An open
circuit method for measuring residual air.
J. Clin. Invest. 19: 609 - 618.
256. COMROE, J.H., Jr., & FOWLER, W.S. (1951).
Lung function studies. VI. Detection of uneven alveolar
ventilation during a single breath of oxygen.
Amer. J. Med. 10: 408-413.
257. HICKAM, J.B., BLAIR, E. & FRAYSER, R. (1954).
An open-circuit helium method for measuring functional residual
capacity and defective intrapulmonary gas mixing.
J. Clin. Invest. 33: 1277-1286.

258. BARGER, A.C., RICHARDSON, G.S. & LANDIS, E.M. (1948).
A Geiger-Müller counter-system for tracer studies of gas exchanges in man.
Fed. Proc. 7: 5.
259. FOWLER, W.S. (1949).
Lung function studies III. Uneven pulmonary ventilation in normal subjects and in patients with pulmonary disease.
J. Appl. Physiol. 2: 283-299.
260. OTIS, A.B., MCKERROW, C.B., BARTLETT, R.A., MEAD, J., McILROY, M.B., SELVERSTONE, N.J. & RADFORD, E.P. Jr. (1956).
Mechanical factors in distribution of pulmonary ventilation.
J. Appl. Physiol. 8: 427-443.
261. SIKAND, R., CERRETELLI, P. & FARHI, L.E. (1966).
Effect of \dot{V}_A and \dot{V}_A/\dot{Q} distribution and of time on the alveolar plateau.
J. Appl. Physiol. 21: 1331-1337.
262. BUIST, A.S. & ROSS, B.B. (1973).
Predicted values for closing volumes using a modified single breath nitrogen test.
Amer. Rev. Resp. Dis. 107: 744-752.
263. BUIST, A.S. & ROSS, B.B. (1973).
Quantitative analysis of the alveolar plateau in the diagnosis of early airway obstruction.
Amer. Rev. Resp. Dis. 108: 1078-1087.
264. BATES, D.V. & CHRISTIE, R.V. (1950).
Intrapulmonary mixing of helium in health and in emphysema.
Clin. Sci. 9: 17-29.
265. ROSSING, R.G. (1970).
A comparison of rate variables for the description of the nitrogen wash-out curve.
Math. Biosci. 6: 283-293.
266. FOWLER, W.S., CORNISH, E.R. Jnr. & KETY, S.S. (1952).
Lung function studies VIII. Analysis of alveolar ventilation by pulmonary N_2 clearance curves.
J. Clin. Invest. 31: 40-50.
267. GOMEZ, D.M. (1963).
A mathematical treatment of the distribution of tidal volume throughout the lung.
Proc. Nat. Acad. Sci. U.S. 49: 312-319.
268. ROSSING, R.G. & DANFORD, M.B. (1968).
A comparison of continuous distributions of parameters of exponential decay curves.
Biometrics, 24: 117-134.

269. BRISCOE, W.A. & Cournand, A. (1959).
Uneven ventilation of normal and diseased lungs studied
by an open-circuit method.
J. Appl. Physiol. 14: 284-290.
270. VAN LIEW, H.D. (1967).
Graphic analysis of aggregates of linear and exponential
processes.
J. Theoret. Biol. 16: 43-53.
271. NAKAMURA, T., Takishima, T., Okubo, T., Sasaki, T., Takahashi, H.
(1966).
Distribution function of the clearance time constant in
lungs.
J. Appl. Physiol. 21: 227-232.
272. SCHEID, P. & Piiper, J. (1971).
Analysis of test gas washout from lungs with varying tidal
volume: Theory.
J. Appl. Physiol. 31: 292-295.
273. INGRAM, R.H., & Schilder, D.P. (1967).
Association of a decrease in dynamic compliance with a change
in gas distribution.
J. Appl. Physiol. 23: 911-916.
274. SAIDEL, G.M., Salmon, R.B., Chester, E.H. (1975).
Moment analysis of multibreath lung washout.
J. Appl. Physiol. 38: 328-334.
275. COURNAND, A., Yarmush, I.G., Riley, R.L. (1941).
Influence of body size on gaseous nitrogen elimination during
high oxygen breathing.
Proc. Soc. Exp. Biol. Med. 48: 280.
276. LUNDIN, G. (1955).
Alveolar ventilation (in normal subjects) analysed breath
by breath as nitrogen elimination during oxygen breathing.
Scand. J. Clin. Lab. Invest. 7 (supp. 20): 39-51.
277. ROSSING, R.G., Danford, M.B., Bell, E.L., Garcia, R. (1967).
Mathematical models for the analysis of nitrogen washout curve.
School of Aerospace Medicine Tech. Report 67 - 100.
278. HASHIMOTO, T., Young, A.C., Martin, C.J. (1967).
Compartmental analysis of the distribution of gas in the lungs.
J. Appl. Physiol. 23: 203-209.
279. CUMMING, G. (1967).
Gas mixing efficiency in the human lung.
Resp. Physiol. 2: 213-224.

280. PROWSE, K., Cumming, G. (1973).
Effects of lung volume and disease on the lung nitrogen decay curve.
J. Appl. Physiol. 34: 23-33.
281. LEWIS, J., Murray-Smith, D.J., Pack, A.I. (1976).
A simulation study of the nitrogen decay curve.
(In preparation).
282. NYE, R.E. Jr. (1961).
Theoretical limits to measurement of uneven ventilation.
J. Appl. Physiol., 16: 1115-1124.
283. VAN LIEW, H.D. (1962).
Semilogarithmic plots of data which reflect a continuum of exponential processes.
Science, 138: 682-683.
284. BRISCOE, W.A., Cournand, A. (1959).
Uneven ventilation of normal and diseased lungs studied by an open-circuit method.
J. Appl. Physiol. 14: 284-290.
285. BRISCOE, W.A. (1959).
A method for dealing with data concerning uneven ventilation of the lung and its effects on blood gas transfer.
J. Appl. Physiol. 14: 291-298.
286. BRISCOE, W.A. (1959).
Comparison between alveolar arterial gradient predicted from mixing studies and the observed gradient.
J. Appl. Physiol. 14: 299-304.
287. BRISCOE, W.A., Cree, E.M., Filler, J., Houssay, J.E.H., Cournand, A. (1960).
Lung volume, alveolar ventilation and perfusion interrelationships in chronic pulmonary emphysema.
J. Appl. Physiol. 15: 785-795.
288. BRISCOE, W.A., Nash, E.S. (1965).
The slow space in chronic obstructive pulmonary disease.
Ann. N.Y. Acad. Sci. 121: 706-722.
289. NASH, E.S., Briscoe, W.A., Cournand, A. (1965).
The relationship between clinical and physiological findings in chronic obstructive disease of the lungs.
Med. Thorac. 22: 305-327.
290. FILLEY, G.F., Beckwitt, H.J., Reeves, J.T., Mitchell, R.S. (1968).
Chronic obstructive bronchopulmonary disease. II. Oxygen transport in two clinical types.
Amer. J. Med. 44: 26-38.

291. KING, T.K.C., Briscoe, W.A. (1967).
Bohr integral isopleths in the study of blood gas exchange in the lung.
J. Appl. Physiol. 22: 659-674.
292. KING, T.K.C., Briscoe, W.A. (1967).
Blood gas exchange in emphysema: An example illustrating a method of calculation.
J. Appl. Physiol. 23: 672-682.
293. KING, T.K.C., Briscoe, W.A. (1968).
The distribution of ventilation, perfusion, lung volume and transfer factor (diffusing capacity) in patients with obstructive lung disease.
Clin. Sci. 35: 153-170.
294. ARNDT, H., King, T.K.C., Briscoe, W.A. (1970).
Diffusing capacities and ventilation: perfusion ratios in patients with the clinical syndrome of alveolar capillary block.
J. Clin. Invest. 49: 408-422.
295. BELLMAN, R., Kalaba, R.E., Lockett, J.A. (1966).
Numerical Inversion of the Laplace Transform,
New York: Elsevier.
296. POST, E.L. (1930).
Generalised differentiation.
Trans. Am. Math. Soc. 32: 723-781.
297. WIDDER, D.V. (1934).
The inversion of the Laplace Integral and the related moment problem.
Trans. Am. Math. Soc. 36: 107-200.
298. LENFANT, C., Okubo, T. (1968).
Distribution function of pulmonary blood flow and ventilation-perfusion ratio in man.
J. Appl. Physiol. 24: 668-677.
299. PESLIN, R., Dawson, S., Mead, J. (1971).
Analysis of multicomponent exponential curves by the Post-Widder's equation.
J. Appl. Physiol. 30: 462-472.
300. WEBER, J., Bouhuys, A. (1959).
Theoretical considerations on lung clearance.
Acta. Physiol. Pharmacol. Neerlandica. 8: 121-136.

301. WISE, M.E., Defares, J.E.G. (1959).
A model for unequal ventilation of the lungs assuming a common dead space and two separate dead spaces.
Bull. Math. Biophys. 21: 343-362.
302. PAIVA, M., Demeester, M. (1971).
Gas transport in the air phase of the lung simulated by a digital computer.
Comput. & Biomed. Res. 3: 675-689.
303. SAIDEL, G.M., Militano, T.C., Chester, E.H. (1971).
Pulmonary gas transport characterization by a dynamic model.
Resp. Physiol. 12: 305-328.
304. HIRATA, T. (1974).
A compartmental lung model to simulate open-circuit nitrogen washout.
Ph.D. Thesis, Rice University, Houston, Texas.
305. Build and Blood Pressure Study. (1959).
Chicago, Vol. I. Society of Actuaries. Quoted in Documenta Geigy.
306. BEKEY, G.A. & McGhee, R.B. (1964).
Gradient methods for the optimization of dynamic system parameters by hybrid computation. In Computing Methods in Optimization Problems.
Editors, Balakrishnan, A.V., Neustadt, L.W.
Academic Press, New York.
307. MEISSINGER, H.F. & Bekey, G.A. (1966).
An analysis of continuous parameter identification methods.
Simulation 6: 94-102.
308. TOMOVIC, R. (1963).
Sensitivity Analysis of Dynamic Systems.
McGraw-Hill Book Co., New York.
309. RADFORD, E.P. Jnr. (1955).
Ventilation standards for use in artificial respiration.
J. Appl. Physiol. 7: 451-460.
310. SALAZAR, E. & Knowles, J.H. (1964).
An analysis of pressure-volume characteristics of the lungs.
J. Appl. Physiol. 19: 97-104.
311. PEDLEY, T.J., Schroter, R.C. & Sudlow, M.F. (1970).
Energy losses and pressure drops in models of human airways.
Resp. Physiol. 9: 371-386.

312. PEDLEY, T.J., Schroter, R.C. & Sudlow, M.F. (1970).
The prediction of pressure drop and variation of resistance
within the human bronchial airways.
Resp. Physiol. 9: 387-405.
313. MILIC-EMILI, J., Henderson, J.A.M., Dolovich, M.B., Trop, D.,
Kaneko, K. (1966).
Regional distribution of inspired gas in the lung.
J. Appl. Physiol. 21: 749-759.
314. KOLER, J.J., Young, A.C., Martin, C.J. (1959).
Relative volume changes between lobes of the lung.
J. Appl. Physiol. 14: 345-347.
315. YOUNG, A.C., Martin, C.J. (1966).
The sequence of lobar emptying in man.
Resp. Physiol. 1: 372-381.
316. KRUEGER, J.J., Bain, T., Patterson, J.L. Jnr. (1961).
Elevation gradient of intrathoracic pressure.
J. Appl. Physiol. 16: 465-468.
317. TURNER, J.M. (1962).
Distribution of lung surface pressure as a function of
posture in dogs.
Physiologist 5: 223.
318. DALY, W.J., Bondurant, S. (1963).
Direct measurement of respiratory pleural pressure changes
in normal man.
J. Appl. Physiol. 18: 513-518.
319. MILIC-EMILI, J., Mead, J., Turner, J.M. (1964).
Topography of esophageal pressure as a function of posture
in man.
J. Appl. Physiol. 19: 212-216.
320. FARHI, L., Otis, A.B., Proctor, D.F. (1957).
Measurement of intrapleural pressure at different
points in the chest of the dog.
J. Appl. Physiol. 10: 15-18.
321. PROCTOR, D.F., Caldini, P., Permutt, S. (1968).
The pressure surrounding the lungs.
Resp. Physiol. 5: 130-144.
322. GLAZIER, J.B., Hughes, J.M.B., Maloney, J.E., West, J.B. (1967).
Vertical gradient of alveolar size in lungs of dogs frozen
intact.
J. Appl. Physiol. 23: 694-705.

323. FRANK, N.R. (1963).
A comparison of static volume-pressure relations of excised pulmonary lobes of dogs.
J. Appl. Physiol. 18: 274-278.
324. FARIDY, E.E., Kidd, R., Milic-Emili, J. (1967).
Topographical distribution of inspired gas in excised lobes of dogs.
J. Appl. Physiol. 22: 760-766.
325. GLAISTER, D.H., Schroter, R.C., Sudlow, M.F., Milic-Emili, J. (1973).
Bulk elastic properties of excised lungs and the effect of a transpulmonary pressure gradient.
Resp. Physiol. 17: 347-364.
326. GLAISTER, D.H., Schroter, R.C., Sudlow, M.F., Milic-Emili, J. (1973).
Transpulmonary pressure gradient and ventilation distribution in excised lungs.
Resp. Physiol. 17: 365-385.
327. BURGER, E.J.Jnr., Macklem, P. (1968).
Airway closure: demonstration by breathing 100% O₂ at low lung volumes and by N₂ washout.
J. Appl. Physiol. 25: 139-148.
328. SUTHERLAND, P.W., Katsura, T., Milic-Emili, J. (1968).
Previous volume history of the lung and regional distribution of gas.
J. Appl. Physiol. 25: 566-574.
329. ANTHONISEN, N.R., Danson, J., Robertson, P.C. & Ross, W.R.D. (1969/70).
Airway closure as a function of age.
Resp. Physiol. 8: 58-65.
330. DOLLFUSS, R.E., Milic-Emili, J. & Bates, D.V. (1967).
Regional ventilation of the lung studied with boluses of 133 Xenon.
Resp. Physiol. 2: 234-246.
331. BRYAN, A.C., Bentivoglio, L.G., Beerel, F., Macleish, H., Zidulka, A., & Bates, D.V. (1964).
Factors affecting regional distribution of ventilation and perfusion in the lung.
J. Appl. Physiol. 19: 395-402.
332. FOWLER, K.T. (1964).
Relative compliance of well and poorly ventilated spaces in the normal human lung.
J. Appl. Physiol. 19: 937-945.

333. ROBERTSON, P.C. Anthonisen, N.R. & Ross, D. (1969).
Effect of inspiratory flow-rate on regional distribution
of inspired gas.
J. Appl. Physiol. 26: 438-443.
334. BASHOFF, M.A. Ingram, R.H. Jnr., Schilder, D.P. (1967).
Effect of expiratory flow rate on the nitrogen concentrations
vs. volume relationship.
J. Appl. Physiol. 23: 895-901.
335. MILLETTE, B., Robertson, P.C., Ross, W.R.D. and Anthonisen, N.R.
(1969).
Effect of expiratory flow rate on emptying of lung regions.
J. Appl. Physiol. 27: 587-591.
336. JONES, J.G., Clarke, S.W. (1969).
The effect of expiratory flow rate on regional lung emptying.
Clin. Sci. 37: 343-356.
337. YOUNG, A.C., Martin, C.J., Pace, W.R. Jnr. (1963).
Effect of expiratory flow patterns on lung emptying.
J. Appl. Physiol. 18: 47-50.
338. ANTHONISEN, N.R., Robertson, P.C., Ross, W.R.D. (1970).
Gravity dependent sequential emptying of lung regions.
J. Appl. Physiol. 28: 589-595.
339. ENGEL, L.A., Utz, G., Wood, L.D.H., Macklem, P.T. (1974).
Ventilation distribution in anatomical lung units.
J. Appl. Physiol. 37: 194-200.
340. SUDA, Y., Martin, C.J., Young, A.C. (1970).
Regional dispersion of volume to ventilation ratios in the
lungs of man.
J. Appl. Physiol. 29: 480-485.
341. MACKLEM, P.T., Mead, J. (1967).
Resistance of central and peripheral airways measured by a
retrograde catheter.
J. Appl. Physiol. 22: 395-401.
342. GEORG, J., Lassen, N.A., Mellempgaard, K., Vinther, A. (1965).
Diffusion in the gas phase of the lung in normal and
emphysematous subjects.
Clin. Sci. 29: 525-532.
343. CUMMING, G., Horsfield, K., Jones, J.G. & Muir, D.C.F. (1967).
The influence of gaseous diffusion on the alveolar plateau
at different lung volumes.
Resp. Physiol. 2: 386-398.

344. JOHNSON, L.R. & Van Liew, H.D. (1974).
Use of arterial pO_2 to study convective and diffusive gas mixing in the lungs.
J. Appl. Physiol. 36: 91-97.
345. KVALE, P.A., Davis, J., Schroter, R.C. (1975).
Effect of gas density and ventilatory pattern on steady state CO uptake by the lung.
Resp. Physiol. 24: 385-398.
347. DUBOIS, A.B., Fenn, W.O. & Britt, A.G. (1952).
CO₂ dissociation curve of lung tissue.
J. Appl. Physiol. 5: 13-16.
348. CHINARD, F.P., Enns, T., Nolan, M.F. (1960).
Contributions of bicarbonate ion and dissolved CO₂ to expired CO₂ in dogs.
Amer. J. Physiol. 198: 78-88.
349. CHINARD, F.P. (1966).
The permeability characteristics of the pulmonary blood-gas barrier. In Advances in Respiratory Physiology. C.G. Caro, Editor. Edward Arnold Ltd. (Publishers), London.
350. CHINARD, F.P., Enns, T., Nolan, M.F. (1962).
The permeability characteristics of the alveolar capillary barrier.
Trans. Assoc. Am. Physicians, 75: 253-261.
351. BERFENSTAM, R. (1952).
Carbonic anhydrase activity in fetal organs.
Acta. Paediat. 41: 310-315.
352. FEISAL, K.A., Sackner, M.A., Dubois, A.B. (1963).
Comparison between the time available and time required for CO₂ equilibration in the lung.
J. Clin. Invest. 42: 24-28.
353. DUBOIS, A.B. (1952).
Alveolar CO₂ and O₂ during breath holding, expiration and inspiration.
J. Appl. Physiol. 5: 1-12.

354. SACKNER, M.A. Feisal, K.A., Dubois, A.B. (1964).
Determination of tissue volume and carbon dioxide dissociation slope of the lungs in man.
J. Appl. Physiol. 19: 374-380.
355. HYDE, R.W., Puy, R.J.M., Raub, W.F., Forster, R.E. (1968).
Rate of disappearance of labelled carbon dioxide from the lungs of humans during breath-holding: a method for studying the dynamics of pulmonary CO₂ exchange.
J. Clin. Invest. 47: 1535-1552.
356. CANDER, L., Forster, R.E. (1959).
Determination of pulmonary parenchymal tissue volume and pulmonary capillary blood flow in man.
J. Appl. Physiol. 14: 541-551.
357. SONI, J., Feisal, K.A., Dubois, A.B. (1963).
The rate of intrapulmonary blood gas exchange in living animals.
J. Clin. Invest. 42: 16-23.
358. FARHI, L.E., Rahn, H. (1960).
Dynamics of changes in carbon dioxide stores.
Anaesthesiology, 21: 604-614.
359. FREEMAN, F.H., Fenn, W.O. (1953).
Changes in carbon dioxide stores of rats due to atmospheres low in oxygen or high in carbon dioxide.
Amer. J. Physiol. 17: 422-430.
360. RAHN, H. (1962).
The gas stores of the body with particular reference to carbon dioxide. In Man's Dependence on the Earthly Atmosphere, Editor, K.E. Schaefer. McMillan, New York.
361. SULLIVAN, S.F., Patterson, R.W., Papper, E.M. (1964).
Tissue carbon dioxide stores. Magnitude of the acute change in the dog.
Amer. J. Physiol. 206: 887-890.
362. FOWLE, A.S.E., Campbell, E.J.M. (1964).
The immediate carbon dioxide storage capacity of man.
Clin. Sci. 27: 41-49.
363. CHERNIACK, N.S., Longobardo, G.S. (1970).
Oxygen and carbon dioxide stores of the body.
Physiol. Rev. 50: 196-243 (219 references).
364. FOWLE, A.S.E., Matthews, C.M.E., Campbell, E.J.M. (1964).
The rapid distribution of ³H₂O and ¹¹CO₂ in the body in relation to the immediate carbon dioxide storage capacity.
Clin. Sci. 27: 51-56.

365. CHERNIACK, N.S., Longobardo, G.S., Staw, I., Heymann, M. (1966).
Dynamics of carbon dioxide stores changes following an alteration
in ventilation.
J. Appl. Physiol. 21: 785-793.
366. MATTHEWS, C.M.E., Laszlo, G., Campbell, E.J.M., Read, D.J.C. (1968).
A model for the distribution and transport of CO₂ in the body
and ventilatory response to CO₂.
Resp. Physiol. 6: 45-67.
367. CHERNIACK, N.S., Tuteur, P.G., Edelman, N.H., Fishman, A.P. (1972).
Serial changes in CO₂ storage in tissues.
Resp. Physiol. 16: 127-141.
368. STAW, I. (1968).
Dynamics of mammalian carbon dioxide stores.
Ph.D. Thesis, Columbia University, New York.
369. NICHOLS, G. Jnr. (1958).
Serial changes in tissue carbon dioxide content during acute
respiratory acidosis.
J. Clin. Invest. 37: 1111-1122.
370. MAREN, T.H. (1967).
Carbonic anhydrase: chemistry, physiology and inhibition.
Physiol. Rev. 47: 595-781.
371. DAVENPORT, H. W. (1969).
The ABC of Acid-Base Chemistry.
University of Chicago Press, Chicago & London.
372. ROUGHTON, F.J.W. (1964).
Transport of oxygen and carbon dioxide. In 'Handbook of Physiology,
Section 3: Respiration.'
Editors, W.O. Fenn & H. Rahn.
American Physiological Society, Washington.
373. VAN SLYKE, D.D. (1921).
The carbon dioxide carriers of the blood.
Physiol. Rev. 1: 141-176.
374. FERGUSON, J.K.W., Roughton, F.J.W. (1935).
The chemical relationships and physiological importance of
carbamino compounds of CO₂ with haemoglobin.
J. Physiol. Lond., 83: 87-102.
375. HENDERSON, L.J. (1928).
Blood.
Yale University Press, New Haven.
376. ROSSI-BERNARDI, L., Roughton, F.J.W. (1967).
The specific influence of carbon dioxide and carbamate compounds
on the buffer power and Bohr effects in human haemoglobin solutions.
J. Physiol. 189: 1-29.

377. OLSZOWKA, A.J., Farhi, L.E. (1968).
A system of digital computer subroutines for blood gas calculations.
Resp. Physiol. 4: 270-280.
378. HOMER, L.D., Denysyk, B. (1975).
Estimation of cardiac output by analysis of respiratory gas exchange.
J. Appl. Physiol. 39: 159-165.
379. VISSER, B.F. (1960).
Pulmonary diffusion of carbon dioxide.
Phys. Med. Biol. 5: 155-166.
380. KIM, T.S., Rahn, H., Farhi, L. E. (1966).
Estimation of true venous and arterial pCO_2 by gas analysis of a single breath.
J. Appl. Physiol. 21: 1338-1344.
381. CHRISTIANSEN, J., Douglas, C.G. Haldane, J.S. (1914).
The absorption and dissociation of carbon dioxide by human blood.
J. Physiol (London)., 48: 244-277.
382. HENDERSON, L.J., Bock, A.V., Field, H.Jr., Stoddard, J.L. (1924).
Blood as a physicochemical system. II.
J. Biol. Chem. 59: 379-431.
383. DILL, D.B., Edwards, H.T., Consolazio, W.V. (1937).
Blood as a physicochemical system. XI. Man at rest.
J. Biol. Chem. 118: 635-648.
384. DITTMER, D.S., Grebe, R.M. (1958). (Editors).
Handbook of Respiration.
W.B. Saunders, Philadelphia and London.
385. FOWLER, W.S. (1948).
Lung function studies. II. The respiratory dead space.
Amer. J. Physiol. 154: 405-416.
386. PEARSON, K.G. (1975).
Parameter estimation techniques applied to a model of human respiratory gas exchange processes.
Ph.D. Thesis, University of Glasgow.
387. ROSENBROCK, H.H. (1960).
An automatic method for finding the greatest or least value of a function.
Computer J. 3: 175-184.
388. DAVIDON, W.C. (1959).
Variable metric method for minimisation.
AEC Research and Development Report, ANL - 5990. (Cited in 389).

389. FLETCHER, R., Powell, M.J.D. (1963).
A rapidly convergent descent method for minimisation.
Computer J. 6: 163-168.
390. ADBY, P.R., Dempster, M.A.H. (1974).
Introduction to Optimisation Methods.
Chapman and Hall, London.
391. BOX, M.J., Davies, D., Swann, W.H. (1969).
Nonlinear Optimisation Techniques. I.C.I. Monograph No.5,
Oliver and Boyd, Edinburgh.
392. DIXON, L.C.W. (1972).
Nonlinear Optimisation.
English Universities Press, London.
393. POWELL, M.J.D. (1970).
A survey of numerical methods for unconstrained optimisation.
SIAM Review, 12: 79-97.
394. WHITE, R.C. (1970).
A survey of random methods for parameter optimisation.
Internal Report, Department of Electrical Engineering,
Technological University, Eindhoven, Netherlands.
395. LILJESTRAND, G., Lindhard, J. (1920).
The determination of circulation rate in man from the arterial
and venous tension and the CO₂-output.
J. Physiol. (Lond). 53: 420-430.
396. BARR, D.P., Peters, J.P. (1921).
The carbon dioxide absorption curve and carbon dioxide
tension of the blood in severe anaemia.
J. Biol. Chem. 45: 571 - 592.
397. DILL, D.B., Talbott, J.H., Consolazio, W. V. (1937)
Blood as a physicochemical system. XII. Man at high altitudes.
J. Biol. Chem. 118: 649-666.
398. PETERS, J.P. Bulger, H.A., Eisenman, A.J. (1924).
Studies of the carbon dioxide absorption curve of human blood.
IV. The relation of the haemoglobin content of blood to the
form of the carbon dioxide absorption curve.
J. Biol. Chem. 58: 747-768.
399. MCHARDY, G.J.R. (1967).
The relationship between the differences in pressure and content
of carbon dioxide in arterial and venous blood.
Clin. Sci. 32: 299-309.

400. LACQUET, L.M., Van Der Linden, L.P., Paiva, M. (1975).
Transport of H_2 and SF_6 in the lung.
Resp. Physiol. 25: 157-173.
401. PACK, A., Nixon, W., Hooper, M., Taylor, J.C. (1976).
A computational model of pulmonary gas transport incorporating
effective diffusion.
Resp. Physiol. (In press).
402. ENGEL, L.A., Wood, L.D.H., Utz, G., Macklem, P.T. (1973).
Gas mixing during inspiration.
J. Appl. Physiol. 35: 18-24.
403. HAMILTON, W.F. (1962).
Measurement of the cardiac output. In 'Handbook of Physiology:
Circulation, Volume I,' pg. 551-584. Editor, Hamilton, W.F.
American Physiological Society, Washington, D.C.
404. BUTLER, J. (1965).
Measurement of cardiac output using soluble gases.
In 'Handbook of Physiology: Respiration, Volume 2', pg. 1489-1503.
Editors, Fenn, W.O., Rahn, H.
American Physiological Society, Washington, D.C.
405. FARHI, L.E. & Haab, P. (1967).
Mixed venous blood gas tensions and cardiac output by "bloodless"
methods; recent developments and appraisal.
Resp. Physiol. 2: 225-233.
406. GUYTON, A.C., Jones, C.E., Coleman, T.C. (1973).
Circulatory Physiology: Cardiac Output and its Regulation.
W.B. Saunders Co., Philadelphia.
407. GROLLMAN, A. (1929).
The determination of the cardiac output of man by the use of
acetylene.
Amer. J. Physiol. 88: 432-445.
408. BECKLAKE, M.E., Varvis, C.J., Pengelly, L.D., Kenning, S.,
McGregor, M., Bates, D.V. (1962).
Measurement of pulmonary blood flow during exercise using
nitrous oxide.
J. Appl. Physiol. 17: 579-586.
409. DEFARES, J.G. (1958).
Determination of P_{CO_2} from the exponential CO_2 rise during rebreathing.
J. Appl. Physiol. 13: 159-164.
410. JONES, N.L., Campbell, E.J.M., McHardy, G.J.R., Higgs, B.E., Clode, M.
(1967).
The estimation of carbon dioxide pressure of mixed venous blood
during exercise.
Clinical Science, 32: 311-327.

411. JENERUS, R., Lundin, G., Thomson, D. (1963).
Cardiac output in healthy subjects determined with a CO₂ rebreathing method.
Acta Physiol. Scand. 59: 390-399.
412. FERGUSON, R.J., Faulkner, J.A., Julius, S., Conway, J. (1968).
Comparison of cardiac output determined by CO₂ rebreathing and dye dilution methods.
J. Appl. Physiol. 25: 450-454.
413. DENISON, D. (1968).
Mixed venous blood gas tensions and respiratory stress in man.
Ph.D. Thesis, University of London.
414. GODFREY, S., Davies, C.T.M., Wozniak, E., Barnes, C.A. (1971).
Cardio-respiratory response to exercise in normal children.
Clin. Sci. 40: 419-431.
415. BAR-OR, O., Shephard, R.J., Allen, C.L. (1971).
Cardiac output of 10 to 13 year old boys and girls during submaximal exercise.
J. Appl. Physiol. 30: 219-223.
416. GODFREY, S., Wolf, E. (1972).
An evaluation of rebreathing methods for measuring mixed venous pCO₂ during exercise.
Clin. Sci. 42: 345-353.
417. WINSBOROUGH, M.M. (1974).
A measurement of the carbon dioxide capacitance of the lungs and of the pulmonary capillary blood flow.
Ph.D. Thesis, Council for National Academic Awards.
418. YU, C.J., Lutherer, B., Guyatt, A., Otis, A.B. (1973).
Comparison of blood and alveolar gas composition during rebreathing in the dog lung.
Resp. Physiol. 17: 162-177.
419. CERRETELLI, P., Sikand, R., Farhi, L.E. (1966).
Adjustments in cardiac output and gas exchange during exercise and recovery.
J. Appl. Physiol. 21: 1345-1350.
420. DAVIES, C.T.M., Di Prampero, P.E., Cerretelli, P. (1972).
Kinetics of cardiac output and respiratory exchange during exercise and recovery.
J. Appl. Physiol. 32: 618-625.
421. HLASTALA, M.P., Wranne, B., Lenfant, C.J. (1972).
Single-breath method of measuring cardiac output - a re-evaluation.
J. Appl. Physiol. 33: 846-848.

422. TANNER, J.M. (1949).
The construction of normal standards for cardiac output in man.
J. Clin. Invest. 28: 567-582.
423. DONALD, K.W., Bishop, J.M., Cumming, G., Wade, O.L. (1953).
The effect of nursing positions on the cardiac output in man.
Clin. Sci. 12: 199-216.
424. BEVEGÅRD, S., Freyschuss, U., Strandell, T. (1966).
Circulatory adaptation to arm and leg exercise in supine and sitting position.
J. Appl. Physiol. 21: 37-46.
425. STENBERG, J., Åstrand, P-O., Ekblom, B., Royce, J., Saltin, B. (1967).
Haemodynamic response to work with different muscle groups, sitting and supine.
J. Appl. Physiol. 22: 61-70.
426. BEVEGÅRD, S., Holmgren, A., Jonsson, B. (1960).
The effect of body position on the circulation at rest and during exercise, with special reference to the influence on the stroke volume.
Acta. Physiol. Scand. 49: 279-298.
427. THOMASSON, B. (1957).
Cardiac in normal subjects under standard basal conditions.
The repeatability of measurements by the Fick method.
Scand. J. Clin. Lab. Invest. 9: 365-376.
428. HOLMGREN, A., Pernow, B. (1960).
The reproducibility of cardiac output determination by the direct Fick method during muscular work.
Scand. J. Clin. Lab. Invest. 12: 224-227.
429. SELZER, A., Sudrann, R.B. (1958).
Reliability of the determination of cardiac output in man by means of the Fick principle.
Circ. Res. 6: 485-490.
430. ÅSTRAND, P-O., Cuddy, T.E., Saltin, B., Stenberg, J. (1964).
Cardiac output during submaximal and maximal work.
J. Appl. Physiol. 19: 268-274.
431. DONALD, K.W., Bishop, J.M., Cumming, G., Wade, O.L. (1955).
The effect of exercise on cardiac output and circulatory dynamics of normal subjects.
Clin. Sci. 14:37-73.
432. HOLMGREN, A., Jonsson, B., Sjöstrand, T. (1960).
Circulatory data in normal subjects at rest and during exercise in recumbent position, with special reference to the stroke volume at different work intensities.
Acta. Physiol. Scand. 49: 343-363.

433. JULIUS, S., Amery, A., Whitlock, L.S., Conway, J. (1967).
Influence of age on the hemodynamic response to exercise.
Circulation 36: 222-230.
434. REEVES, J.T., Grover, R.F., Filley, G.F., Blount, S.G. Jr. (1961).
Circulatory changes in man during mild supine exercise.
J. Appl. Physiol. 16: 279-282.
435. ALTMAN, P.L., Dittmer, D.S. (1971).
Handbook of Respiration and Circulation.
Federation of American Societies for Experimental Biology.